EARTH OBSERVATION-BASED ASSESSMENT OF SPATIAL AND TEMPORAL TRENDS IN INUNDATION EXTENT IN THE BAROTSE WETLAND, WESTERN ZAMBIA

By

Henry Musonda Zimba

A thesis submitted to the University of Zambia, School of Mines, in partial fulfilment of the requirement for the Master of Science Degree in Integrated Water Resources Management

University of Zambia
LUSAKA

DECLARATION

This thesis was written and submitted in accordance with the rules and regulations governing the award of the Master of Science in Integrated Water Resources Management in the School of Mines of the University of Zambia. I further declare that the thesis has neither in part nor in whole been presented as substance for award of any degree, either to this or any other university. Where other people's work has been drawn upon, appropriate and adequate acknowledgment has been made.

Signature of author: …….

Date: …….

APPROVAL

This thesis of Henry Musonda Zimba is approved as fulfilling the requirements of the Degree of Master of Science in Integrated Water Resources Management of the University of Zambia.

Signature: Chairperson ……..

1st Examiner ……..

2nd Examiner …….

External Examiner ……..

ABSTRACT

Climate change, construction of the Mongu-Kalabo Road coupled with increased mining activities in the upper catchment of the Barotse Wetland could alter the inundation extent dynamics and impact the flood dependent ecosystem. There is very little information available in public domain on inundation extent dynamics of the wetland. This study investigated trends in inundation extent in the Barotse Wetland in Western Zambia. The study methods included statistical analysis of inundation extent time series generated with the Desert Flood Index from MODIS satellite imagery, in-situ hydrological and climatological time series, and land cover change assessment with Landsat imagery. Variations in inundation extent were analysed with the one-way Repeated Measure Analysis of Variance test. The Mann-Kendall trends test was used to characterise trends in inundation extent, hydrological and climatological time series. The Pearson r and the Paired t test were used to analyse correlations between hydrological and climatological time series. The Pettit test was used to test for homogeneity in the time series. Land cover change statistics were derived from the Maximum Likelihood algorithm classified maps which were validated with ground truthing data.

The results show that across the period 2003 to 2013 there were significant variations in inundation extent with the *F-Ratios* (27.21 and 15.73) greater than the *F-critical* values (2.35 and 2.17) and *p-values* <0.05 in the ascending/peak and descending periods respectively. In the same period inundation extent showed a significant (*p value* <0.05) rising trend with a Mann-Kendall Z statistic of 1.87. A very strong correlation, with coefficient of determination (R^2) of 0.91, between inundation extent and discharge was observed. From 1984 to 2015 the change in forest cover was observed at 9.78 percent with an annual rate of decrease of 0.32 percent. Overall, the Mann-Kendall trend test showed significant declining trends in mean annual discharge for the period from 1952 to 2003 at Senanga and 1952 to 2004 for Lukulu (Z statistics of -3.38 and -2.88, *p-values* <0.05 in both scenarios, at alpha level 0.05). For the period 1974 to 2012, the rainfall time series at Kabompo Station, upstream of the wetland catchment, showed a generally insignificant declining trend with Z statistic of -1.14 and *p-value* of 0.12 at alpha level 0.05. Rainfall and discharge showed a significant (*p-value* < 0.05) positive correlation with a coefficient of 0.36. Maximum temperature correlated negatively with discharge and inundation extent with correlation coefficients of -0.44 and -0.16 respectively. The study shows that trends in inundation extent follow trends in discharge. By inference, between 1952 and 2004 inundation extent in the Barotse Wetland was in downward trend as was the trend in discharge. Between 2003 to 2013 inundation extent trend was on the rise as was the trend in water level (from 2000 to 2011).

Overall, the downward trend in discharge and reduction in forest cover could negatively affect inundation extent patterns and the Barotse wetland's ecosystem as a whole. In view of the results of the study the Government of Zambia must ensure that deforestation in the wetland catchment is addressed and that no extensive alterations are made to the current wetland landscape as such actions have potential to alter the flow regimes and inundation extent patterns with consequences on the wetland ecosystem.

DEDICATION

To my late wife Alice, who told me the doors at the university were open for me and that I should go as far as possible. I will keep the promise;

and

To my son Rione and my daughter Thelg, you are my inspiration.

ACKNOWLEDGEMENTS

Words fail me on how to express my heartfelt gratitude to my supervisors, Professor Imasiku Anayawa Nyambe and Doctor Kawawa Banda, for their unwavering support and unequalled professional guidance throughout the preparation of this thesis. I am forever indebted and bound to emulate their passion and dedication to hold to excellency in research work and all things in life. At first I was like an eagle without feathers having the frame of passion and potential to fly but with no feathers to give me the ability to fly. Not only have they helped me acquire the feathers they have also taught me how to fly and sow like a noble eagle. Armed with this knowledge I know I have become more useful to my nation.

I always wanted to pursue graduate studies but I fail short on financial resources. I am eternally grateful to the Southern Africa Science Service Centre for Climate Change and Adaptive Land-use Management (SASSCAL) for the financial and technical support that enabled the successful completion of this research. I am thankful for the opportunity and financial support that enabled me attend the SASSCAL training in Research Methodologies at the Okavango Research Institute, University of Botswana in Gaborone, Botswana and the study exchange visit to the University of Jena in German. The exposure and the skills I acquired through these experiences greatly contributed to the completion of this work.

The night and early morning journeys to the Barotse Land were always enjoyable in the company of Mr Wilson Kakusa Phiri aka Professor Namunshakende (PhD Student-UNZA) and Mr Anthony Chabala (MSc. Student- UNZA). I am thankful for their support during data collection and valuable comments at the writing stage of this thesis. Special thanks to Markus Meinhard (PhD Student -University of Jena, German) Dr Peter Selsam (University of Jena, German) and Dr Matthias Mück (German Aero Space Centre) for the technical support and comments both during data collection and at the writing of this thesis.

I am grateful to the Department of Water Affairs and the Zambia Meteorological Department in Mongu for the hydrological and weather data used in this thesis. Lastly, I would like to thank the Integrated Water Resources management (IWRM) Centre at the University of Zambia for the opportunity to be enrolled at the centre and the facilities accorded to me during this research.

TABLE OF CONTENTS

LIST OF FIGURES

LIST OF TABLES

Page

LIST OF APPENDICES

Page

LIST OF ABBREVIATIONS

ACA	Atmospheric Correction Algorithm
AER	Agro-Ecological Zone
ANOVA	Analysis of Variance
ARC	Annual Rate of Change
ASAR AP	Advanced Synthetic Aperture Radar Alternating Polarization mode
ASTER	Advanced Space borne Thermal Emission and Reflection Radiometer
AWEI	Automated Water Extraction Index
BRDF	Bidirectional Reflectance Distribution Function
CBD	Convention on Biological Diversity
CC	Correlation Coefficient
CD	Coefficient of Determination
CDAT	Change Detection After Thresholding
CSO	Central Statistics Office
DEM	Digital Elevation Model
DFI	Desert Flood Index
DJF	December, January, February
DN	Digital Number
DWA	Department of Water Affairs
EFD	European Flood Directive
EMR	Electro Magnetic Radiation
ENVISAT	Environment Satellite
EOS AM	Earth Observation System Ante Meridiem
EOS PM	Earth Observation System Post Meridiem
EXCIMAP	European Exchange CIrcle on flood Mapping
FAO	Food and Agriculture Organisation
FD	Forest Department
FLAASH	First Line –of-sight Atmospheric Analysis of Hypercubes
FWV	Forest Wood Vegetation
GeoTIFF	Geospatial Tagged Image File Format

GL	Grassland
GPS	Global Positioning System
GRZ	Government of the Republic of Zambia
GSB	Grassland Shrubland Bare sand
HDF	Hierarchical Data Format
HSI	Hyperspectral Imagery
IFRC	International Federation of the Red Cross
ILUA	Integrated Land Use Assessment
IPCC	Inter-governmental Panel on Climate Change
IR	Infra-Red
IUCN	International Union for Conservation of Nurture
ITCZ	Inter Tropical Convergence Zone
IWRM	Integrated Water Resources Management
JM	Jefferies Matusita
KLM	Keyhole Markup Language
LANDSAT	Land remote sensing SATellite
LCUCD	Land Cover and Use Change Detection
L2G	Level 2 Gridded
MAM	March, April, May
MERIS	MEdium Resolution Imaging Spectrometer
MNDWI	Modified Normalised Difference Water Index
MODIS	Moderate-resolution Imaging Spectrometer
MODTRAN	MODerate resolution atmospheric TRANsmission
MRT	MODIS Reprojection Tool
NASA	National Aeronautics and Space Administration
NDVI	Normalised Difference Vegetation Index
NDWI	Normalised Difference Water Index
NLAPS	National Land Archive Production System
OLI-TIRS	Operational Land Imager Thermal Infrared Sensor
PC	Percentage Change
RADARSAT	Radar Satellite

ROI	Region of Interest
SAR	Synthetic Aperture Radar
SON	September, October, November
SPOT	Satellite Pour l'Observation de la Terre
STRP	Scientific and Technical Review Paper
TM	Thematic Mapper
TOA	Top Of Atmosphere
UNDP	United Nations Development Programme
UNEP	United Nations Environmental Programme
UNESCO	United Nations Educational, Scientific and Cultural Organization
UNFCCC	United Nations Framework Convention on Climate Change
UNZA	University of Zambia
vis-SWIR	Visible Short Wave Infrared
WL	Wetland
ZMD	Zambia Meteorological Department
ZFD	Zambia Forest Department

LIST OF SYMBOLS

A_ρ	Reflectance additive scaling factor for the band
$B_{rescale}$	Band-specific rescaling factor units of (units of W/ (m^2. sr. μm))
d	Earth-Sun distance in astronomical units
$ESUN_\lambda$	Mean solar exoatmospheric irradiances
$G_{rescale}$	Band-specific rescaling factor units of (W/ (m^2. sr. μm)/DN)
H_a	Alternative Hypothesis
H_0	Null Hypothesis
J_{ij}	The Jefferies-Matusita separability measure for two classes
K_t	Pettit Statistic
k	Kappa Coefficient
$LMIN_\lambda$	The spectral radiance that is scaled to Qcalmin in W/ (m^2. sr. μm)
$LMAX_\lambda$	The spectral radiance that is scaled to Qcalmax in W/ (m^2. sr. μm)
L_λ	Spectral Radiance at the sensor's aperture in W/ (m^2. sr. μm)
M_ρ	Reflectance multiplicative scaling factor for the band
MS_B	Mean of squares between groups
MS_W	Mean of squares within groups
n_d	Discordant pairs
n_c	Concordant pairs
P_s	Pixel size
Q	Discharge (m^3)
Q_i	Sense's slope estimate
Q_{cal}	The quantized calibrated pixel value in Digital Number
Q_{calmin}	The minimum quantized calibrated pixel value (DN=0) corresponding to $LMIN_\lambda$
Q_{calmax}	The maximum quantized calibrated pixel value (DN=255) corresponding to $LMAX_\lambda$
r	Pearson Correlation Coefficient
S	Mann-Kendall's Statistic
SS_B	Between groups sum of squares

SS_T	Total sum of squares
SS_W	Within the group sum of squares
S_k	Seasonal Mann-Kendall Statistic
t_i	Number of ties to the extent i
U_{tN}	Pettit Homogeneity Test statistic
Z_s	Standard test statistic which measures the strength of the trend
Z_{sk}	Standardized Mann-Kendall Statistic
Var [s]	Adjusted Variance
σ^2	Variance for the S statistic
α	Probability Level
τ	Kendall's tau
σ^2	Variance for the S statistic
α	Probability Level
τ	Kendall's tau
ρ_{λ}	Top-of-Atmosphere Planetary Spectral Reflectance, without correction for solar angle.
p^P	Unit less planetary reflectance
θ_s	Solar zenith angle in degrees
p^{Green}	Reflectance value for the Green Band
p^{NIR}	Reflectance value for the Near Infra-Red Band
p^{Red}	Reflectance value for the Red Band

p^{SWIR}	Reflectance value for the Short Wave Infra-Red
$(n)P$	Total number of inundated pixels
ρ	Significance Probability
U_{tN}	Pettit Homogeneity Test statistic
.h1	Header file
.wo	Work Order report
$\sigma_w^2(t)$	Otsu weighted sum of variances at a given threshold value

CHAPTER ONE: INTRODUCTION

1.1 Background

According to the Convention on Biological Diversity (CBD) "the future of humanity depends on wetlands" (UNEP, 2015). This is because many future challenges such as food, water security, human health, disaster risk reduction and climate change resilience can be addressed through conservation and sustainable utilization of wetlands. Wetlands particularly provide water-related services and are productive areas for plant life, animals and wetland agriculture. They are known to regulate water quality, flow regimes, groundwater recharge and flooding. They are also key in carbon sequestration and storage (Bullock and Acreman, 2003; Foster *et al*. 2012; UNEP, 2015). Despite the highlighted significant roles of wetlands, it is estimated that over 64 percent of the world's wetlands have disappeared since 1960, which implies a degradation in freshwater supply to billions of people worldwide as well as a 76 percent decline in biodiversity between 1970 and 2010 (UNEP, 2015). Global climate change and land use change are the major drivers of the degradation in freshwater, biodiversity and impact on the flooding regimes of wetlands (Erwin, 2009; IPCC, 2014; UNEP, 2015).

Flooding is a significant natural occurrence for continued existence and the ecological functioning of wetlands (Millennium Ecosystem Assessment, 2005). The European Flood Directive (EFD) defines "flood" as "a temporary covering by water of land normally not covered by water". This definition encompasses floods from rivers, mountain torrents, Mediterranean ephemeral water courses, floods from the sea in coastal areas, and may exclude floods from sewerage systems (EXCIMAP, 2007). Flooding is key in the delivery of many wetland ecological services to the millions of people who are dependent on it for flood-recession agriculture, pasture and fishing activities (Erwin, 2009; Foster *et al*. 2012). However, Erwin (2009), IPCC (2014) and the UNEP (2015) point to the fact that climate change will have effects on the hydrology of individual wetland ecosystems due to changes in precipitation and temperature regimes. Climate change impacts on wetlands will vary globally and adaptation to these effects will be anchored on information generated in individual habitats (Erwin, 2009). One of the basic information in wetland

management is the understanding of the hydrological dynamics such as base flows, extent, depth and hydro-period that govern the function of the wetland (Erwin, 2009). The Barotse Wetland, is an annually flooded wetland susceptible to the effects of climate change (Beilfuss, 2012), is rich in biodiversity and supports a diverse human systems including agriculture, fisheries, transport and other livelihood streams (Timberlake, 2000; IUCN, 2003; Fanshawe, 2010). Erwin (2009) points to the fact that key to the efficient management of wetland resources is availability of habitat based information. In the case of the Barotse Wetland, one of the fundamental habitat specific piece of data is inundation patterns. This is significant because crucial precondition for tackling future challenges of the Barotse Wetland is foresighted management. The challenges include resource over-exploitation, flood control (to protect house and technical infrastructure such as the newly constructed Mongu-Kalabo Road), land drainage, encroachment for agriculture, and interference with river hydrology for large-scale hydropower and irrigation schemes (Turpie *et al*. 1999). However, due to the difficulty associated with traditional ground based inundation mapping there is paucity of data on inundation regimes. The difficulties associated with traditional ground based (field survey) inundation mapping methods underscore the importance of employing techniques that effectively capture the spatial and temporal distribution of inundation. Nevertheless, earth observation methods such as the use of satellite based remote sensing provides a pragmatic platform that facilitates the acquisition of the type and quantity of data needed to assess inundation dynamics across a vast area and time space. Various water feature extraction algorithms have been developed and successfully used to map inundation extent (McFeeters, 1996; Xu, 2006; Wang, 2007; Di Baldassarre, 2012; Meire, 2012, Wang *et al*. 2013).

Application of satellite based remote sensing techniques in inundation extent assessments provides an important avenue for data collection on the dynamic state of inundation, especially for vast wetlands where ground based methods are virtually impractical. With the advantage of area coverage (spatial resolution), regular revisit time (temporal resolution) and acquisition of data in a wide range of the electromagnetic spectrum (spectral resolution), the remote sensing approach is best suited for study of inundation dynamics as compared to conventional mapping methods (Ticehurst *et al.* 2013; Ticehurst *et al.* 2014). A host of satellite sensors are currently generating enormous amounts of data at various resolutions that form the core for both historical and continued monitoring of inundation regimes and other landforms. Among the vast spectrum of

uses, earth observation based data has increasingly become an important source of information for water use planning, monitoring and management at various levels of management such as field, catchment and regional scale (Mu *et al.* 2007).

1.2 Statement of the problem

It has been noted that one of the major challenges that constrains adaptation to climate change, in Africa and Southern Africa in particular, is lack of skills, access to tools and the information needed to make decisions on climate change (Boko *et al*. 2007). This scenario makes it difficult to perform detailed synthesis and understanding of hydrological implications and analysis of the significance of the different flow components (Stisen *et al.* 2008). In the Zambezi Basin, this challenge is compounded by inadequate and dilapidated hydro-meteorological stations (Cohen *et al*. 2014). In many cases, this problem is so severe that even the application of conventional prediction tools is severely limited in this part of Africa (Cohen *et al*. 2014). In Zambia, like in many Southern African countries, the scantiness of geological, hydrological and land cover change data implies paucity of habitat based information on ecosystems such as wetlands (Stisen *et al.* 2008; Cohen *et al*. 2014). However, use of earth observation-based remote sensing is seen as a cheaper and more efficient method of acquiring the kind and quantity of data needed for effective management of ecosystems and water resources in general (Mu *et al*. 2007; Schumann *et al*. 2007).

It is critical that hydrological variables such as wetland inundation patterns in the Barotse Wetland are monitored. This is because the continued function and resource utilization of the Barotse Wetland ecosystem, as is the case with wetlands worldwide (Erwin, 2009), is largely dependent on the flow regimes and flooding extent, which are prone to climate change (Erwin, 2009). There is irrefutable evidence that the Barotse Wetland is prone to climate variability (Thurlow *et al.* 2009; Yamba *et al*. 2009; Beilfuss, 2012; GRZ, 2013) manifesting through variables such as temperatures and rainfall which directly impact on the hydrological regimes. Further, the wetland is located in a region with high rates of evapotranspiration (Kasimona and Makwaya, 1995; Beilfuss, 2012; Phiri, 2013) which could cut into the residence time of the water and consequently affect the efficient ecological functioning of the wetland. The wetland is also the most agriculture productive area in western Zambia (GRZ, 2013) where agricultural systems and changes in land cover for agriculture have been noted (Erwin, 2009; Millennium Ecosystem Assessment, 2005; UNEP, 2015) as being some of the major drivers of wetland degradation. Further, the construction

of the Mongu-Kalabo Road across the wetland entails modification in the flow regimes within the wetland and can potentially affect the flood extent patterns and biodiversity in the wetland. Despite the noted significance of the hydrological dynamics, such as inundation extent, to the existence and functioning of the wetland there is paucity of data on inundation extent regimes and the potential drivers of these regimes as they relate to hydrological, climatological and anthropogenic variables. There is also a general assumption that has not fully been verified for the Barotse Wetland: that wetlands attenuate flow, thus, reduce the risk of downstream flooding (Millennium Ecosystem Assessment, 2005) by acting as a sponge that soak up water during wet periods and release it during dry periods. It is plausible that the behaviour of the Barotse Wetland may be at variance with this assumption as the case is with other wetlands (Millennium Ecosystem Assessment, 2005). Thus, this study employed a coupled approach in which satellite remote sensing and in-situ hydrological and climatological data were used to assess trends in wetland inundation extent regimes. This was done in order to ascertain the nature of trends in inundation extent regimes and the potential contributing factors to these trends.

1.3 General objective of the study

The general objective of the study was to provide an assessment of the spatial and temporal trends in inundation extent using satellite remote sensing data thereby contribute a valuable data resource in the water resources, biodiversity and disaster management framework for the Barotse Wetland of Western Zambia.

1.3.1 Specific Objectives

The specific objectives of the study were:

- To quantify the inundated area in each flood cycle between 2003 to 2013 using MODIS satellite data;
- To establish trends in the wetland's inundation extent for the period 2003 to 2013;
- To evaluate the role of the Barotse Wetland in downstream flow regimes;
- To establish long term trends in discharge, rainfall and maximum temperature time series for the study area; and
- To ascertain land cover changes over time,1984 to 2015, in the immediate catchment of the Barotse Wetland.

1.4 Research Questions

The study sought to answer the following questions:

- What are the estimates of inundated area in each flood cycle for the period 2003 to 2013 in the Barotse Wetland?
- What trend(s) existed in inundation extent over the period 2003 - 2013?
- What relationship (s) exist between stream discharge/water level and the inundation extent?
- Does the Barotse Wetland play any role in downstream flow regimes?
- What are the potential drivers of the noted (if any) trends/variations in inundation patterns in the Barotse Wetland?

    (i) Are there changes in stream flow, precipitation and temperature in the Barotse Wetland? If these changes exist, what are the patterns of the changes, for instance, are the changes increasing or decreasing? Are the changes gradual or abrupt? In which year and months do these changes occur? What correlations exist between the variables?

    (ii) What changes have occurred in the land cover overtime? If the changes have occurred, what are the potential impacts on inundation extent regimes in the wetland?

1.5 Significance of the study

It has been noted that habitat based information is fundamental in the application of wetland climate change adaptation strategies (Erwin, 2009). This assertion by Erwin (2009) is in tandem with the view by Agrawal (2008) that climate adaptation is inevitably local and that adaptation strategies must be tailored around locally-generated information. The impacts of climate change on the hydrology of the Zambezi River Basin, in which the Barotse Wetland is located, have been adequately highlighted by Beilfuss (2012) and have been particularly noted in GRZ (2013) and IFRCS (2008) with flood and drought events as some of the major impacts. Further, Fanshawe (2010) indicated that there is increasing pressure on land covers such as forests due to a rising

population. A rise in developmental activities and population quintessentially results in clearing of forests for settlements, agriculture and other livelihood streams. Coupled with climate factors, changes in land cover and land use are likely, in the long term, to have a negative impact on the flood regimes, the role of the wetland in flow-regime regulation and consequently biodiversity in the Barotse Wetland. Flood extent patterns and the role of the wetland in flow-regime regulation, is very important. Turpie *et al.* (1999) pointed out crucial future climate challenges in the Barotse Wetland which included resource over-exploitation, flood control to protect house and technical infrastructure, land drainage, encroachment for agriculture, and interference with river hydrology for large-scale hydropower and irrigation schemes. Such challenges require a foresighted wetland management plan which requires habitat based data. The need to assess the trends in inundation extent and the potential drivers is key in the provision of baseline data for the implementation of climate adaptation strategies for the Barotse Wetland. Further, in light of the construction of the Mongu-Kalabo Road across the wetland, there is need for constant generation of inundation extent data so as to progressively monitor the impact of the infrastructure on the wetland's inundation extent regimes. It is impractical to employ ground-based methods in the assessment of temporal and spatial trends in inundation extent as the wetland is vast and changes in inundation extent would not be effectively captured. The satellite based technique therefore, is not only affordable but provides for instant detection in time of the wetland and archives of data exists for comparison across temporal space which is critical in change or trend assessment studies (Ticehurst *et al.* 2013; Ticehurst *et al.* 2014).

The results of this study could prove useful to many stakeholders involved in natural resources management both at local government and community level. Institutions such as the Ministry of Energy and Water Development, Ministry of Lands, Natural Resources and Environmental Protection, Ministry of Agriculture and Ministry of Livestock and Fisheries Development as well as the Disaster Management and Mitigation Unit under the office of the Vice President in Zambia might find this information useful. These institutions are key planners in the utilization of the Barotse Wetland and the implementation of key climate adaptation strategies. The inspiration of this study was anchored on the fact that flooding regimes play a critical role in determining the ecological health of the wetland which is a source of livelihood for many households and further effects downstream flow regimes.

1.6 Description of the study area

1.6.1 Location of the study area in the larger Zambezi River Basin

The Barotse Wetland is situated in the Barotse Sub-basin within the larger Zambezi River Basin (Figure 1) and is geographically located between 13-17^{o} South and 22-24^{o} East of western Zambia in Southern Africa. The wetland is defined as the area extending from Lukulu to downstream of Senanga (Figures 1 and 2).

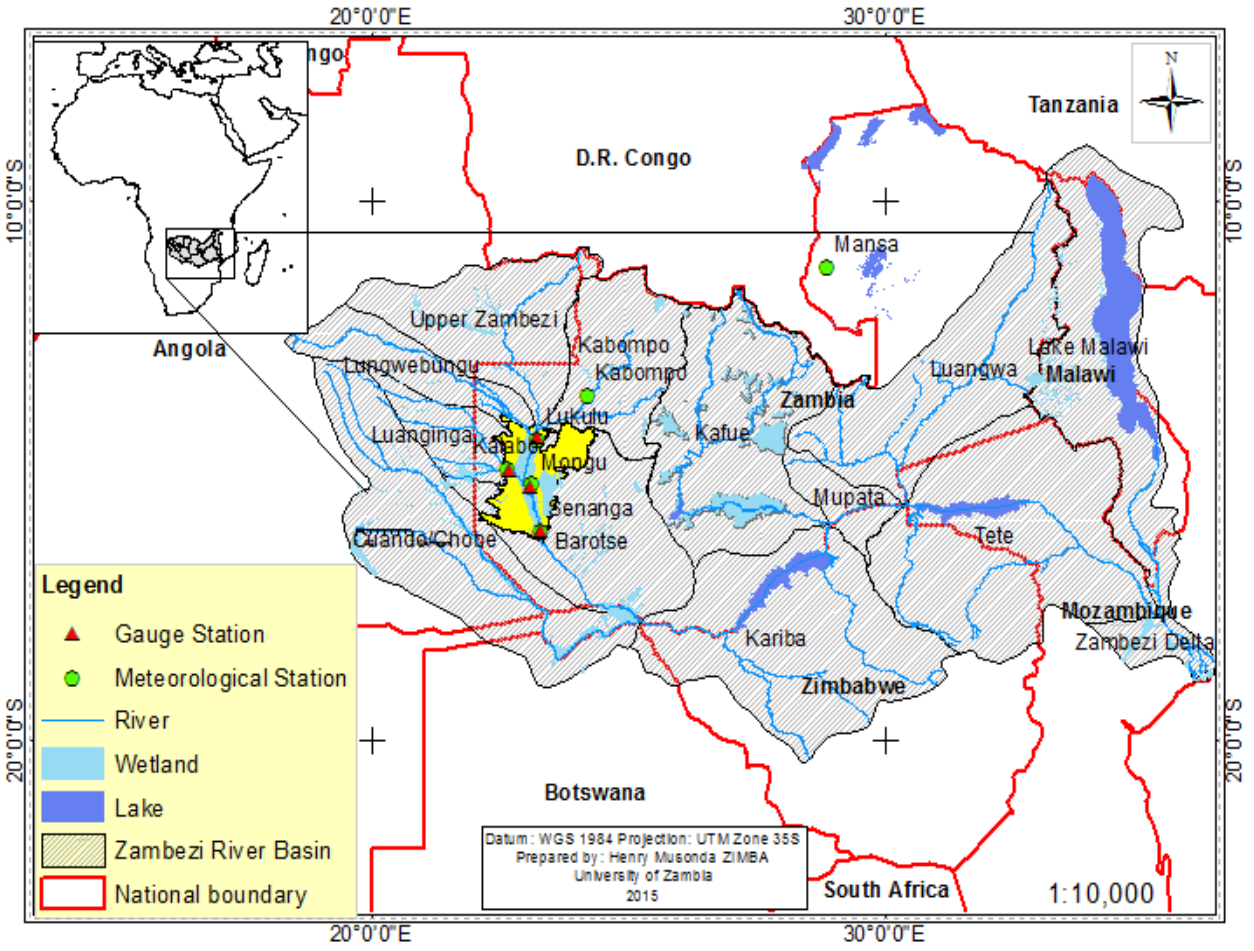

Figure 1: Location of the study area in the larger Zambezi River Basin in Western Zambia, Southern Africa.

Flooding in the Barotse Wetland is a consequence of the breaking of the banks of the Zambezi River during periods of high water flows in the rainy season between October and May of a hydrological year. The actual size of the wetland is unknown but is estimated to be at 1.2 million hectares (IUCN, 2003).

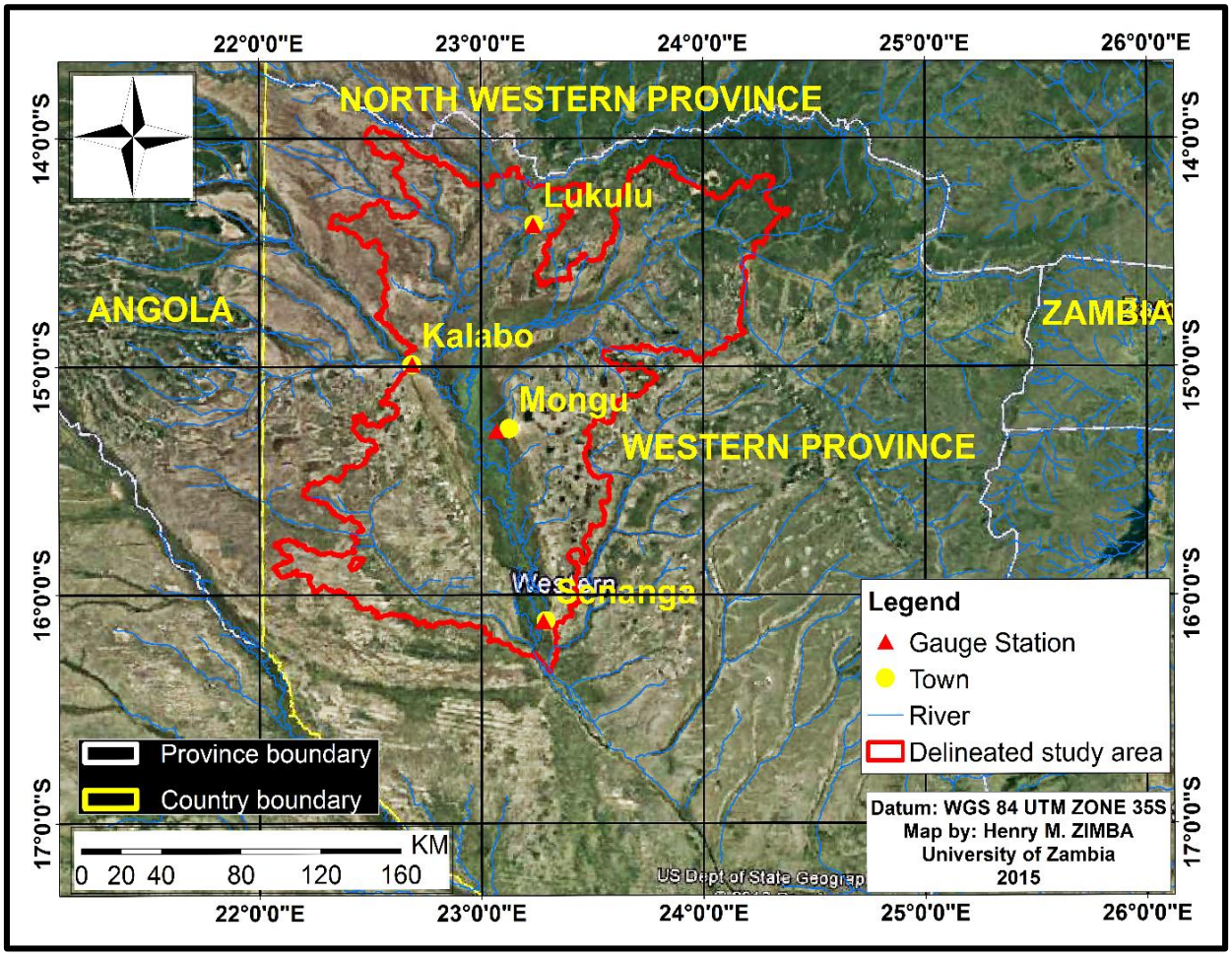

Figure 2: Google Earth image showing the location of the Barotse Wetland in Western Zambia.

The wetland is a sanctuary to variety of biodiversity both flora and fauna some of which are confined to the wetland. The flood provides aquatic habitats for fish such as tiger fish and bream, crocodiles, hippopotamus, water birds, fish-eating birds, lechwe and the wading antelope. After the flood, the plain is a habitat for grazing animals such as wildebeest, zebra, tsessebe and small antelope such as oribi and steenbok, and their predators (Timberlake, 1997; IUCN, 2003).

1.6.2 Topography and Drainage

The land elevation over the study area ranges from 1192 metres above sea level in the north eastern part to about 900 metres above sea level in the southern part (Figure 3). The lower areas form part of the floodplain. The drainage pattern is trellis with all major rivers/streams, which include the Luanginga and Kabompo, being tributaries of the Zambezi River. The Zambezi River and its tributaries account for the flooding in the Barotse Wetland (Timberlake, 1998; IUCN, 2003).

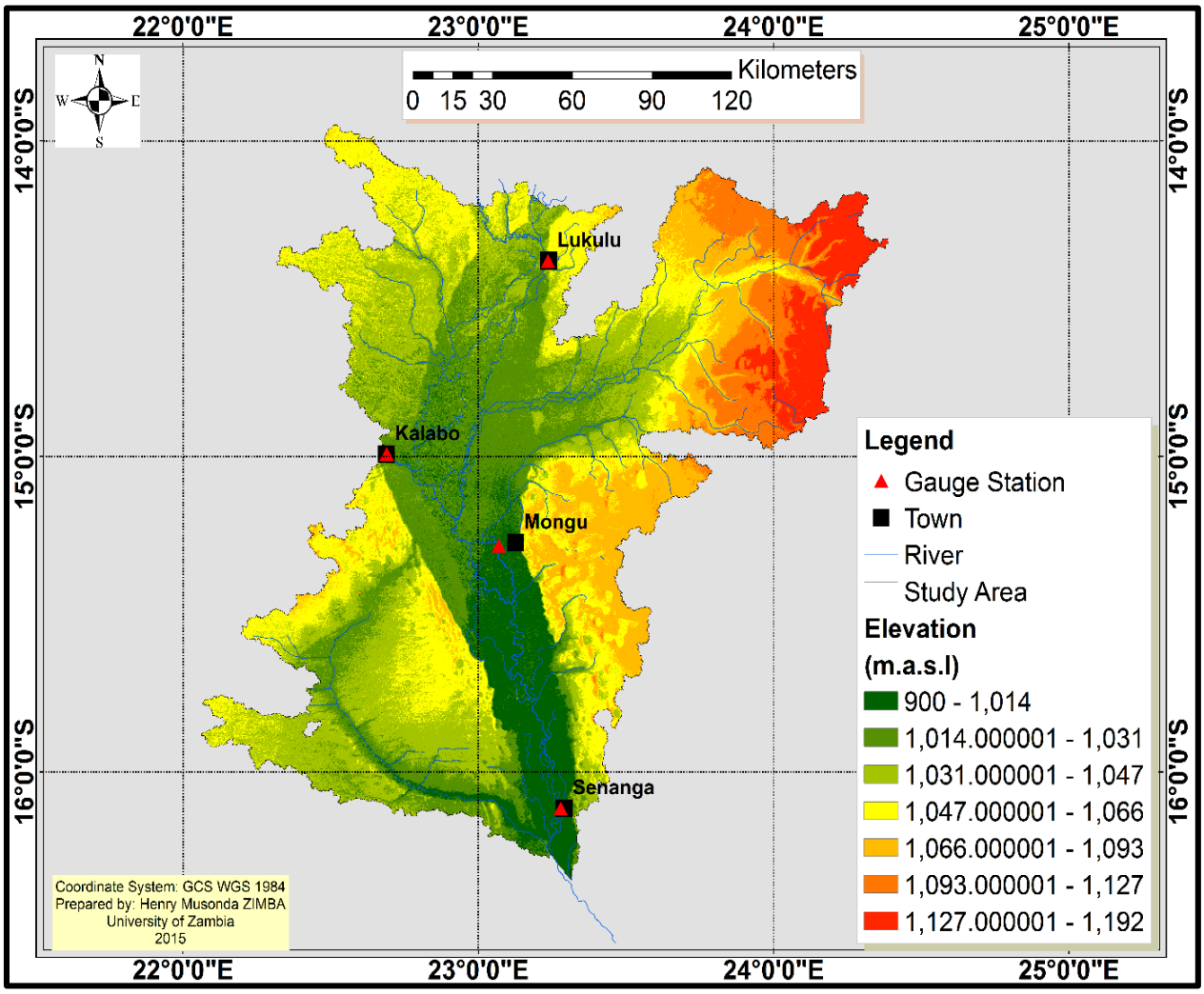

Figure 3: Elevation (m) of the study area as derived from the ASTER 30 m resolution digital elevation model (DEM), Western Zambia.

1.6.3 Soils

The Kalahari sands are underlain by rocks of the Karoo Supergroup. The sands are a Pleistocene deposit, the erosion product of the weak Upper Karoo sandstones. They vary in colour from pallid to orange, are moderately acidic and contain 3 to 12 percent silt plus clay. The sands are not very fertile; the nitrogen content is particularly low where the humus has been disturbed by cultivation. There is no erosion problem as the area is so flat, but heavy population pressure in some areas has resulted in land degradation (Fanshawe, 2010).

1.6.4 Vegetation and land use

The Barotse Sub-basin is predominantly grassland with breaks of semi-evergreen forest, evergreen forest, deciduous forest and shrub land. Other land cover types include mosaic cropland, water bodies and regularly flooded vegetation which covers the Barotse Wetland (Figure 4). The evergreen and semi-evergreen forest is composed of swamp and riparian woodlands while the deciduous forest is of Kalahari and Munga Woodland. The major land uses are cropland and timber production (Fanshawe, 2010; Mukosha, 2014). There are a variety of underground trees or suffrutices some of which are confined to the wetland. They have a dwarf habit with the main woody stem underground. The underground growth nature is attributed to adaptation to the high water table and anaerobic conditions on seasonally-flooded plains. The above ground shoots are often destroyed by fire or frost. The trees spread by means of rhizomes (Timberlake, 2000).

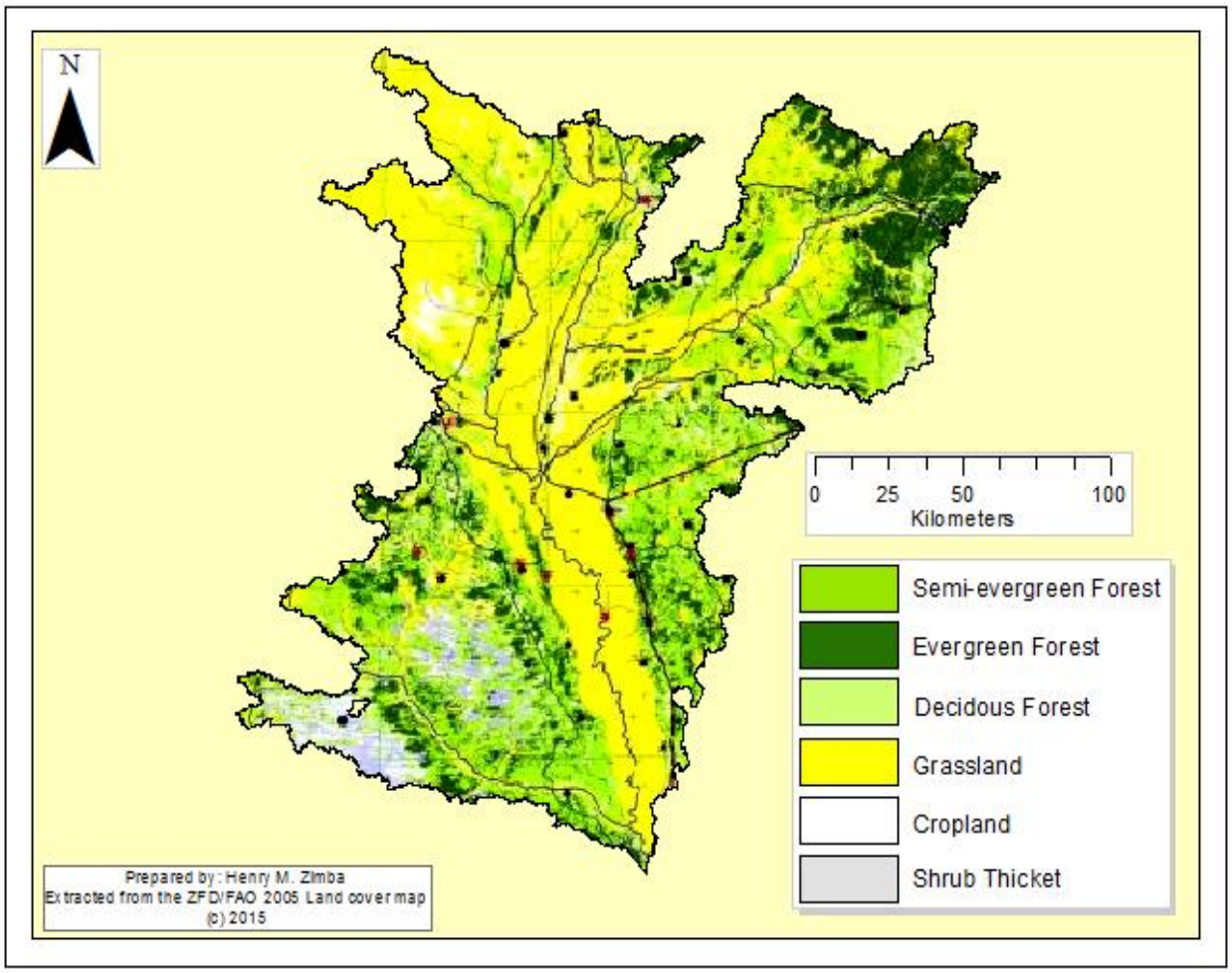

Figure 4: Land cover and use map of the study area in Western Zambia extracted from the ZFD/FAO 2005 ILUA I land cover and use map.

1.6.5 Precipitation, temperature and humidity

Monthly precipitation for Kabompo illustrates the rainfall pattern for the upper catchment of the wetland (Figure 5a). Much of the discharge into the Barotse Wetland is from upstream in Angola and North Western Zambia, which receives an average of above 1000 mm of rainfall as illustrated by the Kabompo annual rainfall time series (Figure 5 b). Rainfall over the study area is a result of the movements of the Inter-Tropical Convergence Zone (ITCZ) over Zambia between October and April of a hydrological year (IUCN, 2003; Fanshawe, 2010). High temperatures are experienced between October and April with maximum temperature of around 34 degrees Celsius and minimum temperature of about 12 degrees Celsius (Figure 5 c). The highest relative humidity is about 70 percent in the months November to March (Figure 5 c)**.**

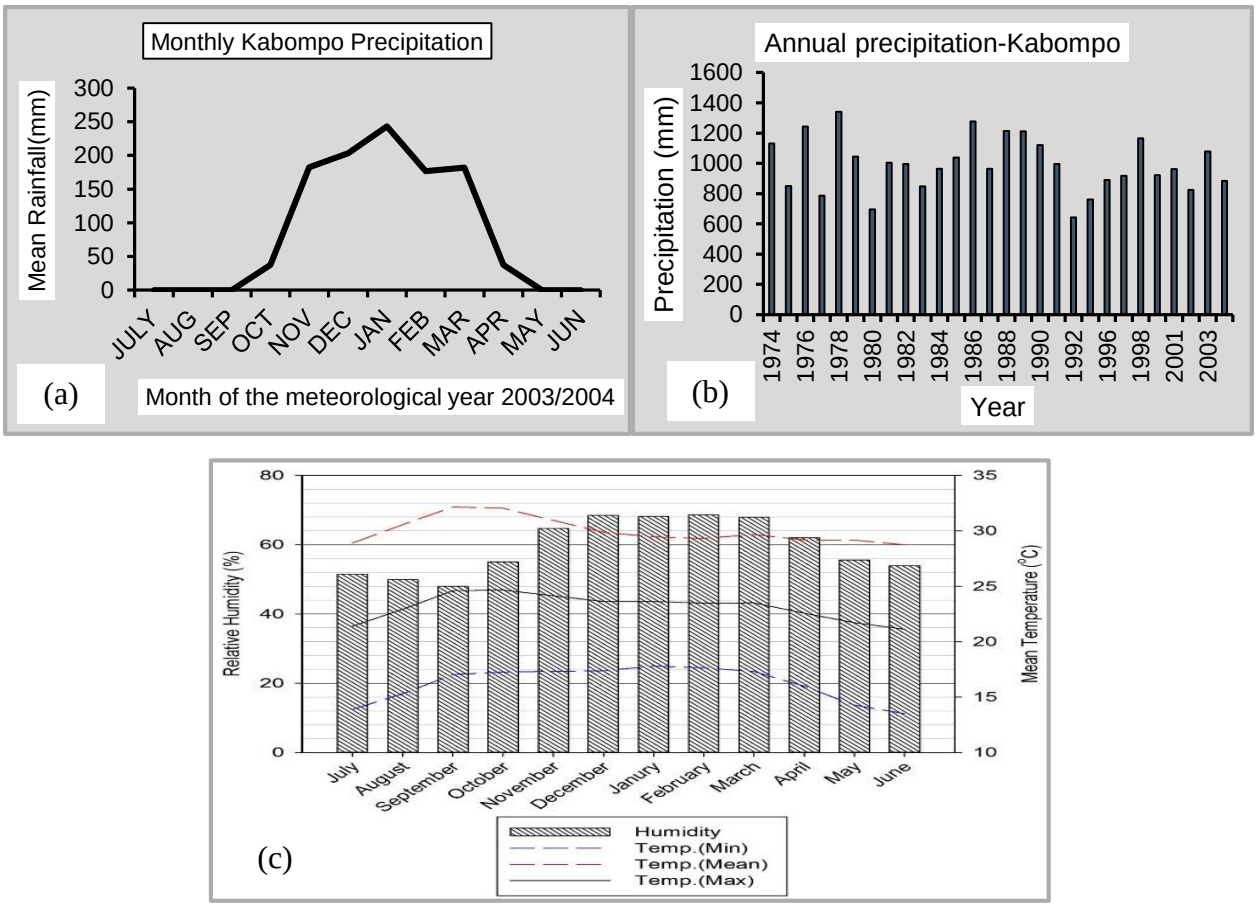

Figure 6: (a) Monthly (October-April, 2003/2004) precipitation for Kabompo Station (b) Annual mean precipitation for Kabompo Station from 1974 to 2004, (upstream of the wetland), (c) 2003/2004 annual temperature and humidity at Mongu Station in the study area, Western Zambia. (Source: ZMD, Mongu, Western Province, Zambia). (Refer to Figure 1 for location of meteorological stations).

1.6.6 Population and social- economic attributes in the study area

The Barotse Wetland hosts about 250,000 people with settlements concentrated along the levee of the Zambezi River and at the edge of the floodplain. The Zambezi River forms a critical life line in the wetland for both humans and wildlife. The population is largely involved in crop, livestock and fisheries activities. The wetland is cited as the most agriculturally productive area in western Zambia. Flooding plays a crucial role in agriculture as the flood waters bring into the plains sediments that are rich in nutrients essential for crop production when the flood recedes. Crops grown include maize, cassava, rice, sweet potatoes and sugar cane. The population of cattle in the wetland is as much as the human population estimated at over 250,000 with the grassland in the wetlands providing grazing pasture for cattle. Fish consumption is five times higher than the national average. At the peak of the flood, fish traps and spears are used for fishing while gill nets and spears are used in the lagoons left behind by the falling flood. The wetland is also home to a rich cultural ceremony known as the Kuomboka which entails annual migration with the coming of the flood to the upland. It is an annual event whose hosting is dependent on the flood water levels (Timberlake, 2000; IUCN, 2003; CSO, 2010).

CHAPTER TWO: LITERATURE REVIEW

Globally and in Zambia some studies have been done on wetland inundation mapping and trends assessment. From the review, it was observed that there was scanty information on wetland inundation dynamics in Zambia and the Barotse Wetland in particular. This chapter highlights the reviewed literature on climate change trends and the impact on wetlands. Furthermore, the interlinkages between wetlands and other ecosystems such as forests were reviewed. Earth Observation-based methods to map wetland inundation and how to analyse trends in hydrological and climatological variables such as discharge were also reviewed. Thus, through the review, gaps in knowledge were noted and thereafter this study was formulated to contribute to the narrowing of the gaps in inundation extent dynamics in the Barotse Wetland.

2.1.1 Regional Studies on Climate Change Trends

According to New *et al.* (2005) there had been little work on precipitation or temperature related extremes in Africa. They attributed this to a lack of easily available data for the various regions of Africa. However, reviewed literature such as Frich *et al.* (2002), Christensen *et al*. (2007) including New *et al.* (2005), indicated that there has been more variability in precipitation than change in the pattern of rainfall. Historical evidence through the use of multi-model data indicated that in the late 20th Century, Southern Africa experienced a 20 percent increase in the frequency of extreme dry austral winters and springs while the frequency of extremely wet austral summers doubled (Christensen *et al.* 2007). Further, Christensen *et al.* (2007) projected that rainfall in the Southern African region was likely to decrease in much of the winter rainfall region and on western margins as well as a delay in the onset of the rains. The picture on the large-scale is one of drying in much of the tropics and/or little change in precipitation in the tropics, increasing the rainfall gradients. "This is a plausible hydrological response to a warmer atmosphere, a consequence of the increase in water vapour and the resulting increase in vapour transport in the atmosphere from regions of moisture divergence to regions of moisture convergence" (Christensen *et al.* 2007).

New *et al.* (2005) indicated that "there are few consistent and statistically significant trends in precipitation indices. Regionally-averaged dry spell length, average rainfall intensity and annual 1-day maximum rainfall all show statistically significant increasing trends, and a general pattern

of increasing trends across the region, but few trends at individual stations are statistically significant". Additionally, the study revealed that "there is an indication of decreasing total precipitation, accompanied by increased average rainfall intensity; the fact that extreme precipitation indices (R95p, R99p, RX1day and RX5day) have on average increased while total precipitation and less-extreme precipitation (R10 mm and R20 mm) have decreased suggests that increased average intensity is concentrated on extreme precipitation days. This indicates that time-averaged measures of rainfall may fail to capture these changes as increases in intensity may compensate for decreases in frequency" (New *et al.* 2005).

The Frich *et al.* (2005) global analysis which included precipitation data from Southern Africa region capturing countries such as South Africa, Zimbabwe, Mozambique and Zambia indicated that there had been more variable patterns over the region revealing an increase in maximum five-day rainfall during the second half of the twentieth century. The general rainfall trend for the Southern African region shows an increasing trend in dry spells with decreasing total precipitation and less extreme precipitation.

2.1.2 Climate Change Trends studies on Zambia

Several studies have been done on Zambia's climate scenarios. Thurlow *et al.* (2009), Yamba *et al.* (2009), Jain (2007) as well as the UNDP country climate profile for Zambia gives an overview of the country's' climate scenario. The results of these studies with regard to precipitation are highlighted below. Both the historical trends as well as projected future trends are presented. The focus of the review was on rainfall as it is the major contributor to hydrological scenarios. Thurlow *et al.* (2009) who considered the period 1976-2007 in the three Agro-Ecological Regions(AER) of Zambia (Figure 6), revealed interesting and valuable aspects of the country's rainfall patterns. The study looked at all three Agro-Ecological Regions I, II and III (AER II is subdivided into IIa and IIb).

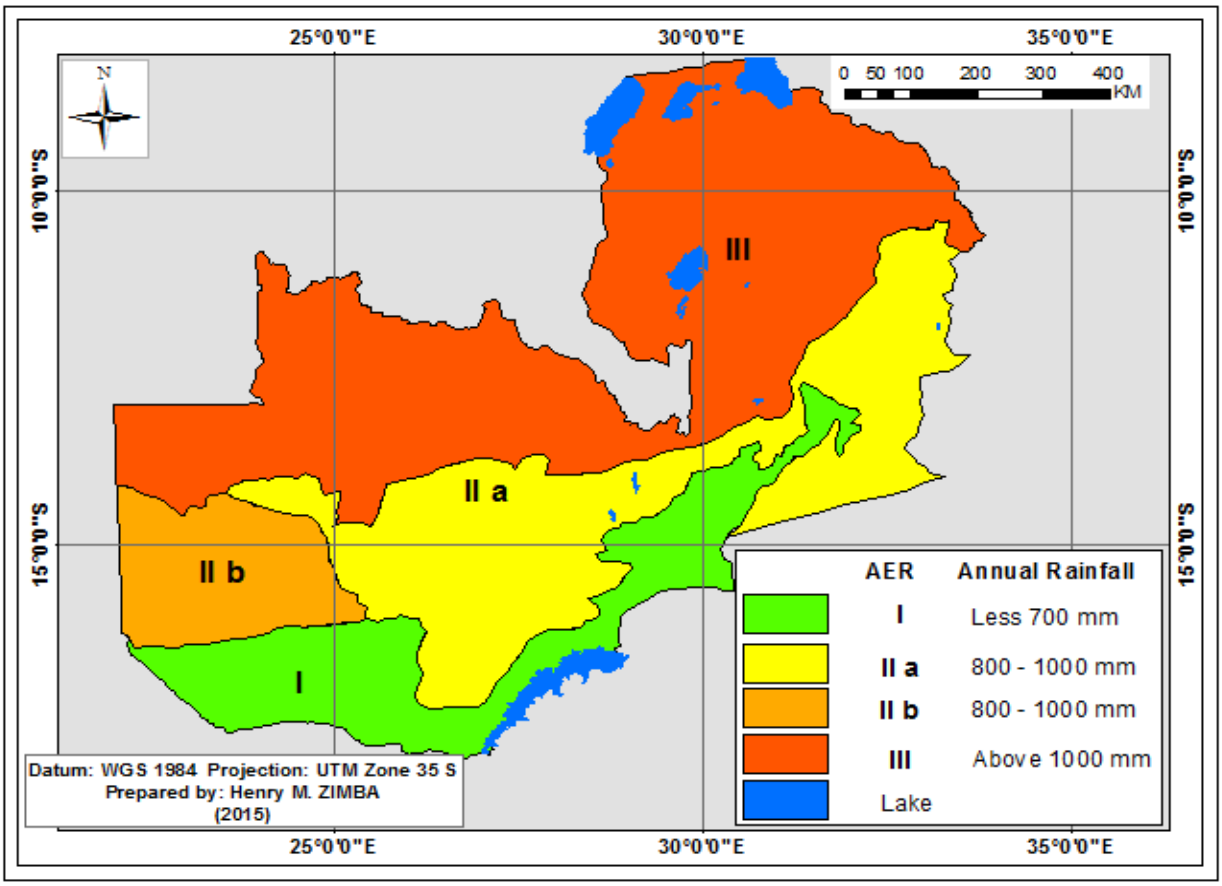

Figure 6: Agro-ecological Regions of Zambia (Ministry of Agriculture and Cooperatives, 2005 map).

Their study revealed that year to year, variations in rainfall patterns were generally higher in regions (from the south) with low rainfall and low in wetter regions towards the north. Annual precipitation coefficients differed over the agro-ecological regions with regions I and II having the highest inter-annual rainfall variability with coefficients of 0.18 and 0.20 respectively (Thurlow *et al.* 2009). Agro-ecological region III showed more stability in rainfall with a precipitation coefficient of 0.09 (Thurlow *et al.* 2009). The study established that rainfall deviations in regions I and II frequently exceeded 20 percent of the mean and approached 30 percent deficits in major drought years. These variations have negative impact on agriculture productivity (Thurlow *et al.* 2009). The situation is different for region III which showed only moderate inter-year rainfall variation, with rainfall in most years lying within 10 percent of the mean and rarely failing below 1100 mm (Thurlow *et al.* 2009). The report indicated that agro-ecological regions I and II were predominantly disposed to both floods and droughts whereas region III showed fairly stable

weather conditions with no severe drought over the last three decades (Thurlow *et al.* 2009). The report concluded that "Zambia is prone to droughts and floods" and that there was "a high chance that at least one agro-ecological region will experience an abnormal weather event in any given year" (Thurlow *et al.* 2009). Jain (2007) established that rainfall variability across the Agro-Ecological Regions of Zambia was not uniform. The report indicated that from the 1990/1991 to 2003/2004 rainfall seasons each one of the AER's had experienced at least 10 years of below normal rainfall (Jain, 2007). Further, Jain (2007) revealed that from the year 1970 to 2000 the southern region (Agro-Ecological Region I) experienced more severe dry seasons than the other regions (AER II and III). Jain (2007) clearly agreed with Thurlow *et al.* (2009) in asserting that in any given year normal rainfall is not guaranteed in any of the Agro-Ecological Regions of Zambia though AER III is more stable than the other regions.

The study done by Yamba *et al*. (2009) was site specific focusing on three districts of Zambia each representing an agro-ecological region. The study covered a historical time period from 1961 - 2007 and a future time period from 2010 -2070. Yamba *et al.* (2009) findings were in many ways similar to those of Thurlow *et al.* (2009) revealing that precipitation variability differed across the country depending on the agro-ecological region. Yamba *et al.* (2009) indicated that Mwansabombwe in AER III had a variability index of 15.63 percent with Kapiri Mposhi in AER II having an index of 23.71 percent while that of Sesheke in AER I was found to be 32.80 percent. These findings clearly agreed with Thurlow *et al.* (2009) in noting that variability in precipitation increased as one moved from the north to the south of the country. High variability, such as reported for regions I and II, is a crucial factor in wetland inundation extent, crop yield and livestock productivity. The report further gave a historical trend which showed that regions I and II had been more prone to climate extremes such as drought and floods while region III had been normally stable. Future projections of rainfall seem to align with the historical trends for all three regions (Yamba *et al.* 2009). According to the UNDP climate country profile for Zambia (http://www.undp.org), there were strong indications that mean annual rainfall do not show large changes. This implies that the future rainfall scenario for Zambia is likely to oscillate within the historical trends as revealed by Thurlow *et al.* (2009), Jain (2007) and Yamba *et al.* (2009) as well as within the Yamba *et al.* (2009) future projections. The UNDP Zambia climate profile further projected that September, October and November (SON) rainfall will decrease while December,

January, February (DJF) and March, April and May (MAM) rainfall will increase. Projections were that maximum 1- and -5 day rainfalls may increase in magnitude in DJF and MAM.

From reviewed literature on rainfall trends for the Agro-Ecological Regions of Zambia, the probability that these trends will continue for a foreseeable future is certainly high. Variations in rainfall patterns will continue across all regions of Zambia. The variations in rainfall have a bearing on the wetland inundation extent patterns and effects on wetland biodiversity as has been cited by Erwin (2009). The Barotse Wetland is in the Agro-Ecological Zone IIa. EAR IIa is characterised by a historic and projected potential for a high precipitation variability index and occurrence of both extreme wet and dry events. However, AER III where much of the discharge emanates has been noted to be stable (Thurlow *et al.* 2009) though projections for Southern Africa show a downward trend in precipitation (Christensen *et al.* 2007).

2.1.3 Impact of climate change on wetlands

Six percent of the earths land surface is covered by wetlands and contains 12 percent of the global carbon, hence playing a critical role in global carbon cycle (IPCC, 1996; Sahagian and Melack 1998; Ferrati *et al*. 2005). How climate change will affect wetland dynamics is one of the biggest unknowns of the near future as it relates to element dynamics and matter fluxes (IPCC 2001; Paul *et al.* 2006). However, evidence of climate change impact on wetlands has now been noted in numerous studies. For instance, a study by Kim *et al*. (2012) on the impact of climate change on wetland revealed that climate change had altered the inundation depth of the wetland. The Ramsar's Scientific Technical Review Paper (SRTP) (2008) and Gitay *et al.* (2011) pointed out examples of what will result from the projected changes in extreme climate scenarios which include: changes in base flows, alterations in the hydrology (depth and hydro period); an increase in soil erosion; an increase in flood runoff which will result in a decrease in recharge of some floodplain aquifers and a decrease in water resource quantity and quality. According to the UNESCO (2009), managing water in the past had been about managing naturally occurring variability. But the advent of climate change threatens to bring about dramatic occurrences manifesting in greater variability, a shift and increase in intensity in the occurrences of extreme events, and the introduction of greater uncertainty in the quantity and quality of supply over the long term. Climate change will lead to a decline in precipitation, surface runoff and groundwater recharge and a rise in evaporation and transpiration. Climate change can directly affect the

hydrologic cycle and, through it, the quantity and quality of water resources (UNESCO, 2009). However, Erwin (2009) indicated that the impact of climate change on the hydrology of individual wetland ecosystems which is mostly through changes in precipitation and temperature regimes will greatly vary across the globe. From "the perspective of assessment of climate variability and the effect on wetlands, these ecosystems need to be viewed in the broader context of their spatial location in a watershed within a specific region" (Erwin, 2009). Variations in stream flow (discharge) regimes have been claimed to be "the most serious and continuing threat to ecological sustainability of rivers and their associated wetlands" (Naiman *et al.* 1995; Sparks, 1995). Adducing from the four principles about the influence of flow regimes on aquatic biodiversity Bunn and Arthington (2002) highlighted: (i) flow is a major determinant of physical habitats in streams; (ii) aquatic species have evolved life history strategies primarily in direct response to their natural flow regimes; (iii) maintenance of natural patterns of longitudinal and lateral connectivity is essential to the viability of populations of many riverine species and the invasion and; (iv) success of exotic and introduced species in rivers is facilitated by the alteration of flow regimes. According to Koster and Suarez (1999) and Zhao *et al.* (2011), spatial rainfall variability is the main source of variability in discharge.

2.1.4 Changes in forest cover and its impact on wetlands

Given the critical role of wetlands to biodiversity and human livelihoods, it is necessary to consider how various ecosystems are linked to wetlands (Blumenfeld *et al.* 2009). One critical example is the link between forests and wetlands. In most cases these interdependent ecosystems are viewed as total independent entities instead of an interrelated unit with a critical role in the hydrological cycle and preservation of water resources. Understanding the linkage between forest cover and wetlands will provide critical information for formulation of policies and management practices to protect water resources (Blumenfeld *et al.* 2009). Deforestation has been cited as one of the major contributors to wetland degradation mainly through increased catchment erosion and nutrient loading (Blumenfeld *et al*. 2009; Fanshawe, 2010). However, some studies like Woodward *et al.* (2014) pointed to contrary effect of deforestation on wetlands in which they showed that wetland extent and water level had increased over time as a consequence of deforestation in the catchment.

2.1.5 Studies on the role of wetlands in flow attenuation in the Zambezi River Basin

Wetlands are known to regulate flow (Millenium Ecosystem Assessment, 2005). Bullock and Acreman (2003) argue that many studies draw conclusions on the categorisation of wetlands in terms of reducing or increasing river flows which in many cases are taken out of context and do not answer the basis for the conclusions. They argue that categorization of wetlands must be based on comparative scenarios. They give a set of comparative scenarios used internationally for categorization of wetlands among which is the comparison of inflows and outflows of a wetland system as a baseline for inference. In the Barotse Wetland two notable studies , Beilfuss and Santos (2001) and McCartney *et al.* (2013) attempted to assess the role of the wetland in flow attenuation. Beilfuss and Santos (2001) compared the before and after catchment volumes to arrive at their conclusion that the wetland attenuated flow. McCartney *et al.* (2013) used hydrological models to quantify the voulumes that were attenuated by the wetland. However, they indicated that their method had many limitations and that the results were inconclusive. At regional level, Murwira *et al* .nd compared rates of change in upstream and downstream time series with a paired t-test to evaluate the role of the Okavango wetlands in flow attenuates. Using this method they concluded that the Okavango wetlands attenuated flow.

2.1.6 Studies on change detection and trends analysis in the Zambezi River Basin

Some studies such as Beilfuss (2012) and Kampata *et al*. 2008 analysed trends in hydrological and meteorological variables in the Zambezi Basin. Beilfuss (2012) observed a significant abrupt change in the annual means of discharge in the entire Zambezi River Basin in 1980. Kampata *et al.* (2008) analysed trends in rainfall in the headstreams of the Zambezi River Basin in Zambia. They used the Mann-Kendall trends test to analyse trend in rainfall between 1945 and 2005. They concluded that the trend was insignificant but that the rainfall was generally decreasing.

2.1.7 Studies on Land cover change assessment in Zambia

A major land cover assessment project by the Zambia Forest Department (ZDF) and the Food and Agriculture Organization (FAO) was carried out to ascertain land cover changes for Zambia for the period 1990 to 2005. The Integrated Land Use Assessment programme used Landsat TM imagery with a supervised classification method. The overall picture for the country was that of downward trend in forest cover with an estimated annual loss 0.62 during the period. Western and

North Western provinces (which is part of the Barotse wetland catchment) in the same period had forest annual rate of loss of 0.07 and 1.04 respectively. A total of 816,020 hectares of forest cover was lost in the 1990 to 2005 period for Western and North Western Provinces (Mukosha, 2014).

2.1.8 Satellite imagery data based methods for detecting inundated area

The argument for satellite remote sensing is that it provides a platform for collection of data in a timely, cheap and efficient manner than the conventional in-situ based mechanisms. Further, satellite data are readily and uniquely suitable for automated processing in computers (Okoye and Koeln, 2003; Ticehurst *et al.* 2014). In a lower income country like Zambia where resources for conducting in-situ data collection are scarce, availability of satellite data provides an affordable and reliable platform for data acquisition for natural resource management and monitoring. Various satellite-based remote sensing pragmatic algorithms and techniques have been developed to detect inundation extent on the earth's surface from both optical and radar satellite imagery.

Several satellite data from sensors such as Landsat, MODIS, MERIS, ENVISAT, RADARSAT, ASTER, SPOT and many more are available on various platforms and can be used to detect inundation extent (Townsend, 2002; Xu, 2006; Kudahetty, 2012; Meier, 2012; Long *et al.* 2014; Zhai *et al.* 2015). For instance, Kudahetty (2012) mapped flood extent with SAR data in ENVI using the Parallelepiped, Minimum Distance, Maximum Likelihood and Mahalonobis Distance algorithms to map flooding scenarios in Kelani Ganga and Bolgodo basins in Siri-Lanka. Townsend (2002) used Radarsat SAR to map seasonal flooding in a forested wetland using the arbitrary recursive classifier (classification tree). Long *et al.* (2014) mapped flood extent in the Chobe Floodplain in Namibia using Synthetic Aperture Radarsat (SAR) using band math and image thresholding and segmentation method. The method included the use of image subtraction, decision-based classification with threshold values, and segmentation of SAR images. The study looked only at flood peak period (Jan-Mar) and considered only a period of 6 years. There was no attempt to relate the flood patterns to any hydrological or land cover and use variables. For optical data the Modified Normalized Difference Index (MNDWI) developed by Xu (2006) is mostly used in mapping open water features. For instance (Meier, 2012) mapped inundation in the Kafue floodplains using the MNDWI on MODIS data. Supervised classification methods are also used as evidenced by Cai *et al.* (2015) who used the supervised classification with the Maximum Likelihood algorithm, with Landsat data, to map flood extent in the Barotse Wetland from 1984 to

2014. Surface water extraction methods based on satellite data can be classified into four types: thematic classification, linear spectral immixing, single-band threshold, and two-band spectral indices (Zhai *et al.* 2015). When it comes to satellite imagery data mostly used for flood extent mapping the MODIS data presents a better option for large wetland inundation mapping (Ticehurst *et al.* 2013; Ticehurst *et al.* 2014). Despite the inherent limitation of cloud cover MODIS is advantageous because all historical data from 2000 to the present are readily available for free, its near-global spatial (250m – 1km) and a better temporal scale (1-2 times/day) and can easily be processed with most available satellite imagery data processing software such as ArcGIS, ENVI, QGIS and many more (Ticehurst *et al.* 2013; Ticehurst *et al.* 2014).

As for the mapping of open water features with optical satellite imagery what was noted from literature is that the use of indices is the most common practice. There are various spectral based water features extraction indices which have been developed and include the Normalised Difference Vegetation Index (NDVI) (Rouse *et al.* 1973), Normalised Difference Water Index (NDWI) (McFeeters, 1996), Modified Normalised Difference Water Index (MNDWI) (Xu, 2006), Automated Water Extraction Index (AWEI) (Feyisa *et al.* 2014), and the Desert Flood Index (DFI) developed by Wang *et al*. (2013). The NDWI developed by McFeeter (1996) and the MNDWI by Xu *et al.* (2006) are the most utilized water feature extraction indices in the extraction of water features from satellite imagery (Wang *et al.* 2013). However, Wang *et al.* (2013) discovered that under all the experimental conditions they subjected the DFI and MNDWI, the DFI performed better. The performance assessment of the two indices was carried out on MODIS and Landsat images in a flooding season of the Indus River in Pakistan. The DFI focuses on more precision in the calculation of water proportion at sub pixel level and the increasing of the contrast between water and non-water features. The other multi-band based indices such as the NDWI and the MNDWI are focused on differentiating the water body information from the non-water-body information by using pixel scales instead of the proportion of the water area, which critically affects precision in water information extraction (Wang, 2007; Wang *et al.* 2013).

2.1.9 Satellite remote sensing based wetland mapping in Zambia

Wetland flooding in Zambia occurs in the rain season between November and May of each hydrological year (IUCN, 2003; Meire, 2012). Wetland inundation in Zambia, like world over, has significant biodiversity, economic and cultural implications (IUCN, 2003; Baidu-Forson *et al.*

2014). Very few remote sensing based studies on wetland inundation extent have been done in Zambia. Notable among the few are the Tiger Initiative (2008), Aduah and Mantey (2012), Meire (2012) and the Cai *et al.* (2015). Tiger Initiative (2008), Aduah and Mantey (2012), Meire (2012) studies were conducted in the Kafue wetlands in the Kafue River sub-basin while the Cai *et al.* (2015) study was conduceted in the Barotse wetland in the Barotse sub-basin. Tiger Initiative (2008) used ASAR AP, MODIS and LANDSAT data and employed various supervised and unsurpevised image classification methods to map the inundation extent. The study also assessed vegetation cover with Landsat and ASTER data. Aduah and Mantey (2012) used Landsat data employing the supervised classification with the maximum likelihood algorith to map inundation. The study also performed regression analysis to establish the relation between rainfall and inundation extent. The study by Meir (2012) used satellite imagery to detect and quantity inundation extent in the Kafue flats using MODIS (MOD09) and and radar (ENVISAT ASAR) imagery. The study used the NDWI to map inundated area with MODIS data while the stepwise classfication approach was with ENVISAT ASAR data. The generated inundated area data derived from MODIS and ENVISAT ASAR were used as input in the Real-time hydrologic and flood model for the Kafue Wetland. Cai *et al.* (2015) used Landsat 5 TM to generate time series for flood extent in the Barotse Wetland which was compared to the perceptions that the locals had on the pattern of flooding in the wetland. Cai *et al*. (2015) used Landsat data with the Maximum Likelihood supervised classification algorithm to generate the flood extent time series data for the Barotse Wetland from 1984 to 2014. They discovered that inundation extent varied from year to year and that the frequency was reducing but the magnitude of the floods was on the rise.

2.2.1 Band characteristics of MODIS and Landsat data

The MODIS was launched by NASA in 1999 and 2002 on board the Terra (EOS AM) and the Aqua (EOS PM) satellites respectively. The MODIS is designed for acquisition of large scale global dynamics measurements. The MODIS MOD09A1 data provides surface reflectance Bands 1 to 7 (Table 1) at 500-meter resolution in an 8-day gridded level-3 product in the sinusoidal projection. Each pixel in the Level-3 product MOD09A1 contain the best possible L2G observation during an 8-day period. It has high-observation coverage, low-view angle, absence of clouds or cloud shadow, and aerosol loading (Vermote *et al.* 2011) and has been espoused as suitable for mapping floodplain inundation (Ticehurst *et al.* 2013).

Table 1: Band characteristics of MODIS data

Band	Wavelength	Spectral Range (nm)	Resolution (m)
1	Visible(Red)	620-670	500
2	Visible(NIR)	841-876	500
3	Visible(Blue)	459-479	500
4	Visible(Green)	545-565	500
5	Visible	1230-1250	500
6	Visible(SWIR)	1628-1652	500
7	Panchromatic	2105-2155	500

Landsat 5 TM was launched by NASA in 1984 and continued to acquire imagery in 7 spectral bands (Table 2) until November 2011 while Landsat 8 OLI-TIRS was launched in 2013 and acquires imagery in 11 spectral bands (Table 3). The Landsat satellites were intended to be of use to a diversity of fields like forestry, agriculture, geology, and land-use planning. The selection of spectral bands for the Landsat satellites was biased toward discriminating different types and amounts of vegetation (Chander and Markham, 2003; USGS, 2015).

Table 2: Band characteristics of Landsat 5TM data

Landsat 5 TM			
Band	Ground Resolution (m)	Sensitivity Spectrum (μm)	Nominal Spectral Location
1	30	0.45 - 0.52	Blue
2	30	0.52 - 0.60	Green
3	30	0.63 - 0.69	Red
4	30	0.76 - 0.90	Near IR
5	30	1.55 - 1.75	SWIR-1
6	120	10.40 - 12.50	Thermal IR-1
7	30	2.08 - 2.35	SWIR-2

Table 3: Band characteristics of Landsat 8 –OLI-TIRS data

Landsat 8 OLI-TIRS			
Band	Ground Resolution (m)	Sensitivity Spectrum (µm)	Nominal Spectral Location
1	30	0.435-0.451	Costal/Aerosol
2	30	0.452-0.512	Blue
3	30	0.533-0.590	Green
4	30	0.636-0.673	Red
5	30	0.851-0.879	Near IR
6	30	1.566-1.651	SWIR-1
7	30	2.107-2.294	SWIR-2
8	15	0.503-0.676	Panchromatic
9	30	1.363-1.384	Cirrus
10	100	10.60 11.19	Thermal IR-1
11	100	11.50 12.51	Thermal IR-2

2.2.2 Radiometric calibration for Landsat data

Whenever multi-temporal Landsat or satellite-based data are used for change analysis there is need for radiometric calibration (Coppin *et al.* 2004; Varjo, 1996). This is done to reduce the effect of the variations in atmospheric conditions which may arise due to differences in relative radiometric response between sensors and changes in satellite sensor calibration over time such as aging. Also differences in illumination and observation angles, variation in atmospheric effects, reflectance anisotropy as BRDF effects, topography for instance slope-aspect effects, and actual changes in target reflectance (Chander and Markham, 2003; Paolini *et al.* 2006). Radiance is the amount of radiation from an object and is influenced by both the properties of the object and the sun energy hitting the object. Radiance is therefore, not the preferred data value for analysis as it varies with time of day and atmospheric conditions. Converting radiance data to reflectance data provides more useful information about the properties of the object being analysed (Paolini *et al.* 2006).

Equation [1] is used to performed radiometric calibration (Chander and Markham, 2003; Lillesand *et al.* 2004; USGS, 2015);

$$L_\lambda = \left(\frac{LMAX_\lambda - LMIN_\lambda}{Q_{calmax}}\right) Q_{cal} + LMIN_\lambda \ldots\ldots\ldots\ldots\ldots\ldots\ldots\ldots\ldots\ldots\ldots\ldots\ldots [1]$$

Where

L_λ: Spectral Radiance at the sensor's aperture in W/ (m^2. sr. µm)

Q_{cal}: The quantized calibrated pixel value in Digital Number (DN)

Q_{calmin}: The minimum quantized calibrated pixel value (DN=0) corresponding to $LMIN_\lambda$

Q_{calmax}: The maximum quantized calibrated pixel value (DN=255) corresponding to $LMAX_\lambda$

$LMIN_\lambda$: The spectral radiance that is scaled to Qcalmin in W/ (m^2. sr. µm)

$LMAX_\lambda$: The spectral radiance that is scaled to Qcalmax in W/ (m^2. sr. µm)

Equation 1 can also be expressed as (Eq. 2) (Chander and Markham, 2003):

$$L_\lambda = G_{rescale} * Q_{cal} + B_{rescale} \ldots\ldots\ldots\ldots\ldots\ldots\ldots\ldots\ldots\ldots\ldots\ldots\ldots [2]$$

Where

$$G_{rescale} = \left[\frac{LMAX_\lambda - LMIN_\lambda}{Q_{calmax}}\right] \ldots\ldots\ldots\ldots\ldots\ldots\ldots\ldots\ldots\ldots\ldots\ldots\ldots [3]$$

$$B_{rescale} = LMIN\lambda \ldots\ldots\ldots\ldots\ldots\ldots\ldots\ldots\ldots\ldots\ldots\ldots\ldots [4]$$

$G_{rescale}$ (units of (W/ (m^2. sr. µm))/DN) (Eq. 3) and $B_{rescale}$ (units of W/ (m^2. sr. µm)) (Eq. 4) are band-specific rescaling factors typically given in the NLAPS product header file (.h1) and the product generation work order report (. wo). Band-specific $LMAX_\lambda$ and $LMIN_\lambda$ parameters and the corresponding $G_{rescale}$ and $B_{rescale}$ values used at different times for the NLAPS are provided in Table 4.

Table 4: Post-Calibration Dynamic ranges for Landsat 5 TM used in this study.

L-5 TM Post-Calibration Dynamic Ranges for U.S. Processed NLAPS Data								
Spectral Radiances, Lmin and Lmax in W/(m^2.sr.um)								
Processing Date	From March 1st 1984 to May 4th 2003				After May 5th 2003			
Band	Lmin	Lmax	Grescale	Brescale	Lmin	Lmax	Grescale	Brescale
1	-1.52	152.1	0.602431	-1.52	-1.52	193	0.76282	-1.52
2	-2.84	296.81	1.1751	-2.84	-2.84	365	1.44251	-2.84
3	-1.17	204.3	0.805765	-1.17	-1.17	264	1.03988	-1.17
4	-1.51	206.2	0.814549	-1.51	-1.51	221	0.87259	-1.51
5	-0.37	27.19	0.108078	-0.37	-0.37	30.2	0.11988	-0.37
6	1.2378	15.303	0.055158	1.2378	1.2378	15.303	0.05516	1.2378
7	-0.15	14.38	0.05698	-0.15	-0.15	16.5	0.06529	-0.15

2.2.3 Atmospheric calibration for Landsat 5 TM data

For water delineation it is a recommended practice that raw (radiance based) imagery be processed to reflectance products that can then be used to extract water features as evidenced by Gilmore *et al.* (2015). The spectral radiances obtained from equation [1] are converted to Top of Atmosphere (exoatmospheric) reflectance using equation [5] (Chander and Markham, 2003; Lillesand *et al*. 2004):

$$p^{\mathrm{P}} = \frac{\pi . L_{\lambda} . d^2}{ESUN_{\lambda} . \cos\theta_s} \ldots\ldots\ldots\ldots\ldots\ldots\ldots\ldots\ldots\ldots\ldots\ldots\ldots\ldots\ldots\ldots [5]$$

Where:

p^{P}: Unit less planetary reflectance

L_{λ}: Spectral radiance at the sensor's aperture

d: Earth-Sun distance in astronomical units

$ESUN_{\lambda}$: Mean solar exoatmospheric irradiances

θ_s: Solar zenith angle in degrees

2.2.4 Atmospheric calibration for Landsat 8 OLI-TIRS

Digital Numbers (DN) values of Landsat 8 OLI level 1 products can be converted to Top of Atmosphere (TOA) reflectance (Eq. 6) (USGS, 2015) as follows:

$$\rho_{\lambda} = M_{\rho} * Q_{cal} + A_{\rho} \ldots\ldots\ldots\ldots\ldots\ldots\ldots\ldots\ldots\ldots\ldots\ldots\ldots\ldots\ldots\ldots [6]$$

Where:

ρ_{λ} = Top-of-Atmosphere Planetary Spectral Reflectance, without correction for solar angle (Unitless).

M_{ρ} = Reflectance multiplicative scaling factor for the band (REFLETANCE_MULT_BAND_n from the metadata).

A_{ρ}= Reflectance additive scaling factor for the band (REFLECTANCE_ADD_BAND_N from the metadata).

Q_{cal} = Level 1-pixel value in DN

It is of significance to note that ρ_{λ}', does not contain a correction for the solar elevation angle hence is not true TOA Reflectance. To convert to true TOA reflectance solar elevation angles for each scene is used according to equation (USGS, 2015):

$$\rho_{\lambda} = \frac{\rho_{\lambda}}{\sin(\theta)} \ldots\ldots\ldots\ldots\ldots\ldots\ldots\ldots\ldots\ldots\ldots\ldots\ldots\ldots\ldots\ldots [7]$$

where:

ρλ = Top-of-Atmosphere Planetary Reflectance. (Unit-less)

θ = Solar Elevation Angle (from the metadata, or calculated).

2.2.5 Atmospheric correction with FLAASH algorithm

The interaction between the electromagnetic radiation (EMR) from the sun, the atmosphere and the earth's surface results in distortions in the radiation characteristics. The EMR recorded by satellites in the solar spectrum is modified due to the scattering and absorption of the EMR by gases and aerosols as it passes through the atmosphere from the earth's surface to the sensor. What determines the need for correction of these distortions is the information needed from the data and the corresponding analytical methods employed to extract the information (Song *et al.* 2001; Lillesand *et al*. 2004; Gilmore *et al*. 2015). The First Line-of-sight Atmospheric Analysis of Hypercubes (FLAASH) is an Atmospheric Correction Algorithm (ACA) used in application of

remotely sensed Hyperspectral Imagery (HSI) data to correct for the effects of atmospheric propagation on measurements acquired by air and space-borne systems (Cooley *et al.* 2002; Lillesand *et al.* 2004). It corrects for HSI in the visible through the shortwave infrared (vis-SWIR) spectral regime. FLAASH physics-based mathematics is derived from MODTRAN4 (Cooley *et al.* 2002; Lillesand *et al.* 2004).

2.2.6 The Desert Flood Index

The Desert Flood Index focus on more precision in the calculation of water proportion at subpixel level and increases contrast between water and non-water features. The other multi-band based indices are focus on differentiating the water body information from the non-water-body information by using pixel scales instead of the proportion of the water area, which critically affects precision in water information extraction (Wang, 2007; Wang *et al.* 2013).

The Desert Flood Index (Eq. 8) (Wang *et al.* 2013) is a multi-band index expressed as:

$$DFI = (p^{Green-}p^{SWIR} + 0.1)/[(p^{Green} + p^{SWIR})(NDVI + 0.5)] \dots\dots\dots\dots\dots\dots\dots\dots\dots\dots [8]$$

$NDVI$ (Eq. 9) is the Normalized Difference Vegetation Index, expressed as:

$$\frac{(p^{NIR} - p^{Red})}{(p^{NIR} + p^{Red})} \dots\dots\dots\dots\dots\dots\dots\dots\dots\dots\dots\dots\dots\dots\dots\dots\dots [9]$$

in which p^{NIR} and p^{Red} are the values of reflectance for the 4th and 3rd bands of Landsat TM while 2nd and 1st bands of MODIS respectively. The $(NDVI + 0.5)$ in the denominator is for the reduction of the influence of vegetation on DFI values. NDVI in denominator is used to preclude the inclusion of vegetation as water in those pixels where water proportion is relatively small and thresholds for vegetation are also set at relatively low values. An empirical value of 0.5 is added to the NDVI in order to prevent out of range results which may arise from the NDVI value of the pure water pixel which may be at zero or negative. For the numerator $(p^{Green-}p^{SWIR} + 0.1)$, it considers the background and the DFI values of the water body with the constant 0.1 having been obtained through a large number of experimental observations (Wang *et al.* 2013).

2.2.7 The Otsu thresholding method

Image segmentation is based on separating the foreground from the background. The Otsu thresholding method (Otsu, 1979) is one of the best and the most widely used in image

segmentation processes (Jassim and Altaani, 2013). In Otsu's method, the aim is to determine the threshold that minimizes the intra-class variance (the variance within the class), defined as a weighted sum of variances of the two classes (Eq. 10) (Otsu, 1979):

$$\sigma_w^2(t) = \omega_1(t)\sigma_1^2(t) + \omega_2(t)\sigma_2^2(t) \dots\dots\dots\dots\dots\dots\dots\dots\dots\dots\dots\dots\dots\dots [10]$$

Where ω_i are the probabilities of the two classes separated by a threshold (t) and σ_i^2 are variances of these classes. Otsu (1979) shows that minimizing the intra-class variance is the same as maximizing inter-class variance (Eq. 11):

$$\sigma_b^2(t) = \sigma^2 - \sigma_\omega^2(t) = \omega_1(t)\omega_2(t)[\mu_1(t) - \mu_2(t)]^2 \dots\dots\dots\dots\dots\dots\dots\dots [11]$$

which is expressed in terms of class probabilities ω_i and class means μ_i.

The class probability $\omega_1(t)$ (Eq. 12) is computed from the histogram as (t) (Eq. 13):

$$\omega_1(t) = \sum_0^t \rho\,(i) \dots\dots\dots\dots\dots\dots\dots\dots [12]$$

while the class mean $\mu_1(t)$ is:

$$\mu_1(t) = \frac{[\sum_0^t \rho(i)\chi(i)]}{\omega_1} \dots\dots\dots\dots\dots\dots\dots\dots [13]$$

where $\chi(i)$ is the value at the centre of the i^{th} histogram bin. Similarly, $\omega_2(t)$ and μ_2 can be computed on the right-hand side of the histogram for bins greater than (t). The class probabilities and class means can be computed iteratively.

2.3.1 The one –way Repeated Measure ANOVA

The one-way RM ANOVA is a typical parametric test which helps to ascertain whether samples in more than two groups have the same central value (mean or median) or whether one of the groups has the central value different from others (Hirsch and Helsel, 2002). Reliability of the one-way ANOVA is dependent on the fulfilment of the following assumptions;

- Response variable residuals are normally distributed (or approximately normally distributed).

- Variances of populations are equal.

Based on these assumptions the data is corrected for outliers, tested for equal variance and normality test (Kolmogorov-Smirnov Test) (Hirsch and Helsel, 2002). Equal variance analysis can be done by comparing the standard deviations of the data. In general, if n observations are sampled from each of k populations (groups), the total number of observations is $N = nk$ (Hirsch and Helsel, 2002). The following notation is used:

- y_{ij} represents the j^{th} observation in i;
- $\overline{y_i}$ represents the mean in group i; and
- $\bar{y}$ represents the mean of all the observations.

The total variation of all the observations about the overall mean is measured by what is called the Total Sum of Squares, given by equation 14 (Hirsch and Helsel, 2002):

$$SS_T = \sum_{i=1}^{k}\sum_{j=1}^{n}\left(y_{ij} - \bar{y}\right)^2 \ldots\ldots\ldots\ldots\ldots\ldots\ldots\ldots\ldots\ldots\ldots\ldots [14]$$

If there is need to ascertain within and between groups variations, there is need to split into two components:

- the variation of the group means about the overall mean (between-group variation); and
- the variation of the individual observations about their group mean (within-group variation)

The two components are segregated as in equation 15 (Hirsch and Helsel, 2002):

$$\sum_{i=1}^{k}\sum_{j=1}^{n}\left(y_{ij} - \bar{y}\right)^2 = n\sum_{i-1}^{k}(\bar{y}_i - \bar{y})^2 + \sum_{i=1}^{k}\sum_{j=1}^{n}\left(y_{ij} - \bar{y}_i\right)^2 \ldots\ldots\ldots\ldots\ldots\ldots\ldots [15]$$

In another form it can be expressed (Eq. 16) (Hirsch and Helsel, 2002);

$$SS_T = SS_B + SS_W \ldots\ldots\ldots\ldots\ldots\ldots\ldots\ldots\ldots\ldots [16]$$

Where:

SS_T= total sum of squares;

SS_B= between groups sum of squares; and

SS_W= within the group sum of squares.

The null hypothesis (H_0) is that there are no differences in the population means while the alternative hypothesis (H_a) is that there is difference in the population means. To test for the null hypothesis (H_0) $\mu_1 = \mu_2 = \cdots = \mu_k = \mu$ the F statistic which is expressed as $F = \frac{MS_B}{MS_W}$ is used in which MS_B and MS_W are mean of squares between groups and mean of squares within groups respectively. The F statistic is compared with the F distribution with $k - 1$ and $N - k$ degrees of freedom. The F statistic is approximately equal to 1 if the null hypothesis is true but will be larger than 1 if there are differences between the population means. Significance of the variations in the population means is ascertained by the *p*-value which simply expresses the probability of having the means constant or not constant. If the means are constant or are not further apart, the *p*-value is very large (no significant variations) whereas if the means are wide or further apart (significant variation exists), the *p*-value is very small (< 0.00001) (Hirsch and Helsel, 2002).

2.3.2 The Pearson's r

Pearson's r is the most commonly used measure of correlation. It is sometimes referred to as the linear correlation coefficient because of its measure of linear association between two variables (Hirsch and Helsel, 2002). Pearson's r is a dimensionless property obtained by standardizing, dividing the distance from the mean by the sample standard deviation as shown in Equation 17 (Hirsch and Helsel, 2002).

$$r = \frac{1}{n-1}\sum_{i=1}^{n}\left(\frac{x_i - \bar{x}}{S_x}\right)\left(\frac{y_i - \bar{y}}{S_y}\right) \ldots\ldots\ldots\ldots\ldots\ldots\ldots\ldots\ldots\ldots\ldots\ldots\ldots\ldots\ldots\ldots [17]$$

The significance of r is determined by testing whether r differs from zero. The test statistic is computed by the following equation [18] (Hirsch and Helsel, 2002) and compared to a table of the t distribution with n-2 degree of freedom.

$$\mathrm{t_r} = \frac{\sqrt[\mathrm{r}]{\mathrm{n}-2}}{\sqrt{1-\mathrm{r}^2}} \ldots\ldots\ldots\ldots\ldots\ldots\ldots\ldots\ldots\ldots\ldots\ldots\ldots\ldots [18]$$

The null hypothesis is that y is not linearly dependent on x. The alternative hypothesis is that y is linearly dependent on x. Before the Pearson r test is conducted the data has to be examined for outliers. This is because outliers influence the reliability of statistical results and it is recommended that they are appropriately dealt with before the data are analysed (Hirsch and Helsel, 2002). The

Dixon test for outliers is mostly used (Hirsch and Helsel, 2002). The null hypothesis (H_0) is that there is no outlier in the data whereas the alternative hypothesis (H_a) is that the minimum or maximum value is an outlier. If the computed *p*-value is higher than the alpha threshold, the H_0 is accepted and if less than the alpha threshold, then the H_0 is rejected and H_a is accepted.

2.3.3. The paired t-test

The paired t-test [eq. 21] (Hirsch and Helsel, 2002) is the most commonly used test for evaluation of matched pairs of data. The Paired t-test is a parametric approach used to compare two population means in samples that are correlated. Observations in one sample are paired with observation in another sample. Normally, the paired t-test is used when there is one measurement variable and two nominal variables. It is used in 'before-after' studies, or when the samples are the matched pairs, or when it is a case-control study (Hirsch and Helsel, 2002). The paired t-test is performed based on the following assumptions:

Let X = before observation(s); Y = the after observation(s).

To apply the test equations 19 and 20 are used (Hirsch and Helsel, 2002), let

$$\widehat{X}_\iota = (X_i - \bar{X}) \dots\dots\dots\dots\dots\dots\dots\dots\dots\dots\dots [19]$$

$$\widehat{Y}_\iota = (Y_i - \bar{Y}) \dots\dots\dots\dots\dots\dots\dots\dots\dots\dots\dots\dots\dots\dots [20]$$

Then t is defined by equation 21 (Hirsch and Helsel, 2002).

$$t = (\bar{X} - \bar{Y}) \sqrt{\frac{n(n-1)}{\sum_{i=1}^{n} \left(\widehat{X}_\iota - \widehat{Y}_\iota\right)^2}} \dots\dots\dots\dots\dots\dots\dots\dots\dots\dots\dots [21]$$

With $n - 1$ degrees of freedom a table of Student's t-distribution confidence intervals is used to ascertain the significance level at which two distributions differ. When the computed *p*-value is < 0.05 it implies that the two distributions differ significantly (Hirsch and Helsel, 2002).

2.4. Supervised classification - Maximum Likelihood classification algorithm

The Maximum Likelihood classification is one of the most widely used systems in remote sensing (Ahmad and Quegan, 2012). The maximum likelihood method is derived from the Bayes Theorem which states that the posteriori distribution P (i |ω), for instance the probability that a particular pixel with a feature vector **ω** belongs to class **i** is given by the equation 22 (Lillesand *et al*. 2004; Ahmad and Quegan, 2012):

$$P(i + \omega) = \frac{P(\omega|i)P(i)}{P(\omega)} \dots\dots\dots\dots\dots\dots\dots\dots\dots\dots\dots\dots\dots\dots\dots\dots\dots\dots\dots\dots [22]$$

Where $P(\omega|i)$ is the likelihood function, $P(i)$ is the priori information such that the probability that class i occurs in the study area, $P(\omega)$ is the probability that ω is observed and can also be expressed as equation 23 (Lillesand *et al.* 2004; Ahmad and Quegan, 2012):

$$P(\omega) = \sum_{i=1}^{m} P(\omega|i)P(i) \dots\dots\dots\dots\dots\dots\dots\dots\dots\dots\dots\dots [23]$$

Where *m* is the number of classes while $P(\omega)$ is regarded as the normalization constant to ensure $\sum_{i=1}^{m} P(i|\omega)$ sums to 1. Pixel X is assigned to class i by the rule (Eq. 24):

$$X \in i \ \ if\ P(i|\omega) > P(j|\omega) \ \ for\ all \ \ J \neq i \dots\dots\dots\dots\dots\dots\dots\dots\dots [24]$$

Maximum likelihood assumes that the data within a given class obeys a multivariate Gaussian distribution. It is therefore appropriate to define the log likelihood or the discriminant function as (Eq. 25) (Lillesand *et al.* 2004; Ahmad and Quegan, 2012):

$$g_i(\omega) = \ln P\,(\omega|i) = -{}^{1}/_{2}\,(\omega - \mu_i)^t C_i^{-1}(\omega - \mu_i) - \frac{N}{2}\ln(2\pi) - \frac{1}{2}\ln(|C_i|) \dots\dots\dots [25]$$

Since log is a monotonic function it implies that equation 25 is equivalent to equation 26 (Lillesand *et al*. 2004; Ahmad and Quegan, 2012).

$$X \in i \ \ if\ g_i\,(\omega) > g_i(\omega)\ for\ all \ \ J \neq i \dots\dots\dots\dots\dots\dots\dots\dots\dots [26]$$

Each pixel is allotted to the class with the Maximum Likelihood or characterised as unclassified if the probability values are all below the chosen threshold by the user. A general procedure for Maximum Likelihood classification used in the classification is as outlined below:

- Determine the number of classes to be investigated based on the knowledge about the study area and the imagery data;
- Delineate training regions or areas of interest (ROI's) and measure their separability using the Jefferies-Matusita (JM) Distance. The ROI's with the best JM statistics are used for classification. The Jefferies-Matusita measures class separability of the chosen ROI's (Ahmad and Quegan, 2012). For normally distributed classes, the JM separability measure for two classes J_{ij}, is defined as equation 27 (Lillesand *et al*. 2004; Ahmad and Quegan, 2012):

$$J_{ij} = \sqrt{2(1 - e^{-\alpha})} \ldots\ldots\ldots\ldots\ldots\ldots\ldots\ldots\ldots\ldots [27]$$

Where α is the Bhattacharyya Distance given by equation 28 ((Lillesand *et al*., 2004; Ahmad and Quegan, 2012);

$$\alpha = \frac{1}{8}(\mu_i - \mu_j)^t \left[\frac{(C_i + C_j)}{2}\right]^{-1} (\mu_i - \mu_j) + \frac{1}{2}\ln\left[\frac{\left|\frac{C_i + C_j}{2}\right|}{\sqrt{|C_i||C_j|}}\right] \ldots\ldots\ldots\ldots\ldots\ldots\ldots\ldots\ldots [28]$$

Where μ is class mean and C is class. J_{ij} ranges from 0 to 2.0, where $J_{ij} > 1.9$ indicates good separability of classes, moderate separability for $1.0 \leq J_{ij} \leq 1.9$ and poor separability for $J_{ij} < 1.0$ (Lillesand *et al*. 2004; Ahmad and Quegan, 2012):

- The training pixels are then used to estimate the mean vector and covariance matrix of each class; and
- Finally, every pixel in the image is assigned into one of the desired land cover types or labelled as unclassified.

In Maximum Likelihood classification, each class is bounded in a region in multispectral space in which its discriminant function is larger than that of all other classes. The decision boundaries separate class regions and the decision boundary between class i and j occurs when (Eq. 29) (Lillesand *et al*. 2004; Ahmad and Quegan, 2012);

$$g_i(\omega) = g_j(\omega) \ldots\ldots\ldots\ldots\ldots\ldots\ldots\ldots [29]$$

In the case of multivariate normal distribution, it is expressed as [eq. 30] (Lillesand *et al.* 2004; Ahmad and Quegan, 2012);

$$-\frac{1}{2}(\omega-\mu_i)^t C_i^{-1}(\omega-\mu_i)-\frac{N}{2}\ln(2\pi)-\frac{1}{2}\ln(|C_i|)$$
$$-\left(-\frac{1}{2}(\omega-\mu_j)^t C_j^{-1}(\omega-\mu_j)-\frac{N}{2}\ln(2\pi)-\frac{1}{2}\ln(|C_j|)\right)=0\ldots\ldots[30]$$

The expression can also be written as a quadratic function in N dimensions as follows (Eq.31) (Lillesand *et al*. 2004; Ahmad and Quegan, 2012):

$$-(\omega-\mu_i)^t C_i^{-1}(\omega-\mu_i)-\ln(|C_i|)+(\omega-\mu_j)^t C_j^{-1}(\omega-\mu_j)+\ln(|C_j|)=0\ldots\ldots\ldots[31]$$

This implies that if only two classes are considered, the decision boundaries are conic sections such as parabolas, circles, ellipses or hyperbolas (Lillesand *et al*. 2004; Ahmad and Quegan, 2012).

2.4.1 Supervised classification – validation with the Error (confusion) matrix

A confusion matrix (sometimes called error matrix) compares, on a class-by class basis, the relationship between reference data (ground truth) and the corresponding results of a classification (Lillesand *et al.* 2004). Such matrices are square, with the number of rows and columns equal to the number of classes. The confusion matrix is used to establish the following statistical parameters about the classification (Lillesand *et al.* 2004):

(a) Overall accuracy: The overall accuracy is calculated by summing the number of pixels classified correctly and dividing by the total number of pixels. The ground truth image or ground truth ROIs define the true class of the pixels. The pixels classified correctly are found along the diagonal of the confusion matrix table which lists the number of pixels that were classified into the correct ground truth class. The total number of pixels is the sum of all the pixels in all the ground truth classes;

(b) Commission: Errors of commission represent pixels that belong to another class that are labelled as belonging to the class of interest. The errors of commission are shown in the rows of the confusion matrix;

(c) Omission: Errors of omission represent pixels that belong to the ground truth class but the classification technique has failed to classify them into the proper class. The errors of omission are shown in the columns of the confusion matrix;

(d) Confusion matrix (Percent): The Ground Truth (Percent) table shows the class distribution in percent for each ground truth class. The values are calculated by dividing

the pixel counts in each ground truth column by the total number of pixels in a given ground truth class;

(e) Producer accuracy: The producer accuracy is a measure indicating the probability that the classifier has labelled an image pixel into Class A given that the ground truth is Class A;

(f) User accuracy: User accuracy is a measure indicating the probability that a pixel is Class A given that the classifier has labelled the pixel into Class A; and

(g) Kappa Coefficient: The kappa coefficient (k) is another measure of the accuracy of the classification (Lillesand *et al*. 2004). It is calculated by multiplying the total number of pixels in all the ground truth classes (N) by the sum of the confusion matrix diagonals (X_{kk}), subtracting the sum of the ground truth pixels in a class times the sum of the classified pixels in that class summed over all classes $\left(X_{k\sum}X_{\sum k}\right)$, and dividing by the total number of pixels squared minus the sum of the ground truth pixels in that class times the sum of the classified pixels in that class summed over all classes expressed as indicated in equation 32 (Lillesand *et al.* 2004);

$$\frac{N_K X_{kk} - X_{k\sum}X_{\sum k}}{N^2 - X_{k\sum}X_{\sum k}} \dots\dots\dots\dots\dots\dots\dots\dots\dots\dots\dots [32]$$

2.5.1 Pettit test for data homogeneity – Change point detection

The Pettit (1979) Homogeneity test approach is a common non-parametric application in change point detection studies involving hydrological or climate series which are known to be non-normal data (Pohlert, 2014; Hirsch and Helsel, 2002). It tests the null hypothesis (H_0) that the T variables follow one or more distributions that have the same location parameter (no change) or simply put the data are homogenous. The alternative hypothesis (H_a) is that there is a point at which a change in the data occurs. The test verifies whether two samples X_1..., X_t and X_t+1..., X_N are from the same population or not. The test statistic counts the number of times a member of the first sample exceeds a member of the second sample. The test statistic is given as in equation 33 (Hirsch and Helsel, 2002):

$$U_{tN} = U_{t-1,N} + \sum_{j=1}^{N} sgn(X_t - X_j) \; for \; t = 2, \ldots . N \ldots \ldots \ldots \ldots \ldots \ldots . [33]$$

Its statistic K_t and associated probabilities employed in significance testing are given as in equations 34 and 35 (Hirsch and Helsel, 2002):

$$K_T = \max|U_t T| \ldots \ldots \ldots \ldots \ldots \ldots \ldots \ldots [34]$$

Where $$U_t T = \sum_{i=1}^{t} \sum_{j=t+1}^{T} sgn(X_i - X_j) \ldots \ldots \ldots \ldots \ldots \ldots \ldots \ldots \ldots [35]$$

The change-point of the series is located at K_T provided that the statistic is significant. The significance probability of K_T is approximated for $\rho \leq 0.05$ as in equation 36 (Hirsch and Helsel, 2002).

$$\rho \cong 2 \; exp\left(\frac{-6K_T^2}{T^3 + T^2}\right) \ldots \ldots \ldots \ldots \ldots \ldots \ldots \ldots \ldots \ldots \ldots . . [36]$$

When the change point is found significant, the time series is divided into two parts at the location of the change point t.

2.5.2 Accounting for serial correlation

It is recommended that time series data is corrected for serial correlation before trends analysis is executed (Hirsch and Helsel, 2002). Serial correlation is when a variable correlate with itself over successive time intervals (past and future). Serial correlation is also sometimes referred to as autocorrelation or lagged correlation. The consequence of serial correlation is that chances of detecting a trend where it is non-existent are increased and the opposite is also true that chances to not detect a trend when it actually exists is increased. A modified Mann-Kendall trends test that corrects for serial correlation by removing the apparent trend was proposed by Hamed and Rao (1998) in the form of an adjusted variance (Equations 37 and 38) (Hirsch and Helsel, 2002) given as:

$$\text{Var}\,[\text{s}] = \frac{1}{18}[\text{N}(\text{N}-1)(2\text{N}+5)]\frac{\text{N}}{\text{NS}^*} \ldots \ldots \ldots \ldots \ldots \ldots \ldots \ldots \ldots \ldots . [37]$$

Where,

$$\frac{\mathrm{N}}{\mathrm{NS}^{*}} = 1 + \frac{2}{\mathrm{N}(\mathrm{N}-1)(\mathrm{N}-2)} \sum_{\mathrm{i}=1}^{\mathrm{p}} (\mathrm{N}-\mathrm{i})\,(\mathrm{N}-\mathrm{i}-1)(\mathrm{N}-\mathrm{i}-2)\mathrm{p_s}(\mathrm{i}) \ldots\ldots\ldots\ldots\ldots [38]$$

N is the number of observations in the sample, NS^{*} is the effective number of observations to account for autocorrelation in the data, $\mathrm{p_s}(\mathrm{i})$ is the autocorrelation between ranks of the observations for lag i, and p is the maximum time lag under consideration (Hirsch and Helsel, 2002).

2.5.3 The Mann-Kendall Test statistic

The Mann-Kendall Test possesses advantage over other tests because it is a non-parametric test which does not need the data to be normally distributed and has low sensitivity to abrupt changes due to inhomogeneity in time series data (Hirsch and Helsel, 2002). In general terms, the Mann-Kendall Test seeks to establish whether monotonic changes are present in a given set of random values. It is a test for whether Y values tend to increase or decrease with T expressed in the following relationships (Eq. 39) (Hirsch and Helsel, 2002):

$$\mathrm{H0: Prob}\left[Y_j > Y_i\right] = 0.5, \text{where time } T_j > T_i \ldots\ldots\ldots\ldots\ldots\ldots\ldots\ldots\ldots [39]$$

$$\mathrm{H1: Prob}\,[Y_j > Y_i \neq 0.5\ (2-\text{sided test}).$$

There is no need for assumption of normality in data but it is required that there be serial correlation if the resulting *p*-value is to be correct. The test is typically applied to ascertain whether the central value or median changes over time (Hirsch and Helsel, 2002).

The Mann-Kendall Statistic is given as in equations 40 and 41 (Hirsch and Helsel, 2002):

$$S = \sum_{i=i}^{n-1} \sum_{j=i+1}^{n} sgn(T_j - T_i) \ldots\ldots\ldots\ldots\ldots\ldots\ldots\ldots [40]$$

$$sgn(T_j - T_k) = \begin{cases} 1 & if\ T_j\_T_i > 0 \\ 0 & if\ T_j - T_i = 0 \\ -1 & if\ T_j - T_i < 0 \end{cases} \ldots\ldots\ldots\ldots\ldots [41]$$

Where T_j and T_i are sequential data values for the time series data of length n. T_j and T_i are the n values in years j and i, $j > i$ respectively. The test statistic represents the number of positive differences minus the number of negative differences for all the differences between adjacent points in the time series. Positive values indicate an upward trend while negative values indicate a downward trend. If n < 10 the value |S| is obtained by direct comparison to the theoretical distribution of S derived by Mann and Kendall (Hirsch and Helsel, 2002). At a set probability level (α) level, the Null Hypothesis (H_0) is rejected in favour of the Alternative Hypothesis (H_a). In the case where the absolute value of S equals or exceeds a specified value $S_{\sigma/2}$,'where $S_{\sigma/2}$ is the smallest S which has the probability less than $a/2$ to appear in case of no trend. Trend interpretation is such that a positive value of S shows an upward trend while a negative value indicates a downward trend. The two tailed test is used. For n > 10, the statistic S is approximately normally distributed with the mean and variance as follows (Eq. 42) (Hirsch and Helsel, 2002):

$$E(S) = 0 \dots\dots\dots\dots\dots\dots\dots\dots\dots\dots [42]$$

The variance (σ^2) for the S-statistic is given by equation 43 (Hirsch and Helsel, 2002):

$$(\sigma^2) = \frac{1(n-1)(2n+5) - \sum t_i(i)(i-1)(2i+5)}{18} \dots\dots\dots\dots\dots\dots\dots\dots\dots [43]$$

Where t_i denotes the number of ties to the extent i. The summation term in the numerator is applied only when the data series has tied values. The standard test statistic Z_s (Eq. 44) is calculated as follows (Hirsch and Helsel, 2002):

$$Z_s = \begin{cases} \frac{S-1}{\sigma} & \text{if } S > 0 \\ 0 & \text{if } S = 0 \\ \frac{S+1}{\sigma} & \text{if } S < 0 \end{cases} \dots\dots\dots\dots\dots\dots\dots\dots\dots\dots [44]$$

The Z_s statistic is used to test the null hypothesis and is a measure of the strength of the trend. For instance if |S| is greater than $S_{\sigma/2}$ where α shows the chosen significant level, such as 0.5 with $Z_{0.025} = 1.96$, the trend is concluded to be insignificant (Hirsch and Helsel, 2002).

2.5.4 The Kendall's Tau

Another significant statistic that is coupled with the running of the Mann-Kendall Test is the Kendall's Tau. Kendall's Tau is a correlation parameter that measures the strength of the relationship between variables. Kendall's Tau is performed on the ranks of the data. This implies that for each specific variable the values are put in order and numbered for instance, 1 for the lowest value, 2 for the next lowest until the n^{th} value is numbered. As is the case with other measures of correlation, Kendall's Tau takes values between -1 and +1, in which a positive correlation indicates that the ranks of both variables increase together while a negative correlation denotes opposite directions in the ranks of the variables (rank of one variable increases, the other decreases). In essence, Kendall's Tau represents a difference between the probability that the observed data are in the same order versus the probability that the observed data are not in the same order. The Kendall's Tau (Eq.45) (Hirsch and Helsel, 2002) is expressed as follows:

$$\tau = \frac{n_c - n_d}{n(n-1)/_2} \ldots\ldots\ldots\ldots\ldots\ldots\ldots\ldots [45]$$

where n_c denotes concordant pairs and n_d are discordant pairs. When the rank of the second variable is greater than the rank of the former variable the pair is said to be concordant. When the rank of the second variable is equal to or less than the rank of the first variable, the pair is considered as discordant (Hirsch and Helsel, 2002).

If there are tied values (same values) then τ_b (Eq. 46) (Hirsch and Helsel, 2002) is used:

$$\tau_b = \frac{S}{\sqrt{[n\,(n-1)/2 - \sum_{i-1}^{t} t_i\,(t_i-1)/2][n\,(n-1)/2] - \sum_{i-1}^{u} u_i\,(u_i-1)/2}} \ldots\ldots\ldots [46]$$

Where t_i is the number of observations tied at a particular rank of x, and u_i is the number of ties at a rank of y (Hirsch and Helsel, 2002).

2.5.5 Accounting for seasonality – Seasonal Kendall Test

Hydrological variables are influenced by seasonality within and across the temporal space and seasonality is a major source of variations. To discern the trend in these hydrological variables, overtime there is need to account for the seasonality by the use of the seasonal Kendall Test as proposed by Hirsch *et al.* (1984). Accounting for seasonality by the Seasonal Kendall test is done by computing separately the Mann-Kendall Test on each of the *m* seasons and thereafter combining the results (Hirsch and Helsel, 2002). Kendall's statistic S_i for each season is summed up to form the overall statistic S_k (Eq. 47) (Hirsch and Helsel, 2002):

$$S_k = \sum_{i=1}^{m} S_i \dots\dots\dots\dots\dots\dots\dots\dots [47]$$

Estimation of S_k by a normal distribution can be made quite well when the product of number of seasons and number of years is more than 25 since the expectation equals to the sum of expectations (zero) of the individual S_i under the null hypothesis with the variance equalling the sum of their variances. Standardisation of S_k (Eq. 48) (Hirsch and Helsel, 2002; Salmi *et al*. 2002) is by subtracting its expectation μ_k (Eq. 49) and dividing by its standard deviation Q_{sk} (Eq. 50):

$$Z_{sk} = \begin{cases} \dfrac{S_k - 1}{Q_{sk}} & \text{if } s_k > 0 \\ 0 & \text{if } s_k = 0 \\ \dfrac{S_k + 1}{Q_{sk}} & \text{if } s_k < 0 \end{cases} \dots\dots\dots\dots\dots\dots [48]$$

Where

$$\mu_{sk} = 0 \dots\dots\dots\dots\dots\dots\dots [49]$$

$$Q_{sk} = \sqrt{\sum_{i=1}^{m}(n_i/18)} * (n_i - 1) * (2n_i + 5) \dots\dots\dots\dots\dots\dots [50]$$

$$n_i = number\ of\ data\ in\ the\ i^{th} season.$$

The null hypothesis is rejected at significance level α if $|Z_{sk}| >$ Zcrit where Zcrit is the value of the standard normal distribution with a probability of exceedance of α/2 (Hirsch and Helsel, 2002; Salmi *et al*. 2002).

2.5.6 Sens's slope estimates

To estimate the true slope of an existing trend the Sen's nonparametric method is used. The Sen's method can be used in cases where the trend can be assumed to be linear using equation 51 (Salmi *et al.* 2002):

$$f_{(t)} = Q_t + B \text{..... [51]}$$

where *f(t)* is a continuous monotonic increasing or decreasing function of time, Q is the slope and B is a constant. To get the slope estimate Q in equation 51 first calculate the slopes of all data value pairs using equation 52 (Salmi *et al.* 2002):

$$Q_i = \frac{x_j - x_k}{j-k} \text{..... [52]}$$

Where j > k.

If there are *n* values x_j in the time series, get as many as $N = n(n-1)/2$ slope estimates Q_i. The Sen's estimator of slope is the median of these *N* values of Q_i. The *N* values of Q_i are ranked from the smallest to the largest and the Sen's estimator equation 53 or 54 (Salmi *et al*. 2002) is used:

$$Q = Q_{[(N+1)/2]} \text{ if } N \text{ is odd..... [53]}$$

$$Q = \frac{1}{2}\left(Q_{[N/2]}\right) + Q_{[(N+2)/2]} \text{ if } N \text{ is even..... [54]}$$

A 100(1-α) % two-sided confidence interval about the slope estimate is obtained by the nonparametric technique based on the normal distribution. The method is valid for *n* as small as 10 unless there are many ties (Salmi *et al*. 2002). The procedure in MAKESENS computes the confidence interval at two different confidence levels; α = 0.01 and α = 0.05, resulting in two different confidence intervals. With equation 55 (Salmi *et al*. 2002) the first interval is computed.

$$C_\alpha = Z_{1-\alpha/2}\sqrt{VAR(S)} \text{ ..... [55]}$$

Where *VAR(S)* has been defined in equation 37, and $Z_{1-\alpha/2}$ is obtained from the standard normal distribution. Then $M_1 = (N - C_\alpha)/2$ and $M_2 = (N - C_\alpha)/2$ are computed. The lower and upper limits of the confidence interval , Q_{min} and Q_{max} are the $M_1{}^{\text{th}}$ largest and the $(M_2 + 1)^{\text{th}}$ largest of the N ordered slope estimates Q_i. If M_1 is not a whole number the lower limit is interpolated. In like manner, if the $M_2$is not a whole number the lower limit is interpolated. To obtain an estimate of B in equation 51 the *n* values of differences $x_i - Qt_i$ are calculated. The median of these values gives an estimate of B (Sirois, 1998). The estimates for the constant B of lines of the 99% and 95% confidence intervals are calculated by a similar procedure.

2.6 Gap analysis

The impact of climate change on wetlands and the need for habitat based information for adaptation to the same has been clearly noted (Diaz, 2006; Agrawal, 2008; Erwin, 2009). Globally, a number of studies on inundation extent mapping have been done using a variety of satellite imagery and methods (Kudahetty, 2012; Wang *et al*., 2013; Long *et al*.,2014 and many others as highlighted in section 2.1.5 of this chapter). In Zambia a few studies mapped wetland inundation extent with satellite imagery mostly in the Kafue Flats (Tiger Initiative, 2008; Meir, 2012; Aduah and Mantey ,2012 and Cai *et al*., 2015). However, the studies did not statistically establish trends in inundation extent and never attempted to link inundation patterns with trends in hydrological and climatological variables. The only study (Cai *et al*. 2015) in the Barotse Wetland was inconclusive on the characterisation of inundation patterns and did not ascertain variables that could be impacting on the spatial extent trends. For instance, Cai *et al*. (2015) used Landsat imagery to assess inundation patterns. They used Landsat data to generate time series across the seasons (1984 to 2014) and came up with the average inundation extent for each year. However, they experienced difficulties in generating sufficient cloud free images thus failed to ascertain inundation extent for some years (1996, 2010, 2011 and 2012). They also did not statistically ascertain the trend in inundation extent.

Some studies on the role of wetlands in flow attenuation in the Zambezi River Basin have been done (Murwira *et al*. nd; Beilfuss and dos Santos, 2001; McCartney et al. 2013). Beilfuss and dos Santos (2001) and McCartney *et al*. (2013) concluded that the Barotse Wetland attenuates flow.

Beilfuss and dos Santos (2001) compared the hydrographs of the Barotse sub-basin inflows and outflows after which they attributed the differences to the wetland. Despite the complicated modelling methods used by McCartney *et al*. (2013) they admitted that the study had numerous limitations and that it was inconclusive. Unlike Murwira *et al*. nd, the studies in the Barotse wetland did not statistically show how significant the differences in the changes in the volumes of the before and after scenarios were.

Though some publications (Kasimona and Makwaya ,1995; Timberlake,1998, 2000; Beilfuss and Santos, 2001; Fanshawe, 2010) cited minimal or negligible change in land cover in the Barotse Wetland they presented no quantified evidence of change. The land cover change assessment by FAO and the Zambia Department of Forest (Mukosha, 2014) is limited in temporal coverage (1990 to 2005) and the spatial extent was too wide (entire Zambia) which could have affected the accuracy of the classification. At the time of this study, there were no publications in public domain on both short and long-term trends of hydrological and climatological data for the Barotse Wetland. Significantly, most studies done on the Barotse Wetland such as Simwinji (1997), IUCN (2003) and Baidu-Forson *et al*. (2014) have tended to focus on the biodiversity and the social-economic value aspect of the wetland.

Arising from the observed gaps in data on inundation extent, role of the wetland in flow attenuation, land cover change and trends in hydrological and climatological variables this study was formulated to add to the body of knowledge on the highlighted aspects and thus contribute to filling of the gaps for the Barotse Wetland.

CHAPTER THREE: METHODOLOGY

3.1 Study approach and data used

From the literature review, it was noted that supplementing the detection, quantification and characterization of inundation regimes with land cover change detection, as well as the analysis of some hydrological and climate variables such as discharge, rainfall and temperature would provide a widened perspective and valuable platform for identification, planning and implementation of targeted adaptation measures for the wetland. Therefore, the formulated objectives of the study as outlined in Chapter 1 gave rise to a multidimensional methodological approach, as given in Figures 7 (a – b). The remote sensing approach (Figure 7a) involved the use of MODIS and Landsat satellite imagery. The arrows show the flow of the data analysis process (Figure 7a). The MODIS data were used to generate inundation extent masks through the use of the Desert Flood Index.

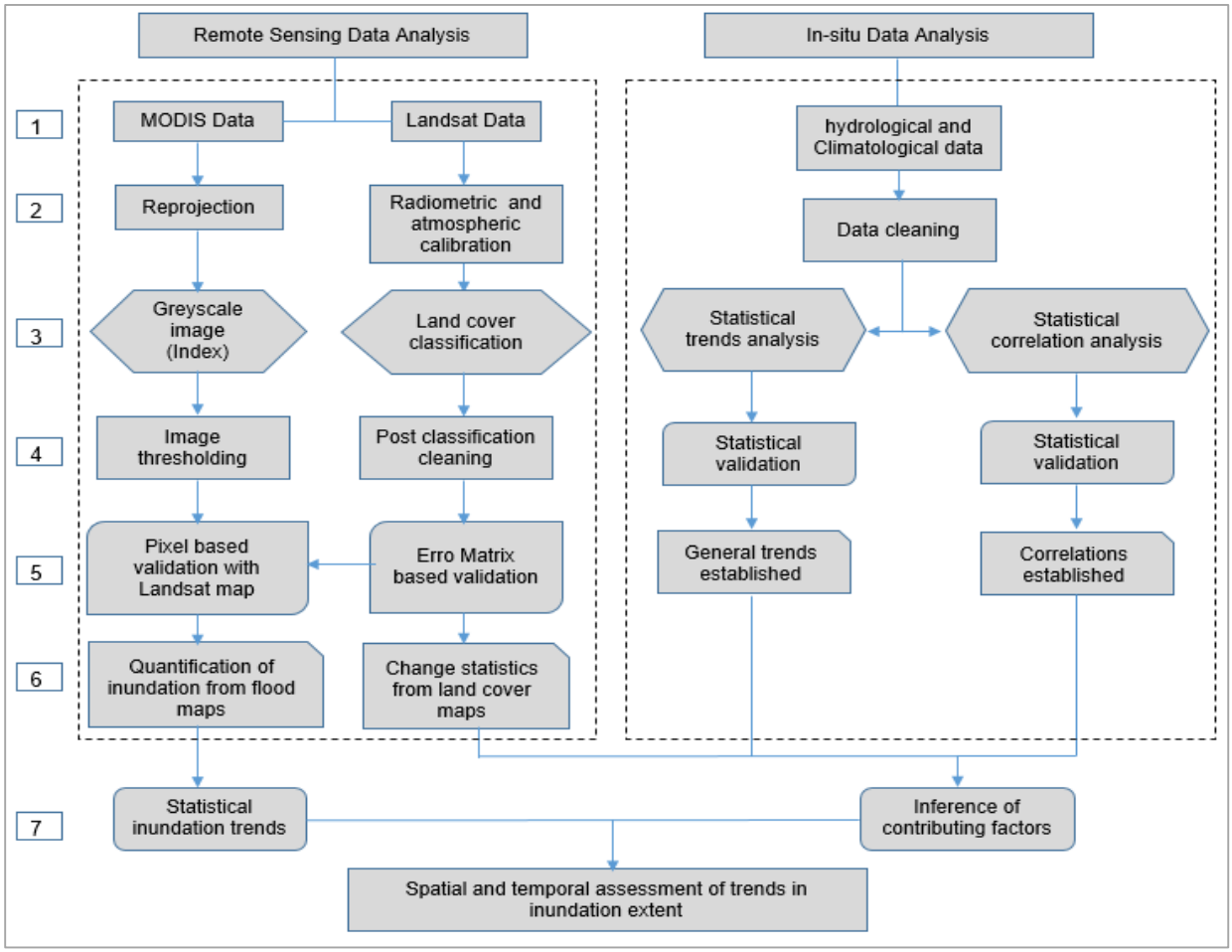

Figure 7a: Study approach to assess spatial and temporal trends in inundation in the Barotse Wetland, Western Zambia.

The flood masks were then validated using Landsat 8 OLI-TIRS land cover classified maps data after which inundation extent for each MOD09A1 day was calculated for the temporal space 2003 to 2013. The RM ANOVA and Mann-Kendall tests were then applied on the inundation extent time series to analyse the variations and trends. Other than being used for validation of the inundation extent maps the Landsat 5 TM and Landsat 8 OLI-TIRS images were used to perform the land cover change assessment, as indicated with the arrows in Figure 7a. The Landsat data based land cover classifications were validated using the error matrix with ground truth data after which change statistics were evaluated by comparing the changes in the land cover classifications across the time space June 1984 to June 2015. The in-situ hydrological and climatological analysis approach involved the analysis of time series of stream discharge, rainfall and temperature using statistical methods to establish correlations and trends in the variables. The land cover change assessment, correlations and the trends established among the variables were then used to make inferences on the potential contributing factors to the trends in inundation extent (Figure 7a). Further, the correlations were used to analyse the role of the wetland in regulating flow. Figure 7b shows how each objective of the study was achieved using given data sets, methods applied, data processing and analysis tools used.

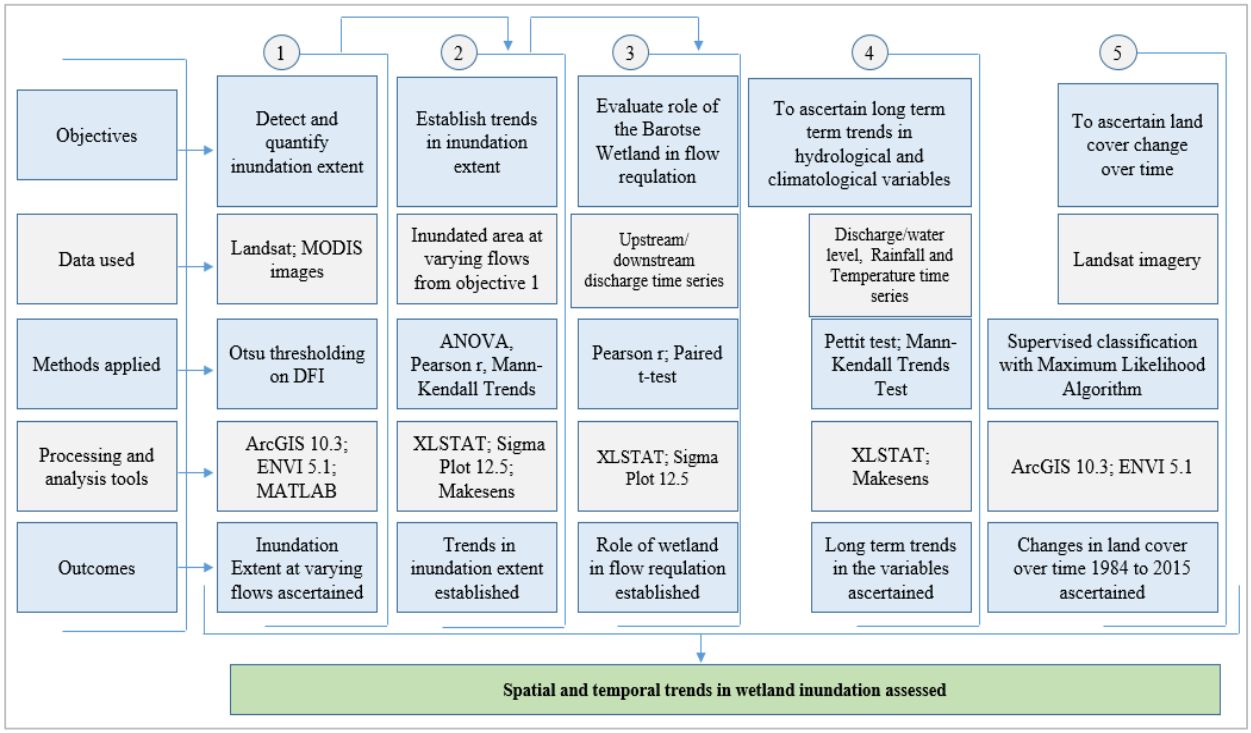

Figure 7 (b): Objectives, data, methods and analysis techniques used to assess spatial and temporal trends in inundation in the Barotse Wetland, Western Zambia.

The arrows show the flow of the processes and the interlinkages of objectives. For instance, the results from objective one were the inputs for objective two. The results from object two were part of the inputs for objective three. All five objectives of the study were interlinked as indicated by the arrows (Figure 7b). The assessment of inundation was categorised into two phases based on the characterization of discharge (flows) and these were: the rising or ascending/peak and the falling or descending periods. The ascending/peak period is normally from November to April of each hydrological year (October to September) (Figure 8). The peak in flows is ordinarily achieved between March and April while the descending to regular flows generally is from May to July (Figure 8). The temporal space considered was an eleven-year period from 2003 to 2013. This period was chosen primarily based on two considerations; availability of MODIS imagery and the representative nature of hydrological and climatological regimes experienced during this period. The MODIS platform started capturing data in the year 2000 hence no assessment of inundation could be done with MODIS prior to this period. In terms of climatological and hydrological variables the period 2003 -2013 experienced a myriad of both extreme wet and dry events which were critical for inclusion in the assessment of inundation trends.

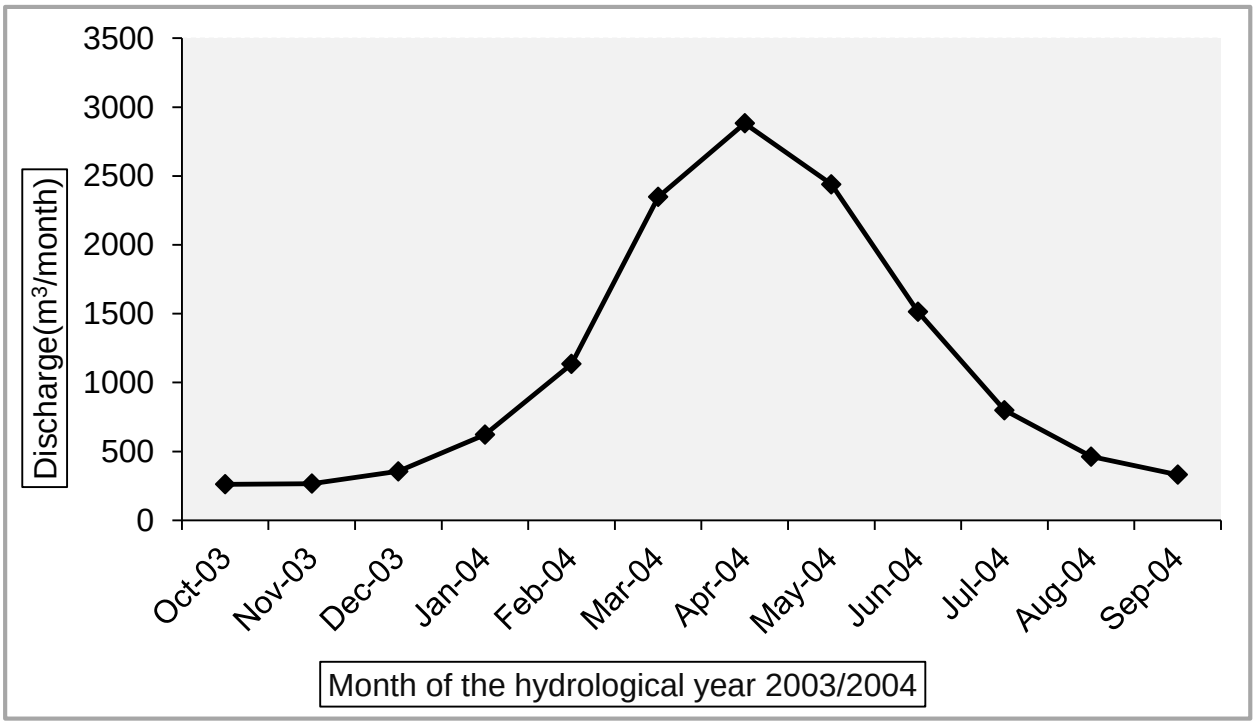

Figure 8: Hydrograph of mean monthly discharge (m^3/month) for Senanga Gauge Station Western Zambia, in the hydrological year 2003/2004 characterising flow regimes.

The satellite approach was anchored on the spatial and temporal robustness of MODIS and Landsat platforms. MODIS provided temporal leverage as the product used in this study, the MOD 09A1, has an eight-day repeat cycle with a 500 m spatial resolution suitable for assessment of inundation covering large areas. The MOD 09A1 gives the best image available in terms of absence of cloud cover and other parameters in the eight-day period. Since the focus of the study was the rainy season, which is prone to cloud cover on most days, the eight-day revisit time was deemed adequate for the purposes of this study. Landsat 5 TM and Landsat 8 OLI-TIRS on the other hand have a relatively higher spatial resolution (30 m) than MODIS but have a longer revisit time, 16 days, which proved difficult to generate "sufficient" data sets for adequate time-series analysis of inundation extent. Very few cloud free Landsat imagery were available during the flooding period. The Landsat images available, during the flood season, differed on the dates they were acquired each year hence the decision to settle for MODIS imagery which had several images available on the same dates each year. The MODIS imagery data made it possible to compare inundation extent on each particular day of the year across the years. However, taking advantage of its spatial resolution and the ground truthing process, Landsat data was used to validate inundation extent as detected by MODIS. Further, Landsat imagery was used to assess the land cover changes over time. Details of each of the satellite data used in the study are given in the proceeding sections of this chapter. To enhance the characterisation of inundation behaviour in the wetland, there was need to understand the relationship between inundation extent and hydrological parameters discharge and water level. This was done by first establishing relationship(s) between discharge, water level and inundation extent in the wetland. Thereafter, the established relationship(s) was used to further understand and characterise water retention and discharge behaviour of the wetland drawing conclusions on how such phenomenon potentially affected downstream stream flooding regimes. The relationship between inundation extent and discharge was also used to draw conclusions on the potential effects of the observed changes in land cover on inundation in the wetland. Finally, statistical analysis of hydrological and meteorological variables to establish general trends was performed. Establishing the general trends in the hydrologic and meteorologic parameters was, by relational inference, aimed at establishing whether there was a trend in inundation extent and the direction of this trend.

3.2 Acquisition of satellite data

The Moderate-resolution Imaging Spectroradiometer (MODIS) MOD 09A1, Landsat 5 TM and Landsat 8 OLI-TIRS (Operational Land Imager Thermal Infrared Sensor) imagery were accessed from NASA (National Aeronautics and Space Administration) via the internet portal glovis (http://glovis.usg.gov). The shape file covering the study area was used to cut out and download MODIS 09A1 data for the years 2003 to 2013. Landsat TM and OLI-TIRS data were downloaded from scenes at paths 174 to 176 with rows at 070 to 071. Details of the Landsat data used in this study are in Appendix 1.

3.3 Satellite imagery data pre-processing

The web based MODIS Reprojection Tool (MRT) was used to pre-process MOD09A1 data. MOD 09A1 is a reflectance product hence there was no need to convert from digital numbers (DN) to reflectance values before use in the study. The data were first re-projected and thereafter converted from the native HDF to GeoTIFF a usable format in ArcGIS 10.3. Data and information by Landsat 5 TM and Landsat 8 OLI-TIRS is acquired and stored as digital numbers ranging between 0 and 255 and 0 and 65535 respectively. Hence, needed to be converted to reflectance through the process of radiometric and atmospheric calibration as explained in the proceeding sections.

3.4 Radiometric and atmospheric calibration

In this study, the critical information needed from satellite data was the detection of change in land cover across years. For land cover change studies, it is a recommended practice that raw (Digital Number-based) imagery be processed to reflectance products that can then be used to extract the desired information (Lillesand *et al*. 2004; Gilmore *et al*. 2015). The spectral radiances obtained from equation [1] are converted to Top of Atmosphere (exoatmospheric) reflectance using equation [5] (Chander and Markham, 2003; Lillesand *et al*. 2004, USGS, 2015).

3.4.1 Radiometric and atmospheric calibration for L5 TM and L8-OLI-TIRS data

For Landsat 5 TM, the meta data file (MTL.txt) for each scene was used to input data in the radiometric calibration module (RCM) in ENVI 5.1 classic (Figure 9). Recommended calibration parameters from Table 4 were inputted for each band after which the radiance product was obtained.

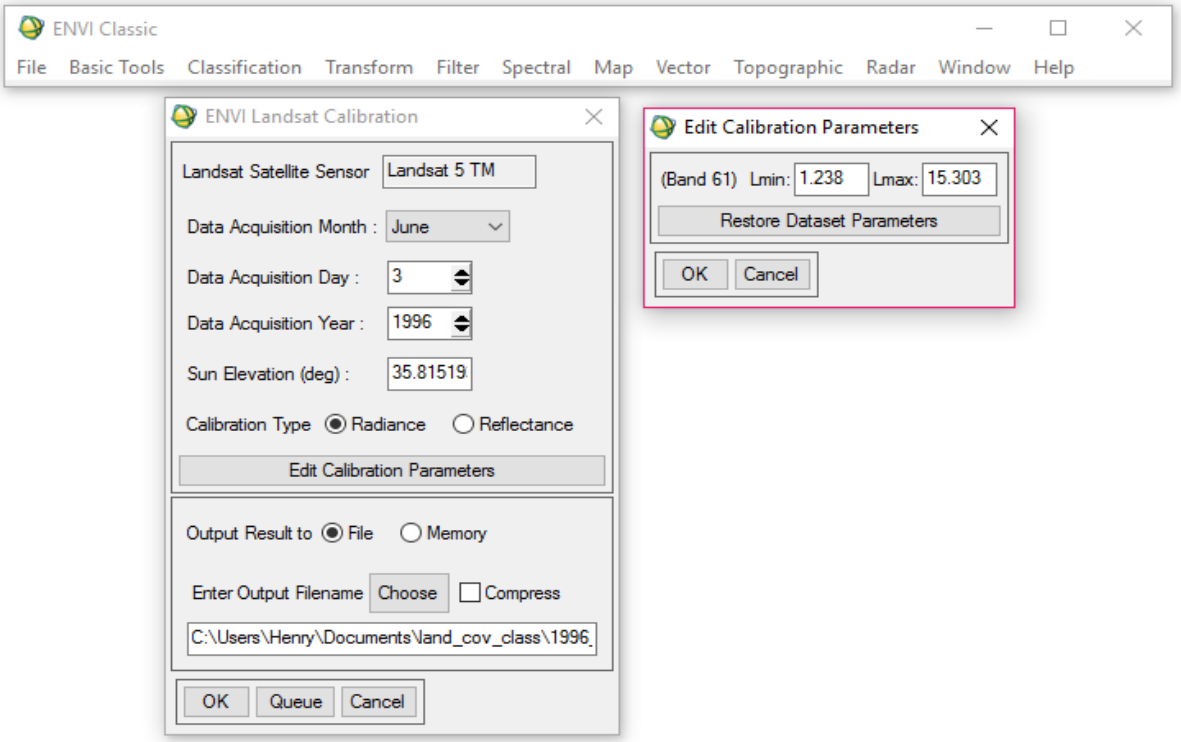

Figure 9: Radiometric calibration for Landsat 5 TM.

For Landsat 8 OLI-TIRS, radiance was calculated using the Radiometric callibration tool in ENVI 5.1. The data was inputted using the MTL.txt file. The output interleave was set to Band-Interleaved by –Line (BIL) format. The output data type was set to float point data. The scaling factor was automatically set at 0.1 (Figure 10).

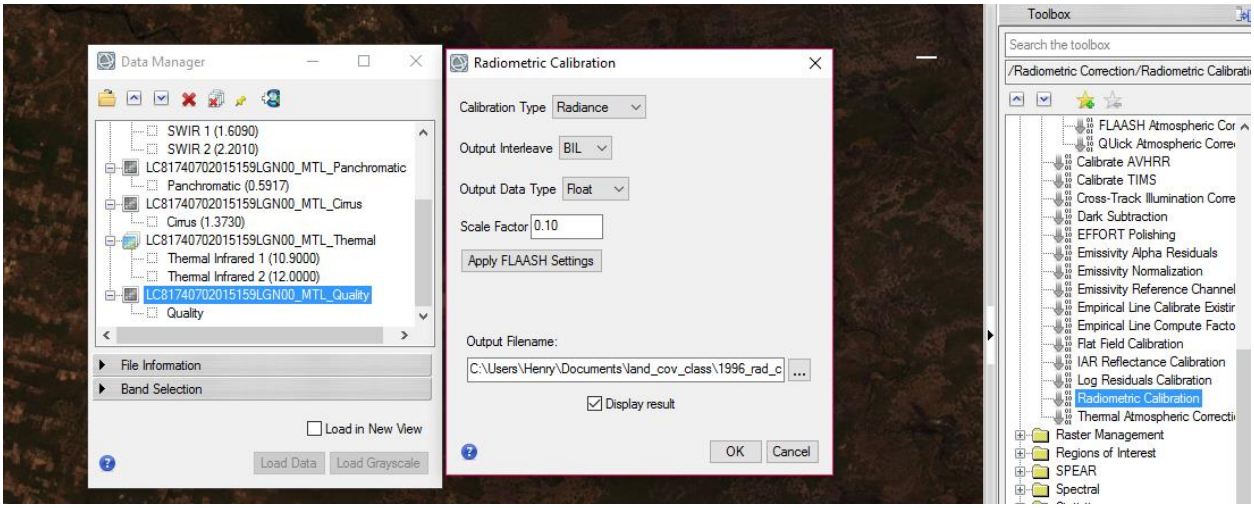

Figure 10: Radiometric calibration for Landsat 8 OLI- IRS.

To obtain an atmospheric corrected refelectance product, in both L5TM and L8 OLI-TIRS, the radiance file was inputted in the FLAASH atmospheric calibration module (Figure 11). The module automatically inputs some parameters from the radiance image while other parameters such as the flight date and time and ground elevation had to be manually inputted. Atmospheric model was set to tropical, Aerosal model to rural, Aerosal retrieval was automatically set to 2 – Band K-T (Kaufman-Tanre method). The input paramaeters differed from scene to scene. All reflectance products had values between 0 and 1. Landsat 5 TM bands 3,4,5 and 7 and Landsat 8 OLI-TIRS bands 4,5,6 and 7 were used.

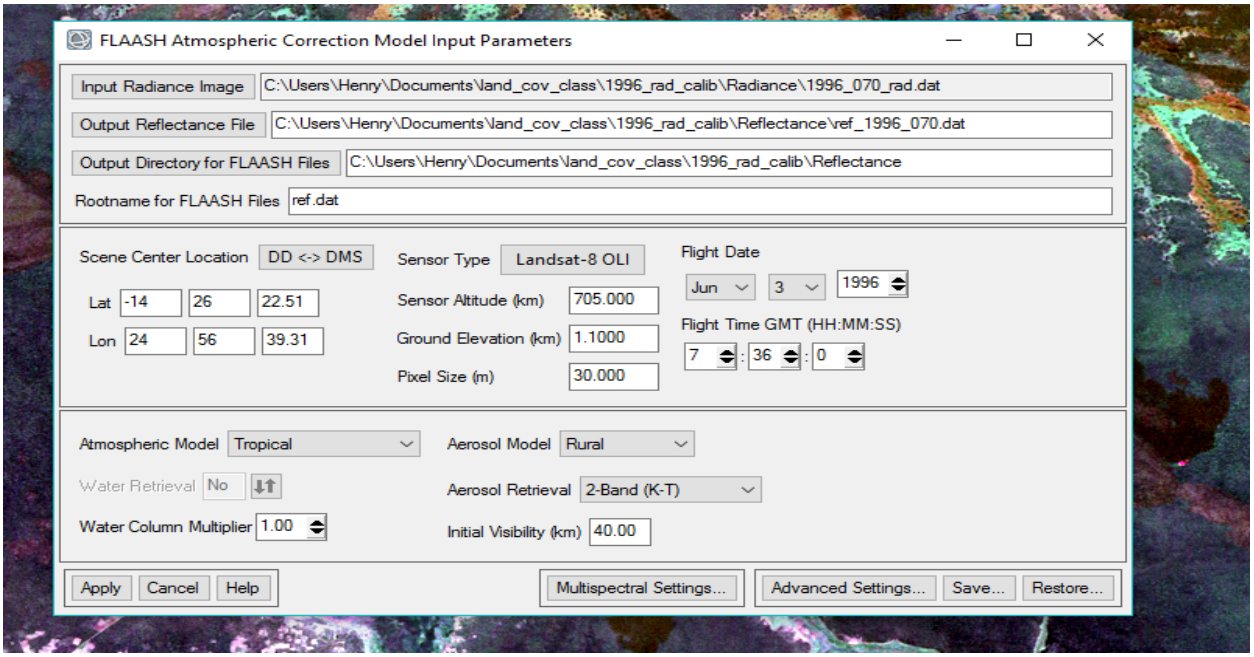

Figure 11: FLAASH atmospheric calibration for Landsat 5 TM and Landsat 8 OLI-TIRS.

To come up with the complete image for the study area the reflectance products for individual scenes were mosaicked in ENVI 5.1 using the seemless mosiac tool.

3.5 Detection and quantification of inundated area

Detection of the inundated area was done using the DFI for MODIS data and the Maximum likelihood classification process for Landsat data. Quantification of inundated area was based on the number of pixels within the delineated study area that were detected to contain water. The processes are explained in the proceeding sections.

3.5.1 Detection of inundated area

The detection of the inundated area from MODIS MOD901A was done using the Desert Flood Index algorithm (Equation 8; section 2.2.6). The raster calculator in ArcMap 10.3 was used to calculate the DFI from the MOD09A1 bands 1, 2, 4 and 6 as given in Table 1. For Landsat 8 OLI-TIRS the inundated area was detected using the maximum likelihood classification (equations 22 to 32; Section 2.4) in ENVI 5. (Full classification process is explained in section 3.8).

3.5.2 Determining image thresholding values for the DFI

The generated DFI indices from MODIS data were transferred into the Matlab environment for stretching and thresholding. The indexed greyscale images had intensities between -1 and 1 which had to be stretched to convert to all positives for thresholding in Matlab environment. After stretching, the threshold values were obtained using equation 10 in Matlab. Threshold values were then used to generate binary images with the 0:1 scale where 0 represented non inundated pixels and 1 for inundated pixel. See appendix 2 for calculated threshold values. In a few instances when the Otsu method in Matlab couldn't generate suitable threshold values, google earth image and the thermal band were used to aid with manually select threshold value. The object identifier tool was used to select the stretch value from pixels that were inundated. The raster calculator was then used to get a binary mask from the greyscale index with the manually generated value.

3.5.3 Pixel based validation of inundation extent with ground truth data

Validation of the DFI derived inundation extent maps was based on the use of classified image with Landsat 8 OLI-TIRS data. The Landsat flood mask was generated from a land cover classification class wetland/regularly flooded grassland, as explained in Section 3.8. The class wetland/regularly flooded grassland was extracted from the classified image which was validated with ground truth data as described in Sections 3.8 and 4.7. The extraction was done using the class identification number with the raster calculator in ArcMap 10.3. The portions of the same area for MOD09A1 and Landsat 8 OLI-TIRS binary masks were then compared.

3.5.4 Quantification of inundated area

Quantifying inundation extent was based on the number of pixels detected in the image as having been containing water at the time the image was captured. In the inundation mask, all pixels

containing water had a value of 1 while non-water containing pixels had a value of 0. The number of flooded and non-flooded pixels was obtained from the attribute table of each binary mask. The inundated area was then obtained by multiplying the number of water containing pixels with the pixel size, 500m by 500m in the case of MOD09A1 and 30 m by 30 m for Landsat 5TM. To obtain inundated area equation 56 was used (Wang et al. 2013).

$$A_i = (n)P_I * P_s \dots\dots\dots\dots\dots\dots\dots\dots\dots\dots\dots\dots\dots\dots\dots\dots\dots . [56]$$

Where; A_i = area inundated, $(n)P$= total number of inundated pixels in the image and P_s= pixel size of the imagery.

3.6 Analysis of variation, trend and correlation in inundation extent, hydrological and meteorological variables

Analysis of variation in inundation extent was done to ascertain the significance of the variations. There was need to characterise the direction of the trend in inundation extent for the period 2003 to 2013. Correlation analysis of inundation extent, hydrological and meteorological variables was done to appreciate the degree to which they are tied together. Daily discharge and water level data where obtained from the Department of Water Resources Development in Mongu, Western Zambia. Meteorological data was obtained from the Zambia Meteorological Department in Mongu, Western Zambia. The analyses were carried as described in the proceeding sections.

3.6.1 Analysis of variation in inundation extent with a one-way Repeated Measure ANOVA

After estimating inundated area for each given day of the study period a one-way Repeated Measure Analysis of Variance (RM ANOVA) was performed on selected dates (based on the MOD09A1 capture dates) from each data set, for ascending/peak and receding flood periods from 2003 to 2013, to test for significance in variations in inundation extent. In this study the inundation extent data for the period 2003 to 2013 was taken to represent the entire population. Each year represented a sample population made up of inundation extent on selected MOD09A1 based days of the year falling within the defined ascending/peak and receding categories of inundation cycles. The different compound hydrological, climatological and anthropogenic parameters experienced in each different year were taken as the treatments (categorically independent). The resultant inundation extent in each year was taken as the dependent variable. The rates of change in inundation extent were calculated using equation 57:

$$\frac{(I_i - I_k)}{\Delta T} \ldots\ldots\ldots\ldots\ldots\ldots\ldots\ldots\ldots [57]$$

Where I_i is inundation extent on day *i*, I_k is inundation extent on day *k* and ΔT is the change in time (number of days in this case). The changes in inundation extent were obtained and analysed using graphs.

3.6.2 Ascertaining trend in inundation extent

To ascertain the trend in inundation extent the Mann-Kendal test (equations 39 – 46; section 2.5.3) was used (Hirsch and Helsel, 2002). The inundation extent for the ascending and descending periods in each year were added and the mean obtained. The means were then used to determine the trend with the Mann-Kendall trend test for the period 2003 to 2013.

3.6.3 Correlation analysis of inundation extent, hydrological and meteorological variables

The Pearson r correlation (equations 17 and 18; section 2.3.2) was used to ascertain the extent to which inundation extent, discharge, water level, rainfall and temperature correlated. All data sets used were tested for outliers using the Dixon test (Hirsch and Helsel, 2002). Thereafter, the data sets were tested for homogeneity using the Pettit test (equations 34 to 37; section 2.5.1). The Pearson r correlation test was applied after the data sets were tested for outliers and homogeneity (Hirsch and Helsel, 2002). The data were analysed as guided in sections 2.3.2. and 2.5.1).

3.7 Evaluation of the role of the wetland in downstream flood regimes – the visual analysis of hydrographs and the statistical approaches

After establishing the correlation between inundation extent and the hydrologic variable discharge, the role of the wetland in downstream flow modulation was investigated using the rate of change in discharge upstream at Lukulu and downstream at Senanga Gauging stations. The assumption was that the flow into the wetland must equal the flow out of the wetland with Lukulu Gauge Station upstream as the entry point whereas Senanga Gauge Station at the downstream as the outlet as per recommended international guidelines by Bullock and Acreman (2003) for assessing if the wetland regulates flow. The difference between the inflows and the outflows was taken to account for the retention capacity of the wetland. Daily discharge data for each month during the ascending/peak and receding periods for the two stations for the year 1997 were used for analysis.

Prior to the construction of hydrographs, the two data sets were tested for normality in data distribution using the Kolmogorov-Smirnov Test (Hirsch and Helsel, 2002) and established their correlation using the Pearson r coefficient of correlation (equations 17 and 18; Section 2.3.2). The normality and correlation tests were prerequisite for determining the type of statistical test with which to analyse the data. For normality testing the data sets were split into three parts; the ascending/peak period from January to April, the receding period May to July and overall January to July. Normality tests were carried out for each month in the three splits of the data. The data were normally distributed, hence, a parametric test –paired t-test was used to test for significance in variations in the rate of change of daily discharge for the two stations. Hydrographs of daily discharge data were constructed and visually analysed. Then rates of change in daily discharge for each gauging station during ascending/peak and receding flood periods were calculated and analysed for variation using the paired t-test algorithm. The rate of change was calculated using equation 58 where Q_i and Q_k were the discharge for day *i* and day *k*. ΔT is the change in time between Q_i and Q_k..

$$\frac{(Q_i - Q_k)}{\Delta T} \dots\dots\dots\dots\dots\dots\dots\dots [58]$$

Murwira *et al.* (undated) used this approach to assess the role of Eastern Caprivi Wetland in downstream flood mitigation. In this study the rates of discharge for Lukulu and Senanga Gauge stations were paired. The data were drawn from the period January to July 1997 which was considered based on the analysis of discharge characterisation of the hydrological year (October 2003 to September 2004) hydrograph (Figure 8) and in tandem with flooding regimes in the wetland. The alpha threshold was set at 0.05. The results are presented in Chapter Four in form of descriptive statistics, tables and hydrographs.

3.8 Detection of land cover changes using the Maximum Likelihood Algorithm

Land cover-use change detection and analysis were done based on Landsat 5TM and Landsat 8 OLI-TRS imagery for the month of June in the years 1984, 1996, 2004 and 2015. The month of June was chosen to avoid overestimation of grassland and underestimation of forest land if the assessment is done when deciduous plants would have shade off leaves. Land cover classification maps were generated for each of the aforementioned years. The classification maps were then

compared in ENVI 5.1 and change statistics generated. Reflectance products as explained in Sections 2.2.2 to 2.2.5 were used in the land cover change detection exercise.

3.8.1 Supervised classification with Maximum Likelihood algorithm

Classification was done in ENVI 5.1 using the Maximum Likelihood Classification algorithm (Equations 23 – 32). Classification was based on Regions of Interest (ROI's) also known as training areas for each class. Selection of ROI's was based on uniformity and representation of the same class across the image. During the reconnaissance survey, a number of coordinate points from various land cover and use scenes were taken using a handheld Trimble Juno 3D Global Position System (DGPS) with accuracy level of 2 to 5 metres. These points were used to facilitate for creation of ROI's. Before classification was done statistics were generated to establish spectral separability. The ROI's and bands with the best separability statistics were used to construct, for instance, the spectral separability graph for Landsat 8 OLI-TIRS (Figure 12). The selected bands and ROI's for each year were eventually used for classification.

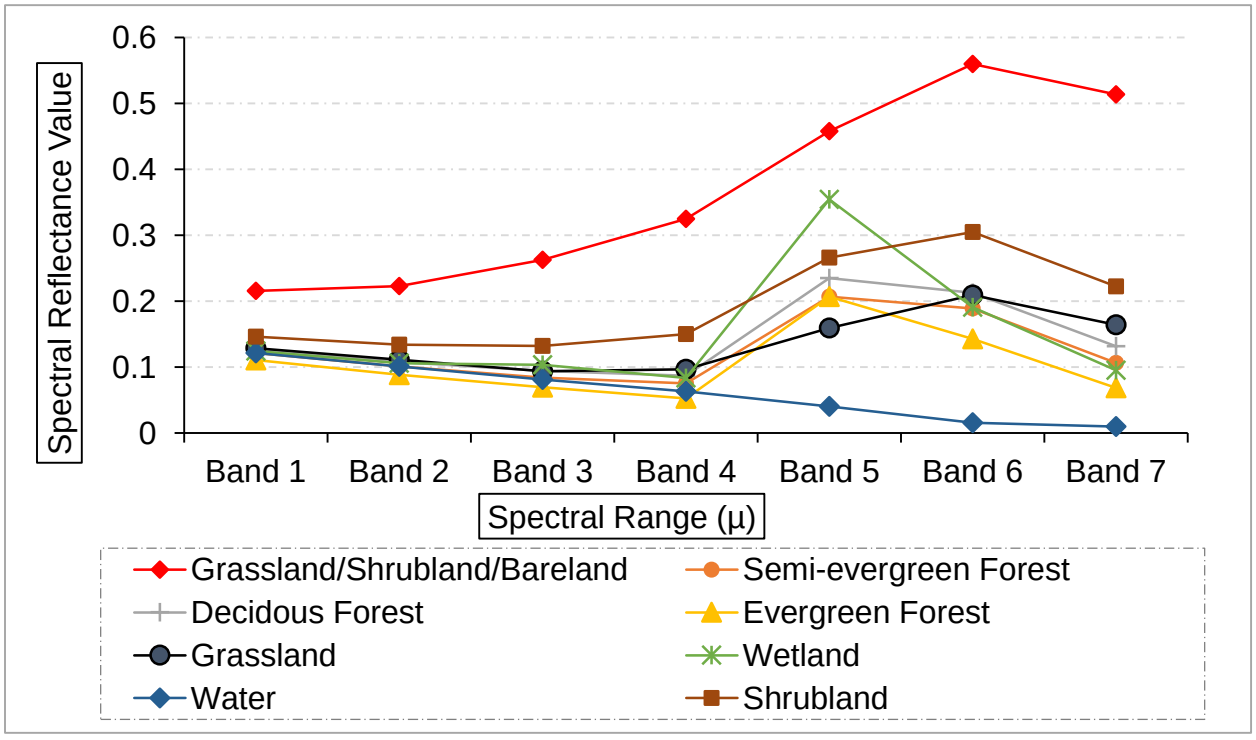

Figure 12: Spectral separability graph for Landsat 8 OLI-TIRS land cover classification for June 2015 for the study area in Western Zambia.

Landsat 5 TM bands 3,4,5 and 7 and Landsat 8 OLI-TIRS bands 4,5,6 and 7 were used in the study. The Jefferies-Matusita (JM) distance for all classes was between 1.99 and 2 which is an indication of good class separability (Lillesand *et al.* 2004; Ahmad and Quegan, 2012) of the selected ROI's. The Maximum Likelihood classification algorithm was then applied using the ROI's. In all Landsat images processed (for the years 1984, 1996, 2004 and 2015) and analysed the grassland/shrubland/bareland class had the highest separability factor and was followed by water bodies. Wetland and grassland were also relatively easy to separate from other classes. Forest classes had very similar spectral characteristics. Shrubland class had spectral characteristics similar to forest and grassland classes. For easy of extraction of statistics for analysis classes with similar parameters such as forest types and grasslands were merged to form compound classes such as forest land and grassland.

3.8.2 Post classification cleaning

Post classification cleaning was done before performing the accuracy assessment and the extraction of classification statistics. To solve the problem of isolated pixels occurring in classification images, the classes were sieved. Sieving of classes serves to remove isolated classified pixels using blob grouping. The sieve classes method looks at the neighbouring 4 or 8 pixels to determine if a pixel is grouped with pixels of the same class. If the number of grouped pixels in a class is less than the chosen value those pixels are removed from the class leaving black or unclassified pixels (ENVI user guide, 2009). In this study the sieving parameters were a group mean threshold of 2 and 4 neighbouring pixels. The parameters for the majority analysis were a majority kernel size of 7 by 7 with the centre pixel weight of 2. The majority analysis is used to change spurious pixels within a large single class to that class. When a chosen kernel size is applied the centre pixel in the kernel will be replaced with the class value that the majority of the pixels in the kernel has (ENVI user guide, 2009). Classes with similar attributes such as the various forest types were merged into a single class for easy of quantification and change assessment.

3.8.3 Accuracy assessment using the Confusion Matrix with ground truthing data

In this study, accuracy assessment of the land cover classification was done using the confusion matrix. The confusion matrix was generated based on ground truthing data. A minimum of 50 ground truthing points per class (the number of points increasing with the size of land cover classes) were generated using the stratified method in ENVI 5.1. A total of 350 points for ground-

truthing were generated. The shape file of the generated ground truthing points in ENVI 5.1 where converted to a compatible format KLM file in ArcGIS 10.3 for use in the Trimble Juno 3D GPS and Google Earth. The 2015 land cover classification map was validated with ground truth points. A hybrid method of obtaining ground truth data was used in which field obtained data and Google Earth based data were combined to validate the classification. During the field work campaign in June 2015 a total of 10 points for each class was validated based on actual ground data while the rest of the points for each class were validated using high resolution Google Earth software with the image for the month of June. The 10 ground based data were used as control for the Google Earth data. Accuracy assessment for the 1984 and 1996 classification map was done based on the 1986 and 1997 topographical maps while the 2005 FD/FAO land cover map was used to assess the accuracy of the 2004 land cover classification map. The accuracy assessment was done using the ground-truth with ROI's tool in the post classification module in ENVI 5.1.

3.8.4 Change detection and extraction of classification statistics

After the accuracy assessment, change detection was done using the Change Detection Module in ENVI 5.1. There was no need to perform a manual image co-registration as the input images were pixel based and the ENVI 5.1 change detection module automatically performs the function when the "initial state" and "final state" classification images are fed into the module. The co-registration is done using the initial state image as the base if re-projection or resampling is required (Lillesand et al. 2004). Change statistics were obtained for each period 1984 -1996, 1996 – 2004 and 2004 - 2015. Finally change statistics between 1984 and 2015 were obtained and analysed.

3.9 Trends analysis of hydrological and meteorological variables

Trends analysis is done to establish whether the probability distribution from which a given set of series of observation of a random variable arises has changed overtime. In this study, it was crucial that trends in some hydrological and meteorological variables were ascertained so as to help make inferences on the possible historical trends in inundation extent. The hydrological variable considered in this study was discharge and water level. The meteorological variables considered were rainfall and temperature. Data from two gauging stations namely Lukulu in the upstream and Senanga at the outlet of the wetland (Figure 3) were evaluated. Point based rainfall data for Mongu on the edge of the wetland and Kabompo Station in the upstream were considered. To validate the

rainfall trends for Kabompo Station, the Mansa Meteorological Station rainfall data were used. Mansa Station is in the same agro-ecological zone as Kabompo Station but in the far north east in Luapula Province of Zambia (Figure 13).

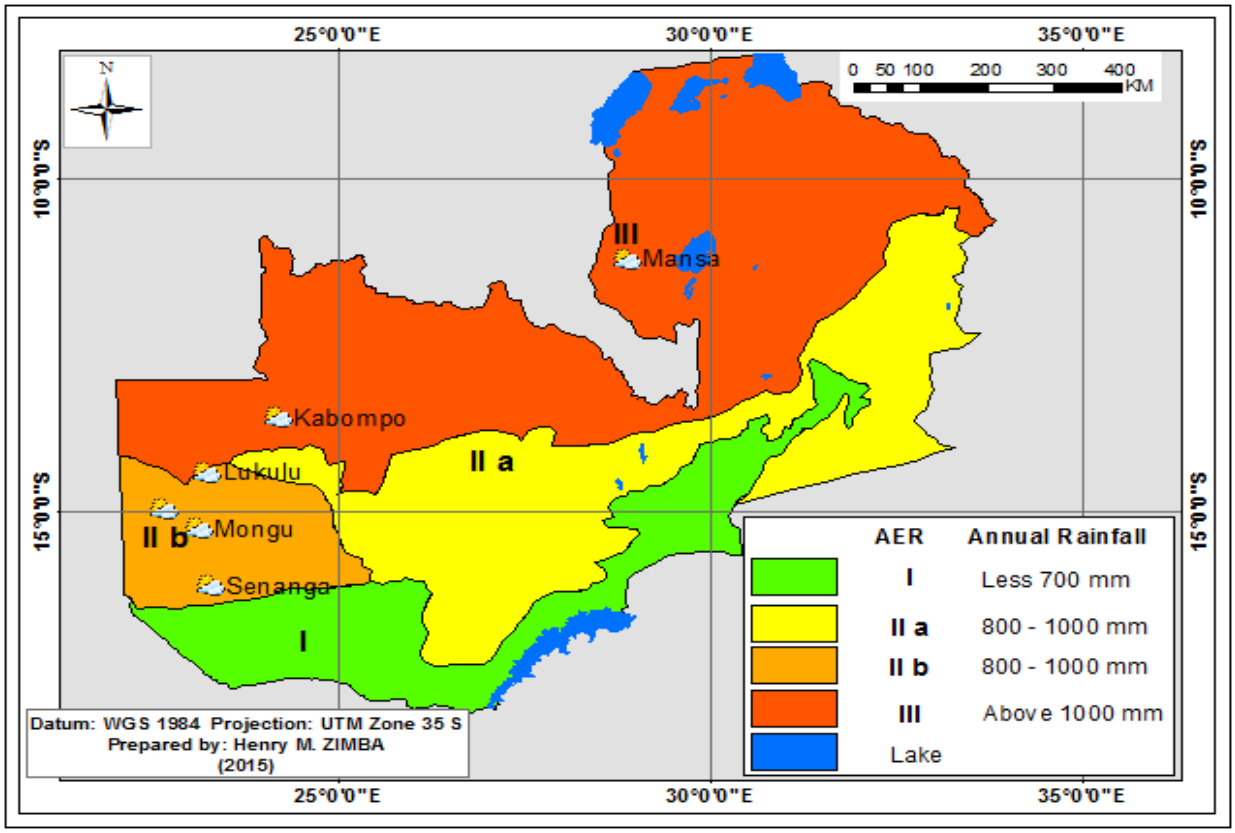

Figure 13: Location of meteorological stations used in the study in the Agro-Ecological Regions of Zambia.

Hydrological and meteorological data are known to be non-normal (Hirsch and Helsel, 2002); hence, for this study, a non-parametric test approach by way of the Pettit (equations 34 to 37; section 2.5.1) and the Mann-Kendall Test (equations 38 to 49; section 2.5.3) was used to evaluate data homogeneity and monotonic trends in discharge data for the period 1952 – 2003, 1952 – 2004 at Lukulu and Senanga hydrometric stations respectively. Only water level data for Senanga Gauge Station was available for the period 2000 to 2011. Hence, the trend in water level data was used to compare with the trend in inundation extent in the period 2003 to 2013. First, abrupt changes and trends were investigated in the mean monthly discharge time series with the seasonal Mann-Kendall Test. This was done to establish the months in which the changes occurred and also to evaluate the trends in monthly time series. Then the abrupt changes and trends in mean annual

discharge, rainfall and temperature time series were investigated. Based on the correlation between discharge and inundation extent, the trends in inundation extent were inferred from the trends analysis of the discharge data. The Pettit homogeneity test and the trends analysis with Mann-Kendall tests were performed in XLSTAT and MAKESENS. The change point detection and the trends test were done following procedures outlined in sections 2.5.1 to 2.5.6.

3.10 Data processing procedure in XLSTAT and MAKESENS

All data sets were prepared and inputted as per each software specifications. Computations of the time series data for trends analysis were done using statistical packages XLSTAT and MAKESENS. The homogeneity and seasonal Mann-Kendall tests were also performed in XLSTAT and the MAKESENS software. In XLSTAT, test parameters were pre-set, as highlighted below, before running the analysis. For the Pettit Homogeneity Test the alpha level was set at 0.05. For the Seasonal Mann-Kendall trends test, on the mean monthly discharge values, the parameters set were; alpha level (α) at 0.05, Hamed and Rao auto-correction at 0.05 and 0.01 confidence intervals and run at 12-month cycle serial dependence. In the two tailed test the Null Hypothesis (H_0) was that there was no trend in the time series while the Alternative Hypothesis (H_a) was that there was a trend. If the computed *p-value* was < 0.05 the H_0 was rejected and the H_a accepted. If the computed *p-value* was > 0.05 the H_0 was accepted. For the mean annual discharge, rainfall and temperature time series, the Excel based application Makesens was used to analyse the trends with alpha levels at 0.1, 0.01, 0.05 and 0.001. The Sens slope helped to visualise the trends and also gave the annual rate of change values for each variable. The results of the trends analysis are presented in Chapter Four in form of descriptive statistics, tables and graphs.

CHAPTER FOUR: RESULTS

The findings of the study are addressed in this chapter with reference to the five objectives given in Chapter 1.

4.1. Detection of inundated area with the DFI and extraction of inundation binary masks

The inundation binary mask generated from the DFI grey scale image aligned with the composite image of the MODIS data (Figure 14A-C). The number of inundated pixels were extracted from the attribute table of each binary mask (Figure 14 C). The pixels with the value 0 (Black in Figure 14 C) represented non-inundated areas whereas pixels with the value 1 (White in Figure 14 C) represented inundated areas.

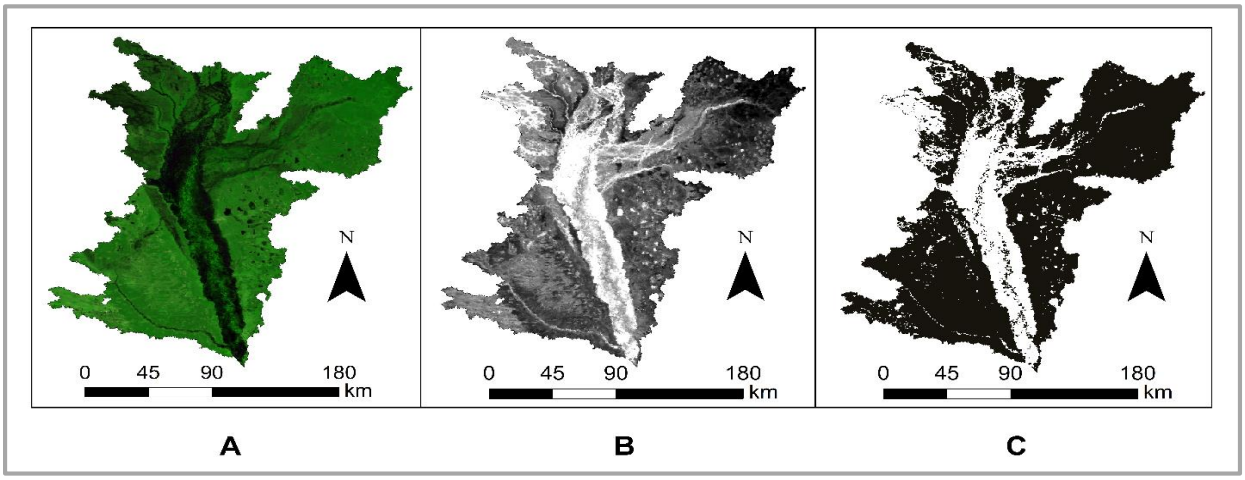

Figure 14: Images of the false colour composite (A), Stretched greyscale DFI (B) and the resultant binary mask (C) for the Barotse Wetland, Western Zambia.

4.2 Pixel based validation of flood maps

Segments of Landsat 8 OLI-TIRS (A) and MOD09A1 (B) flood masks for the month of June, 2015 obtained on the 06th and 07th of the month respectively were compared (Figure 15). Landsat and MODIS have different capture and revisit times. The inundation extent on 7th June, 2015 under MOD09A1 was at 1,356 Km^2 while inundation extent for Landsat 8 OLI-TIRS on the 6th of June, 2015 was 1,341.71 Km^2 a difference of 14.29 Km^2 (Table 5).

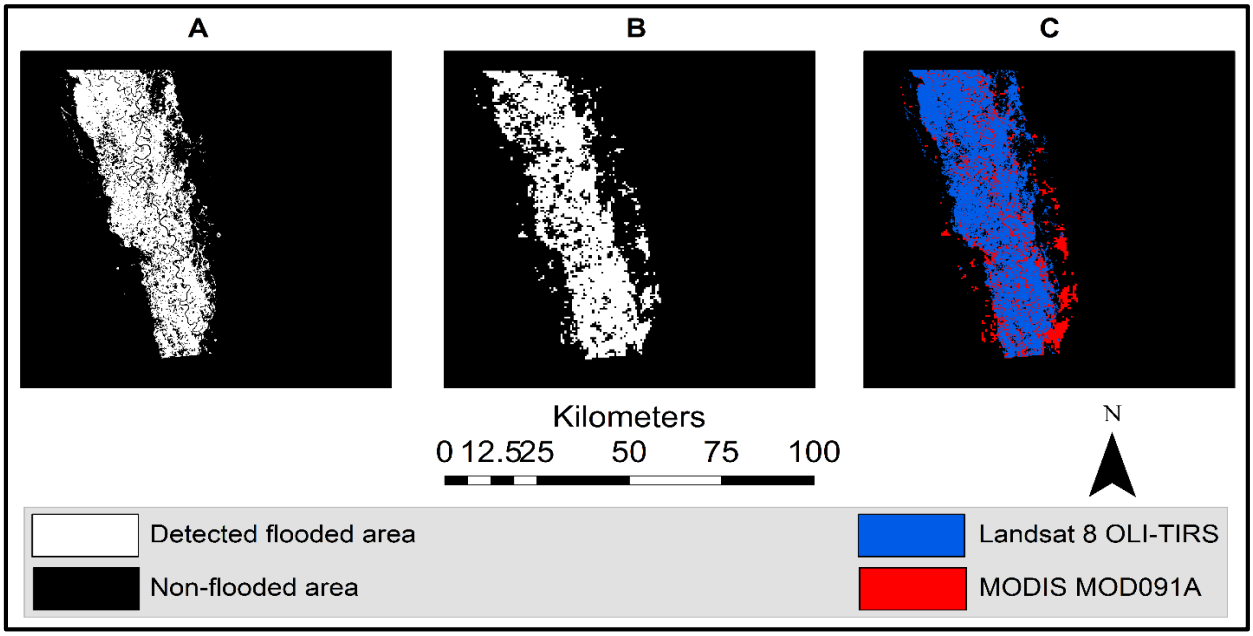

Figure 15: Comparison of Landsat 8 OLI-TIRS (A) and MOD09A1(B) inundation masks. Images acquired on the 6th and 7th June, 2015 for Landsat and MODIS respectively. In C is an overlay of Landsat 8 OLI-TIRS mask on MOD09A1 inundation mask for the Barotse Wetland, Western Zambia.

Table 5: Comparison of estimated inundation extent under Landsat 5TM and MOD09A1 DFI indices for April in the Barotse Wetland, Western Zambia.

Data Type	Day	Date	Pixel count	Pixel size(Km^2)	Area (Km^2)
Landsat	160	06th June, 2015	1490790	0.0009	1,341.71
MODIS	161	07th June, 2015	5424	0.25	1,356.00
Difference Area					**14.29**
Accuracy Percent(%)					**98.95**

The accuracy percentage between the DFI generated flood mask and the Maximum Likelihood Classification, validated with ground truthing data, was 98.95 (Table 4). The difference in inundated area can be attributed to the differences in the spectral and spatial resolutions of Landsat 8 OLI-TIRS and MODIS as well as the methods used to extract the flood masks. For instance,

Landsat has a spatial resolution of 30m by 30m while the MOD09A1 used has a 500m by 500m resolution.

4.3 Quantification of inundated area

Inundation extent at different days of a flood cycle was detected (Figure 16). For example, inundated areas at varying flows, ascending/peak (days 313, 033 and 097) and for receding period (days 113, 161 and 185) of the hydrological year 2003/2004 were observed (Figure 16).

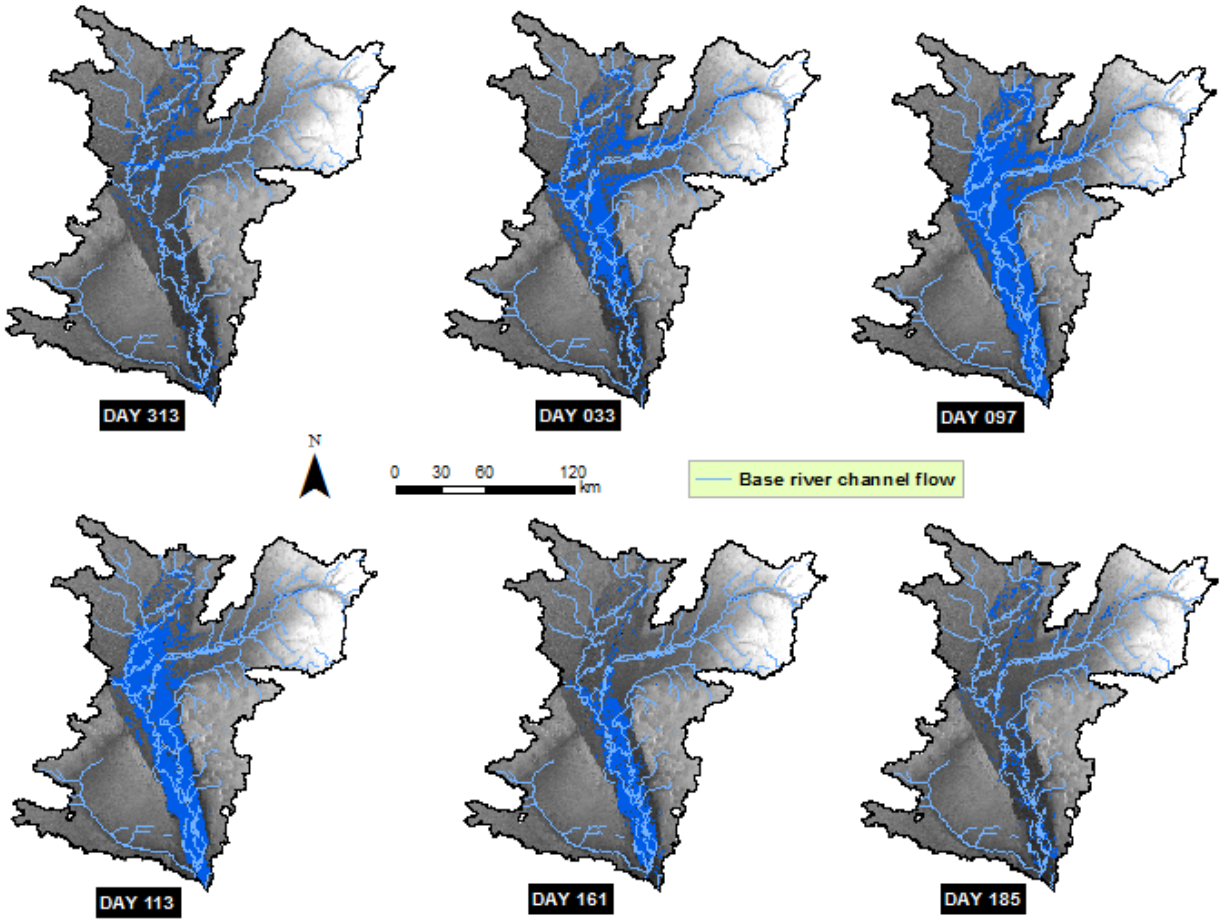

Figure 16: Changes in wetland inundated area (Blue) on; (A) 9th November, 2003 (Day 313), (B) 2nd February,2004 (Day 033), (C) 6th April (Day 097) (D),22nd April (Day 113), (E) 9th June (Day 161) and (F) 3rd July (Day 185) of the hydrological year 2003/ 2004 - overlaid a Digital Elevation Model (DEM).

Flood maps showed that the first areas to be inundated were also the first to have the floods recede and the last areas to be inundated were also last to have the flood recede. For instance, in Figure 16, on day 033, the upstream and the middle part of the wetland was more flooded than the

downstream. On the other hand, day 161 shows receded inundation in the upstream while the middle and downstream areas were still inundated. This phenomenon indicates differences in the onset and recession of flood within the wetland. Quantification of the detected inundated area was pixel based as shown in the calculations for the year 2004 in Table 6. The calculated area during ascending/ peak and receding flood periods in the study period (2003 to 2013) is given in Appendix 2. Two inundation extent peaks in 2004 with the first occurring on day 089 in March at 6102.24 Km^2 and the second on day 105 in April at 6372.75 Km^2 were observed. The day 097 in April showed a minimal reduction in the inundation extent from 6102.24 Km^2 on day 089 to 5,837.5 Km^2 on day 097 rising to 6,372.75 Km^2 on day 105 and eventually starting to steadily decline from day 113. Inundation extent starts to increase from day 305 in November (Table 6 and Figure 17) which is at the start of the rain season.

Table 6: Computed estimates of inundated area based on the MOD09A1 derived DFI's for the year 2004, Barotse Wetland, Western Zambia.

Day	Pixel count	Pixel size(Km^2)	Area (Km^2)	Day	Pixel count	Pixel size(Km^2)	Area (Km^2)
33	14304	0.25	3576.00	209	3977	0.25	994.25
89	24409	0.25	6102.24	217	3759	0.25	939.75
97	23350	0.25	5837.50	225	1851	0.25	462.75
105	25491	0.25	6372.75	233	1320	0.25	330.00
113	19191	0.25	4797.75	241	1205	0.25	301.25
121	18450	0.25	4612.50	249	1188	0.25	297.00
129	16754	0.25	4188.50	257	1123	0.25	280.75
137	15028	0.25	3757.00	265	1105	0.25	276.25
145	13910	0.25	3477.50	273	1098	0.25	274.50
153	11671	0.25	2917.75	281	1088	0.25	272.00
161	9938	0.25	2484.50	289	1069	0.25	267.25
169	7849	0.25	1962.25	297	1078	0.25	269.50
185	4486	0.25	1121.50	305	1835	0.25	458.75
193	5088	0.25	1272.00	313	2532	0.25	633.00
201	4646	0.25	1161.50	345	2589	0.25	647.25

The differences in inundation extent within a hydrological year is shown in Figure 17. As expected, inundation extent was widest during the high flow and water level period between day 089 and

day 105 (March – April) of the year 2004 (Figure 17). It was difficult to obtain cloud free images for the ascending/peak period, between day 297 to day 081, hence inundation on those cloudy days could not be assessed resulting in fewer data as compared to the receding period, day 105 to day 257 which had more due to many cloud free days (Figure 17).

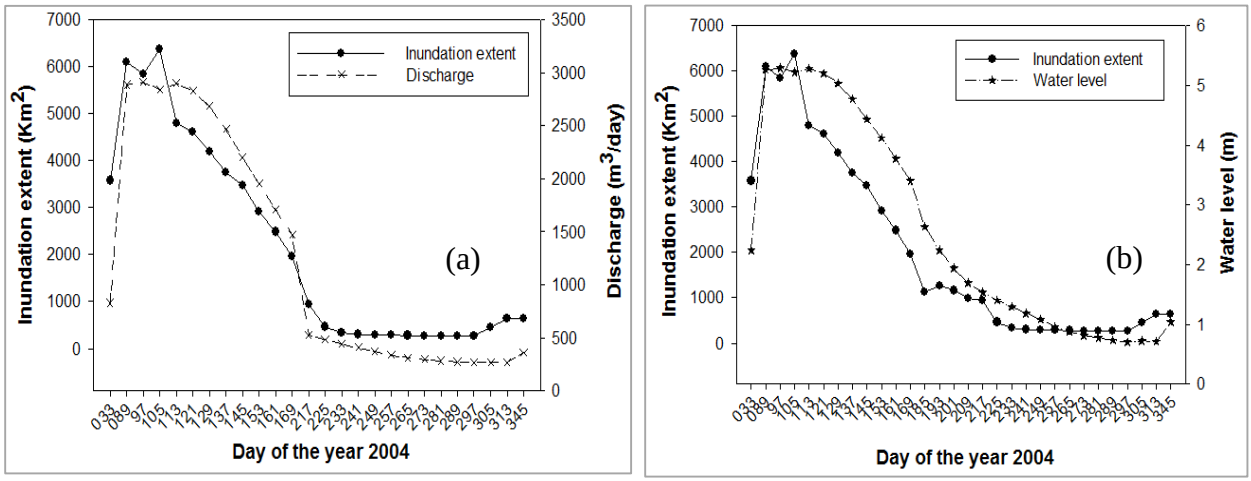

Figure 17: (a) Inundation extent and discharge (b) Inundation extent and water level at Senanga Gauge Station in the hydrological year 2003/2004 in the Barotse Wetland, Western Zambia.

Inundation extent related to discharge and water level in the same way. Inundation extent increased or decreased with increase or decrease in discharge and water level (Figure 17). The annual distribution of inundation extent was very much similar to the annual distribution of stream discharge and water level with peak periods between the 75th and 105th day of the year (March-April) (Figure 17). Even during the driest period, from about day 225 to day 281 (August to October), there was a significant area of about 300 Km^2 inundated (Table 6 and Figure 17). The inundation extent begins to recede from Day 113 (end of April) and completes retreats by Day 217 (end of July) and thus follows the stream discharge and water level pattern (Figure 17).

4.4 Variations and trend in inundation extent during the period 2003 to 2013

4.4.1 Within and inter-annual variations in inundation extent for the period 2003 to 2013

The one-way repeated measure ANOVA test revealed significant (*p-value* = 0.005) variations across inundation cycles from 2003 to 2013. During the ascending/peak period the lowest mean in inundation extent was noted in 2005 at 2856.5 Km^2 while the highest mean was recorded in the year 2010 at 6362.75 Km^2 (Table 7). Varying standard deviations (SD) were observed in each year

within the ascending period with the highest SD ± 513.91 recorded in 2009 and the lowest SD ± 30.748 recorded in 2010 (Table 7). The value of the SD's indicates the magnitude of the variations in inundation extent within a particular year.

Table 7: ANOVA statistics for the inundation extent during the ascending/peak period for the years 2003 to 2013 in the Barotse Wetland, Western Zambia.

Year	N	Missing	Mean	SD	SEM
2003	3	0	5408.98	428.90	247.63
2004	3	0	6104.16	267.63	154.52
2005	3	0	2856.50	274.07	158.23
2006	3	0	5429.67	340.86	196.80
2007	3	0	5508.08	377.84	218.15
2008	3	0	5568.00	466.66	269.43
2009	3	0	5930.75	513.91	296.71
2010	3	0	6362.75	30.75	17.75
2011	3	0	6214.42	148.58	85.78
2012	3	0	5785.75	376.97	217.64
2013	3	0	6214.58	67.69	39.08

N= Number of observations, SD = Standard Deviation, SEM = Standard Error of Mean

With degrees of freedom (10,20) (Table 8) a critical value of 2.35 was obtained from the F-distribution table at $\alpha = 0.05$. According to the RM-ANOVA (Hirsch and Helsel, 2002) if the Fcal (27.211) > Fcrit (2.35) and *p-value* of <0.001 (which is < 0.05), the results are significant at the 95 percent confidence level. The null hypothesis (H_0) for the ascending/peak period was that there was no variation in inundation extent while the alternative hypothesis (H_a) was that there was variation in the inundation extent.

Table 8. ANOVA statistics of inundation extent during the ascending/ peak period for the period 2003 to 2013 in the Barotse Wetland, Western Zambia.

Source of Variation	DF	SS	MS	F	P
Between Subjects	2	424666.26	212333.10		
Between Treatments	10	27997791.80	2799779	27.21	<0.01
Residual	20	2057798.64	102889.9		
Total	32	30480256.70			

DF= degree of freedom, SS= Sum of squares, MS = Mean of squares, F= F-ratio (test statistic), P= significace level

As the test was significant (*p-value* < 0.05) the H_0 that there was no difference was rejected and the H_a that there was difference was accepted. This result means that differences in the mean values of inundation extent among the ascending/peak days in each year assessed (2003-2013) were greater than would be expected by chance indicating existence of a statistically significant differences. The box plots (Figure 18) augment the RM-ANOVA test results (Table 8) as they show that the location of mean values in inundation extent during the ascending/peak period differed in each year confirming existence of variation. The smaller the box plot the less within group variations existed and the bigger the box plot the more within group variations existed. Year 2010 had the highest mean and the least within group variations while the year 2005 had the lowest but the year 2009 had the most within group variations (Figure 18).

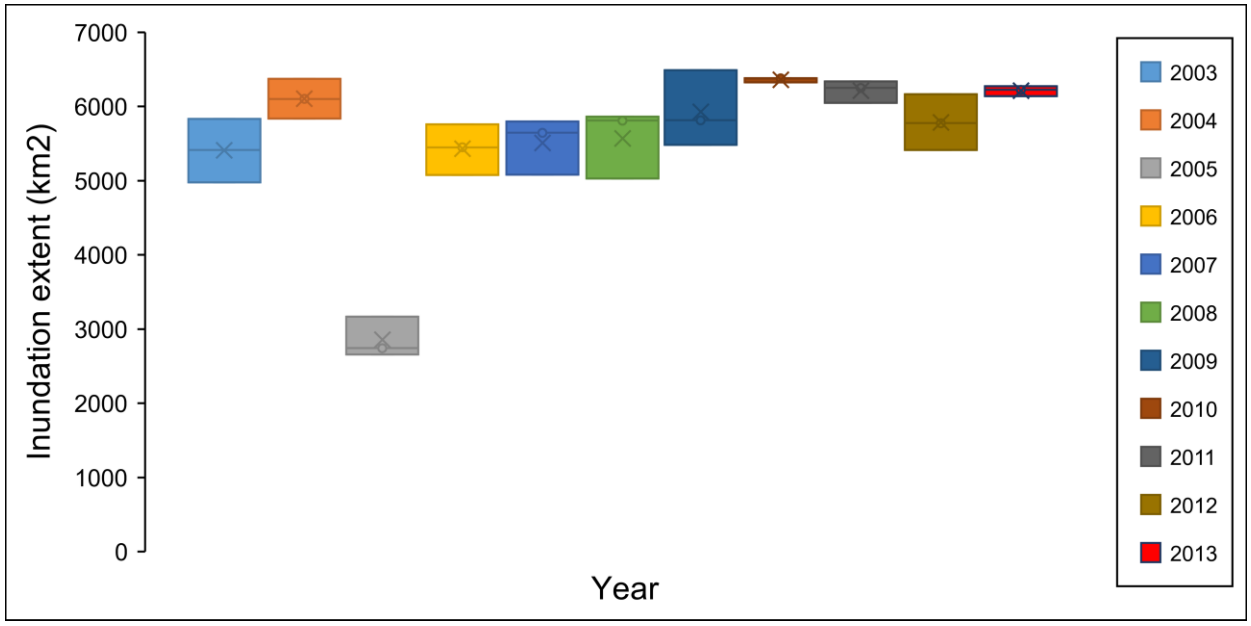

Figure 18: Box plots showing location of the mean in inundation extent during the ascending/peak period from 2003 to 2013 in the Barotse Wetland, Western Zambia.

Isolation of the significant from the non-significant difference of means with all Pairwise Multiple Comparison Procedure (Holm, 1979) at overall significance level = 0.05 showed that only the years 2005 differed significantly with other years with the highest mean difference between the year 2005 and 2010 and lowest between 2003 and 2005 (Table 9) (full results in Appendix 3a).

Table 9: All Pairwise Multiple comparison results for the ascending/peak period in the Barotse Wetland, Western Zambia.

Comparison	Difference of Means	P value	P value <0.05
2010 vs. 2005	3506.25	<0.01	Yes
2013 vs. 2005	3358.08	<0.01	Yes
2011 vs. 2005	3357.92	<0.01	Yes
2004 vs. 2005	3247.66	<0.01	Yes
2009 vs. 2005	3074.25	<0.01	Yes
2012 vs. 2005	2929.25	<0.01	Yes
2008 vs. 2005	2711.5	<0.01	Yes
2007 vs. 2005	2651.58	<0.01	Yes
2006 vs. 2005	2573.17	<0.01	Yes
2003 vs. 2005	2552.48	<0.01	Yes

In the receding period the year 2005 had the lowest SD at ±294.508 Km^2 while the highest SD was recorded in the year 2011 at ±1107.71 Km^2 (Table 10). The different SD's indicate existence of variations in inundation extent within flood season across the years. The lower the SD the less the variation and the higher the SD the more the variations in inundation extent within a flood cycle. The lowest mean in inundation extent was observed in 2005 at 2470.63 Km^2 while the highest mean was recorded in the year 2011 at 5099.56 Km^2 (Table 10).

Table 10: ANOVA statistics for the inundation extent for the receding period for the years 2003 to 2013 in the Barotse Wetland, Western Zambia.

YEAR	N	Missing	Mean	SD	SEM
2003	4	0	4185.69	848.35	424.17
2004	4	0	4338.94	464.27	232.13
2005	4	0	2470.63	294.51	147.25
2006	4	0	4300.50	778.40	389.20
2007	4	0	4135.06	672.13	336.07
2008	4	0	3883.44	523.24	261.62
2009	4	0	4059.63	739.05	369.53
2010	4	0	4680.94	585.95	292.98
2011	4	0	5099.56	330.23	165.11
2012	4	0	4450.81	471.23	235.61
2013	4	0	4377.44	1107.71	553.85

N= Number of observations, SD = Standard Deviation, SEM = Standard Error of Mean

The RM-ANOVA test produced degrees of freedom (10,30) and F-value of 15.73 (Table 11). From the F-distribution table a critical value of 2.17 was obtained at $\alpha = 0.05$. The Fcal (15.733) > Fcrit (2.17) and *p-value* of <0.01 (which is < 0.05) indicating that the results were significant at the 95 percent confidence level. The H_0 that there was no variation in inundation extent during the receding period was rejected and the H_a that there was variation was accepted.

Table 11: ANOVA statistics for the inundation extent for the receding period for the year 2003 to 2013 in the Barotse Wetland, Western Zambia.

Source of Variation	DF	SS	MS	F	P
Between Subjects	3	11142465	3714155		
Between Treatments	10	17100357	1710036	15.733	<0.01
Residual	30	3260753	108691.8		
Total	43	31503575			

DF= degree of freedom, SS= Sum of squares, MS = Mean of squares, F= F-ratio (test statistic), P= significace level

The box plots for the mean values (Figure 19) show that there were variations in the location of mean of inundation extent during the receding period with the highest and lowest means recorded in 2011 and 2005 respectively. The year 2005 had the least within group variation while the year 2013 had the highest within group variation.

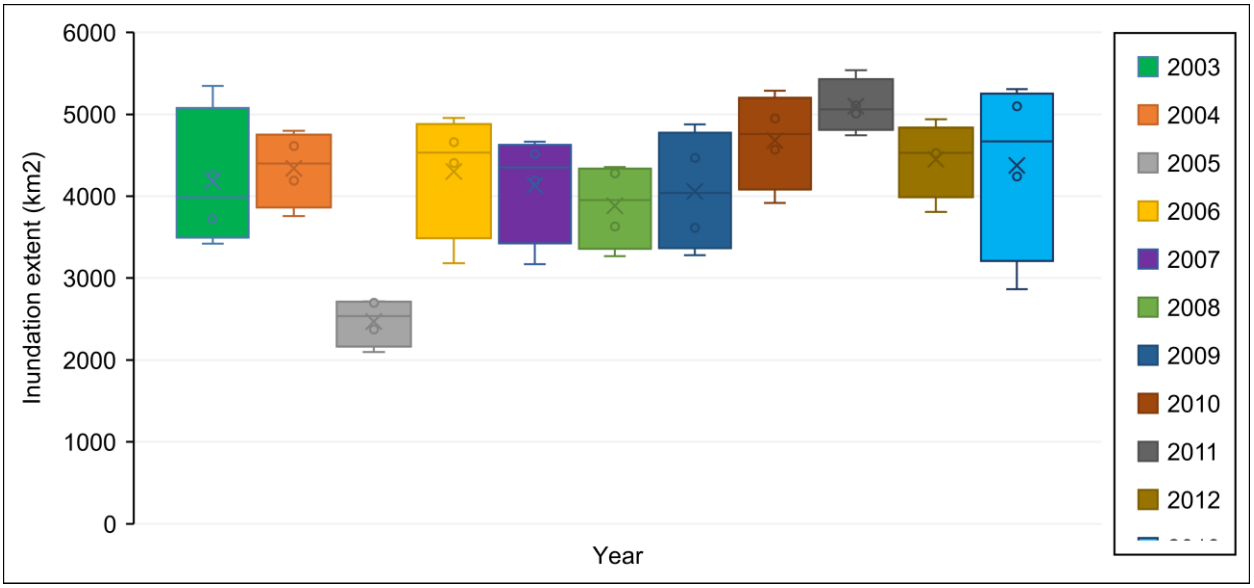

Figure 19: Mean inundation extent during the receding period between 2003 and 2013 in the Barotse Wetland, Western Zambia.

The all Pairwise Multiple Comparison Procedures (Holm-Sidak method) with an overall significance level of 0.05 showed significant diffrences in the means of inundation extent between several years. The highest difference of mean of 2628.94 Km^2 observed between the year 2005 and 2011 and the lowest of 1412.81 Km^2 observed between 2005 and 2008. Other significant variations were observed between the year 2011 and 2007, 2008, 2009 with the lowest mean difference of 964.50 Km^2 between the year 2007 and 2011 (Table 12). The results of the all pair wise comparison (Table 12) which shows the highest mean difference between the year 2005 and 2011 augments the observations made in Figure 19 (full results in Appendix 3b).

Table 12: All Pairwise Multiple comparison results for the receding period inundation extent for the year 2003 to 2013 in the Barotse Wetland, Western Zambia.

Comparison	Difference of Means	P value	P value <0.050
2011 vs. 2005	2628.94	<0.05	Yes
2010 vs. 2005	2210.31	<0.05	Yes
2012 vs. 2005	1980.19	<0.05	Yes
2013 vs. 2005	1906.81	<0.05	Yes
2004 vs. 2005	1868.31	<0.05	Yes
2006 vs. 2005	1829.88	<0.05	Yes
2003 vs. 2005	1715.06	<0.05	Yes
2007 vs. 2005	1664.44	<0.05	Yes
2009 vs. 2005	1589.00	<0.05	Yes
2008 vs. 2005	1412.81	<0.05	Yes
2011 vs. 2008	1216.13	<0.05	Yes
2011 vs. 2009	1039.94	<0.005	Yes
2011 vs. 2007	964.50	<0.005	Yes

When the rates of change in inundation extent were computed and analysed it was observed that from year to year there were differences in how long it took for the inundation extent to increase or decrease. For example, the year 2004, during the ascending period between day 033 and day 089 there was a positive rate of change indicating an increase in the inundation extent (Figure 20). On the other hand, the period between day 089 and day 097 showed significant negative rate of change indicating decrease in inundation extent. From day 113 the trend is that of reduction in inundation though at varying rates. The downward trend seen from day 113 signifies the onset of the recession in the inundation extent (Figure 20) and corresponds to the start of reduction in stream discharge as indicated in Figure 8.

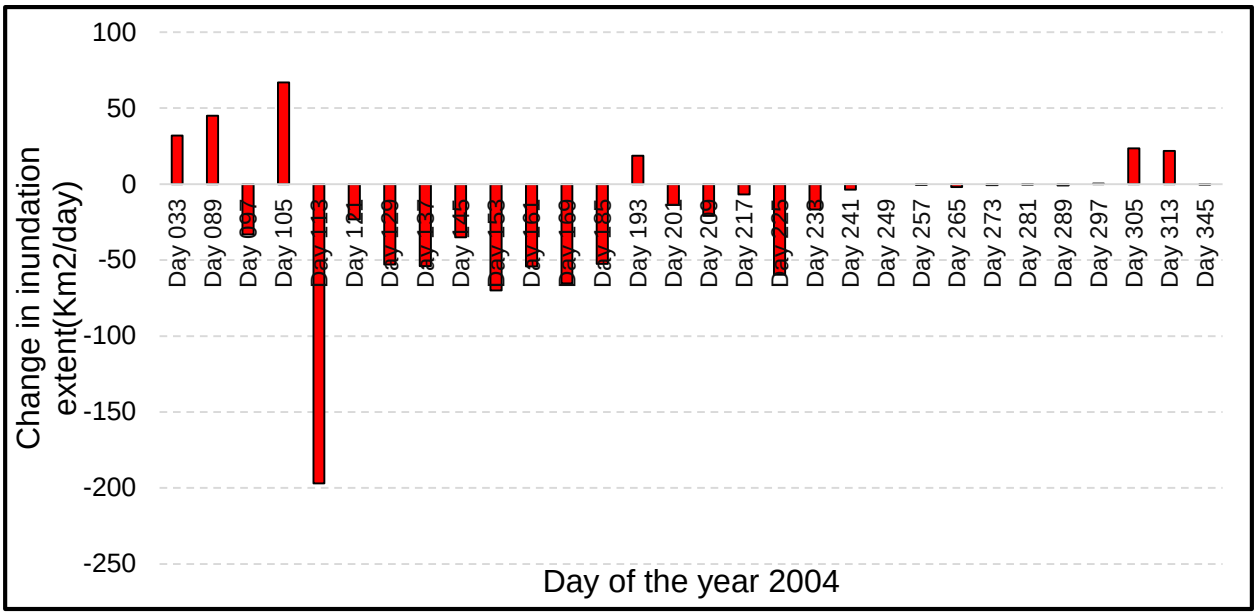

Figure 20: Indexes of the rate of change in increase and decrease in inundation extent during the ascending period and the descending period for the year 2004 in the Barotse Wetland, Western Zambia.

Further analysis showed negative rate of change between day 201 and day 305. From day 305 (end of October) inundation extent begins to increase with a significant rise in the rate of increase between day 305 and day 313 (November) (Figure 20). Inundation extent rate of change indices for each year were as shown in Appendix 4. The rates of change in inundation extent across the period 2003 to 2013 showed that there were variations in the rates (appendix 4). For instance, on day 081 (March) the rate of change in inundation extent was highest in the year 2006 and lowest in the year 2012. On day 129 (May) the year 2010 recorded the highest rate of change while 2005, 2006 and 2011 had the lowest rates of change in inundation extent during the same period. In contrast, on the same day 129 the year 2007 recorded a negative rate of change as opposed to the rest of the years that recorded a positive rate of change in inundation extent (appendix 4). On day 137 in the year 2010 there was a significant positive rate of change in inundation extent while the rest of the years assessed recorded a negative rate of change (appendix 4). Other interesting observations made are those for the years 2007 and 2013 on day 049 (in February) and day 073 (in March) respectively (appendix 4), that recorded negative rates in inundation extent in the time when the flood extent is expected to increase.

4.4.2 Trend in inundation extent for the period 2003 to 2013

For the period 2003 to 2013, the Mann- Kendall test showed a significant rising trend (Figure 21) in inundation extent with Z statistic of 1.87 and *p-value* <0.05 at alpha level 0.05 (see full results in Appendix 3c).

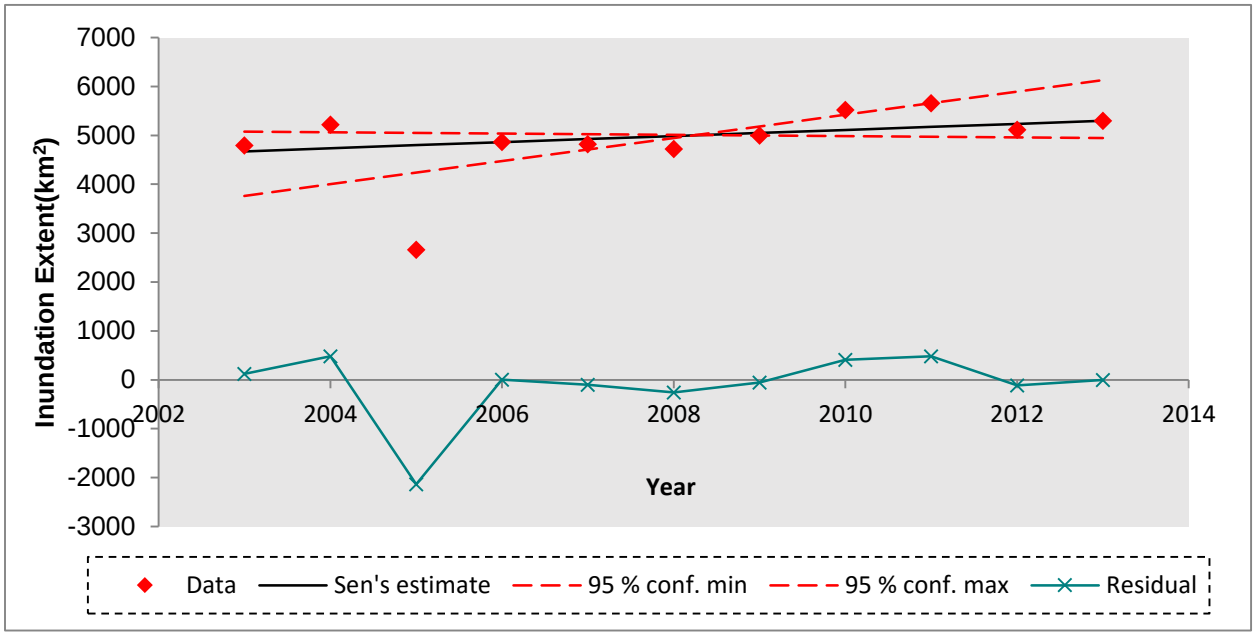

Figure 21: Mann- Kendall Trend of the annual means of inundation extent for the time space 2003 to 2013 in the Barotse Wetland, Western Zambia.

4.5 Correlation between inundation extent, discharge and trend in water level

The inundated area and the outflow at Senanga Gauge Station for the year 2004 were significantly correlated throughout the year with correlation coefficient of 0.95. The coefficient of determination (R^2) was 0.91 with *p-value* < 0.01 at alpha of 0.05 (Table 13 and Figure 22). When compared water level with inundation extent showed a similar relationship as was the case with discharge with a coefficient of correlation (R) of 0.94 and coefficient of determination (R^2) of 0.89 (Table 13). The interpretation is that inundation extent increases or decrease with increase or decrease in discharge and water level (Figure 22 a-b). The Mann-Kendall trends tests showed a rising trend in water level for the period 2000 to 2011 with Z statistic of 2.67 with p-value <0.05 at alpha level 0.5 (Figure 22 c) (full test results in appendix 3 d). The trend in water level is very similar to the trend in inundation extent (Figure 21) for the period (discharge data for the period 2003 to 2013 was not available. Water level data was only available up to 2011).

Table 13: Pearson r correlation for inundation extent, discharge and water level at Senanga Gauge Station for the year 2004, Barotse Wetland, Western Zambia.

Var	Obs	Min	Max	Mean	SD	R	R^2	P value	Alpha
Q	26	263.54	2905.43	1251.49	1096.03	0.95	0.91	< 0.05	0.05
WL	26	0.7	5.29	2.61	1.91	0.94	0.89	<0.05	0.05
IE	26	267.25	6372.75	2146.01	2139.34				

Var = Variable, IE = Inundation Extent, Q = discharge, Obs = Number of observations, SD = Standard Deviation, R = Coefficient of Correlation, R^2 = coefficient of determination

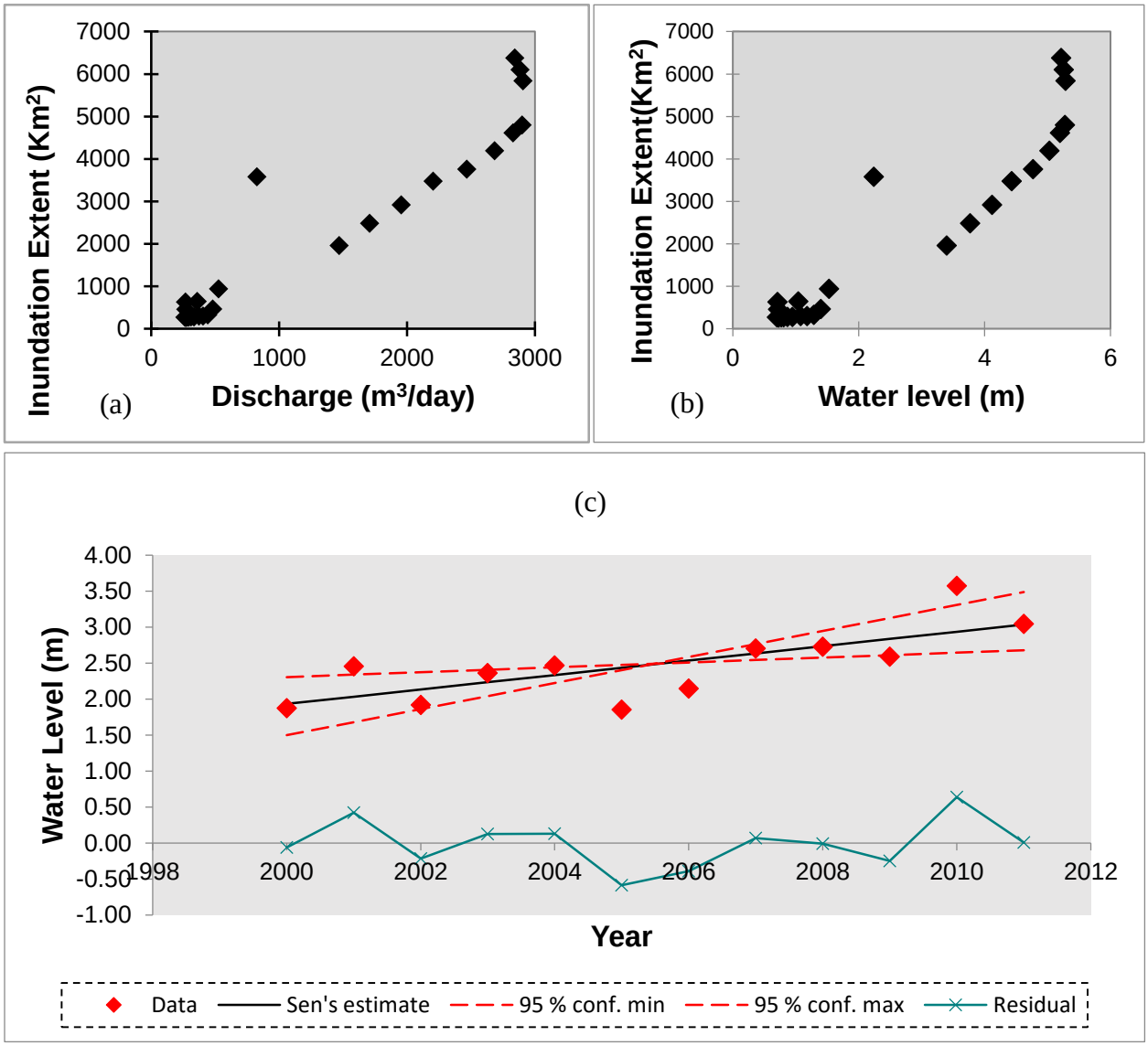

Figure 22: (a –b) Relationship between inundation extent, discharge and water level for the year 2004 at Senanga Gauge Station, (c) Trend in water level for the period 2000 to 2011 at Senanga Gauge Station in the Barotse Wetland, Western Zambia.

4.6 Evaluation of the role of the Barotse Wetland in downstream flooding

The Jan – Jul discharge at Lukulu and Senanga stations were significantly correlated with a Pearson Coefficient of 0.67 and a *p-value* < 0.0001 as shown in Table 14. This correlation implies that discharge at Senanga Gauge Station increases or reduces with increase or decrease in discharge at Lukulu Gauge Station.

Table 14: Pearson correlation for Lukulu Gauge Station discharge and Senanga Gauge Station discharge data from January to July during the year 1997, Barotse Wetland, Western Zambia.

Variable	Obs	Min	Max	Mean	SD	R	R^2	p-value
Lukulu (Q)	207	272.67	1703.76	815.65	482.24	0.67	0.45	< 0.0001
Senanga(Q)	207	336.05	1747.80	1017.57	497.73			

Q = discharge (m^3), SD = Standard Deviation, Obs = Observations, Min = minimum, Max= maximum

This relationship was then used to analyse the behaviour of the wetland with regard to retention and release of water in the months during the ascending/peak and receding flood period using discharge hydrographs (Figure 23).

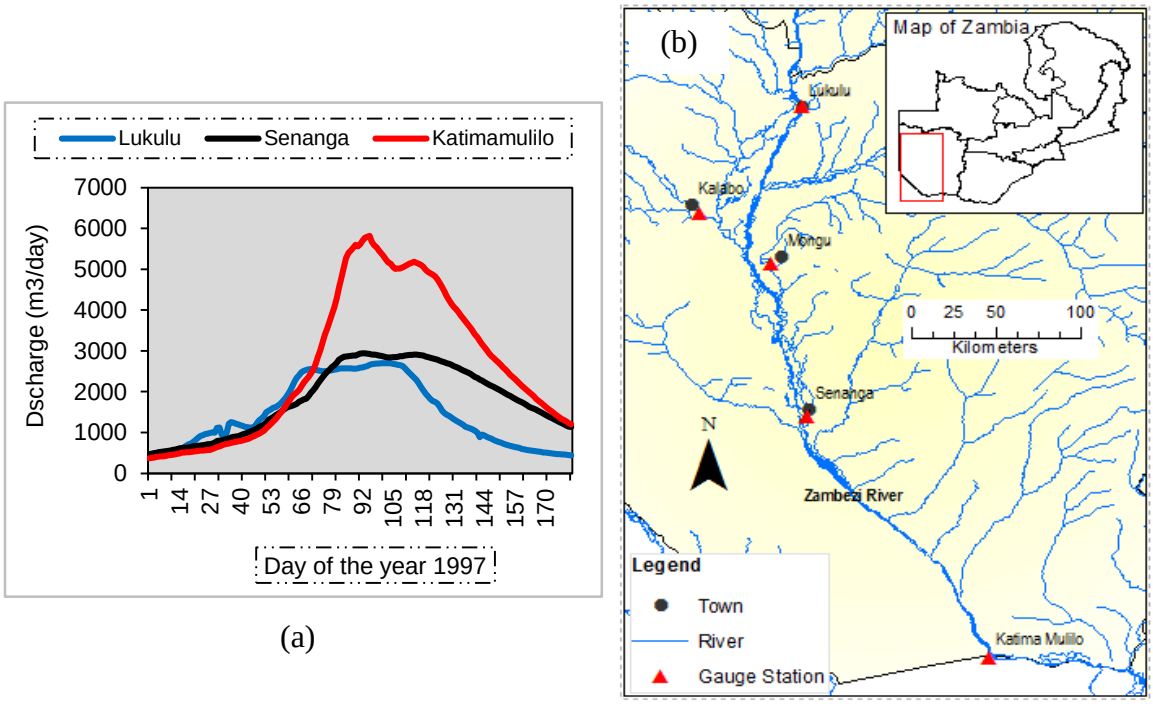

Figure 23: (a) the discharge ($m^3.day^{-1}$) hydrographs for Lukulu, Senanga and Katima Mulilo gauge stations on the Zambezi River for the year 1997 and (b) Location of the gauge stations.

During the rising limb (Figure 23), discharge at Lukulu Gauge Station in the upstream is higher than the discharge downstream at Senanga and Katima Mulilo. However, this scenario begins to change after day 70 (March). The difference in the discharge at Lukulu and Senanga gauge stations during the rising limb is indicative of water "absorption" or "soaking" capacity of the wetland. During the peak period, day 073 to day 105 (March to April) Lukulu and Senanga hydrographs show a similar flattened nature signifying similarities in the discharge values at both stations. This scenario may imply that the wetland has reached the "water absorption" capacity resulting in almost similar inflow and outflow volumes in the wetland. During the falling limb the scenario changes with Senanga Station exhibiting significantly higher discharge values than Lukulu Station. This behaviour signifies the end of the rain season and results in inflows being lower than the outflows. The noted behaviour suggests that the wetland "soak" in water during the rising and peak periods and releases it afterwards in the receding period. This behaviour suggests a wetland that regulates flow. Further investigation of the hydrographs with the rate of change in discharge (Figure 24) between the upstream at Lukulu and downstream at Senanga showed significant differences. For instance, during the rising limb, high positive rates of change in discharge at Lukulu Gauge Station where not matched by high positive rates of change at Senanga Gauge Station between day 001 - 025, and between day 037 and day 45 (Figure 24).

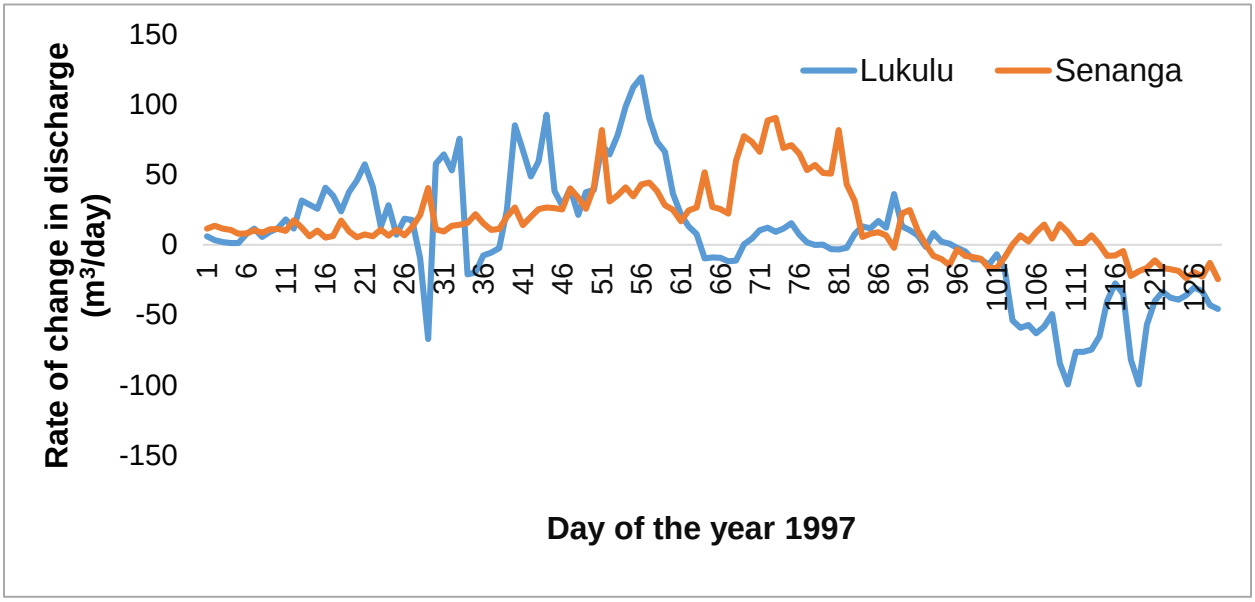

Figure 24: Rate of change in discharge at upstream Lukulu and downstream Senanga gauge stations from January to June 1997, Barotse Wetland, Western Zambia.

A look at the period between day 061 – 083 showed that decrease in the rate of change of discharge at Lukulu station did not translate into a corresponding behaviour at Senanga Gauge Station but showed an increase in the rate of discharge at the downstream station. Between day 001 and day 025 the rate of change of increase in discharge at Lukulu was significantly higher than that of Senanga (Figure 24). On day 028 and day 029 the rate of change in discharge at Senanga was higher than that of Lukulu. However, from day 039 to day 060 Lukulu Gauge Station had a higher change in discharge than Senanga. From day 061 to day 083 Senanga Gauge Station had a higher rate of change in discharge than Lukulu Gauge Station. Between day 101 and day 129, the change in discharge showed higher rates for Senanga than Lukulu Gauge Station (Figure 24). This phenomenon can be attributed to reduced inflow at Lukulu due to reduced rainfall as this is the end of the rain season. But for Senanga Gauge Station this is the period when the flood is just starting to recede and most of the water reaching the downstream as a result the outflows from the wetland are maintained. Overall, peak in discharge at Lukulu and Senanga gauge stations does not occur at the same time. Peaks at Senanga are delayed and do not seem to be of corresponding magnitude as those for Lukulu station (Figure 24).

4.6.1 Role of the wetland - Statistical analysis of discharge and rates of change

The Lukulu and Senanga discharge time series were found to be normally distributed with the Kolmogorov-Smirnov test with p-value < 0.05 in all cases and an overall Pearson Correlation Coefficient of 0.67 (Jan-July) with monthly correlation coefficients of between -0.38 and 0.99 (Table 15).

Table 15: Pearson r Correlation Coefficients (CC) and correlation determinants (CD) between Lukulu and Senanga gauge stations for the year 1997, Barotse Wetland, Western Zambia.

	Month 1997							
	Jan	Feb	Mar	Apr	May	Jun	Jul	Jan-Jul
p-value	< 0.05	< 0.05	< 0.05	<0.05	< 0.05	< 0.05	< 0.05	< 0.05
r (CC)	0.99	0.99	0.88	-0.38	0.91	0.99	0.99	0.67
r^2 (CD)	0.99	0.97	0.78	0.15	0.83	0.99	0.99	0.45

The month of April was the only one with a negative correlation between Lukulu and Senanga discharge time series in the seven months considered, January to July. The significant negative

correlation, R = - 0.38 with *p-value* < 0.05, in discharge time series between Lukulu and Senanga stations in the month of April, 1997 (Table 15) augments the observations in Figure 24 in which a decrease in discharge values at Lukulu did not correspond to declining values at Senanga (day 101 to day 126).

The Paired t-test (Tables 16) revealed differences in the rate of change in discharge at the two gauging stations for the rising limb. For the rising limb, the calculated t = 0.32 was less than the t = 1.990 obtained from the t test distribution table and had a *p-value* = 0.75 (Table 16). Since the t-cal was less than the t-crit with *p*-value greater than the alpha 0.05 the Null Hypothesis that the mean of the discharge time series of Senanga was not greater than or equal to the mean of the discharge time series of Lukulu could not be rejected.

Table 16: Paired t-test summary statistics for the mean rate of change in discharge between Lukulu and Senanga gauge stations, for the year 1997 for the rising limb January to March, 1997, Barotse Wetland, Western Zambia.

Treatment	N	Mean	SD	SEM	d-f	t-cal	t-crit	p-value
Q-Lukulu	90	13.53	15.02	1.58	89	0.32	1.99	0.75
Q-Senanga	90	12.96	6.93	0.73				
Difference	90	0.56	16.47	1.74				

N = Number of observations, SD = Standard Deviation, d-f = Degree of freedom, t-cal = t – calculated, t-crit = t-critical, Q = Discharge (m^3/day), SEM = Standard Error of Mean

Analysis with box plots (Figure 25) showed that the rate of change in discharge at Lukulu Station during the rising limb was 13.53 $m^3.day^{-1}$ and Senanga Station had 12.96 $m^3.day^{-1}$. The rate of change in discharge for Lukulu Station during the rising limb was not significantly different from that for Senanga Station (*p-value* > 0.05) in the same period (Table 16 and Figure 28). The higher SD ± 15.02 indicate more variation in the rate of change in discharge at Lukulu as compared to Senanga Station which showed a small SD ± 6.93 (Table 16 and Figure 25).

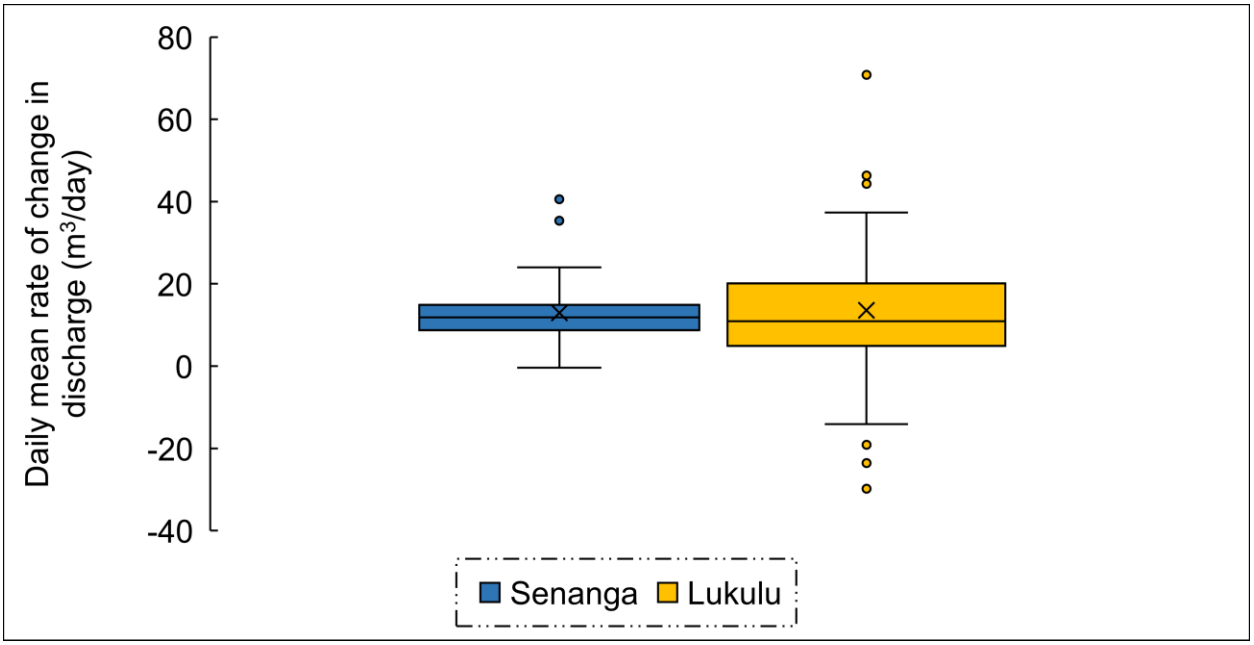

Figure 25: Box plots for the rates of change in discharge for Lukulu and Senanga gauge stations during the rising limb (January - March) 1997, Barotse Wetland, Western Zambia.

This result show that the inflows during this period at Lukulu Gauge Station were not significantly higher than the outflows at Senanga Gauge Station. For the falling limb, the calculated t_{cal} = 2.88 was greater than the t_{crit} = 1.99 obtained from the t-distribution table and had a *p-value* = 0.00491 (Table 17). As the t-cal was greater than the t-crit with *p-value* less than the alpha 0.05 the Null Hypothesis that the mean of the discharge time series at Lukulu was greater than or equal to the mean of the discharge time series at Senanga was rejected. Therefore, the rate of change in discharge at Senanga Station for the falling limb was significantly higher (*p-value* < 0.05) than that of Lukulu Station (Table 17). The two stations show almost the same amount of variation in the rates of change with SD's of ± 11.64 and ±11.44 for Lukulu and Senanga stations respectively.

Table 17: Paired t-test summary statistics for the rate of change in discharge between Lukulu and Senanga gauge stations, for the year 1997 during the falling limb May to July, Barotse Wetland, Western Zambia.

Observation	N	Mean	SD	SEM	d-f	t-cal	t-crit	p-value
Lukulu (Q)	93	-9.50	11.64	1.21	92	2.88	1.99	<0.05
Senanga (Q)	93	-14.85	11.44	1.19				
Difference	93	5.36	17.92	1.86				

N = Number of observations, SD = Standard Deviation, d-f = Degree of freedom, t-cal = t – calculated, t-crit = t-critical, Q = Discharge (m^3/day), SEM = Standard Error of Mean

Table 17 and box plots (Figure 26) showed Senanga had -14.85 $m^3.day^{-1}$ daily change in discharge while Lukulu had -9.50 $m^3.day^{-1}$ during the failing limb. This means that, during the period May –July, the outflows were higher than the inflows into the wetland. This occurrence suggests a type of wetland which stores water during the high flow period which it gradually releases during the flood recession period.

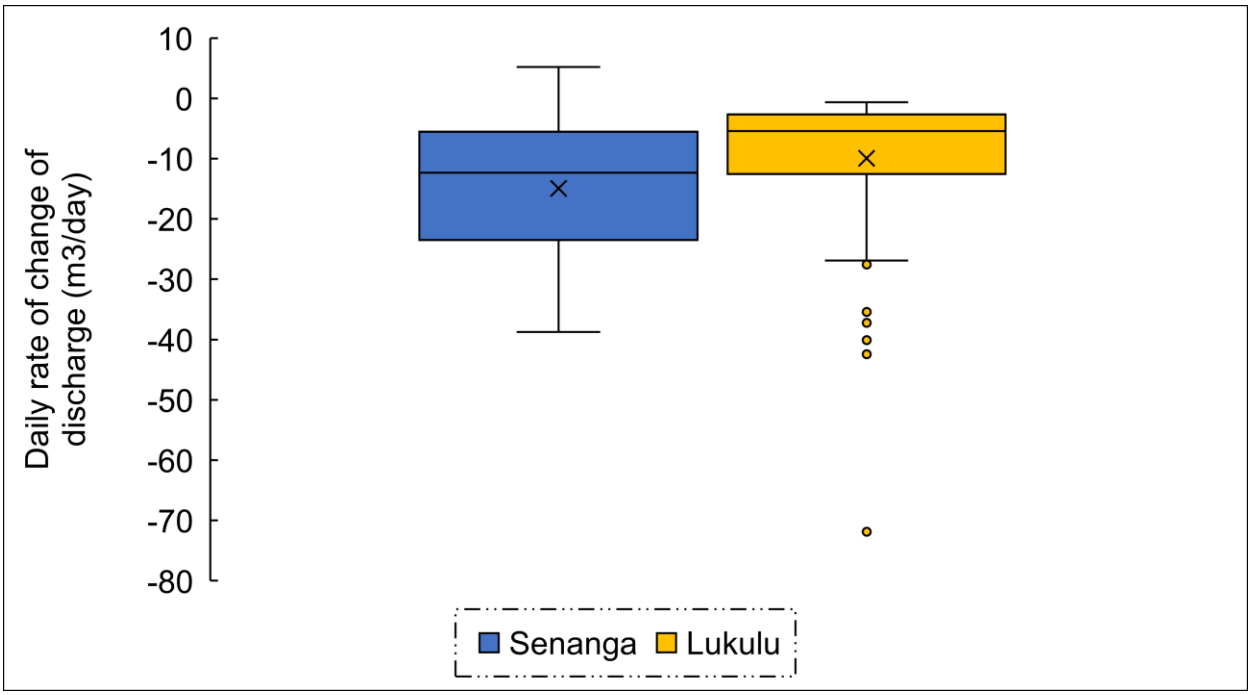

Figure 26: Box plots for the mean rates of discharge for Lukulu and Senanga gauge stations, during the falling limb (May to July) 1997, Barotse Wetland, Western Zambia.

4.7.0 Land cover –use classification and change detection for the period 1984 – 2015

The results of the land cover classification and change statistics are presented here.

4.7.1 Ground truthing and the Error Matrix accuracy assessment

The result of the 2015 land-cover classification was as in Figure 27. The five classes were assessed based on ease of identification and separability. The classes were forest/woody vegetation, wetland, water, grassland and grassland/shrubland/bare sand land. Ground truthing points for the five classes were collected from the study area as described in Section 3.8.3 in Chapter 3 and shown in Figure 27.

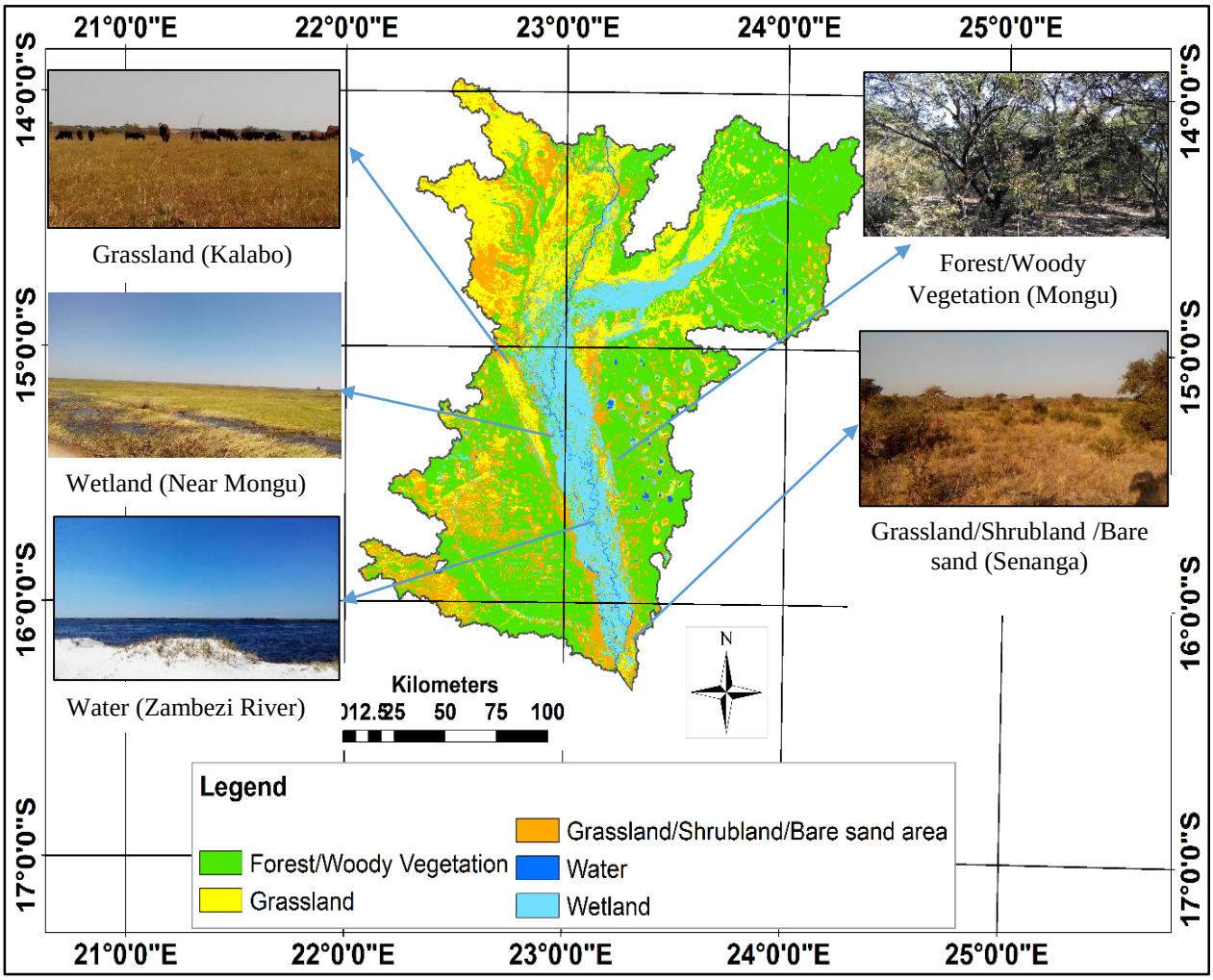

Figure 27: Some of the ground truthing points for the June, 2015 Maximum Likelihood supervised land cover classification map of the study area, Western Zambia.

The results of the ground truth point based accuracy assessment for the June, 2015 land cover classification map are shown in the error matrix (Table 18) as evidenced by the photos in Figure 27.

Table 18: Error Matrix for the 2015 land cover classification of the study area in Western Zambia.

Ground Truth Points(Field and visually interpreted points from high resolution google earth imagery)							Users Acc. (percent)
	FWV	GL	WTL	WT	GSB	TOTAL	
FWV	**128**	15	6	0	1	150	85.33
GL	6	**43**	0	0	1	50	86
WTL	2	3	**47**	0	0	52	90.39
WT	0	4	3	**41**	0	48	85
GSB	2	3	2	0	**43**	50	86
Total	138	68	58	41	45	350	
Prod Acc (percent)	92.75	63.24	81.03	100	95.56	Overall Acc.: 86.29 percent	
						Kappa statistic : 0.83	

FWV= Forest/woody vegetation, GL = Grassland, WTL = Wetland, WT = Water, GSB = Grassland/Shrubland/Bare sand land, Prod Acc = Producer Accuracy, Users Acc = Users Accuracy

The overall accuracy of 86.29 percent and Kappa coefficient of 0.83 were deemed sufficient for the study as the results were an indication of a very good agreement between the June, 2015 classification map and the obtaining real world land cover as observed during the ground truthing mission. ROI's based on the 1986 and 1997 topographic maps and the 2005 Zambia Forest Department land cover classification map were then generated and used as basis for the pixel based accuracy assessment of the 1984, 1996 and 2004 land cover classification maps and the results of which were as presented in Table 19. The land cover classification maps for the periods 1984, 1996, 2004 and 2015 are shown in Figure 28. All classified maps had overall accuracy of above 80 percent with lowest at 86.29 percent for the 2015 classification and highest of 94.43 percent for the 1984 classification with Kappa coefficients of 0.83 and 0.91 respectively (Table 19). The results of the accuracy assessments (Table 18) indicate a very good agreement between the image classifications and the real world. Detailed error matrix results are in Appendix 5.

Table 19: Error Matrix accuracy assessment results for the 1984, 1996, 2004 and 2015 land cover classification maps of the study area in Western Zambia.

	1984		1996		2004		2015	
Class	Prod. Acc.	User Acc.	Prod. Acc.	User Acc.	Prod. Acc.	User Acc.	Prod. Acc.	User Acc.
GL	95.99	87.48	96.78	85.40	67.52	96.15	63.24	86
WTL	87.14	98.61	83.21	94.17	97.48	91.76	81.03	90.39
WT	46.48	100	65.68	95.33	85.64	32.38	100	85
FWV	99.93	96.43	98.56	95.05	99.13	94.19	92.75	85.33
GSB	54.24	80.04	28.57	65.82	82.36	63.23	95.56	86
Overall Accuracy	94.43		92.16		91.65		86.29	
Kappa Coefficient	0.91		0.87		0.86		0.83	

FWV= Forest/woody vegetation, GL = Grassland, WTL = Wetland, WT = Water, GSB = Grassland/Shrubland/Bare sand land, Prod. Acc = Producer accuracy, User Acc = User accuracy.

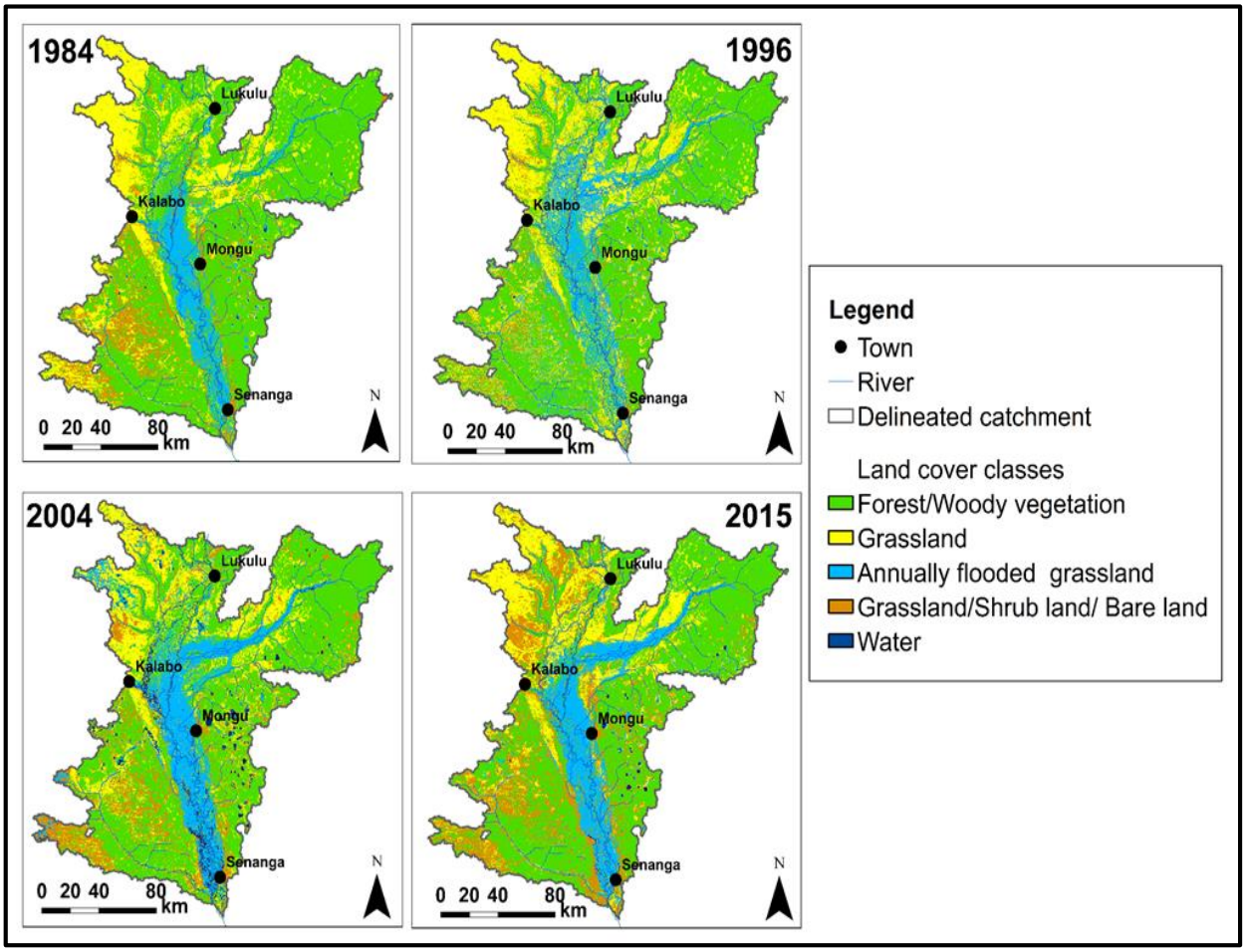

Figure 28: Land cover classification maps in June for the years 1984, 1996, 2004 and 2015 in the study area, Western Zambia,

4.7.2 Land cover change statistics

The estimated areas of different land cover classes and rates of change at each time step are summarized in Table 20. The FWV class was the largest and had a total percentage of area cover of 55.14 percent in 1984 decreasing to 51.46 percent in 1996 and then to 47.39 percent in 2004 and again declining to 45.37 percent in 2015. The GL was second in size occupying 21.16 percent of the total delineated catchment area in 1984, increasing to 28.96 percent in 1996, reducing to 21.07 percent in 2004 and further declining to 18.78 in 2015. The GSB class was 13.12 percent of the total delineated catchment area in 1984, reducing to 3.59 percent in 1996, then increasing to 13.36 percent in 2004 and finally increasing to 21.42 percent in 2015 (Table 20).

Table 20: Land Cover Change in Percentage (%) of Land Cover Classes over the assessed period, Western Zambia.

	1984	1996	2004	2015
Forest/Woody vegetation	55.14	51.46	47.39	45.37
Grassland (Dry grassland)	21.16	28.96	21.07	18.78
Wetland (wet grassland)	9.92	15.44	14.81	13.28
Water	0.67	0.55	3.36	1.16
Mosaic Grassland/Shrubland/Bare sand area	13.12	3.59	13.36	21.42
Total	100	100	100	100

Time Step

Class		1984 - 1996	1996 - 2004	2004 - 2015	1984 - 2015
FWV	PC	-3.68	-4.07	-2.02	-9.77
	ARC	-0.31	-0.51	-0.18	-0.32
GL	PC	7.80	-7.89	-2.29	-2.38
	ARC	0.65	-0.99	-0.19	-0.07
WL	PC	5.52	-0.63	-1.53	3.36
	ARC	0.46	-0.08	-0.14	0.11
WT	PC	-0.12	2.81	-2.20	0.49
	ARC	-0.01	0.35	-0.20	0.02
GSB	PC	9.53	9.77	8.06	8.30
	ARC	0.79	1.22	0.73	0.26

PC = Percentage Change, ARC= Annual Rate of Change

There was a notable decrease in the class FWV of 9.77 percent in the period 1984 to 2015 with an annual rate of decrease of 0.32 percent. The lowest annual rate of decrease in the class FWV of 0.18 percent was noted between the period 2004 to 2015. The highest rate of decrease in the class

FWV of -4.07 percent was between 1996 and 2004 with an annual rate of decrease of 0.51 percent (Table 20; Figure 29). For the period interval 1984 to 2015 a decrease in the class GL of -2.38 with an annual rate of change of -0.07 was noted. Overall annual rate of decrease in GL cover was 0.07 percent per annum with the highest rate of decrease of 0.99 percent noted during the period 1996 to 2004. There was an increase of 7.80 percent in grassland class between 1984 to 1996 while a decrease of a similar magnitude at 7.89 percent occurred during the period 1996 to 2004. The annual rates of change in the class GL during the increase and decrease were 0.65 and -0.99 respectively (Table 20). There were increases in the class GSB of 9.53, 9.77 and 8.06 percent with annual rates of increase of 0.79, 1.22 and 0.73 percent during the periods 1984 to 1996, 1996 to 2004 and 2004 to 2015 respectively. Overall, there was an increase of 8.3 percent with an estimated annual rate of increase of 0.26 in the class GSB for the overall period 1984 to 2015. During the periods when the classes FWV and GL decreased/increased, an increase/decrease in the class GSB was noted (Figure 29).

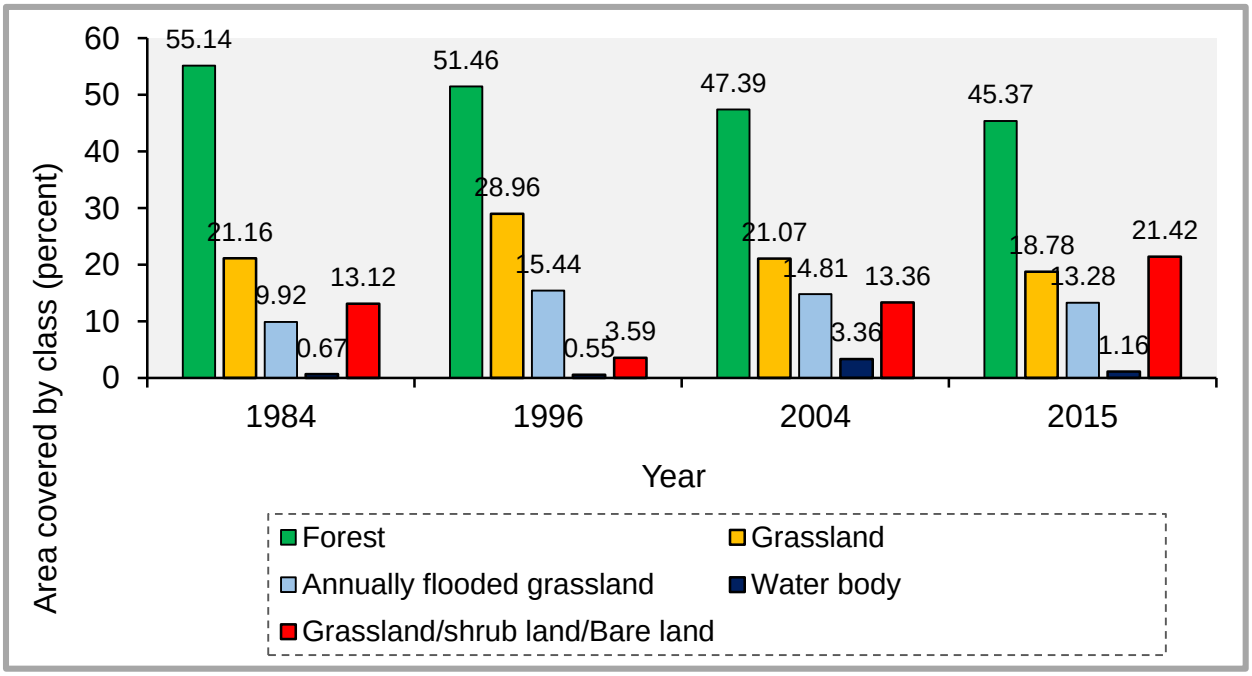

Figure 29: Land Cover Change in Percentage of Land Cover Classes over the assessed period June, 1984 to June, 2015 in the study area, Western Zambia.

As for the class WL, except for the period 1984 to 1996 when there was an increase of 5.25 percent, all other periods had decreases: 0.63 percent in the1996 to 2004 and 1.53 percent in 2004 to 2005. The annual rates of decrease of were -0.08 and -0.14 percent for the periods 1996 to 2004

and 2004 to 2015 respectively. The overall change in the class WL between 1984 to 2015 was an increase of 3.36 percent with an annual rate of increase of 0.11 percent (Table 20; Figure 29). The highest reduction in forest cover was noted during the period 1996 – 2004 (127,257.38 ha) followed by the period 1984 – 1996 (107,057.54 ha) with the period 2004 – 2015 (60,491.42 ha) having the least reduction (Figure 30). Between the periods 1996-2015, there is reduction in forest and grassland land cover class and a notable rise in the grassland/shrubland/bareland land cover class. This is in contrast to the period 1984-1996 in which the grassland land cover class increased while the forest and the grassland/shrubland/bareland classes reduced (Figure 30).

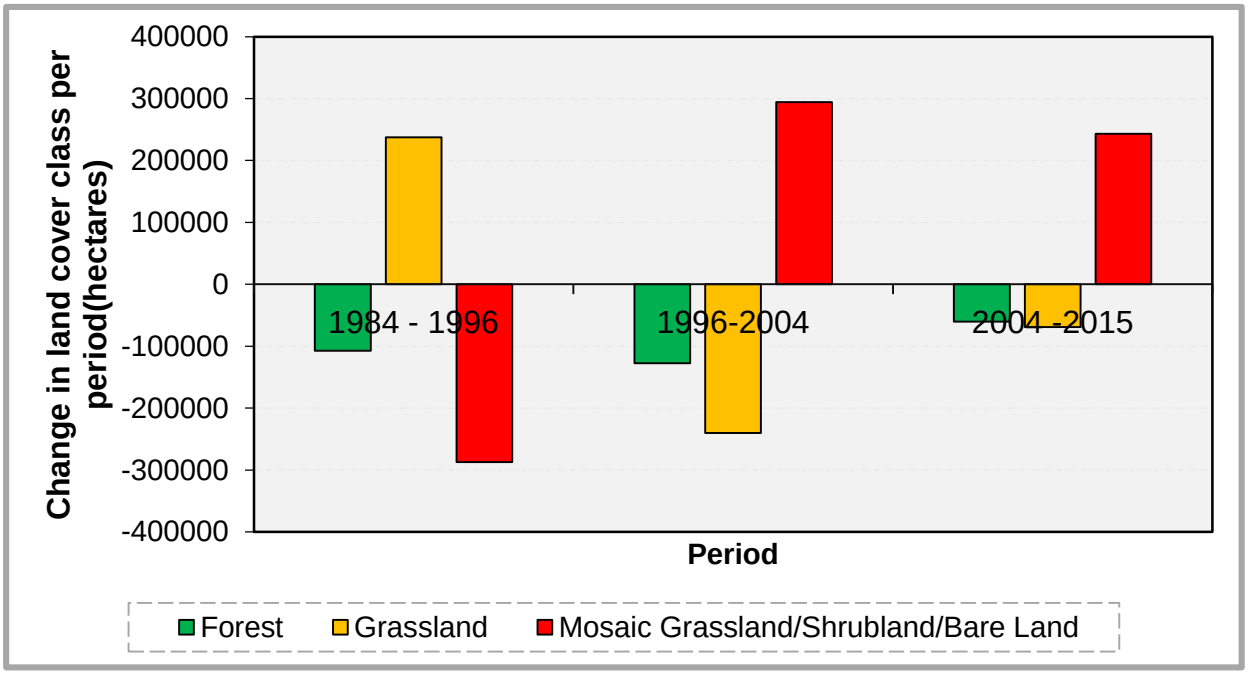

Figure 30: Land Cover Change in hectares of Forest, Grassland and Mosaic Grassland/Shrubland/Bareland classes over the assessed period June, 1984 to June, 2015 in the study area, Western Zambia.

Regarding the intrinsic changes in land cover classes, Table 21 reveals how the various classes transitioned over time. The main focus of this study was the assessment of the changes in the class FWV. During the period 1984 to 1996 about 14.42 percent of the class FWV was converted into the class GL, 1.25 percent was converted to class GSB while about 10.04 percent was converted into class WL. Through the period 1996 to 2004 about 5.19 percent of FWV was converted into WL, 9.01 percent was converted into GL while about 6.21 was converted into GSB. During the period 2004 to 2015 about 8.89 percent of FWV was converted into GSB, about 7.28 percent

was converted into GL while about 3.25 percent was converted into WL. Overall, during the period 1984 to 2015 about 30 percent of the FWV was converted to other classes of which about 12.45 percent was converted into GSB, 9.70 percent was converted into GL while 7.10 percent was converted into WL.

Although transitions from FWV to other classes was noted in all periods there were also transitions from other classes to FWV. For instance, for the period 1984 to 2015, about 10.4 percent of GL, about 30 percent of GSB, about 4.80 percent of WL and about 3.80 percent of WT transitioned into FWV (Table 21). Overall, there was a downward trend in the class FWV and an upward trend in the class GSB (Figure 29). The major drivers, as noted during the field surveys, of the transitions from FWV to other classes, especially GSB and GL, are the conversion to agricultural land and timber harvesting and for energy purposes. It was difficult to classify agricultural land because the spectral signature of grassland and that of crop fields were very similar and the crop fields were too small to be efficiently mapped separately. Figure 31 shows the major drivers of FWV class changes in the delineated catchment as observed during the ground truthing mission in June 2015.

Table 21: Land Cover Change Matrix Showing estimates in the change in Percentage of Land Cover Classes in the study area, Western Zambia.

From 1984 to 1996		1996				
		Wetland	Grassland	Water	Forest/woody vegetation	Grassland/shrub land/bare land
1984	Wetland	73.38	8.55	18.05	10.04	7.06
	Grassland	8.64	74.72	9.80	14.42	36.63
	Water	0.75	0.05	62.48	0.04	0.15
	Forest/woody vegetation	16.77	12.61	6.50	74.18	37.95
	Grassland/shrub land/bare land	0.45	3.96	7.74	1.25	18.14
From 1996 to 2004		2004				
		Wetland	Water	Grassland	Forest/woody vegetation	Grassland/shrub land/bare land
1996	Wetland	59.86	10.11	11.29	5.19	3.77
	Water	4.83	84.79	3.95	1.18	2.26
	Grassland/shrub land/bare land	6.65	2.45	22.92	6.21	58.80
	Grassland	4.94	0.59	46.92	9.01	25.31
	Forest/woody vegetation	23.72	0.85	14.86	78.31	9.81
From 2004 to 2015		2015				
		Wetland	Grassland	Water	Forest/woody vegetation	Grassland/shrub land/bare land
2004	Wetland	70.01	18.93	8.42	3.25	16.14
	Grassland	14.24	48.96	18.50	7.28	18.91
	Water	0.66	0.05	26.06	0.05	0.34
	Grassland/shrub land/bare land	5.35	31.09	12.84	8.89	61.97
	Forest/woody vegetation	9.73	0.94	34.16	80.51	2.61
From 1984 to 2015		2015				
1984		Grassland	Water	Wetland	Forest/woody vegetation	Grassland/shrub land/bare land
	Grassland	51.27	3.08	7.58	9.72	12.28
	Water	0.62	67.24	2.46	0.17	0.44
	Wetland	7.56	21.31	81.90	7.13	2.90
	Forest/woody vegetation	10.37	3.76	4.83	70.50	29.96
	Grassland/shrub land/bare land	30.10	4.62	3.22	12.45	54.39

Figure 31: Major drivers of forest cover change in the delineated catchment: (A) Forest land cleared in June 2015 in preparation for crop production – Lukulu District, Western Zambia; (B) Firewood and charcoal on sale along the Mongu-Senanga Road and; (C) A truck loaded with logs of timber enroute to the urban market, Lukulu District, Western Zambia.

4.8.0 Change point detection and trends analysis of time series

The results of the abrupt change detection and trends analysis of hydrological time series data at Senanga, Lukulu and Kalabo gauge stations as well as the meteorological time series analysis for Mongu, Kabompo and Mansa are given in this section. Mansa Meteorological Station data was used as a validation for the Kabompo Station data as the two stations are located within the Agro-Ecological Region, III, with a similar rainfall pattern.

4.8.1 Change point detection – Mean monthly discharge time series

From the homogeneity Pettit Test, it was observed that there were changes in the mean monthly and annual discharge for all three hydrometric stations evaluated. Lukulu and Senanga stations showed changes in the mean monthly values in the same year but different months, May 1981 and July 1981 respectively and December 1997 for both stations (Table 22; Figures 32 and 33). For Lukulu Station, at confidence level of 99 percent with p-value < 0.01, a change point was observed in May 1981 from 846.52 m^3. $month^{-1}$ to 614.97 m^3. $month^{-1}$ after the change. Further examination of data showed another change point in February 1991 from a mean monthly value of 647.38 m^3. $month^{-1}$ to 606.15 m^3. $month^{-1}$. A final change point was observed in December 1997 from 487.02 m^3. $month^{-1}$ to 888.70 m^3. $month^{-1}$ (Table 22). For Senanga Gauge Station mean monthly discharge time series, only one significant abrupt change was observed in July 1981 from a mean monthly discharge of 1065 m^3. $month^{-1}$ to 828.48 m^3. $month^{-1}$ detected at 99 percent confidence with the computed *p-value* of <0.01 (Table 22).

Since the mean monthly values were based on the hydrological year, October to September, the changes in the mean monthly values of discharge at the two stations occurred in the same hydrological year, 1981.

Table 22: Homogeneity test for hydrological and meteorological mean annual and monthly time series data, Western Zambia.

Station	Period	t	Year	P-value	Alpha(α)	Conf. Level	Mean From	Mean To	Test Decision
LK mean monthly discharge	1967 - 2003	May-81	1981	< 0.05	0.05	99%	846.52	614.97	$p < \alpha$, H_0 rejected
	1982 - 2003	Feb-91	1991	< 0.05	0.05	99%	647.38	606.15	$p < \alpha$, H_0 rejected
	1992 - 2003	Dec-97	1997	< 0.05	0.05	99%	487.02	888.70	$p < \alpha$, H_0 rejected
LK mean annual discharge	1952 - 2003	1980	1980	< 0.05	0.05	99%	810.42	604.66	$p > \alpha$, H_0 accepted
	1980 - 2003	1998	1998	> 0.05	0.05	99%	604.66		$p > \alpha$, H_0 accepted
SNG mean monthly discharge	1967 - 2004	Jul-81	1981	< 0.05	0.05	99%	1065	828.48	$p < \alpha$, H_0 rejected
	1982 -2004	Dec-97	1997	> 0.05	0.05	99%	819.70		$p > \alpha$, H_0 accepted
SNG mean annual discharge	1952 - 2004	1979	1979	< 0.05	0.05	99%	1078	873.26	$p < \alpha$, H_0 rejected
	1980 - 2004	1997	1997	> 0.05	0.05	99%	833.26		$p > \alpha$, H_0 accepted
KLB mean annual discharge	1959 - 1998	1981	1981	< 0.05	0.05	99%	69.09	43.15	*$p < \alpha$, H0 rejected*
	1982 - 1998	1997	1997	> 0.05	0.05	99%	43.15		$p > \alpha$, H_0 accepted
KBM(Prec)	1974 - 2004	1991	1991	> 0.05	0.05	99%	970.29		$p > \alpha$, H_0 accepted
MAS(Prec)	1974 - 2012	1986	1986	> 0.05	0.05	99%	1150.48		$p > \alpha$, H_0 accepted
MNG(Prec)	1974 - 2014	2006	2006	> 0.05	0.05	99%	942.32		$p > \alpha$, H_0 accepted
MNG(Max Temp)	1975-2002	1990	1990	> 0.05	0.05	99%	30.48		$p > \alpha$, H_0 accepted

LK, SNG, KBM, MAS and MNG are respectively Lukulu, Senanga, Kabompo, Mansa and Mongu station; t = time of change.

(discharge in m^3, rainfall in mm and temperature in degrees Celsius)

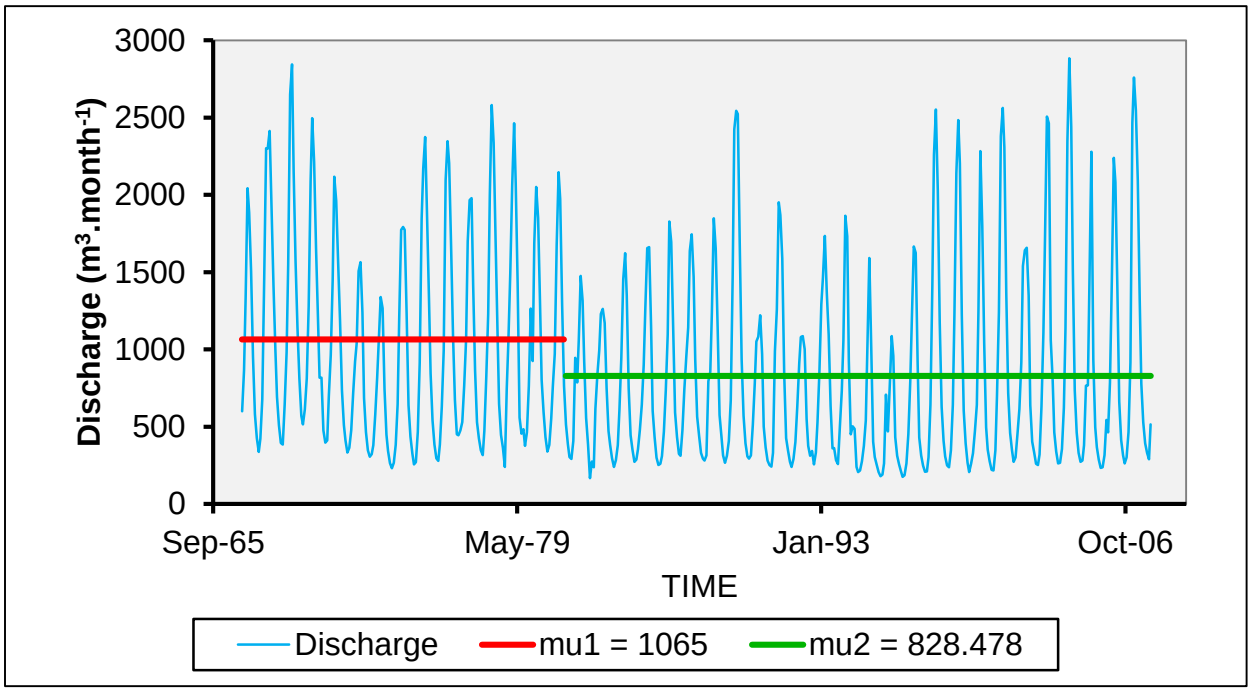

Figure 32: Abrupt change in mean monthly discharge time series for the period 1967 to 2003, for Senanga Gauge Station, Western Zambia.

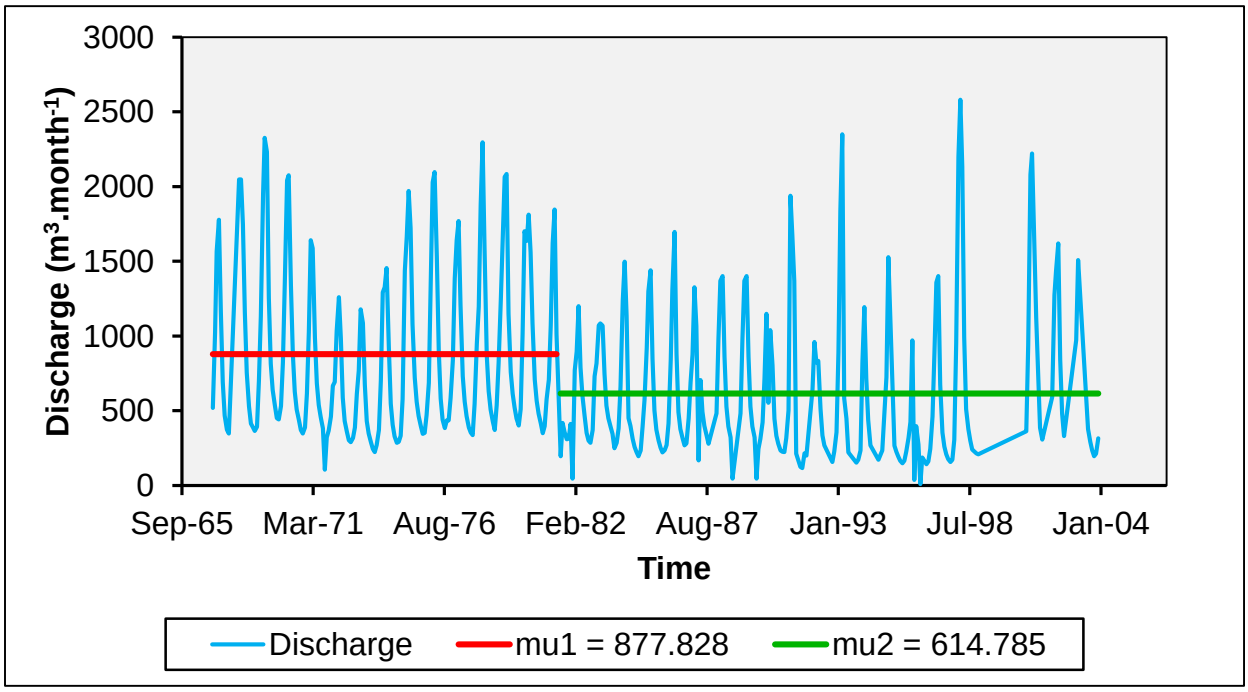

Figure 33: Abrupt change in mean monthly discharge time series for the period 1967 to 2003, for Lukulu Gauge Station, Western Zambia.

4.8.2 Change point detection – Mean annual discharge time series Pettit Homogeneity Test

The mean annual discharge time series showed similar time space for abrupt changes as exhibited in the mean monthly discharge time series. For Lukulu Station, an abrupt change in the annual mean discharge is observed in the hydrological year 1980/1981 from a mean of 810.42 m^3. $year^{-1}$ to 604.66 m^3. $year^{-1}$. Senanga Station time series revealed an abrupt change in the 1979/1980 hydrological year from 1078.00 m^3. $year^{-1}$ to 873.26 m^3. $year^{-1}$ while for Kalabo Station an abrupt change was observed in the 1981/1982 hydrological year from 69.09 m^3. $year^{-1}$ to 43.15 m^3. $year^{-1}$. The changes in the discharge mean in 1997 for Senanga and Kalabo, and 1998 for Lukulu were not adequate to register significance at alpha level 0.05 (Table 22). Generally, significant abrupt changes in the monthly and annual mean rate of discharge were observed in the hydrological years 1979/1980 and 1981/1982 and showed a downward trend.

4.8.3 Change point detection – Mean annual precipitation and maximum temperature time series Pettit Homogeneity Test.

For all meteorological time series examined, the data were found to be homogenous. The p-*values*, in all precipitation and maximum temperature time series, were greater than the significance level alpha =0.05; the Null Hypothesis (H_0) that the time series were homogenous could not be rejected (Table 22). The abrupt changes in the mean annual and monthly discharge values were not reflected in changes in the means of the precipitation and temperature time series for Kabompo, Mongu and Mansa Stations (Table 22).

4.8.4 The Seasonal Mann-Kendall Test analysis on mean monthly discharge time series data.

For Lukulu Station data, with the seasonal Mann-Kendall Test, no significant trends in the mean monthly discharge were observed in the segmented periods 1967 – 1981, 1982 -1997 and 1998 – 2003. However, there was a significant downward trend with a Kendall Statistic of -0.21 with computed *p-value* < 0.05 between the time space 1967 and 2003 (Table 23). Further investigations with the fitting of the linear regression with ordinary least squares revealed insignificant upward trends for the periods 1967 – 1981, 1982-1997 (Table 24).

Table 23: Seasonal Mann-Kendall statistics for the discharge time series at Lukulu and Senanga Gauge Stations, Western Zambia.

Station	M-K	S	*p-value*	Trend	Period	M-K	S	*p-value*	Trend	Period
LK (Q)	-0.07	-96	0.53	[- *]	1967 - 1981	0.09	22	0.33	[+ *]	1982 - 1991
	0	0	1	[N-T]	1992 - 1997	0	0	1	[N-T]	1998 - 2003
	-0.21	-1266	< 0.05	[- +]	1967 - 2003					
SN(Q)	-0.09	-110	0.44	[- *]	1967 - 1981	0.12	468	0.10	[+ *]	1982-2004
	-0.23	-2250	<0.05	[- +]	1967 - 2004					

*M-K, S and p are respectively the Mann-Kendall's Tau statistic, the Kendall Score and the two-sided p-value. [N-T] indicate no trend detected, (+ and – indicate respectively positive trend and negative trend, +, * indicate respectively significant and not significant at confidence level α = 0.05), LK(Q) = Lukulu Station discharge, SN(Q) = Senanga Station discharge.*

Table 24: Slope (m^3. $year^{-1}$) and the linear regression coefficient R^2 for the trends in mean monthly discharge at Senanga and Lukulu gauge stations, Western Zambia.

	Senanga			Lukulu			
Period	1967 - 1981	1982 - 2004	1967 - 2004	1967 - 1981	1982 - 1997	1998 - 2003	1967 - 2003
Slope	-0.04	0.02	-0.02	0.01	0.02	-0.09	-0.03
R^2	0.01	0.01	0.01	<0.05	<0.05	<0.05	0.03

Significant downward trend was noted for the overall period 1967-2003 with slope coefficients of -0.03 and R^2 of 0.03 (Tables 23 and 24). Therefore, the overall trend for monthly discharge at Lukulu Station for the period 1967 to 2003 was downward.

For Senanga Station the Mann-Kendall trends test detected no significant trend in the mean monthly discharge time series for the periods 1967-1981 and 1982-2004. The Kendall Statistic and the computed *p-values* for the two periods were -0.09, 0.12 and 0.44, 0.10 respectively (Table 23). With computed *p-values* > 0.05 in all scenarios the H_0 that there is no trend in the data was accepted. However, the overall Mann-Kendall Test for the period 1967 - 2004 detected a significant downward trend. The Kendall Statistic and the computed *p-value* for this period were -0.23 and <0.05 respectively (Table 23). The computed *p-value* was less than 0.05 the H_0 was, therefore, rejected and the H_a that there was a trend in the discharge time series was accepted. Further investigation with the fitting of the linear regression with ordinary least squares revealed a downward trend for the 1952 - 1981 with a slope coefficient of -0.04 and R^2 of 0.01. The periods 1982-2004 had a slope coefficient of 0.02 and R^2 of 0.01 indicating an upward trend. The overall period 1967 - 2004 had a slope coefficient of -0.02 and R^2 of 0.01 indicating a downward trend in the time series (Table 24).

There was a generally decreasing trend in the mean monthly base flows for the most part of the period 1967 to 2003/4 for both Lukulu and Senanga stations (Figures 32 and 33).

4.8.5 Mann-Kendall trends and Sens's slope estimates for mean annual discharge, precipitation and temperature.

The Mann-Kendall Test and Sens's slope results for the hydrometric and meteorological stations considered in the study are presented in Table 25 and Appendix 6. For the period 1952 – 1979 Senanga discharge time series had no significant trend (*p-value* of 0.56) and no significant trend from 1980 – 2004 (*p*-value of 0.74). However, when the entire period 1952 – 2004 was considered there was a significant trend with a Z statistic value of -3.38, a *p*-value of <0.05 at alpha levels 0.001 with an annual rate of decrease in discharge of 6.94 m^3. $year^{-1}$ (Table 25; Figure 34). For Lukulu Station, upstream of the wetland, there was no significant trend in discharge during the period 1952 to 1980 or the period 1981 to 2003. For the period 1952 – 2003 however, there was a

significant downward trend with a Z statistic value of -2.88, *p-value* of <0.05 at alpha level of 0.01 with an annual rate of decrease of 4.68 m^3. $year^{-1}$ (Table 25; Figure 35). As for Kalabo Station, the discharge time series for the period 1959 - 1998 showed a significant downward trend with a Z statistic value of -3.58 with p-value of <0.01 at alpha level of 0.001 and annual rate of decrease of 1.12 m^3. $year^{-1}$ (Table 25; Figure 36). For the period considered the observed general trend in discharge into the wetland was downward.

Table 25: Mann-Kendall test and Sens's slope statistics for hydrological and meteorological time series, Western Zambia.

			Mann-Kendall trend			Sen's Slope
Time series	**First year**	**Last Year**	**n**	**Test Z**	**Signific.**	**Q**
Discharge-Senanga	1952	2004	51	-3.38	***	-6.94
Discharge-Lukulu	1952	2003	51	-2.88	**	-4.68
Discharge-Lukulu1	1952	1980	29	1.76	+	6.25
Discharge-Lukulu 2	1981	2003	22	-0.28		-1.97
Discharge-Senanga1	1952	1979	28	0.14		0.42
Discharge-Senanga 2	1980	2004	23	0.63		5.83
Discharge- Kalabo	1959	1998	40	-3.58	***	-1.12
Precipitation-Kabompo	1974	2004	30	-1.14		-4.65
Precipitation-Mongu	1974	2013	40	1.22		4.23
Precipitation-Mansa	1974	2012	38	-0.05		-0.33
Maximum temperature Mongu	1975	2002	28	-1.66	+	-0.07

Interpretation of the level of significance and the Sen's slope			
Level of significance		Sen's slope variable	
***	if trend at α = 0.001 level of significance.	Q	Sen's estimator for the true slope of linear trend i.e. change per unit time period (in this case a year).
**	if trend at α = 0.01 level of significance.		
*	if trend at α = 0.05 level of significance.		
+	if trend at α = 0.1 level of significance.		
	If the cell is blank, the significance level is greater than 0.1.		

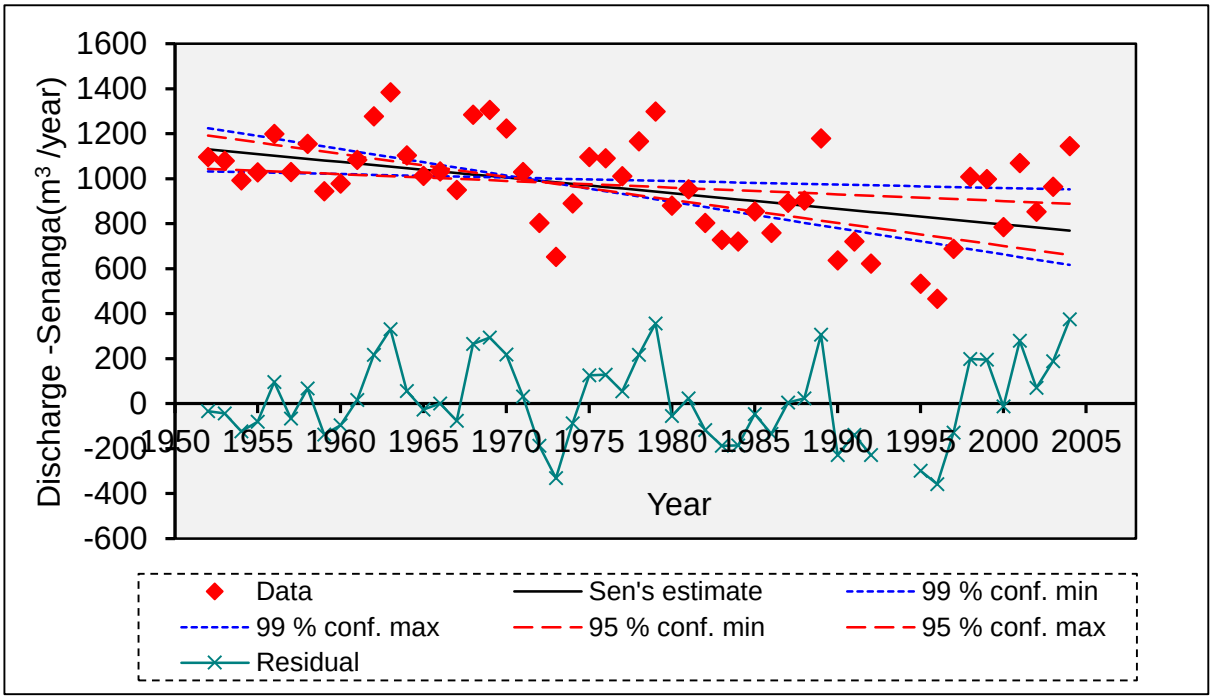

Figure 34: Overall trend in annual mean time series of discharge between 1952 – 2004 for Senanga Station, Barotse Wetland, Western Zambia.

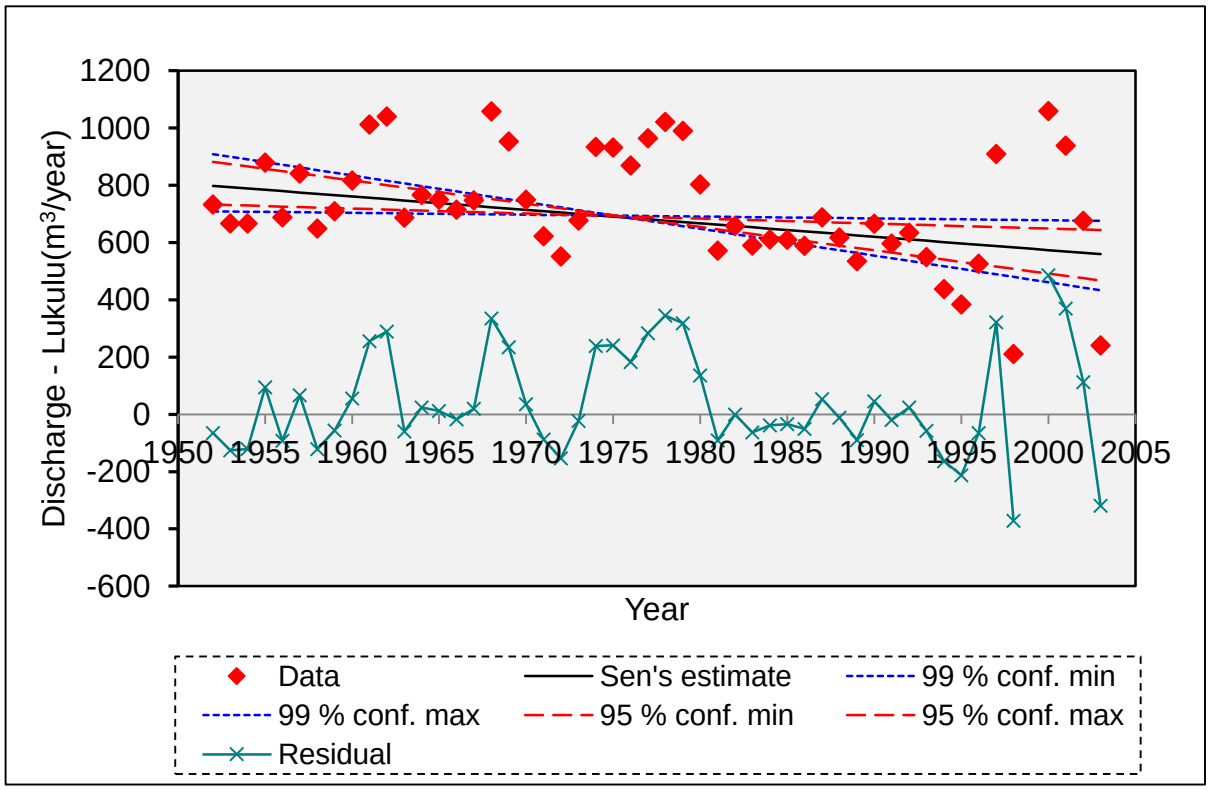

Figure 35: Overall trend in annual mean time series between 1952 – 2003 for Lukulu Station, Barotse Wetland, Western Zambia.

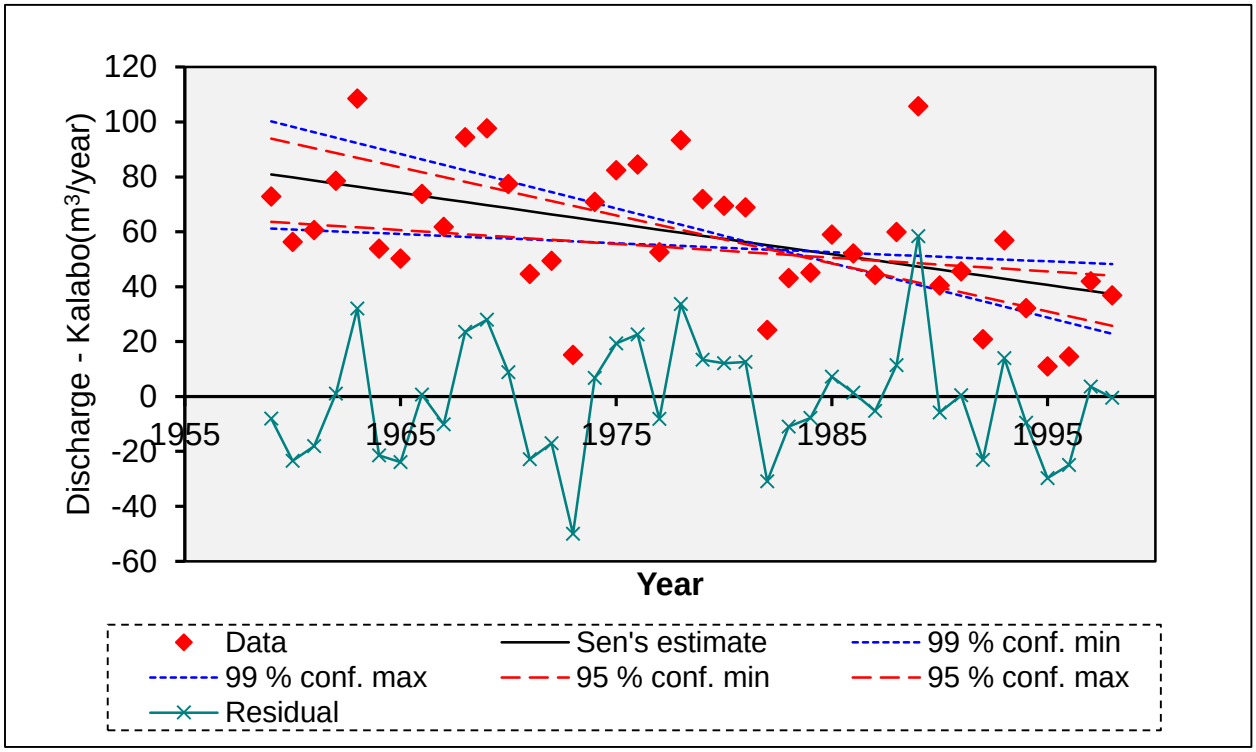

Figure 36: Annual mean time series and trend of discharge between 1952 - 1998 for Kalabo Station, Barotse Wetland, Western Zambia.

As for precipitation in the stations representative of locations in the wetland, wetland catchment and a comparison station, Mansa, from the same rainfall belt as the upstream catchment for the wetland, they showed a generally insignificant downward trend (Table 25 and Figure 36). Generally, there were variations in rainfall patterns for Mongu, Kabompo and the validation station Mansa showing cycles of high and low rainfall periods. For the Mongu station, the period 1980 – 1997 had rainfall values below the mean value with an exception of 1990 and 1993 when the annual rainfall was above the mean value. For instance, in the period 1998 – 2005, Kabompo Station time series showed oscillatory behaviour between above and below the mean annual rainfall. During the period 1994 – 2010 there was annual rainfall above the mean value (Figures 37 and 38). For Kabompo and Mansa, the stations recorded mostly above the mean annual rainfall with a substantial number of years (10 out of 35) in which the annual rainfall was below the mean (Figure 37). The mean annual maximum temperature time series (1975-2002) for Mongu Station, representative of the temperature scenario over the wetland, showed a significant declining trend

in the mean annual maximum temperature with Z-test score of -1.66, *p-value* of 0.049 at alpha level of 0.10 with an annual rate of decrease of 0.07 degrees Celsius. year^{-1} (Table 25; Figure 38).

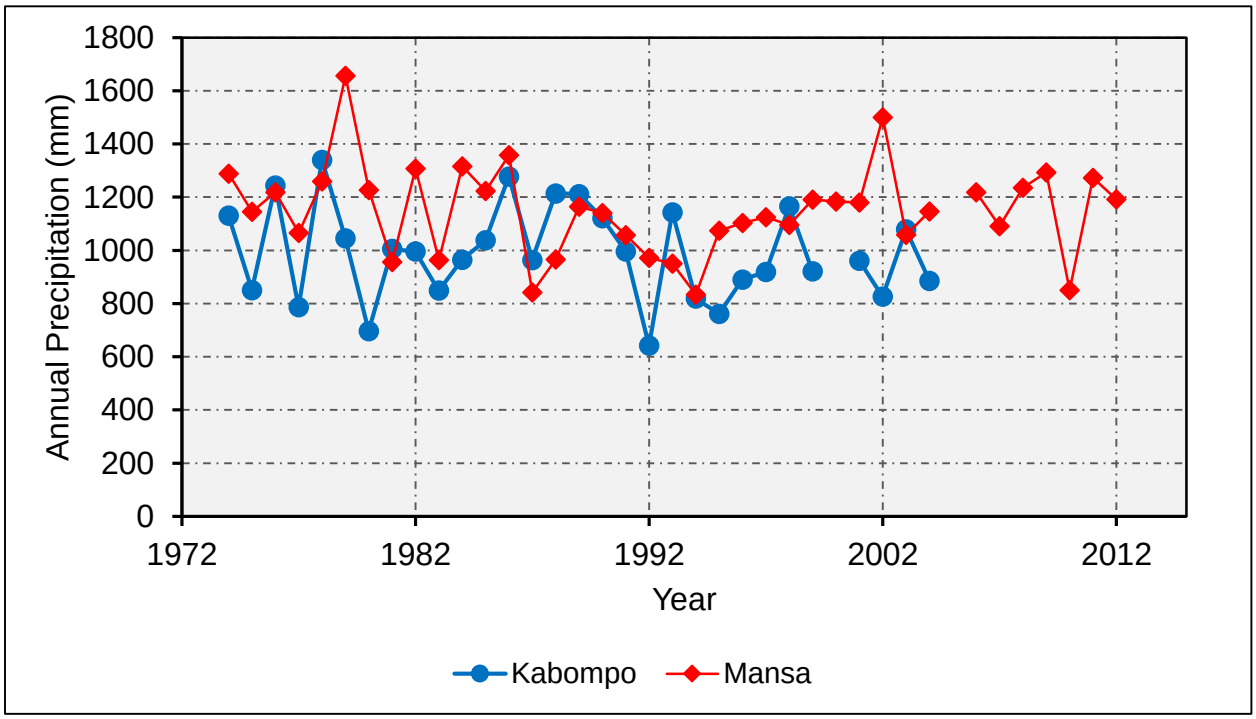

Figure 37: Comparison of annual mean time series of precipitation between Kabompo and Mansa Stations.

4.9.0 Correlation between hydrological and meteorological variables with the Pearson's r

The mean annual rainfall recorded at Kabompo Station correlated with mean annual discharge recorded at Senanga Gauge Station with a correlation coefficient of 0.36 and a *p*-value < 0.05 at significance level alpha = 0.05. This implies that discharge at Senanga Station increases or decreases with increase or decrease in rainfall at Kabompo Station (which is representative of the upstream catchment of the wetland). When mean monthly time series of discharge, maximum temperature, and inundation extent were analysed, the results (Tables 26) showed that there was a significantly strong correlation between discharge at Senanga Station and inundation extent with coefficient of correlation of 0.81 and a *p*-value of <0.05 at 0.05 significance level alpha (Table 26).

Table 26: Pearson correlation coefficients for mean monthly discharge, inundation extent, maximum temperature in the study, Western Zambia.

Variables	Max temp Kabompo	Q-Senanga	I Extent	Max temp Mongu
Max temp Kabompo	**1**	-0.43	-0.38	**0.89**
Q-Senanga	-0.43	**1**	**0.81**	-0.44
I Extent	-0.38	**0.81**	**1**	-0.16
Max temp Mongu	**0.89**	-0.44	-0.16	**1**

Values in bold are different from 0 with a significance level alpha=0.05, Q = Discharge (m^3/month), I = Inundation, Max = Maximum, Temp = Temperature.

A key negative correlation between inundation extent in the Barotse Wetland and maximum temperature at Mongu Station was observed with a coefficient of correlation of -0.16 and *p*-value of 0.63 at 0.05 significance level alpha (Tables 26).

CHAPTER FIVE: DISCUSSION

5.1 Detection and quantification of inundated area

Despite the difficulty in acquiring cloud free MODIS imagery for all eight-day interval period for the considered time space 2003 to 2013 the cloud free images processed and used in this study were adequate to provide data for statistical analysis of trends in inundation extent. The challenge of cloud cover is an inherent attribute of optical satellite data such as MODIS which has been noted by many (Wang, 2007; Di Baldassarre, 2012; Meire, 2012; Ticehurst *et al*. 2014; Proud *et al.* 2011; Ticehurst *et al*. 2013). As noted by Ticehurst *et al*. (2013) concerning MOD09A1 product, few cloud free MODIS images were available during the ascending/peak period as compared to the receding period. Inundation detection and thresholding was easier for images captured during the period when there was a lot of water and high flow period in the wetland. For instance, MODIS images captured in the months January to May were easier to detect inundation extent using the DFI algorithm than the months June to December. This is because during the high flow period, January to April, there was less or no spectral signal interference from under laying elements such as soil and grass. Further, MODIS data is known to detect high moisture content and dark soils as being flooded area while in reality it is not flooded (Ticehurst *et al*. 2013). This challenge was addressed with the aid of google earth image and the thermal band as explained in section 3.5.2. By implication, inundation extent is likely to be overestimated during the flood receding period than the peak period. Calculating the threshold value proved a challenge for low periods. The thresholding challenge was also noted by the developers of the DFI algorithm (Wang *et al.* 2013). Nerveless, from the acquired imagery, MODIS and Landsat, and with the application of the DFI algorithm detection and estimates of inundation extent in the delineated study area were made as indicated in Table 6.

Although Ticehurst *et al.* (2013) observed that some temporal information is lost when mapping wetland inundation with the composite 8-day interval on the MOD09A1 product the temporal loss was considered not to be significant because the flooding in the Barotse Wetland can be assumed as not fast flowing as evidenced by the long resident time of water in the wetland (Kasimona and Makwaya, 1995). Considering the purpose of this study, variation and trend across the years and

not necessarily within a flooding season, the 8-day interval MOD09A1 product was adequate. From the study it is evident that acquiring information on the extent of inundation in a wetland is much easier and faster using the satellite based method, as proved with MODIS supplementing with ground truthing, than employing the costly and time consuming in-situ field surveys.

5.2 Variations and trends in inundation extent

There were differences in inundation extent across seasons (Figure 38 a) with maximum and minimum inundated area estimated at about 660,000 hectares in 2009 and 170,000 hectares in 2005 (Figure 38 b-c). Cai *et al*. (2015) estimated the maximum and minimum inundated area at about 552,000 hectares and 250,000 hectares respectively. Hughes and Hughes (1992) estimated the total inundated area of the floodplains at 7700 Km^2. The difference in the maximum inundated area could be due to the delineation of what were termed as wetland in the two studies as well as the imagery and methods used in each study.

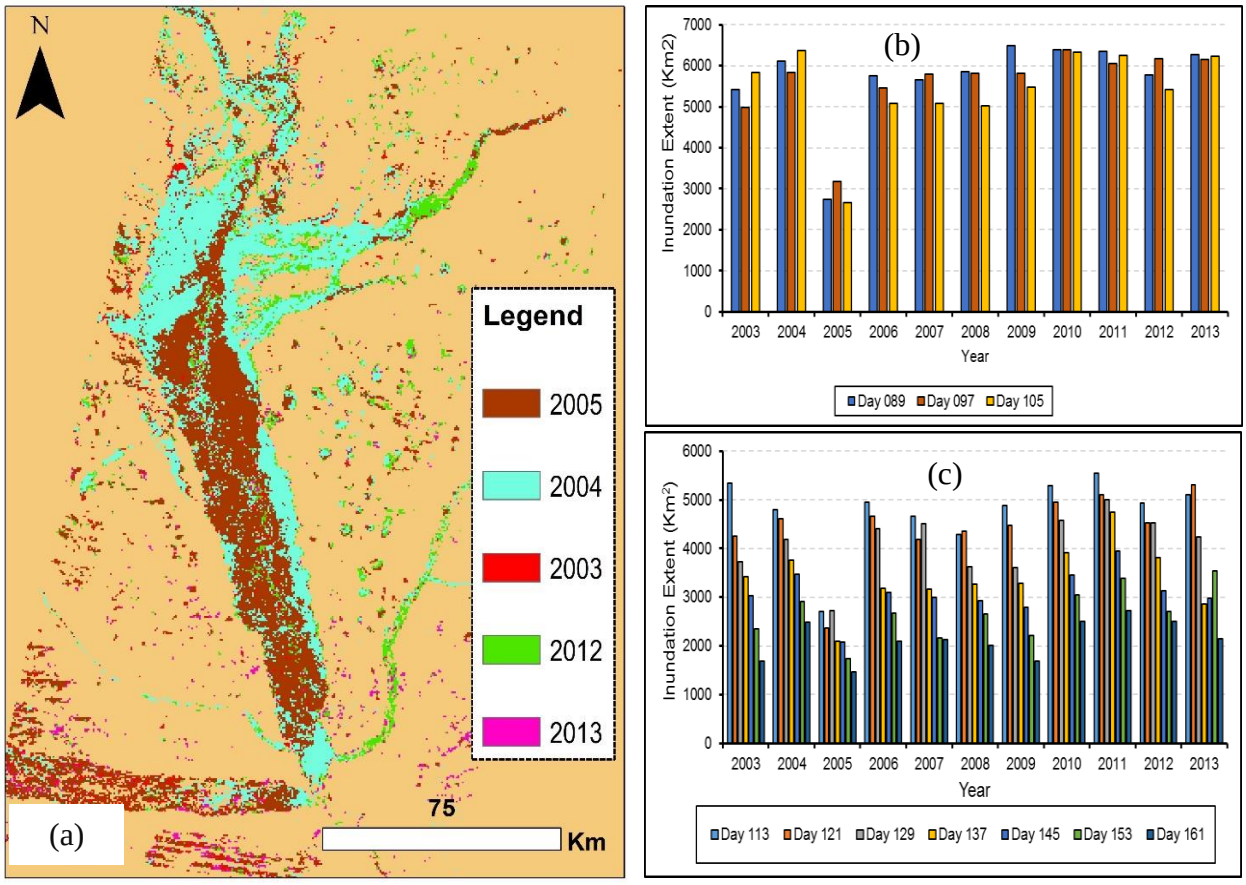

Figure 38: (a) Comparison of inundation extent for Day 097 for the years 2003, 2004, 2005, 2012 and 2013. Trends in inundation extent on given days during the ascending period (a), receding period (b) for the time space 2003 to 2013 in the Barotse Wetland, Western Zambia.

Cai *et al*. (2015) stated that "the flooding patterns are changing, that the magnitude increased, and the timing of on-set and recession also changed". From Figure 20 a-c it was observed that inundation extent on a given day of each year differed from year to year with an increasing trend observed from year 2006 to 2013. Based on the observations in Figure 38 the findings by Cai *et al*. (2015) that "the flooding patterns are changing" has been augmented. For instance, an overlay of inundation masks for day 097 (Figure 38 a) showed that in 2004 there was more inundated area than there was in 2005. Inundation extent on a given day of each year differed from year to year (Figure 38 b, c). This answers to Cai *et al*. (2015), in view of the perceptions by the local people, that the inundation patterns change. That the magnitude of flooding increased can be augmented by the findings of this study which observed an increasing trend in the annual means of the inundation extent (Figure 21). For instance, between 2003 and 2013 the magnitude in inundation extent increased by 62.20 Km^2. This is indicative of increased flood magnitude in the period 2003 to 2013. The rise in inundation extent for the period is validated by the observed rise in the trend in water level which showed an increase in water level of 0.1 m during the period 2000 to 2011 (Figure 22 c and Appendix 3 d). Annual differences in inundated area affects farming activities which are flood dependent. Farming activities in the wetland depend on the rate at which the flood recedes. The higher the rate of recession the earlier the farmers have access to land for farming activities. The advantage with MODIS imagery used in this study over the Landsat imagery used by Cai *et al.* (2015) is that the inundation extent repeat interval is halved hence more images and inundation extent fluxes were obtained for analysis. Furthermore, the MODIS images are taken on the same days each year making it suitable for use in comparative and change studies as suggested by Ticehurst *et al.* 2014.

5.10.3 Correlation between inundation extent, discharge and water level

Discharge and water level into the Barotse Wetland is influenced by runoff from the upper catchment in Angola and North Western Zambia (Timberlake, 1998; IUCN, 2003; Beilfuss, 2012). For instance, the flow data for Senanga Gauge Station at the outlet of the wetland typifies the flows received from the upper catchment during the period 1952 - 2004 (change in annual mean discharge) and 1967 – 2007 (monthly mean discharge). There were differences in the mean annual discharge values with 25 out of the 50 years considered showing mean values which where less than the previous years value (Figure 39). The magnitude of the differences also varied from each

year with some years having very high reduction/increase in values like the year 1989 and 2004 which significantly differed from the means of discharge of the previous years (Figure 39). This implies that in each hydrological year the mean annual discharge values differs. In the recent past 1980 to 2004 the differences in the mean of the annual discharge seem to have taken on a rising trend in both directions (increase/decrease) (Figure 39). The differences in the mean monthly and mean annual flows are high as observed from Figures 40.

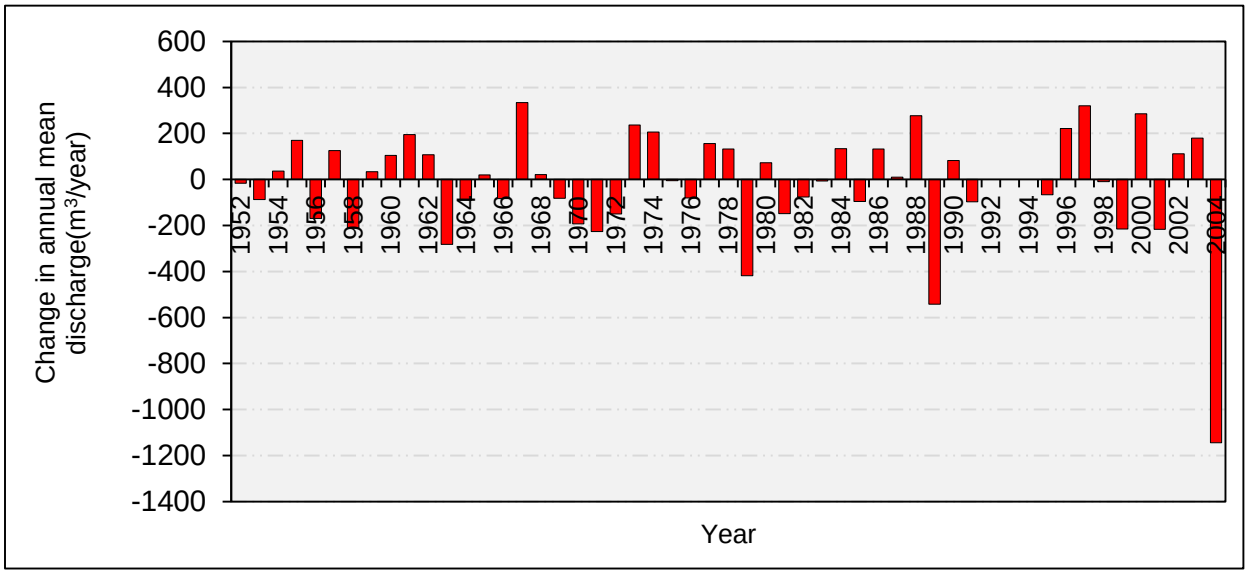

Figure 39: Time series showing differences in the mean annual discharge (1952-2004) for Senanga Gauge Station in the Barotse Wetland, Western Zambia.

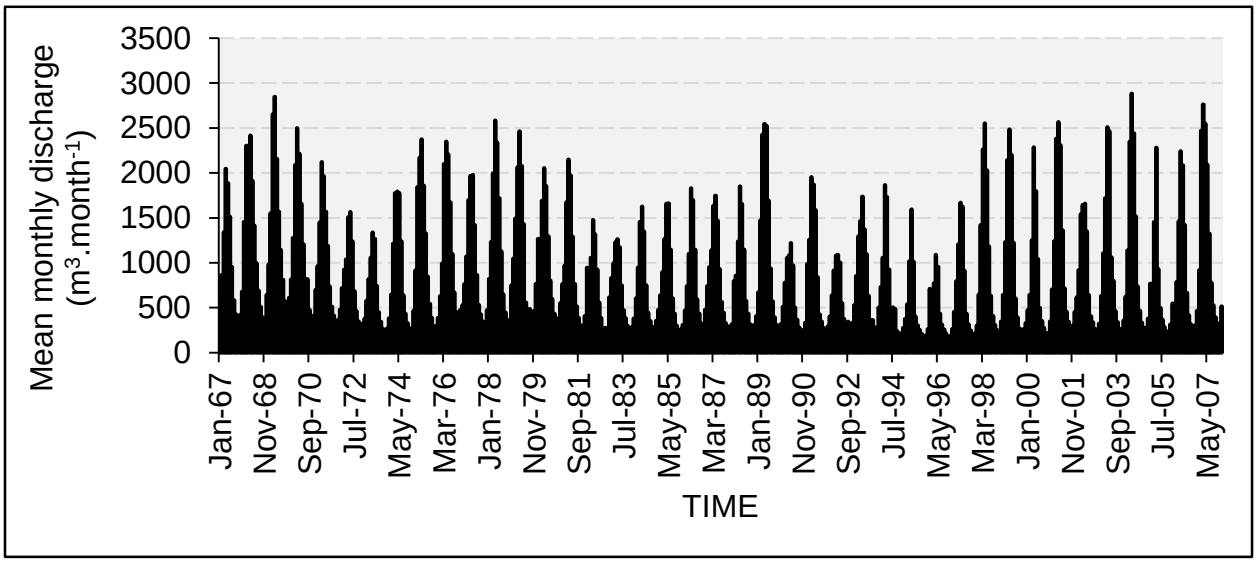

Figure 40: Time series showing the mean monthly discharge for Senanga Gauge Station over the period 1967 – 2007 in the Barotse Wetland, Western Zambia.

Between 1967 and 2004 the highest monthly discharge during the flooding period was 2882.69 $m^3.month^{-1}$ in April, 2004 while the lowest was 1085.46 $m^3.month^{-1}$ in April, 1996 (Figure 40). The discharge regime for Senanga Gauage Station shows cycles of high flows and low flows typical of the Zambezi River Basin. For instance higher annual flows were between 1974 to 1981 followed by lower flows between 1982 to 1997 and again higher flows between 1998 to 2007 (Figure 40). These discharge cycles are similar to the overall Zambezi River Basin cycles as demonstarted by Beilfuss (2012).

Drawing on the established correlation between inundation extent and outflows at Senanga (Figures 17 and 22), an inference is made that there were trends in inundation extent of similar pattern as discharge trends in the Barotse Wetland during the period 1952 to 2007. This result show that the outflows from the wetland increase or decrease with increase or decrease in inundation extent. By inference, trends in inundation extent will show corresponding trends in outflows. The IUCN (2003) indicated that the onset of annual inundation in the wetland varies greatly while Simwinji (1997) explained that inundation is a consequence of the rainfall dependent flow and seepage from the upper catchment. The relationship between inundation extent and discharge/water entails that trends in inundation extent follow trends in discharge/water level. It means that trends in inundation extent increases or decreases with increase or decrease in discharge/water level in the wetland (Figures 22).

5.10.4 Evaluation of the role of the wetland in flow attenuation

Bullock and Acreman (2003) argued that many studies draw conclusions on the categorisation of wetlands in terms of reducing or increasing river flows which in many cases are taken out of context and do not answer the basis for the conclusions. They argue that categorization of wetlands must be based on comparative scenarios. They give a set of comparative scenarios used internationally for categorization of wetlands among which is the comparison of inflows and outflows of a wetland system as a baseline for inference. The results of this study were based on the comparison of the inflows and outflows of the Barotse Wetland, these being inflows as recorded at Lukulu Gauge Station (including Kalabo Gauge Station) and outflows at Senanga

Gauge Station. According to the international guidelines as cited by Bullock and Acreman (2003) the methodology used for the in-out scenario is that hydrological inputs and outputs associated with a single wetland are measured after which the differences between the outputs are attributed to the wetland. However, the assumption for the Barotse Wetland, was that the inflows through runoff, ungauged streams, direct rainfall over the wetland and ground water were negligeable. Thus, to an extent, this study complied with the international guidelines as regards the method used to come to the conclusion on the role of the Barotse Wetland in flow modulation. Anchoring on the suggestions by Bullock and Acreman (2003) and the international guidelines that they cited, it was infered that the observed differences in the discharge hydrograph (Figure 24) and the differences in the rate of change in daily discharge time series (Figures 25, 26) between Lukulu and Senanga gauge stations during the ascending/peak and the receding periods typifies the regulatory role the Barotse Wetland plays in flow regimes. The findings of this study validates the assertions by Beilfuss and Santos (2001) that "overall, the Barotse Plain attenuates runoff from a catchment area of more than 335,000 Km^2 (27 percent of the total Zambezi catchment), with an average annual storage capacity of 8.5 x 109 m^3". The results of this study also give credence to the observations by Kasimona and Makwaya (1995) who suggested that "Although peak runoff from the Northern highlands typically reaches Lukulu by February-March (following the period of peak rainfall), Zambezi floodwaters take 4-6 weeks to pass through the Barotse Plain and peak discharge near the downstream outlet (Senanga Gauging Station) is often delayed until April or early May. Floodwaters recede slowly from the Barotse Plain during the six-month dry season, with high evaporation losses throughout the year".

The behaviour of the Barotse Wetland in flow attenuation is similar to that observed in the Okavango wetlands, also in the Zambezi River Basin, by Murwira et al. (undated). It was observed by Murwira *et al*. (undated) that, depending on the period, high and low flows, the rate of change in daily discharge for the upstream and downstream of the Okavango Wetland were different. This phenomenon made them conclude that the Okavango Wetland regulated flow regimes. Therefore, based on the guidelines as cited by Bullock and Acreman (2003), the results of this study coupled with the observations made by Kasimona and Makwaya (1995) and Beilfuss and Santos (2001), the Barotse Wetland can be characterised as one that regulates flow. Bunn and Arthington (2002) suggest that flow is a major determinant of physical habitat in streams which in turn is a major

determinant of biotic composition. Bullock and Acreman (2003) indicate that flow regulation by a wetland may mitigate downstream flooding. Therefore, this study has augmented the understanding of the role of the Barotse Wetland in flow regimes which is key in the management of the wetland as an ecosystem.

5.10.5 Land covers change assessment

"Given the crucial importance of water to life on Earth, it is necessary to consider how various ecosystems are linked through the hydrological cycle. One key example is the relationship between forests and wetlands. Far too often, these interdependent ecosystems are viewed as completely separate entities instead of a linked unit that plays a crucial role in the hydrological cycle and the preservation of our water resources. A better understanding of the role that these bodies play in the hydrological cycle will enable us to more effectively consider these ecosystems when formulating policies and management practices to protect our water resources" (Blumenfeld *et al*. 2009). The above extract from Blumenfeld *et al*. (2009) underscore the need for land cover assessments when trying to analyse the inundation dynamics of a wetland such as the Barotse Wetland. Though studies such as Timberlake (1998, 2000) and Fanshawe (2010) could not quantify the forest cover changes they all recognised the loss in forest cover in and around the Barotse Wetland. They attributed these losess to a host of anthropogenic induced factors which included:

> (i) the increased pressure for agricultural land expansion; (ii) settlements; (iii) timber production; (iv) energy; and (v) harvesting for other livelihood purposes.

This study, however, undertook to quantify the forest cover changes within the confines of the relief based delineated catchment. Through ground truthing campaigns the study also validated some of the drivers (Figure 31) of forest cover loss as advanced by Timberlake (1998, 2000) and Fanshawe (2010). The estimated total loss in forest cover for the period 1984 to 2015 was 294,806.34 hectares and confirms Tmberlake (1998) and Fanshawe (2010) assertions on the loss of forest cover. The estimated overall annual rate of loss in forest cover of 0.3 percent and the general downward trend in forest cover is in tandem with the Zambia Forest Department (ZFD) and the Food and Agriculture Organization (FAO) 2005 Integrated Land Use Assessment report presented by Mukosha (2014). The Mukosha (2014) report indicated an estimated annual loss of

0.07 percent and a total loss of 101,964 hectares in forest cover for the period 1990 to 2005 for Western Province. The delineated study area is 23.87 percent of the Western Province but captures most of the populated areas of the province with districts such as Mongu, Lukulu, Kalabo and Senanga included in the assessment. Therefore, the results of this study are potentially within the boundaries of actual forest cover loses. Furthermore, the loss of forest cover and its impact on wetlands and water resources in Zambia as a whole have been noted in the World Water Assessment Programme report (UNESCO, 2009) and Blumenfeld *et al*. (2009). Clearly, the highlighted general loss of forest cover in Zambia by the UNESCO (2009) report and as connected to impacts on wetlands by Blumenfeld et al. (2009) is in tandem with the findings of this study showing that there is very high rate of forest cover loss in Western Province with potential impacts on the Barotse Wetland.

The observed loss in forest cover is high and is potentially impacting on both the inundation extent and wetland biodiversity (Blumenfeld *et al*., 2009). This study has, at broad forest level, validated the assertion that "Deforestation in the woodlands flanking the floodplains, both Miombo and *Baikiaea*-dominated, has been marked over the last 40 years, resulting in an opening of the tree canopy and accompanying increase in fire risk and hazard. Soil erosion and loss of valuable nutrients from the generally dystrophic soils has possibly also occurred" (Timberlake, 1998). The loss in forest cover in the wetland catchment exposes bare land, which is largely sandy, and exacerbates soil erosion resulting in high generation of sediments that end up in tributary water bodies and finally pouring into the wetland. From June 1996, there is a notable increase in the grassland/shrubland/bareland land cover class (Figure 30) which implies that more land has become susceptible to sediment yielding. Yields of sediments in water bodies were validated with the field observations made at Sefula Rice fields in Mongu District (Figure 41). The canals that take water into the fields from the upland catchment showed yields of sediments which had blocked some of the side irrigation canals. This accumulation of sediments derived from upland erosion may bring about a decrease in the volume of a wetland, a reduction in the duration the wetland retains water and can, over time, change the structure of the plant community in the wetland (Jurik *et al*. 1994; Blumenfeld *et al*. 2009).

Figure 41: Photographic evidence of sedimentation yield in river channels and the main Barotse Floodplain: (A) and (B) main irrigation canal showing sediment accumulation, (C), (D) and (E) shows sedimentation in the branch irrigation canals and (F) shows sedimentation in the main Barotse Floodplain on the banks of the Zambezi River, Western Zambia.

It is the reduction in the wetland volume and the decrease in the residence time of water in the wetland that can, overtime, contribute to significant variations in inundation extent. This study has already established a significant correlation, with a coefficient of determination of 0.91, between discharge into the wetland and the inundation extent hence factors that impact on the discharge into the wetland consequently contribute to the variations in the inundation extent. It has been observed that there is sediment accumulation taking place in the Barotse Wetland (Figure 41); however, what this study has not determined are the quantities of sediments resulting from the changes in forest cover and the extent to which these sediments affect the inundation extent in the wetland. Pressure on forest resources is likely to take a rising projection due to a rising population, and increased demand for food and timber products has already been noted by Simwinji (1997), Timberlake (1998) and Fanshawe (2010). These pressures will quintessentially result in increased sediment generation if adequate mitigation measures are not put in place by relevant authorities to reduce the rate of deforestation as has been suggested by Blumenfeld et al. (2009) and UNESCO (2009).

However, Beilfuss and Santos (2001) argued that "land use and land cover changes are unlikely to have had a significant effect on Zambezi runoff patterns". Kasimona and Makwaya (1995) also argued that "the Zambezi headwaters region, covered by relatively infertile Kalahari sands, is frequently burned and cleared for small agricultural plots (machambas) but retains dense forest cover over most of the region. Beilfuss and Santos (2001) further, pointed out that "water diversions are currently negligible relative to the mean annual flow, and unlikely to affect runoff patterns in the near future".

5.10.6 Abrupt change point detection and trends analysis

Studies, which include Githui *et al*. (2005) and Khaleghi *et al*. (2014), have been done in various parts of the world to determine abrupt changes and trends in hydrological and meteorological data using the Pettit Homogeneity and Mann-Kendall Trends Tests. For instance, Githui *et al*. (2005) analysed the time series of annual values of rainfall and discharge for the time space 1963-1998 of Yala River Basin in Kenya. The results showed a decreasing trend for the rainfall data, a decreasing slope in the upstream station, and an increasing trend in the downstream station for the discharge data. Khaleghi *et al*. (2014) investigated the trends of river discharges and rainfall in Jajrood Watershed in Iran. Two river gauging stations, Roodak (upstream) and Latyan (downstream), and 6 rainfall stations including Latyan, Roodak, Ahar, Shemshak, Lavasan, and Garmabdarre were used. Their study sought to determine if the

discharge and rainfall values had generally increased or decreased over four decades. Their results showed rainfall data increasing upstream but decreasing downstream. The river discharge variations showed strong negative slope in Latyan station. Both Githui *et al.* (2005) and Khaleghi *et al.* (2014) as well as Hirsch and Helsel (2002) emphasized the need to ensure that time series data is cleaned before use and that seasonality is taken into account. Hirsch and Helsel (2002) and Khaleghi *et al*. (2014) point to the fact that detection or non-detection of trend in time series is based on the quality, quantity of data and other exogenous variables. They emphasise that any given test for trend has a definition of what is meant by "no trend". It includes assumptions generally related to the type of distribution and serial correlation. They indicate that failing to reject H_0 does not mean that it has been adequately proved that there is no trend. It is rather an indication that the evidence available is not sufficient to conclude that there is a trend. This study took into account the recommendations on data cleaning and followed standard procedures as suggested by Hirsch and Helsel (2002).

In Zambia, Kampata *et al.* (2008) used the Mann-Kendall Test to analyse trends in rainfall in the headstreams of the Zambezi River Basin. They analysed rainfall time series between 1945 and 2005 for Kabompo, Kasempa, Mwinilunga, Kaoma and Mongu Meteorological Stations. They concluded that "there was no evidence of significant trends in the annual rainfall at 0.05 significance level for all the individual stations as the computed Z statistics were found to be less than the critical value of 1.96. Although the trends are not significant, the rainfall is generally decreasing as evident from the negative values of the Mann–Kendall-statistics, S". The results of this study agree with those of Kampata *et al.* (2008) for Kabompo and Mongu stations. As observed in this study, the period 1974 to 2012, Kabompo and Mansa time series showed insignificant downward trends. Mongu station showed an insignificant upward trend in rainfall (Table 25). Though Mongu Station, representative of rainfall received in the wetland, showed an upward trend the rainfall received within the wetland does not significantly impact on the inundation (Beilfuss and Santos, 2001; IUCN, 2003 and Fanshawe, 2010). The study observed a generally downward trend in rainfall. The downward trend in rainfall is in tandem with the overall scenario analyses for Southern Africa by Frich *et al.* (2002), New *et al.* (2005) and Christensen *et al.* (2007), which indicate reduction in rainfall.

An insignificant downward trend in the maximum temperatures within the wetland area (as represented by the Mongu Station Maximum Temperature time series) during the period 1975

to 2003 was observed (Table 25). On discharge, the change point detection analysis showed that there were significant changes in the mean discharge in the Barotse Wetland. For instance, one of the major changes in annual mean discharge between 1952 and 2004 occurred in 1981 from 1123 to 808. 38 m^3. $year^{-1}$ and 846.52 to 614.97 m^3. $year^{-1}$ at Senanga and Lukulu Gauge Stations respectively. This change point is also noted by Beilfuss (2012) for the entire Zambezi River Basin. Generally, the trend in discharge into the wetland shows a downward trajectory. At both Lukulu and Senanga stations there was a significant downward trend in discharge between 1952 to 2004 with *p-value* < 0.05. This downward trend can also be visually observed (Figures 34, 35 and 26) as the discharge values varies in a downward direction. Variations in discharge for the period 1952 to 1974 were higher than variation for the period 1975 to 1981 which was higher than that for 1982 to 1997. Although the variations for the period 1998 to 2004 were higher than for the period 1982 to 1997, the amounts were lower than for the period 1967 to 1974 and 1975 to 1981 indicating an overall downward trend in discharge values. The variations in discharge observed in this study are very similar to those observed by Beilfuss (2012) for the Zambezi River Basin. The implications of the trends in discharge on the inundation extent is that by correlation the downward trend in discharge translates into a downward trend in inundation extent in the Barotse Wetland. A downward trend or departure from the normal mean in discharge has significant reparations on water quality and quantity in a river system (Hirsch and Helsel, 2002).

5.10.7 Hydrologic, climatologic and land cover variables correlation with inundation

There was a strong coefficient of determination of 0.91 between mean daily discharge and 8-day interval inundation extent (Table 13 and Figure 22) and a correlation coefficient of 0.81 between mean monthly discharge and mean monthly inundation extent (Table 27). These results correlate with the assertions by Kasimona and Makwaya (1995), Beilfuss and Santos, (2001), IUCN (2003) Fanshawe (2010), Beilfuss (2012) which state that inundation in the Barotse Wetland is as a result of the discharge from the Zambezi River and its tributaries into the wetland. Further, the significant correlation, *p*-value <0.05, between mean annual rainfall time series at Kabompo Station and the mean annual discharge time series at Senanga Station supports the dependence of the inundation extent on the upstream wetland catchment rainfall. The observed relationship between rainfall at Kabompo Station and discharge at Senanga Station is supported by Koster and Suarez (1999) and Zhao *et al.* (2011), who observed that spatial rainfall variability is the main source of variability in discharge. Thus, based on the

observed correlation between discharge and rainfall, the overall downward trend in rainfall at Kabompo Station means that the overall trends in discharge at Kalabo, Lukulu and Senanga gauge stations in the wetland for the period 1952 to 2004 (Figures 34 – 36) was downward as well.

The IPCC (2001), Paul *et al.* (2006) and Kim *et al.* (2012) point to how climate variables such as increased temperature and rainfall variability will impact on wetlands globally through changes in water quantity and quality. According to the Millennium Ecosystem Assessment, (2005), Blumenfeld *et al*. (2009) and Woodward *et al.* (2014) understanding the interlinkages between wetlands, changes in land cover and use and between climate and hydrological variables such as discharge, rainfall and temperature is crucial to the mananagment of water resources in general and wetlands in particular. For instance, changes in land cover and use is one of the major contributors to wetland degradation mainly through increased catchment erosion and nutrient loading (Erwin, 2009; Blumenfeld et al. 2009; Fanshawe, 2010). Woodward *et al.* (2014) observed that reduction in forest cover increased wetland inundation extent and water level. Thus, the long term perspective of this study is that the observed reduction in forest cover in the Barotse Wetland catchment will have significant effects on the hydrology of the wetland. Based on this study's observed trends and correlations between hydrological and climatological variables and the changes in the forest cover Changes in the wetland catchment, these variables will continue to play a significant role in inundation extent trends in the Barotse wetland.

CHAPTER SIX: CONCLUSIONS AND RECOMMENDATIONS

The conclusions derived from the study and the recommendations are presented in this chapter in a summarised form following the study objectives as outlined in Chapter 1. The recommendations seek to point at areas where intervention by way of further studies and action by relevant institutions is required.

6.1 CONCLUSIONS

The following were the conclusions:

(i) The highest inundation extent was observed in 2009 at 6,658.75 Km^2 while the lowest extent was observed in the year 2005 at 3169.25 Km^2.

(ii) Based on the quantified inundation extent and analysed with the one-way RM ANOVA, the Barotse Wetland experienced significant (*p-value* < 0.05) variations in inundation extent in the period 2003 to 2013. Inundation extent on the days assessed during the period 2003 to 2013 differed each year.

(iii) Inundation extent showed an increasing trend in the period 2003 to 2013 with a Mann-Kendall Z statistic of 1.87 at alpha level 0.05. The trend in inundation extent was similar to the water level trend which also showed a rising scenario (Mann-Kendall Z statistic of 2.67) for the period 2000 to 2011. The Pearson correlation coefficient of Inundation extent and water level was 0.89 while discharge and inundation extent showed a coefficient of 0.91. This implies that trends in inundation extent increase or decrease with increase or decrease in water level/discharge trend(s).

(iv) Though data on actual evapotranspiration, runoff, ground water flows and rainfall over the wetland was not obtained to calculate the water balance for the Barotse Wetland, the differences in the hydrographs of inflows and outflows and the rates of change in discharge at Lukulu and Senanga gauge stations suggest the wetland plays a major role in flow attenuation. For instance, during the receding period, that is from mid-April to end of July of a hydrological year, the inflow (discharge) rate of change (for the hydrological year 1996/1997) at Lukulu Gauge Station was lower, 9.50 $m^3.day^{-1}$, than the outflow (discharge), 14.85 $m^3.day^{-1}$, at Senanga

Gauge Station. This phenomenon suggests an attribute that accentuates the Barotse Wetland as a regulator of flow from the upper catchment(s).

(v) Discharge at Senanga Gauge Station correlates positively with rainfall at Kabompo Meteorological Station with a correlation coefficient of 0.36 and *p*-value of < 0.05 at significance level alpha of 0.05. By correlation, variability in discharge in the wetland follows the variability pattern in the spatial rainfall distribution in the upper catchment.

(vi) There were abrupt changes in mean monthly values of discharge in the study area for the period 1967 to 2007. For Lukulu Station, a change point was observed in the month of May 1981 from 846.52 m^3. $month^{-1}$ to 614.97 m^3. month-^{1} after the change. Another change point was observed in February 1991 from a mean monthly value of 647.377 m^3. $month^{-1}$ to 606.152 m^3. $month^{-1}$. A final change point was in December 1997 from 487.024 m^3. $month^{-1}$ to 888.701 m^3. $month^{-1}$. For Senanga Gauge Station, only one significant abrupt change was noted in July 1981 from a mean monthly discharge of 1065 m^3. $month^{-1}$ to 828.478 m^3. $month^{-1}$. There was a significant abrupt change in the annual means of discharge for both Lukulu and Senanga stations. For Lukulu Station an abrupt change in the annual mean discharge was observed in the hydrological year 1980/1981 from a mean of 810.417 m^3. $year^{-1}$ to 604.660 m^3. $year^{-1}$. Senanga Station time series revealed an abrupt change in the 1979/1980 hydrological year from 1078 m^3. $year^{-1}$ to 873.256 m^3. $year^{-1}$. Generally, significant downward abrupt changes in the monthly and annual means of discharge were observed in the hydrological years 1979/1980 and 1981/1982.

(vii) The Mann-Kendall test for trends revealed overall insignificant (*p-value* > 0.05) downward trend in rainfall at Kabompo Station whereas discharge at Lukulu, Kalabo and Senanga gauge stations showed significant (*p-value* < 0.05) overall downward trend. At alpha level 0.05, Senanga and Lukulu stations discharge time series (1952 to 2004) showed significant downward trends with Z-statistics of -3.38 and -2.88 respectively.

(viii) Significant (*p-value* < 0.05) correlation with coefficient of correlation of 0.91 between discharge and inundation extent was observed. Based on this established

relationship it can be inferred that during the period 1952 to 2004, the overall trend in inundation extent in the Barotse Wetland was also in the downward direction in tandem with the downward trend in discharge.

(ix) Forest cover (Forest/wood vegetation) reduced by 9.77 percent during the period June 1984 to June 2015 in the study area. During the same period the class grassland, shrubland and bare land increased by 8.3 percent. The observed rate of decrease in forest cover of 0.3 percent is relatively high and could cause disproportional distortions in the hydrological parameters and affect biodiversity in the wetland especially when viewed from the entire wetland catchment perspective. The rate of decrease in forest cover is linked to increase in land use practices such as agriculture, energy and timber production as observed during the field surveys as well as from the literature reviewed.

(x) By the correlations between variables established in this study, it can be inferred that inundation extent follows the patterns in rainfall in the upper catchment, discharge/water level in the wetland, temperature and also the changes in forest cover in the wetlands catchment.

(xi) Overall, use of remote sensing or earth observation-based systems such as satellite MODIS and Landsat imagery augmented by ground truthing provide a faster, cheaper and timely system for acquiring the type and quantity of inundation extent data needed to inform key wetland management decisions. This is despite the inherent limitations associated with the use of optical satellite imagery data such as cloud cover and the time lag associated with the revisit cycle of satellites over a given location. For developing countries like Zambia where financial resources and other logistical constraints negate field survey based data collection systems, satellite remote sensing provides enormous leverage for data collection with minimal financial resources.

(xii) From this study it has been observed that dynamics of inundation extent and its interactions with other variables such as discharge can statistically be evaluated and used as basis for drawing management frameworks for adaptation to climate change.

6.2 RECOMMENDATIONS

Based on the conclusions of the study the following recommendations are advanced for intervention:

(i) The Government of Zambia through the Ministry of Agriculture and Livestock, the Ministry of Lands, Natural Resources and Environmental protection and other relevant institutions must consider using high resolution remote sensing data such as LIDAR to map and characterize the land cover and use patterns in the entire wetland catchment so as to enhance climate change mitigation and adaptation measures.

(ii) Noting from the successful detection and quantification of inundation extent based on the MODIS and Landsat imagery the Government of Zambia, through the Ministry of Lands, Natural Resources and Environmental protection, must consider setting up an earth observation based approach to capture data, process and utilize the information for wetland monitoring and management. These data are available for free and can easily be processed using simple techniques such as what has been used in this study.

(iii) In view of the high rate of depletion of forest cover in the areas surrounding the wetland the Government of Zambia through the Ministry of Agriculture, Ministry of Livestock and Fisheries, the Ministry of Lands, Natural Resources and Environmental protection and other relevant institutions must upscale existing or devise new integrated forest management interventions to curb, to significantly minimal level, the rate of deforestation going on in the area.

(iv) The Ministry of Agriculture and the Ministry of Livestock and Fisheries Development must pay particular attention to the observed patterns in inundation extent and its relationship with discharge/water level when developing physical infrastructure for climate adaptation in the wetland because inundation extent follows the discharge/water level pattern which is highly variable.

(v) The Integrated Water Resources Management Centre of the University of Zambia must help the Ministry of Agriculture to devise new water management practices and tools especially for small-holder farmers in the Barotse Wetland who are already experiencing the impact of varying inundation scenarios.

(vi) The Government of Zambia must ensure that no extensive alterations are made to the current wetland landscape as such actions have potential to alter the flow regime modulation role of the wetland.

(vii) More research should be done on quantifying the impact of the changes in forest cover and other anthropogenic activities on the wetland inundation regimes and biodiversity. Also, interested researchers should consider carrying out an in-depth study in order to identify and characterize the elements that gives the wetland its capacity to modulate downstream flow regimes.

7.0 REFERENCES

Aduah, M. S. and Mantey, S. (2012), "Remote sensing for mapping wetland floods in Kafue Flats, Zambia", Ghana Mining Journal, pp 33 - 40.

Agrawal, A. 2008: Social Dimensions of Climate Change. The Role of Local Institutions in Adaptation to Climate Change. Social Development Department paper The World Bank, Washington DC, pp 103 - 122.

Ahmad, A. and Quegan, S., 2012. Analysis of Maximum Likelihood Classification on Multispectral data. Applied Mathematical Sciences, 6(129), pp 6425 - 6436.

Baidu-Forson, J.J., Phiri, N., Ngu'ni, D., Mulele, S., Simainga, S., Situmo, J., Ndiyoi, M., Wahl, C., Gambone, F., Mulanda, A., Syatwinda, G. (2014). Assessment of agrobiodiversity resources in the Borotse flood plain, Zambia. CGIAR Research Program on Aquatic Agricultural Systems. Penang, Malaysia. Working Paper: AAS-2014-12, pp 1 - 9.

Beilfuss, R. and Santos, D. d., 2001. Patterns of hydrological change in the Zambezi Delta, Mozambique, Maputo, Mozambique: Programme for the sustainable management of Cahora Bassa Dam, pp 10 - 13.

Beilfuss, R., 2012. A Risky Climate for Southern African Hydro: Assessing hydrological risks and consequences for Zambezi River Basin Dams, 2150 Allston Way, Suite 300, Berkeley, CA 94704, USA: International Rivers, pp 9 - 15.

Boko, M., I. Niang, A. Nyong, C. Vogel, A. Githeko, M. Medany, B. Osman-Elasha, R. Tabo and P. Yanda, 2007: Africa. Climate Change 2007: Impacts, Adaptation and Vulnerability. Contribution of Working Group II to the Fourth Assessment Report of the Intergovernmental Panel on Climate Change, M.L. Parry, O.F. Canziani, J.P. Palutikof, P.J. van der Linden and C.E. Hanson, Eds., Cambridge University Press, Cambridge UK, pp 433 – 467.

Blumenfeld, S., Lu, C., Christophersen, T. and Coates, D., 2009. Water, Wetlands and Forests. A Review of Ecological, Economic and Policy Linkages, Montreal and Gland: Secretariat of the Convention on Biological Diversity and Secretariat of the Ramsar Convention on Wetlands, pp 103 – 123.

Bullock, A. and Acreman, M., 2003. The role of wetlands in the hydrological cycle. Hydrology and Earth System Sciences, 7(3), pp 358 - 389.

Bunn, S. E. and Arthington, A. H., 2002. Basic principles and ecological consequences of altered flow regimes for aquatic biodiversity. Environmental Management, Issue 30, pp 492-507.

Cai Xueliang, Haile Alemseged, Magidi James, Mapedza Everisto, 2015. Living with floods – household perception and satellite observations in the Barotse Floodplain, Zambia. 17th WaterNet/WARFSA/GWPSA Symposium, Mauritius, pp 4 - 8.

Central Statistics Office, 2010. Government of the Republic of Zambia. 2010 census of population and housing. National descriptive tables, Volume 11.

Chander, G. and Markham, B., 2003. Revised Landsat-5 TM Radiometric Calibration Procedures and Post Calibration Dynamic Ranges. IEEE TRANSACTIONS ON GEOSCIENCE AND REMOTE SENSING, 41(11), pp 2674 - 2677.

Christensen, J. H., Hewitson, B., Busuioc, A. et al. 2007. Regional Climate Projections. - In: Solomon, S., Qin, D., Manning, M., Chen, Z., Marquis, M., Averyt, K. B., Tignor, M. and Miller, H. L. (eds.), Climate Change 2007: The Physical Science Basis. Contribution of Working Group I to the Fourth Assessment Report of the Intergovernmental Panel on

Climate Change. Cambridge University Press, Cambridge. United Kingdom and New York, NY, USA. Section 11.2 (Africa), pp 326 -356.

Cohen T. Liechti, Matos J.P., Boillat J.-L., Portela M.M. and Schleiss A.J., (2014): Hydraulic–hydrologic model for water resources management of the Zambezi basin, Journal of Applied Water Engineering and Research, DOI: 10.1080/23249676.2014.958581, pp 80-92.

Cooley, T. et al., 2002. FLAASH, a MODTRAN4-based atmospheric correction algorithm, its application and validation. Geoscience and Remote Sensing Symposium, 3(IGARSS'02), pp 1414-1418.

Coppin, P. et al., 2004. Digital change detection methods in ecosystem monitoring; a review. International Journal of Remote Sensing, Volume 25, 1565–1696.

Diaz, H. and A. Rojas, 2006, "Methodological Frame work for the Assessment of Governance Institutions", working paper prepared for the IACC project. www.parc.ca., pp 1-8

Di Baldassarre, G., 2012. Floods in a changing climate: Inundation Modelling. New York: Cambridge University Press, pp 67 - 86.

ENVI, User's guide, 2009. Research Systems Inc., USA, 2009, pp 92 – 150.

Erwin, K. L., 2009. Wetlands and global climate change: the role of wetland. Springer Science Business Media B.V., 17(DOI 10.1007/s11273-008-9119-1), pp 71 - 83.

European exchange circle on flood mapping, 2007. Hand book on good practices for flood mapping in Europe. Prepared by EXCIMAP (a European exchange circle on flood mapping) Endorsed by Water Directors, 29-30 November 2007, pp 9 - 42.

Fanshawe, B. D., 2010. Vegetation Description of the Upper Zambezi Districts of Zambia, Famona, Bulawayo, Zimbabwe: Biodiversity Foundation for Africa, pp 76 – 130.

Ferrati R, Canziani G. A, Moreno D. R, 2005. Estero del Ibera: hydro meteorological and hydrological characterization. Ecol Model 186, pp 3 – 15.

Feyisa, G. L., Meilby, H., Fensholt, R. and Proud, S. R., 2014. Automated water extraction index: A new technique for surface water mapping using Landsat imagery. Remote Sensing of Environment, Volume 140, pp 23 - 35.

Foster, J., Curtin, A., Hill, B., Ronan, M., Wainwright, P., Blackhall, S., . . . O'Donnell, C. (2012). The Role of Wetlands in the Carbon Cycle. Canberra, Australia: Department of Sustainability, Environment, Water, Population and Communities in consultation with the Wetlands and Waterbirds Taskforce, pp 2 - 9.

Frich, P.; Alexander, L. V.; Della-Marta, P.; Gleason, B.; Haylock, M.; Tank, A. K.; Peterson, T.,2002. Global changes in climatic extremes during the 2nd half of the 20th century. Climate Res, Volume 19, pp 193 - 212.

Gilmore, S. and Saleem, A. and Gilmore, A. 2015. Effectiveness of DOS (Dark-Object Subtraction) method and water index techniques to map wetlands in a rapidly urbanising megacity with Landsat 8 data, in Veenendaal, B. and Kealy, A. (ed), Proceedings of Research@Locate in conjunction with the annual conference on spatial information in Australia and New Zealand, Vol-1323, Mar 10-12 2015, pp 100-108. Brisbane: CEUR-WS.

Gitay, H., Finlayson, C.M. and Davidson, N.C. 2011. A Framework for assessing the vulnerability of wetlands to climate change. Ramsar Technical Report No. 5/CBD Technical Series No. 57. Ramsar Convention Secretariat, Gland, Switzerland and Secretariat of the Convention on Biological Diversity, Montreal, Canada. ISBN 92-9225-361-1 (print); 92-9225-362-X (web), pp 1 – 13.

Githui, F. W., Opere, A. and Bauwens, W. (2005) Statistical and Trend Analysis of Rainfall and River Discharge: Yala River Basin, Kenya. Proceedings of the International Conference of UNESCO Friend/Nile Project: Towards A Better Cooperation; Sharm El-Sheikh, Egipto, pp 171-181.

Government of the Republic of Zambia, Ministry of Finance and National Planning, 2013. Strategic Programme for Climate Resilience. Pilot Programme on climate Resilience, pp 16 - 27

Hamed, K.H, Rao, R. 1998. A Modified Mann-Kendall trends test for autocorrected data. Journal of hydrology, Vol 204, pp 182-196.

Hirsch, R. M., Slack, J. R. and Smith, R. A. (1982) Techniques of trend analysis for monthly water quality data, Water Resources Research, 18(1), pp 107–121.

Hirsch, R. M. and Helsel, D. R., 2002. Statistical Methods in Water Resources. In: Techniques of Water-Resources Investigations of the United States Geological Survey: Hydrologic Analysis and Interpretation. U.S. Geological Survey, pp 137 - 357.

International Federation of the Red Cross (IFRC), 2008. Zambezi River Basin Initiative Project document. Southern Africa. www.ifrc.org. November 8, 2015, pp 1- 8.

IPCC (International Panel on Climate Change) ,1996. Climate change 1996—impacts, adaptations and mitigation of climate change: scientific technical analysis. Contribution of working group II to the second assessment report, pp 141 – 152.

IPCC (International Panel on Climate Change), 2001. Impacts, adaptation, and vulnerability. Technical summary, and summary for policymakers. Third assessment report of working group I of the intergovernmental panel on climatic change, pp 1 – 34. URL: http://www.ipcc.ch

IPCC., 2014. Climate Change 2014. Impacts, Adaptation, and Vulnerability. IPCC WGII AR5 Summary for Policymakers, pp 1 – 34.

IUCN, 2003. Barotse Floodplain, Zambia: Local economic dependence on wetland resources, Harare: The World Conservation Union Regional Office for Southern Africa, pp 1 – 6.

Jain, S., 2007. An Empirical Economic Assessment of Impacts of Climate Change on Agriculture in Zambia. The World Bank Development Research Group, Sustainable Rural and Urban Development Team, pp 1 – 46.

Jassim, F. A. and Altaani, F. H., 2013. Hybridization of Otsu Method and Median Filter for Colour Image Segmentation. International Journal of Soft Computing and Engineering, 3(2), pp 69 - 74.

Jurik, T. W., Van der valk, A. G. and Wang, S. C., 1994. Effects of sediment load on seedling emergence from wetland seed banks. Wetlands, Issue 14, pp 159 - 165.

Kampata, J. M., Parida, B. P., Moalafhi, D. B., 2008. Trend analysis of rainfall in the headstreams of the Zambezi River Basin in Zambia. Physics and Chemistry of the Earth (03), pp 621–625.

Kasimona, V.N., and J.J. Makwaya. 1995. Present planning in Zambia for the future use of Zambezi River waters. pp 49 - 56 in T. Matiza, S. Crafter, and P. Dale., eds. Water resources

use in the Zambezi Basin. Proceedings of a workshop held at Kasane, Botswana, April 28-May 2 1993. Gland: IUCN.

Khaleghi, M., Zeinivand, H. and Moradipour, S., 2014. Rainfall and River Discharge Trend Analysis: A Case Study of Jajrood Watershed, Iran. International Bulletin of Water Resources and Development, II (03), pp 1 - 8.

Kim Duck Gil, Noh Hui Seong, Kang Na Rae, Kim Hung Soo, 2012. Impact of Climate Change on Wetland Functions. Department of Civil Engineering, Inha University, Korea. Hydrology days 2012, pp 43 - 50.

Koster, R. D. and Suarez, M. J., 1999. A simple framework for examining the interannual variability of Land surface moisture fluxes. Journal of Climate, Volume 12, pp 1911-1917.

Kudahetty, C., 2012. Flood Mapping Using Synthetic Aperture Radar in Kelani Ganga and Bolgoda Basins, Sri Lanka. Enschede, Netherlands: University of Twente, pp 1 – 36.

Lillesand, T. M., Kiefer, R. W. and Chipman, J. W., 2004. Remote Sensing and Interpretation. Hoboken(NJ): John Wiley and Sons, pp 397 – 624.

Long, S., Fatoyinbo, T. E. and Policelli, F., 2014. Flood extent mapping for Namibia using change detection and thresholding with SAR. Environmental Research Letters, Volume 9, pp 1 - 10.

McFeeters, S., 1996. The use of the Normalised Difference Water Index (NDWI) in the delineation of open water features. International Journal of Remote Sensing, Volume 17, pp 1425 - 1432.

Millennium Ecosystem Assessment, 2005. “ECOSYSTEMS AND HUMAN WELL-BEING: WETLANDS AND WATER Synthesis,” World Resources Institute, Washington, DC, pp 13-21.

Meire, P., 2012. Real-Time Hydrologic Modelling and Floodplain Modelling in the Kafue River Basin, Zambia. Zürich: ETH Zürich Diss. eth no. 20421, pp 37 - 44.

Ministry of Agriculture and Cooperatives, 2005. Agro-ecological Regions of Zambia map.

Mu Qiaozhen, Faith Ann Heinsch, Maosheng Zhao, Steven W. Running, 2007. Development of a global evapotranspiration algorithm based on MODIS and global meteorology data. Remote Sensing of Environment 111 (2007), pp 519 – 536.

Mukosha, Jackson. 2014. Zambia's historical forest change assessment and future plans. Lusaka: Zambia Forest Department. Extracted from the Integrated Land Use Assessment project report. pp 16 - 18.

Murwira, Amon., Elisha, Madamombe., and Karin. S. Schmidt-Murwira., (undated). Role of wetlands in flood mitigation: The Zambezi Wetlands case study. Harare: University of Zimbabwe, Department of Geography and Environmental Sciences. pp 1 - 21.

Naiman, R. J., Magnuson, J. J., McKnight, D. M. and Stanford, J. A., 1995. The Freshwater Imperative: A research Agenda, Washington D.C: Island Press, pp 58 – 70.

New, Mark; Hewitson, Bruce; Stephenson, David B.; Tsiga, Alois; Kruger, Andries; Manhique, Atanasio; Gomez, Bernard; Coelho, Caio A. S.; Masisi, Dorcas Ntiki; Kalulanga, Elina; Mbambalala, Ernest; Adesina, Francis; Saleh, Hemed; Kanyanga, Joseph; Adosi, Juliana; Bulane, Lebohang; Fortunata, Lubega; Mdoka, Marshall L.; Lajoie, Robert., 2005. Evidence of trends in daily climate extremes over Southern and West Africa. Journal of Geophysical Research – Atmosphere, pp 2 - 24.

Okoye, M. A. & Koeln, G. T., 2003. Encyclopaedia of Life Support Systems. [Online]

Otsu, N., 1979. A threshold selection method from Gray-Level Histograms. IEEE Transactions on Systems, Man, and Cybernetics, SMC-9(1), pp 62 - 66.

Paolini, L. et al., 2006. Radiometric correction effects in Landsat multi-date/multi-sensor change detection studies. International Journal of Remote Sensing, pp 685 – 704.

Paul S, Jusel K, Alewell C,2006. Reduction processes in forest wetlands: tracking down heterogeneity of source/link functions with a combination of methods. Soil Biol. Biochem 38, pp 1028 – 1039.

Phiri, W.K., 2013. Remote sensing estimation of spatial and temporal variability of actual evapotranspiration using the SEBS algorithm in the semi-arid Barotse basin, South-Western Zambia, M.Sc. Thesis, The University of Zambia, Lusaka, Zambia, pp 61 - 109.

Pettit A. N. (1979). A Non-Parametric Approach to the Change-Point Problem. Applied Statistics, 28, pp 126 - 135.

Pohlert, T., 2014. The Pairwise Multiple Comparison of Mean Ranks Package (PMCMR): R package, http://creativecommons.org/licenses/by-nd/4.0: Creative Commons License (CC BY-ND 4.0), pp 1 – 9.

Proud, S. R., Fensholt, R., Rasmussen, L. Y. and Sandholt, l., 2011. Rapid response flood detection using the MSG geostationary satellite. International Journal of applied earth observation and Geoinformatics, 13(4), pp 536 - 544.

Rouse, J. W., Haas, R. H., Schell, J. A. and Deering, D. W., 1973. Monitoring vegetation sytems in the great plains with ERTS, Washington, DC: The 3rd ERTS Symposium, NASA, pp 309 – 317.

Sahagian D and Melack J., 1998. Global wetland distribution and functional characterization: trace gases and the hydrologic cycle. IGBP Report, pp 46.

Salmi, T., Määttä, A., Anttila, P., Ruoho-Airola, T., and Amnell, T. (2002). Detecting trends of annual values of atmospheric pollutants by the Mann-Kendall test and Sen's slope estimates –the Excel template application MAKESENS. Finnish Meteorological Institute (31), pp 11 - 12.

Schumann, G., P. Matgen, F. Pappenberger, R. Hostache, and L. Pfister, 2007. Deriving distributed roughness values from satellite radar data for flood inundation modelling, J. Hydrol.,344, pp 96 – 111.

Simwinji, N., 1997. Summary of the existing Relevant Social-economic and Ecological information on Zambia's Western Province and Barotseland, Harare: IUCN-The World Conservation Union Regional Office for Southern Africa, pp 42 - 48.

Sirois, Allan, 1998. A Brief and Biased Overview of Time Series Analysis or How to Find that Evasive Trend. In WMO report No. 133: WMO/EMEP workshop on Advanced Statistical methods and their Application to Air Quality Data sets (Helsinki, 14-18 September 1998), pp 10 - 24.

Song Conghe, Curtis E. Woodcock, Karen C. Seto, Mary Pax Lenney, and Scott A. Macomber, 2001. Classification and Change Detection Using Landsat TM Data: When and How to Correct Atmospheric Effects? Journal of Remote Sensing of the Environment. Vol 75, pp 230 – 244.

Sparks, R. E., 1995. Need for ecosystem management of large rivers and floodplains. Bioscience, Volume 45, pp 168 - 182.

Stisen, S., Jensen, K. H., Sandholt, I., and Grimes, D. I. F., 2008. A remote sensing driven distributed hydrological model of the Senegal River basin. Journal of Hydrology, 354, pp 131 - 148.

STRP (Scientific and Technical Review Panel of the Ramsar Convention on Wetlands) (2002) New guidelines for management planning for Ramsar sites and other wetlands. ‘‘Wetlands: water. Life, and culture’’ 8th meeting of the conference of the contracting parties to the convention on wetlands (Ramsar, Iran, 1971) Valencia, Spain, 18–26. Nov 2002, pp 1 – 13.

Thurlow, J., Zhu, T. and Diao, X., 2009. Climate Change, Economic Growth and Poverty in Zambia, Washington D.C: International Food Policy Research Institute, pp 1 – 18.

Ticehurst, C. J. et al., 2013. Using MODIS for mapping flood events for use in hydrological and hydrodynamic models: Experiences so far. Adelaide, Australia, 20th International Congress on Modelling and Simulation, pp 1721 -1726.

Ticehurst, C., Guerschmann, J. P. and Chen, Y., 2014. The Strengths and Limitations in Using the Daily MODIS Open Water Likelihood Algorithm for Identifying Flood Events. Remote Sensing, 6(ISSN 2072-4292), pp 11791 - 11809.

Tiger initiative, 2008. Satellite data for monitoring flooding and vegetation changes of the Kafue Flats, Zambia, in relation to the new water management regulations at Zesco Ltd. The Tiger Initiative, 2005 - 2008 report, pp 13.

Timberlake, L., 1997. Biodiversity of the Zambezi Basin Wetlands: A Review of Available Information, Zambezi Society and Biodiversity Foundation for Africa Report to IUCN − The World Conservation Union Regional Office for Southern Africa, Harare, pp 1 - 45.

Timberlake, J., 1998. Biodiversity of the Zambezi Basin Wetlands: Review and preliminary assessment of available information, Harare/Bulawayo: Zambezi Society and the Biodiversity Foundation for Africa, pp 9 – 90.

Timberlake, J., 2000. Biodiversity of the Zambezi Basin. Biodiversity Foundation for Africa, Volume 09, pp 1 - 20.

Townsend, P. A., 2002. Relationships between forest structure and the detection of flood inundation in forested wetlands using C-band SAR. International Journal of Remote Sensing, 23(3), pp 443 - 460.

Turpie, J., Smith, B., Emerton, L., Barnes, J. (1999). Economic value of the Zambesi Basin wetlands. IUCN – The World Conservation Union Regional Office for Southern Africa, Harare, pp 4 - 90.

UNEP, 2015. "Wetlands Meeting the Challenges of the Future,". CBD Press Brief. Secretariat of the Convention on Biological Diversity, UNESCO, Montreal, Quebec, H2Y 1N9.Canada, pp 1 - 2

UNESCO, 2009. "Zambia: The Zambezi and Congo river basins" in World Water Assessment Programme. 2009. The United Nations World Water Development Report 3: Case Study Volume: Facing the Challenges. Paris: UNESCO, and London: Earth scan, pp 15 - 18.

USGS, 2015. Landsat 8 (L8) data user's handbook. Version 1.0 ed. Sioux Falls, South Dakota: EROS, pp 41 – 64.

Varjo, J., 1996. Radiometric correction of multi-temporal Landsat TM data for detecting rapid changes in mineral soil forest land. International Archives of Photometry and Remote Sensing, 33(7), pp 720 - 733.

Vermote E, Xiong X., Wolfe R., Barnes W., Guenther B., Saleous N.Z., Salomonson V., Terra and Aqua MODIS Design, Radiometry and Geometry in Support of Land Remote Sensing. 2011. Land Remote Sensing and Global Environmental Change: NASA's Earth Observing System and the Science of ASTER and MODIS. Series: Remote Sensing and Digital Image Processing, Vol. 11, Springer Verlag. pp 873. ISBN: 978-1-4419-NASA Goddard Space Flight Center Terrestrial Information Systems Laboratory Mail Code 619, Building 32, S036C Greenbelt, MD 20771 USA.

Vermote E. and Kotchenova S. Y. 2011. MODIS Directional surface reflectance product: Method, error estimates and validation. Land Remote Sensing and Global Environmental Change: NASA's Earth Observing System and the Science of ASTER and MODIS. Series: Remote Sensing and Digital Image Processing, Vol. 11, Springer Verlag. pp 873. ISBN: 978-1-4419-6748-0.

Wang, S., 2007. The Quantitative Research on Dynamic Changes between flood and Vegetation in Tarim. Beijing: Beijing Normal University (PhD- Dissertation), pp 1 – 30.

Wang S., Baig, M. H. A. Zhang, . L. G. Jiang, S. Lu and Q. Tong, 2013. “Comparison of MNDWI and DFI for Water Mapping in Flooding Season,” *Chinese Academy of Sciences*, pp 2876 – 2879.

Woodward, C; Shulmeister, J; Larsen, J; Jacobsen, G E; Zawadzki, A., 2014.The hydrological legacy of deforestation on global wetlands. Science, 346(6211), pp 844 - 846.

Xu, H., 2006. Modification of normalised difference water index (NDWI) to enhance open water features in remotely sensed imagery. International Journal for Remote Sensing, pp 3025 – 3033.

Yamba F.D, Chipeta G. B., Walimwipi. H., Jain. S., 2009 Site specific evidence of climate change/variability in Kapiri Mposhi, Mwansabombwe and Sesheke, IUCN Climate Change and Development project background studies, pp 8 – 36.

Zhai, K., Wu, X., Qin, Y. and Du, P., 2015. Comparison of surface water extraction performances of different classic water indices using OLI and TM imageries in different situations. Geo-spatial Information Science, 18(1), pp 32 - 42.

Zhao, F. F., Zhang, L., Chiew, F. H., and Vase, J. (2011). The effect of spatial rainfall variability on streamflow prediction for a South-eastern Australian catchment. Perth, Australia: 19th International Congress on Modelling and Simulation,12 – 16 December, 2011, pp 3684 – 3689.

http://www.undp.org

http://glovis.usg.gov

8.0 APPENDICES

Appendix 1: Landsat Images used in the study for flood extent mapping and assessment of land cover changes, Barotse Wetland, Western Zambia.

QTY	PATH/ROW	RES	FORMAT	SENSOR	PROD TYPE	CC(%)	SCENE TIME	DATE
9	174/070	30	GEOTIFF	L5 TM	L1T	0	07:52:23.4770440Z	1984-07-04
9	175/070	30	GEOTIFF	L5 TM	L1T	0	07:58:14.0630880Z	1984-06-09
9	175/071	30	GEOTIFF	L5 TM	L1T	0	07:58:38.0370060Z	1984-06-09
9	176/070	30	GEOTIFF	L5 TM	L1T	0	08:05:01.8416	1984 07 18
9	176/071	30	GEOTIFF	L5 TM	L1T	0	08:05:25.8046	1984 07 18
9	174/070	30	GEOTIFF	L5 TM	L1T	0	07:36:00.8280310Z	1996-06-03
9	175/070	30	GEOTIFF	L5 TM	L1T	0	07:42:34.5820880Z	1996-06-10
9	175/071	30	GEOTIFF	L5 TM	L1T	0	07:42:58.6180310Z	1996-06-10
9	176/070	30	GEOTIFF	L5 TM	L1T	0	07:49:08.1620310Z	1996-06-17
9	176/071	30	GEOTIFF	L5 TM	L1T	0	07:49:32.1980310Z	1996-06-17
9	174/070	30	GEOTIFF	L5 TM	L1T	0	08:05:36.0340560Z	2004-06-25
9	175/070	30	GEOTIFF	L5 TM	L1T	0	08:11:29.9500000Z	2004-06-16
9	175/071	30	GEOTIFF	L5 TM	L1T	0	08:11:54.0660000Z	2004-06-16
9	176/070	30	GEOTIFF	L5 TM	L1T	0	08:17:25.7930310Z	2004-06-07
9	176/071	30	GEOTIFF	L5 TM	L1T	0	08:17:49.9090310Z	2004-06-07
9	174/070	30	GEOTIFF	L8 OLI	L1T	1.64	08:23:04.6330075Z	2015-06-08
9	175/070	30	GEOTIFF	L8 OLI	L1T	0	08:29:19.4234228Z	2015-06-15
9	175/071	30	GEOTIFF	L8 OLI	L1T	0	08:29:43.3646163Z	2015-06-15
9	176/070	30	GEOTIFF	L8 OLI	L1T	0	08:35:24.6996098Z	2015-06-06
9	176/071	30	GEOTIFF	L5 TM	L1T	0	08:35:48.6391860Z	2015-06-06
9	175/070	30	GEOTIFF	L5 TM	L1T	0	08:18:46.5955231Z	2003-04-19
9	175/070	30	GEOTIFF	L5 TM	L1T	0	08:10:05.9740000Z	2004-04-29
9	175/070	30	GEOTIFF	L5 TM	L1T	0	08:17:09.1920440Z	2005-04-16
9	175/070	30	GEOTIFF	L5 TM	L1T	0	08:19:07.5710440Z	2007-04-06

QTY = Quality, RES = Resolution, PROD = Product

Appendix 2: Calculated estimates of inundated area based on MODIS 09A1 imagery data for the period 2003 -2013 in the Barotse Wetland, Western Zambia.

Year	Day	Threshold	Pixel count	Pixel size(km2)	Area (Km^2)
2003	33	0.45	8491	0.25	2122.75
	97	0.45	19910	0.25	4977.5
	105	0.5	23341	0.25	5835.25
	113	0.5	21392	0.25	5348
	121	0.45	17018	0.25	4254.5
	129	0.45	14884	0.25	3721
	137	0.45	13677	0.25	3419.25
	145	0.45	12115	0.25	3028.75
	153	0.45	9373	0.25	2343.25
	161	0.45	6724	0.25	1681
	169	0.45	6106	0.25	1526.5
	193	0.45	2429	0.25	607.25
	209	0.43	6698	0.25	1674.5
	297	0.4	2429	0.25	607.25
	313	0.41	3398	0.25	849.5
2004	33	0.47	14304	0.25	3576
	89	0.47	24409	0.25	6102.24
	97	0.47	23350	0.25	5837.5
	105	0.5	25491	0.25	6372.75
	113	0.47	19191	0.25	4797.75
	121	0.47	18450	0.25	4612.5
	129	0.47	16754	0.25	4188.5
	137	0.47	15028	0.25	3757
	145	0.48	13910	0.25	3477.5
	153	0.47	11671	0.25	2917.75
	161	0.47	9938	0.25	2484.5
	169	0.47	7849	0.25	1962.25
	185	0.47	4486	0.25	1121.5
	193	0.47	5088	0.25	1272
	201	0.44	4646	0.25	1161.5
	209	0.44	3977	0.25	994.25
	217	0.44	3759	0.25	939.75

Appendix 2 continued.

2005	49	0.45	7718	0.25	1929.5
	57	0.47	9305	0.25	2326.25
	89	0.47	10968	0.25	2742
	97	0.47	12677	0.25	3169.25
	105	0.47	10633	0.25	2658.25
	113	0.45	10791	0.25	2697.75
	121	0.45	9489	0.25	2372.25
	129	0.45	10860	0.25	2715
	137	0.43	8390	0.25	2097.5
	145	0.45	8313	0.25	2078.25
	153	0.45	6936	0.25	1734
	161	0.43	5834	0.25	1458.5
	169	0.42	4896	0.25	1224
	177	0.4	3869	0.25	967.25

2006	73	0.47	25766	0.25	6441.5
	81	0.44	23035	0.25	5758.75
	89	0.46	23038	0.25	5759.5
	97	0.47	21803	0.25	5450.75
	105	0.47	20315	0.25	5078.75
	113	0.47	19820	0.25	4955
	121	0.48	18635	0.25	4658.75
	129	0.47	17623	0.25	4405.75
	137	0.48	12730	0.25	3182.5
	145	0.47	12409	0.25	3102.25
	153	0.45		0.25	0
	161	0.45	8377	0.25	2094.25
	169	0.45	4499	0.25	1124.75
	177	0.47	2893	0.25	723.25

Appendix 2 continued.

2007	41	0.44	24889	0.25	6222.25
	49	0.43	23743	0.25	5935.75
	73	0.46	23777	0.25	5944.25
	81	0.47	23204	0.25	5801
	89	0.47	22587	0.25	5646.75
	97	0.47	23188	0.25	5797
	105	0.48	20322	0.25	5080.5
	113	0.48	18657	0.25	4664.25
	121	0.47	16753	0.25	4188.25
	129	0.48	18063	0.25	4515.75
	137	0.46	12688	0.25	3172
	145	0.45	12009	0.25	3002.25
	153	0.45	8654	0.25	2163.5
	161	0.47	8508	0.25	2127
	169	0.42	2475	0.25	618.75
	185	0.42	2294	0.25	573.5
2008	81	0.44	23247	0.25	5811.75
	89	0.46	23453	0.25	5863.25
	97	0.49	23243	0.25	5810.75
	105	0.49	20120	0.25	5030
	113	0.49	17115	0.25	4278.75
	121	0.46	17423	0.25	4355.75
	129	0.45	14523	0.25	3630.75
	137	0.45	13074	0.25	3268.5
	145	0.45	11739	0.25	2934.75
	153	0.45	10652	0.25	2663
	161	0.45	8053	0.25	2013.25
	169	0.45	6733	0.25	1683.25
	177	0.45	5526	0.25	1381.5
2009	81	0.43	26635	0.25	6658.75
	89	0.44	25970	0.25	6492.5
	97	0.45	23262	0.25	5815.5
	105	0.45	21937	0.25	5484.25
	113	0.45	19503	0.25	4875.75
	121	0.46	17874	0.25	4468.5
	129	0.46	14452	0.25	3613
	137	0.45	13125	0.25	3281.25
	145	0.45	11178	0.25	2794.5
	153	0.45	8874	0.25	2218.5
	161	0.46	6760	0.25	1690
	169	0.46	5172	0.25	1293
	177	0.45	3368	0.25	842

Appendix 2 continued.

2010	81	0.43	25520	0.25	6380
	89	0.44	25524	0.25	6381
	097	0.45	25309	0.25	6327.25
	105	0.45	21147	0.25	5286.75
	113	0.43	19791	0.25	4947.75
	121	0.44	18278	0.25	4569.5
	129	0.45	15679	0.25	3919.75
	137	0.45	13821	0.25	3455.25
	145	0.45	12187	0.25	3046.75
	153	0.45	10031	0.25	2507.75
	161	0.46	7169	0.25	1792.25
	169	0.44	7623	0.25	1905.75
	177	0.44	5000	0.25	1250
2011	81	0.41	24875	0.25	6218.75
	89	0.41	25361	0.25	6340.25
	97	0.45	24202	0.25	6050.5
	105	0.45	25010	0.25	6252.5
	113	0.45	22148	0.25	5537
	121	0.45	20439	0.25	5109.75
	129	0.45	20036	0.25	5009
	137	0.47	18970	0.25	4742.5
	145	0.46	15813	0.25	3953.25
	153	0.45	13524	0.25	3381
	161	0.45	10924	0.25	2731
	169	0.43	8507	0.25	2126.75
	177	0.4	5795	0.25	1448.75
2012	1	0.45	12238	0.25	3059.5
	57	0.43	19488	0.25	4872
	73	0.45	23436	0.25	5859
	89	0.45	23104	0.25	5776
	97	0.45	24670	0.25	6167.5
	105	0.45	21655	0.25	5413.75
	113	0.45	19762	0.25	4940.5
	121	0.47	18106	0.25	4526.5
	129	0.46	18117	0.25	4529.25
	137	0.45	15228	0.25	3807
	145	0.45	12497	0.25	3124.25
	153	0.45	10805	0.25	2701.25
	161	0.45	10038	0.25	2509.5
	169	0.44	6917	0.25	1729.25
	177	0.43	4013	0.25	1003.25

Appendix 2 continued.

2013	25	0.39	21579	0.25	5394.75
	33	0.41	15158	0.25	3789.5
	49	0.35	20727	0.25	5181.75
	57	0.42	26296	0.25	6574
	65	0.42	24334	0.25	6083.5
	73	0.43	22858	0.25	5714.5
	81	0.44	24524	0.25	6131
	89	0.46	25104	0.25	6276
	97	0.49	24568	0.25	6142
	105	0.49	24903	0.25	6225.75
	113	0.5	20386	0.25	5096.5
	121	0.48	21223	0.25	5305.75
	129	0.45	16965	0.25	4241.25
	137	0.44	11465	0.25	2866.25
	145	0.43	11881	0.25	2970.25
	153	0.43	14169	0.25	3542.25
	161	0.40	8614	0.25	2153.5
	169	0.39	9388	0.25	2347
	177	0.38	8471	0.25	2117.75

Appendix 3: All Pairwise Multiple Comparison Procedures (Holm-Sidak method) for inundation extent variations in the Barotse Wetland, Western Zambia.

(a) Ascending period comparisons

Normality Test (Kolmogorov-Smirnov) Passed (P = 0.22)

Equal Variance Test: Passed (P = 0.76)

All Pairwise Multiple Comparison Procedures (Holm-Sidak method):
Overall significance level = 0.05

Comparisons for factor:

Comparison	Diff of Means	t	P	P<0.050
2010 vs. 2005	3506.25	13.39	<0.05	Yes
2013 vs. 2005	3358.08	12.82	<0.05	Yes
2011 vs. 2005	3357.92	12.82	<0.05	Yes
2004 vs. 2005	3247.66	12.40	<0.05	Yes
2009 vs. 2005	3074.25	11.74	<0.05	Yes
2012 vs. 2005	2929.25	11.18	<0.05	Yes
2008 vs. 2005	2711.50	10.35	<0.05	Yes
2007 vs. 2005	2651.58	10.12	<0.05	Yes
2006 vs. 2005	2573.17	9.83	<0.05	Yes
2003 vs. 2005	2552.48	9.75	<0.05	Yes
2010 vs. 2003	953.77	3.64	0.07	No
2010 vs. 2006	933.08	3.56	0.08	No
2010 vs. 2007	854.67	3.26	0.15	No
2013 vs. 2003	805.60	3.08	0.22	No
2011 vs. 2003	805.44	3.08	0.22	No
2010 vs. 2008	794.75	3.04	0.23	No
2013 vs. 2006	784.92	3.00	0.24	No
2011 vs. 2006	784.75	3.00	0.24	No
2013 vs. 2007	706.50	2.70	0.40	No
2011 vs. 2007	706.33	2.70	0.40	No
2004 vs. 2003	695.18	2.65	0.41	No
2004 vs. 2006	674.50	2.58	0.46	No
2013 vs. 2008	646.58	2.47	0.53	No
2011 vs. 2008	646.42	2.47	0.52	No
2004 vs. 2007	596.08	2.28	0.66	No
2010 vs. 2012	577.00	2.20	0.70	No
2004 vs. 2008	536.16	2.08	0.80	No
2009 vs. 2003	521.77	1.99	0.82	No
2009 vs. 2006	501.08	1.91	0.86	No
2010 vs. 2009	432.00	1.65	0.96	No
2013 vs. 2012	428.83	1.64	0.96	No
2011 vs. 2012	428.67	1.64	0.95	No
2009 vs. 2007	422.67	1.61	0.95	No
2012 vs. 2003	376.77	1.44	0.98	No
2009 vs. 2008	362.75	1.39	0.99	No
2012 vs. 2006	356.08	1.36	0.99	No
2004 vs. 2012	318.41	1.22	0.99	No
2013 vs. 2009	283.83	1.08	1.00	No
2011 vs. 2009	283.67	1.08	1.00	No
2012 vs. 2007	277.67	1.06	1.00	No
2010 vs. 2004	258.59	0.99	1.00	No
2012 vs. 2008	217.75	0.83	1.00	No
2004 vs. 2009	173.41	0.66	1.00	No

Appendix 3a continued.

2008 vs. 2003	159.02	0.61	1.00	No
2010 vs. 2011	148.33	0.57	1.00	No
2010 vs. 2013	148.17	0.57	1.00	No
2009 vs. 2012	145.00	0.55	1.00	No
2008 vs. 2006	138.33	0.53	1.00	No
2013 vs. 2004	110.42	0.42	1.00	No
2011 vs. 2004	110.25	0.42	1.00	No
2007 vs. 2003	99.10	0.38	1.00	No
2007 vs. 2006	78.42	0.30	1.00	No
2008 vs. 2007	59.92	0.23	1.00	No
2006 vs. 2003	20.69	0.08	1.00	No
2013 vs. 2011	0.17	0.00	1.00	No

(b) Receding Period comparisons

Normality Test (Kolmogorov-Smirnov) Passed (P = 0.19)

Equal Variance Test: Passed (P = 0.22)

All Pairwise Multiple Comparison Procedures (Holm-Sidak method):
Overall significance level = 0.05

Comparisons for factor:

Comparison	Diff of Means	t	P	P<0.05
2011 vs. 2005	2628.94	11.28	<0.05	Yes
2010 vs. 2005	2210.31	9.48	<0.05	Yes
2012 vs. 2005	1980.19	8.49	<0.05	Yes
2013 vs. 2005	1906.81	8.18	<0.05	Yes
2004 vs. 2005	1868.31	8.01	<0.05	Yes
2006 vs. 2005	1829.88	7.85	<0.05	Yes
2003 vs. 2005	1715.06	7.36	<0.05	Yes
2007 vs. 2005	1664.44	7.14	<0.05	Yes
2009 vs. 2005	1589.00	6.82	<0.05	Yes
2008 vs. 2005	1412.81	6.06	<0.05	Yes
2011 vs. 2008	1216.13	5.22	<0.05	Yes
2011 vs. 2009	1039.94	4.46	<0.05	Yes
2011 vs. 2007	964.50	4.14	<0.05	Yes
2011 vs. 2003	913.88	3.92	<0.05	Yes
2011 vs. 2006	799.06	3.43	0.07	No
2010 vs. 2008	797.50	3.42	0.07	No
2011 vs. 2004	760.63	3.26	0.10	No
2011 vs. 2013	722.13	3.10	0.15	No
2011 vs. 2012	648.75	2.78	0.29	No
2010 vs. 2009	621.31	2.67	0.36	No
2012 vs. 2008	567.38	2.43	0.53	No
2010 vs. 2007	545.88	2.34	0.59	No
2010 vs. 2003	495.25	2.12	0.76	No
2013 vs. 2008	494.00	2.12	0.75	No

Appendix 3b
continued.

2004 vs. 2008	455.50	1.95	0.85	No
2011 vs. 2010	418.63	1.80	0.93	No
2006 vs. 2008	417.06	1.79	0.92	No
2012 vs. 2009	391.19	1.68	0.95	No
2010 vs. 2006	380.44	1.63	0.96	No
2010 vs. 2004	342.00	1.47	0.99	No
2013 vs. 2009	317.81	1.36	0.99	No
2012 vs. 2007	315.75	1.35	0.99	No
2010 vs. 2013	303.50	1.30	1.00	No
2003 vs. 2008	302.25	1.30	1.00	No
2004 vs. 2009	279.31	1.20	1.00	No
2012 vs. 2003	265.13	1.14	1.00	No
2007 vs. 2008	251.63	1.08	1.00	No
2013 vs. 2007	242.38	1.04	1.00	No
2006 vs. 2009	240.88	1.03	1.00	No
2010 vs. 2012	230.13	0.99	1.00	No
2004 vs. 2007	203.88	0.88	1.00	No
2013 vs. 2003	191.75	0.82	1.00	No
2009 vs. 2008	176.19	0.76	1.00	No
2006 vs. 2007	165.44	0.71	1.00	No
2004 vs. 2003	153.25	0.66	1.00	No
2012 vs. 2006	150.31	0.65	1.00	No
2003 vs. 2009	126.06	0.54	1.00	No
2006 vs. 2003	114.81	0.49	1.00	No
2012 vs. 2004	111.88	0.48	1.00	No
2013 vs. 2006	76.94	0.33	1.00	No
2007 vs. 2009	75.44	0.32	1.00	No
2012 vs. 2013	73.38	0.32	1.00	No
2003 vs. 2007	50.63	0.22	1.00	No
2013 vs. 2004	38.50	0.17	1.00	No
2004 vs. 2006	38.44	0.17	0.87	No

Appendix 3 c. Mann-Kendall Test results for the annual means of inundation extent

		Mann-Kendall Trend			Sens Slope estimate
Name	**Years**	**n**	**Test Z**	**Signific.**	**(Km^2)**
Inundation Extent	2003 - 2013	11	1.87	+	62.20

Point values for the chart							
Year	Data	Sen's estimate	99 % conf. min	99 % conf. max	95 % conf. min	95 % conf. max	Residual
2003	4797.33	4673.95	5291.48	3066.80	5073.39	3764.13	123.38
2004	5221.55	4736.16	5221.55	3398.58	5060.35	4000.74	485.39
2005	2663.56	4798.36	5151.62	3730.37	5047.32	4237.35	-2134.80
2006	4865.08	4860.57	5081.69	4062.15	5034.29	4473.95	4.51
2007	4821.57	4922.78	5011.75	4393.93	5021.25	4710.56	-101.20
2008	4725.72	4984.98	4941.82	4725.72	5008.22	4947.17	-259.26
2009	4995.19	5047.19	4871.89	5057.50	4995.19	5183.78	-52.00
2010	5521.84	5109.39	4801.96	5389.29	4982.15	5420.38	412.45
2011	5656.99	5171.60	4732.02	5721.07	4969.12	5656.99	485.39
2012	5118.28	5233.80	4662.09	6052.86	4956.09	5893.60	-115.52
2013	5296.01	5296.01	4592.16	6384.64	4943.05	6130.20	0.00

Appendix 3 d. Mann-Kendall Test results for the annual means of water level for Senanga Gauge Station for the period 2000 to 2011.

		Mann-Kendall Trend			Sens Slope estimate
Name	**Years**	**n**	**Test Z**	**Signific.**	**(m)**
Water Level	2000 - 2013	12	1.87	**	0.10

Point values for the chart

Year	Data	Sen's estimate	99 % conf. min	99 % conf. max	95 % conf. min	95 % conf. max	Residual
2000	1.87	1.93	2.44	1.24	2.31	1.50	-0.06
2001	2.46	2.03	2.45	1.46	2.34	1.68	0.42
2002	1.92	2.13	2.46	1.69	2.37	1.86	-0.21
2003	2.36	2.23	2.46	1.91	2.41	2.04	0.13
2004	2.47	2.33	2.47	2.13	2.44	2.22	0.13
2005	1.85	2.43	2.48	2.36	2.48	2.40	-0.58
2006	2.15	2.53	2.48	2.58	2.51	2.58	-0.39
2007	2.70	2.63	2.49	2.80	2.54	2.76	0.07
2008	2.73	2.73	2.49	3.03	2.58	2.94	-0.01
2009	2.59	2.83	2.50	3.25	2.61	3.13	-0.25
2010	3.57	2.94	2.51	3.47	2.64	3.31	0.64
2011	3.04	3.04	2.51	3.70	2.68	3.49	0.01

Appendix 4: Inundation extent Rate of change indices for each year in the Barotse Wetland, Western Zambia.

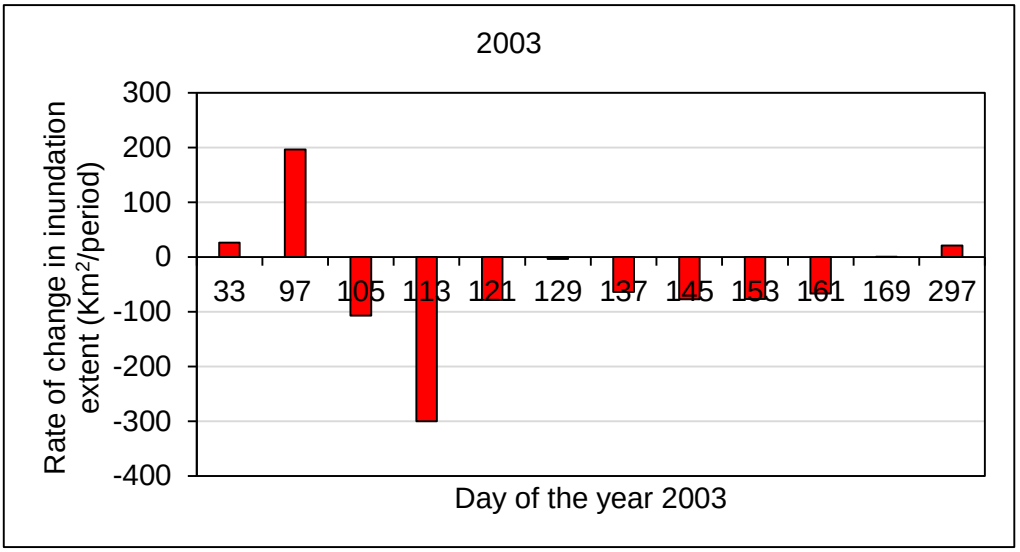

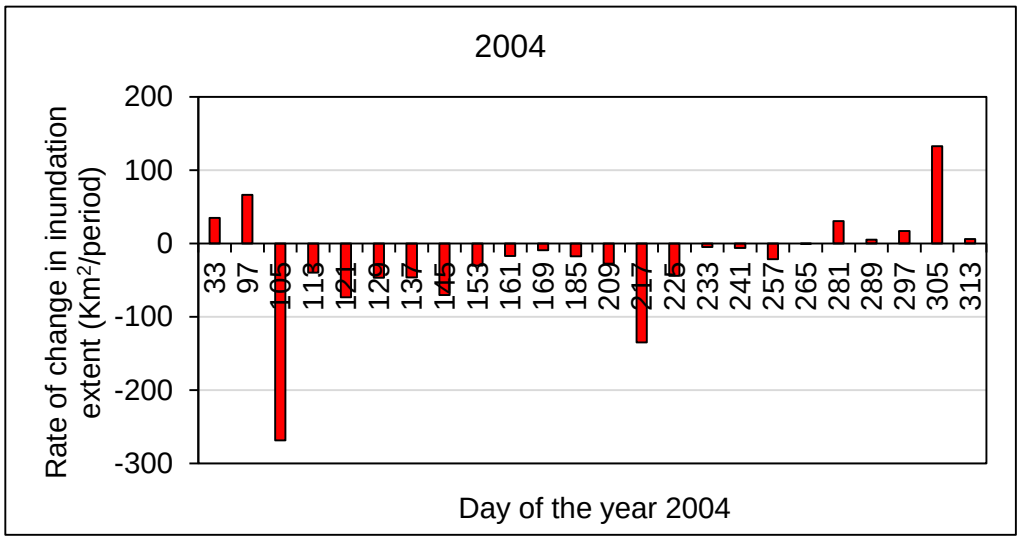

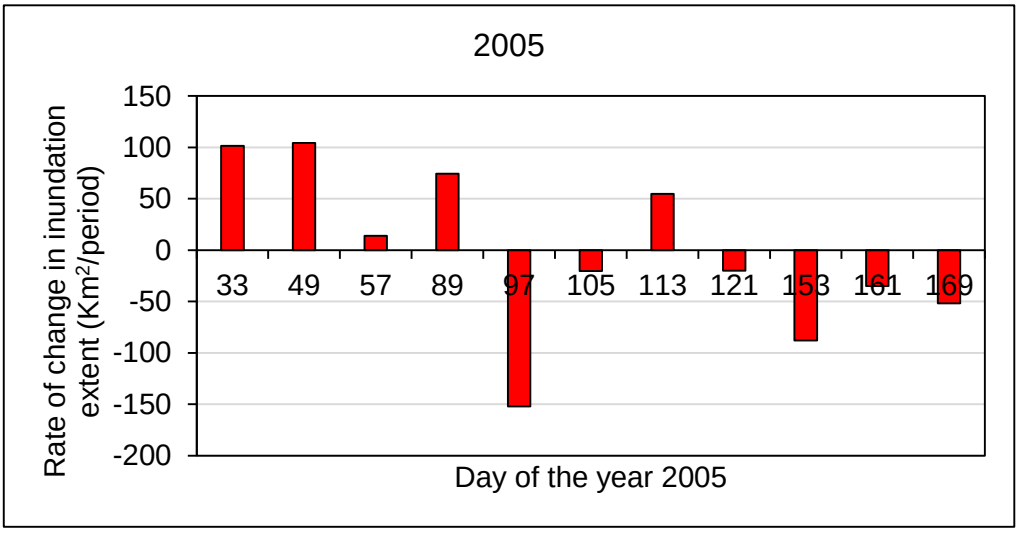

Appendix 4 continued.

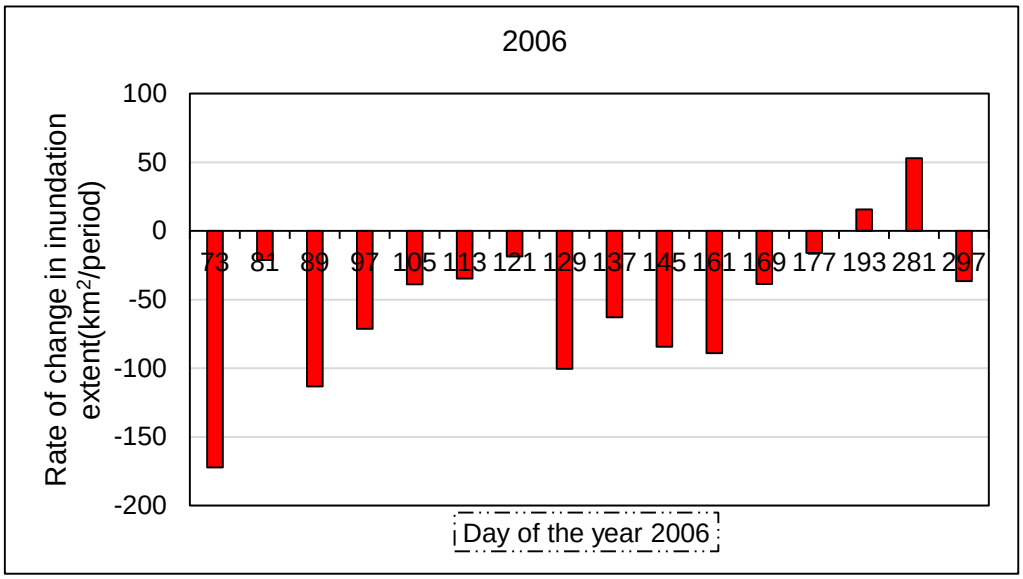

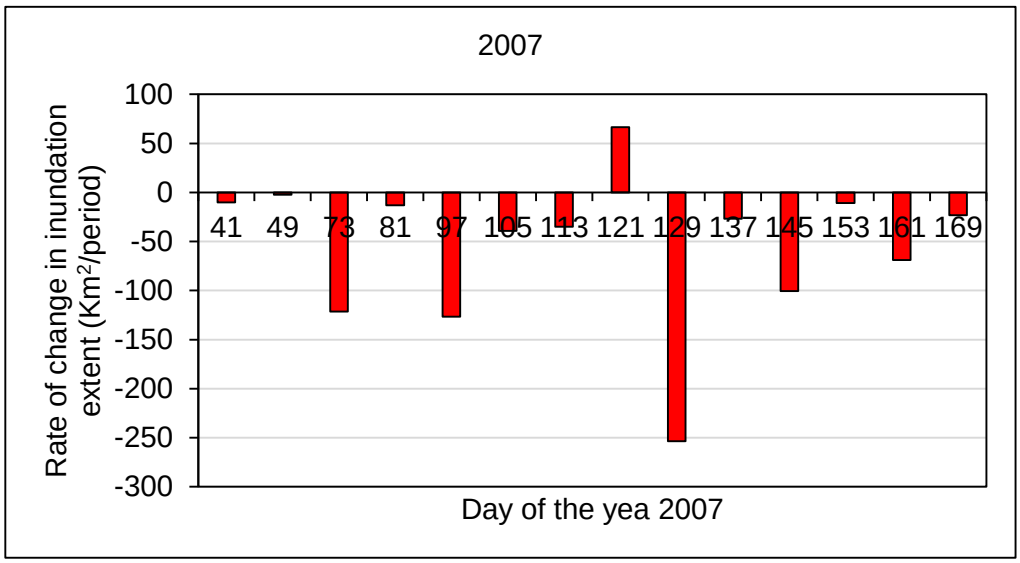

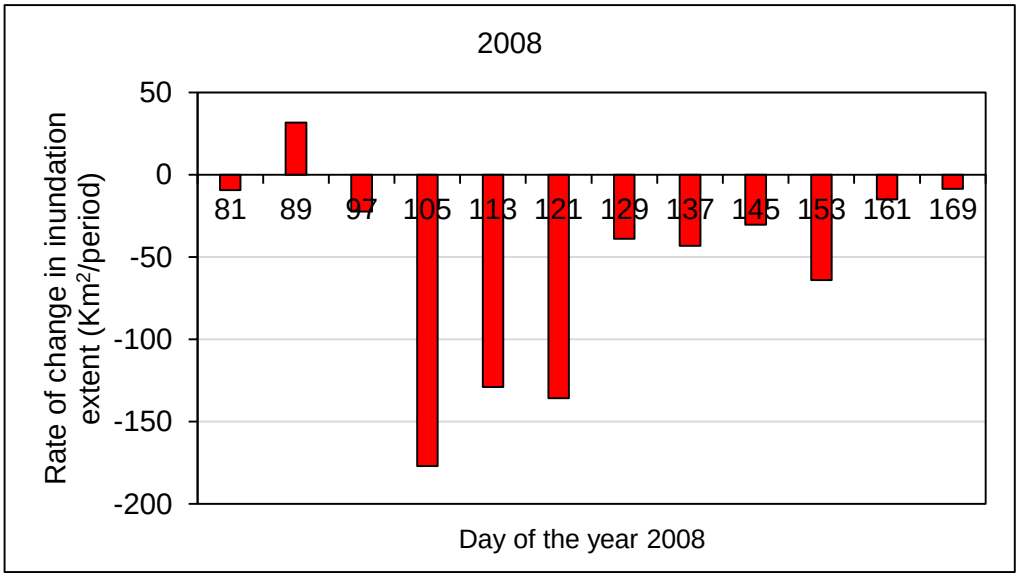

Appendix 4 continued.

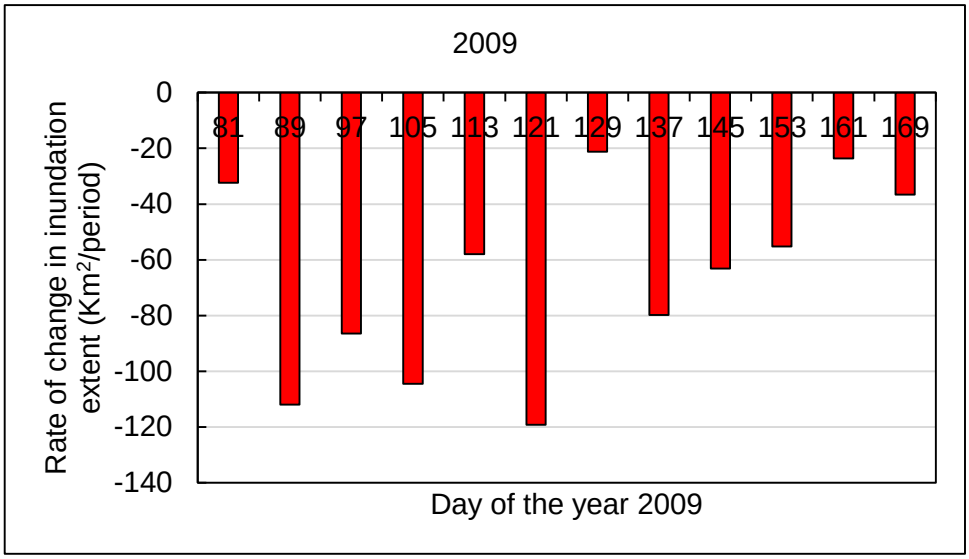

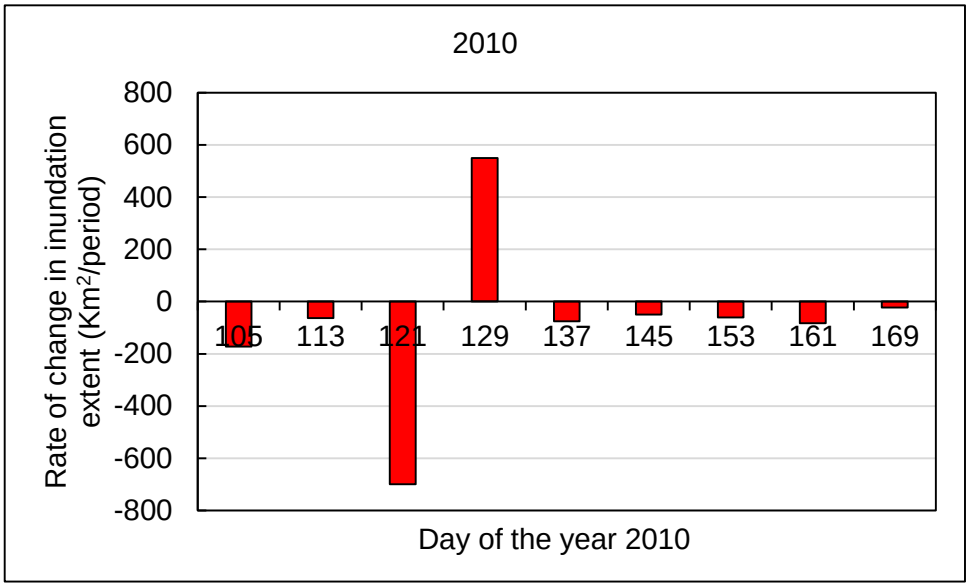

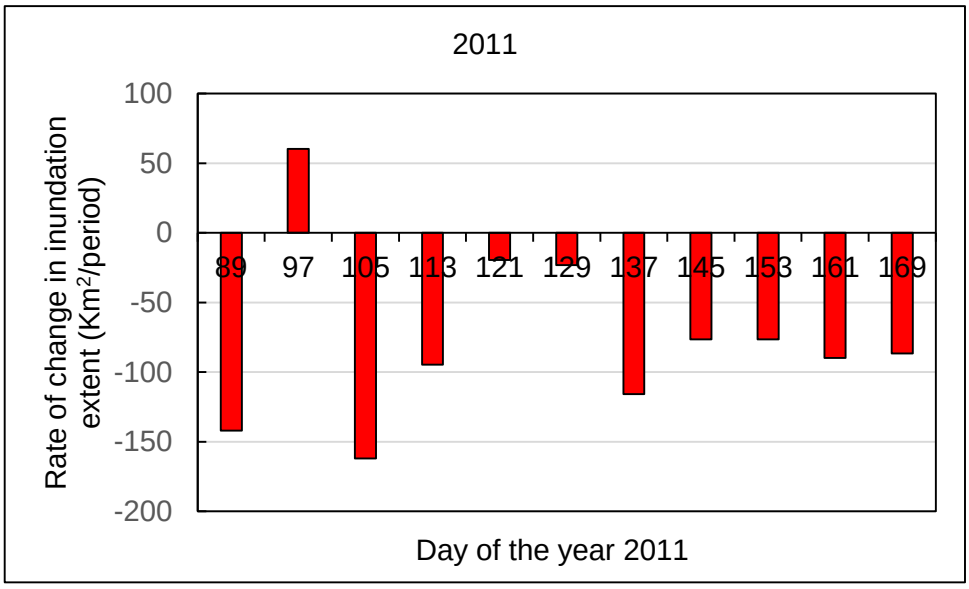

Appendix 4 continued.

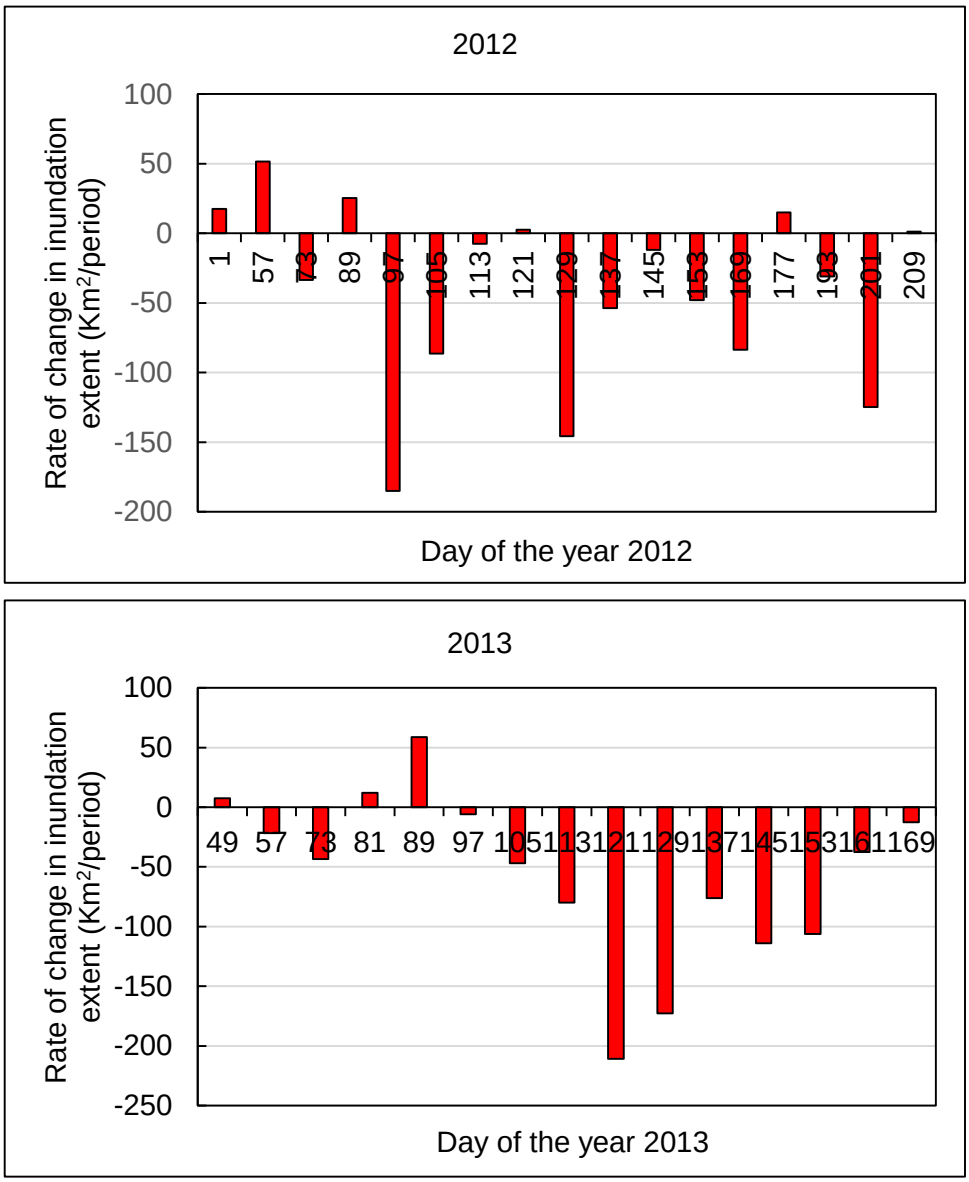

Appendix 5: Land Cover Classification Accuracy Assessment Reports for the Barotse Wetland, Western Zambia.

1984 CLASSIFICATION ACCURACY ASSESSMENT

Overall Accuracy **(134330/142248)** **94.43%**

Kappa Coefficient **0.9091**

	Ground Truth Pixels					
Class	Grassland	Wetland	Water	Forest Land	Grass/Shrub/Bare Land	Total
Unclassified	0	0	0	0	0	0
Grassland	28047	3137	0	51	827	32062
Wetland	36	26702	340	0	0	27078
Water	0	0	343	0	0	343
Forest Land	1012	291	0	76447	1528	79278
Grass/Shrub/Bare Land	124	513	55	4	2791	3487
Total	29219	30643	738	76502	5146	142248

	Ground Truth (Percent)					
Class	Grassland	Wetland	Water	Forest Land	Grass/Shrub/Bare Land	Total
Unclassified	0	0	0	0	0	0
Grassland	95.99	10.24	0	0.07	16.07	22.54
Wetland	0.12	87.14	46.07	0	0	19.04
Water	0	0	46.48	0	0	0.24
Forest Land	3.46	0.95	0	99.93	29.69	55.73
Grass/Shrub/Bare Land	0.42	1.67	7.45	0.01	54.24	2.45
Total	100	100	100	100	100	100

Class	Commission (Percent)	Omission (Percent)	Commission (Pixels)	Omission (Pixels)
Grassland	12.52	4.01	4015/32062	1172/29219
Wetland	1.39	12.86	376/27078	3941/30643
Water	0	53.52	0/343	395/738
Forest Land	3.57	0.07	2831/79278	55/76502
Grass/Shrub/Bare Land	19.96	45.76	696/3487	2355/5146

Class	Prod. Acc. (Percent)	User Acc. (Percent)	Prod. Acc. (Pixels)	User Acc. (Pixels)
Grassland	95.99	87.48	28047/29219	28047/32062
Wetland	87.14	98.61	26702/30643	26702/27078
Water	46.48	100	343/738	343/343
Forest Land	99.93	96.43	76447/76502	76447/79278
Grass/Shrub/Bare Land	54.24	80.04	2791/5146	2791/3487

Appendix 5 continued.

1996 CLASSIFICATION ACCURACY ASSESSMENT

Overall Accuracy	(131390/142559)	92.10%
Kappa Coefficient	0.8718	

Ground Truth Pixels

Class	Water	Wetland	Grassland	Forest Land	Grass/Shrub/Bare Land	Total
Unclassified	0	0	0	0	0	0
Water	490	0	24	0	0	514
Wetland	130	25535	269	1069	114	27117
Grassland	44	3340	28430	34	1443	33291
Forest Land	39	1190	546	75450	2156	79381
Grass/Shrub/Bare Land	43	621	107	0	1485	2256
Total	746	30686	29376	76553	5198	142559

Ground Truth (Percent)

Class	Water	Wetland	Grassland	Forest Land	Grass/Shrub/Bare Land	Total
Unclassified	0	0	0	0	0	0
Water	65.68	0	0.08	0	0	0.36
Wetland	17.43	83.21	0.92	1.4	2.19	19.02
Grassland	5.9	10.88	96.78	0.04	27.76	23.35
Forest Land	5.23	3.88	1.86	98.56	41.48	55.68
Grass/Shrub/Bare Land	5.76	2.02	0.36	0	28.57	1.58
Total	100	100	100	100	100	100

Class	Commission (Percent)	Omission (Percent)	Commission Pixels)	Omission (Pixels)
Water	4.67	34.32	24/514	256/746
Wetland	5.83	16.79	1582/27117	5151/30686
Grassland	14.6	3.22	4861/33291	946/29376
Forest Land	4.95	1.44	3931/79381	1103/76553
Grass/Shrub/Bare Land	34.18	71.43	771/2256	3713/5198

Class	Prod. Acc. (Percent)	User Acc. (Percent)	Prod. Acc. (Pixels)	User Acc. (Pixels)
Water	65.68	95.33	490/746	490/514
Wetland	83.21	94.17	25535/30686	25535/27117
Grassland	96.78	85.4	28430/29376	28430/33291
Forest Land	98.56	95.05	75450/76553	75450/79381
Grass/Shrub/Bare Land	28.57	65.82	1485/5198	1485/2256

Appendix 5 continued.

2004 CLASSIFICATION ACCURACY ASSESSMENT

Overall Accuracy	(130306/142248)	91.65%
Kappa Coefficient	0.8635	

Ground Truth Pixels

Class	Wetland	Water	Grassland	Forest Land	Grass/Shrub/Bare Land	Total
Unclassified	0	0	0	0	0	0
Wetland	29872	81	2603	0	0	32556
Water	257	632	1063	0	0	1952
Grassland	1	0	19729	667	123	20520
Forest Land	0	0	3897	75835	785	80517
Grass/Shrub/Bare Land	513	25	1927	0	4238	6703
Total	30643	738	29219	76502	5146	142248

Ground Truth (Percent)

Class	Wetland	Water	Grassland	Forest Land	Grass/Shrub/Bare Land	Total
Unclassified	0	0	0	0	0	0
Wetland	97.48	10.98	8.91	0	0	22.89
Water	0.84	85.64	3.64	0	0	1.37
Grassland	0	0	67.52	0.87	2.39	14.43
Forest Land	0	0	13.34	99.13	15.25	56.6
Grass/Shrub/Bare Land	1.67	3.39	6.6	0	82.36	4.71
Total	100	100	100	100	100	100

Class	Commission (Percent)	Omission (Percent)	Commission Pixels)	Omission (Pixels)
Wetland	8.24	2.52	2684/32556	771/30643
Water	67.62	14.36	1320/1952	106/738
Grassland	3.85	32.48	791/20520	9490/29219
Forest Land	5.81	0.87	4682/80517	667/76502
Grass/Shrub/Bare Land	36.77	17.64	2465/6703	908/5146

Class	Prod. Acc. (Percent)	User Acc. (Percent)	Prod. Acc. Pixels)	User Acc. (Pixels)
Wetland	97.48	91.76	29872/306432	9872/32556
Water	85.64	32.38	632/738	632/1952
Grassland	67.52	96.15	19729/292191	9729/20520
Forest Land	99.13	94.19	75835/765027	5835/80517
Grass/Shrub/Bare Land	82.36	63.23	4238/5146	4238/6703

Appendix 6: Sens slope estimates for each time series data set assessed in the study, Barotse Wetland, Western Zambia.

Point values for the chart Observed discharge – Senanga Station Overall 1952 -2004

Year	Data	Sen's estimate	99 % conf. min	99 % conf. max	95 % conf. min	95 % conf. max	Residual
1952	1095.98	1130.08	1225.33	1032.99	1192.14	1044.24	-34.11
1953	1078.99	1123.14	1213.62	1031.44	1181.92	1041.25	-44.15
1954	992.09	1116.20	1201.91	1029.89	1171.70	1038.26	-124.11
1955	1028.09	1109.25	1190.20	1028.34	1161.47	1035.27	-81.16
1956	1198.40	1102.31	1178.49	1026.79	1151.25	1032.28	96.09
1957	1029.29	1095.36	1166.78	1025.23	1141.03	1029.29	-66.07
1958	1155.07	1088.42	1155.07	1023.68	1130.81	1026.30	66.66
1959	943.99	1081.47	1143.37	1022.13	1120.58	1023.31	-137.48
1960	978.22	1074.53	1131.66	1020.58	1110.36	1020.32	-96.31
1961	1083.23	1067.59	1119.95	1019.03	1100.14	1017.33	15.64
1962	1277.85	1060.64	1108.24	1017.48	1089.92	1014.34	217.21
1963	1384.63	1053.70	1096.53	1015.92	1079.70	1011.35	330.93
1964	1103.09	1046.75	1084.82	1014.37	1069.47	1008.36	56.34
1965	1012.82	1039.81	1073.11	1012.82	1059.25	1005.37	-26.99
1966	1032.87	1032.87	1061.41	1011.27	1049.03	1002.38	0.00
1967	949.27	1025.92	1049.70	1009.72	1038.81	999.39	-76.65
1968	1284.00	1018.98	1037.99	1008.17	1028.58	996.40	265.03
1969	1305.54	1012.03	1026.28	1006.61	1018.36	993.41	293.51
1970	1223.45	1005.09	1014.57	1005.06	1008.14	990.42	218.37
1971	1029.98	998.14	1002.86	1003.51	997.92	987.43	31.83
1972	803.06	991.20	991.16	1001.96	987.70	984.44	-188.14
1973	652.62	984.26	979.45	1000.41	977.47	981.45	-331.64
1974	889.71	977.31	967.74	998.86	967.25	978.46	-87.60
1975	1095.98	970.37	956.03	997.30	957.03	975.47	125.61
1976	1091.38	963.42	944.32	995.75	946.81	972.48	127.96
1977	1011.19	956.48	932.61	994.20	936.59	969.49	54.71
1978	1166.75	949.53	920.90	992.65	926.36	966.50	217.21
1979	1299.10	942.59	909.20	991.10	916.14	963.51	356.51
1980	880.23	935.65	897.49	989.55	905.92	960.52	-55.42
1981	952.60	928.70	885.78	988.00	895.70	957.53	23.90
1982	803.58	921.76	874.07	986.44	885.47	954.54	-118.18
1983	727.32	914.81	862.36	984.89	875.25	951.55	-187.49
1984	721.34	907.87	850.65	983.34	865.03	948.56	-186.53
1985	854.81	900.93	838.94	981.79	854.81	945.57	-46.12
1986	759.28	893.98	827.24	980.24	844.59	942.58	-134.70
1987	892.42	887.04	815.53	978.69	834.36	939.59	5.38
1988	902.73	880.09	803.82	977.13	824.14	936.60	22.64
1989	1179.84	873.15	792.11	975.58	813.92	933.61	306.69
1990	637.20	866.20	780.40	974.03	803.70	930.62	-229.00
1991	720.25	859.26	768.69	972.48	793.48	927.63	-139.01
1992	623.10	852.32	756.98	970.93	783.25	924.64	-229.22
1993		845.37	745.28	969.38	773.03	921.65	
1994		838.43	733.57	967.82	762.81	918.66	

Appendix 6 continued.

1995	533.03	831.48	721.86	966.27	752.59	915.67	-298.45
1996	466.52	824.54	710.15	964.72	742.36	912.68	-358.02
1997	687.94	817.59	698.44	963.17	732.14	909.69	-129.66
1998	1008.26	810.65	686.73	961.62	721.92	906.70	197.61
1999	999.04	803.71	675.02	960.07	711.70	903.71	195.33
2000	784.33	796.76	663.32	958.51	701.48	900.72	-12.43
2001	1069.80	789.82	651.61	956.96	691.25	897.73	279.98
2002	852.51	782.87	639.90	955.41	681.03	894.74	69.63
2003	964.38	775.93	628.19	953.86	670.81	891.75	188.45
2004	1144.40	768.99	616.48	952.31	660.59	888.76	375.41

Appendix 6 continued.

Point values for the chart
Observed –discharge-
Senanga Station 1952-1979

Year	Data	Sen's estimate	99 % conf. min	99 % conf. max	95 % conf. min	95 % conf. max	Residual
1952	1095.98	1079.03	1214.10	969.81	1177.04	984.70	16.94
1953	1078.99	1079.45	1202.09	980.92	1168.44	992.12	-0.46
1954	992.09	1079.86	1190.07	992.03	1159.84	999.55	-87.78
1955	1028.09	1080.28	1178.06	1003.15	1151.23	1006.98	-52.19
1956	1198.40	1080.70	1166.05	1014.26	1142.63	1014.40	117.70
1957	1029.29	1081.11	1154.03	1025.37	1134.03	1021.83	-51.82
1958	1155.07	1081.53	1142.02	1036.48	1125.42	1029.25	73.55
1959	943.99	1081.94	1130.01	1047.59	1116.82	1036.68	-137.95
1960	978.22	1082.36	1118.00	1058.70	1108.22	1044.11	-104.14
1961	1083.23	1082.78	1105.98	1069.81	1099.62	1051.53	0.46
1962	1277.85	1083.19	1093.97	1080.92	1091.01	1058.96	194.66
1963	1384.63	1083.61	1081.96	1092.03	1082.41	1066.38	301.02
1964	1103.09	1084.02	1069.94	1103.15	1073.81	1073.81	19.07
1965	1012.82	1084.44	1057.93	1114.26	1065.21	1081.23	-71.62
1966	1032.87	1084.85	1045.92	1125.37	1056.60	1088.66	-51.99
1967	949.27	1085.27	1033.91	1136.48	1048.00	1096.09	-136.00
1968	1284.00	1085.69	1021.89	1147.59	1039.40	1103.51	198.32
1969	1305.54	1086.10	1009.88	1158.70	1030.79	1110.94	219.44
1970	1223.45	1086.52	997.87	1169.81	1022.19	1118.36	136.94
1971	1029.98	1086.93	985.85	1180.92	1013.59	1125.79	-56.96
1972	803.06	1087.35	973.84	1192.04	1004.99	1133.22	-284.29
1973	652.62	1087.77	961.83	1203.15	996.38	1140.64	-435.15
1974	889.71	1088.18	949.82	1214.26	987.78	1148.07	-198.47
1975	1095.98	1088.60	937.80	1225.37	979.18	1155.49	7.39
1976	1091.38	1089.01	925.79	1236.48	970.58	1162.92	2.37
1977	1011.19	1089.43	913.78	1247.59	961.97	1170.34	-78.24
1978	1166.75	1089.84	901.76	1258.70	953.37	1177.77	76.90
1979	1299.10	1090.26	889.75	1269.81	944.77	1185.20	208.84

Appendix 6 continued.

Point values for the chart Observed discharge Senanga Station 1980 - 2004

Year	Data	Sen's estimate	99 % conf. min	99 % conf. max	95 % conf. min	95 % conf. max	Residual
1980	880.23	791.93	928.71	641.58	900.04	678.40	88.30
1981	952.60	797.75	914.55	661.52	890.99	694.71	154.85
1982	803.58	803.58	900.38	681.46	881.95	711.01	0.00
1983	727.32	809.41	886.22	701.40	872.90	727.32	-82.08
1984	721.34	815.23	872.06	721.34	863.85	743.63	-93.89
1985	854.81	821.06	857.89	741.28	854.81	759.94	33.75
1986	759.28	826.89	843.73	761.22	845.76	776.25	-67.60
1987	892.42	832.71	829.57	781.16	836.72	792.56	59.70
1988	902.73	838.54	815.40	801.10	827.67	808.86	64.19
1989	1179.84	844.37	801.24	821.04	818.62	825.17	335.47
1990	637.20	850.19	787.08	840.98	809.58	841.48	-212.99
1991	720.25	856.02	772.92	860.92	800.53	857.79	-135.77
1992	623.10	861.85	758.75	880.86	791.48	874.10	-238.75
1993		867.67	744.59	900.80	782.44	890.40	
1994		873.50	730.43	920.74	773.39	906.71	
1995	533.03	879.33	716.26	940.68	764.34	923.02	-346.29
1996	466.52	885.15	702.10	960.61	755.30	939.33	-418.64
1997	687.94	890.98	687.94	980.55	746.25	955.64	-203.04
1998	1008.26	896.81	673.78	1000.49	737.20	971.95	111.45
1999	999.04	902.63	659.61	1020.43	728.16	988.25	96.41
2000	784.33	908.46	645.45	1040.37	719.11	1004.56	-124.13
2001	1069.80	914.29	631.29	1060.31	710.06	1020.87	155.52
2002	852.51	920.11	617.12	1080.25	701.02	1037.18	-67.60
2003	964.38	925.94	602.96	1100.19	691.97	1053.49	38.44
2004	1144.40	931.77	588.80	1120.13	682.92	1069.80	212.63

Appendix 6 continued.

Point values for the chart Observed discharge at Lukulu Station -overall 1952 - 2003

Year	Data	Sen's estimate	99 % conf. min	99 % conf. max	95 % conf. min	95 % conf. max	Residual
1952	733.43	798.41	908.89	708.97	882.01	732.69	-64.98
1953	667.57	793.73	899.57	708.32	873.88	730.94	-126.15
1954	667.57	789.04	890.25	707.68	865.75	729.19	-121.47
1955	879.51	784.36	880.93	707.03	857.62	727.45	95.15
1956	687.87	779.67	871.61	706.38	849.48	725.70	-91.80
1957	841.35	774.99	862.29	705.73	841.35	723.95	66.36
1958	649.25	770.30	852.97	705.09	833.22	722.21	-121.06
1959	709.10	765.62	843.65	704.44	825.09	720.46	-56.52
1960	816.46	760.94	834.33	703.79	816.96	718.71	55.52

Appendix 6 continued.

1961	1012.38	756.25	825.01	703.14	808.83	716.97	256.13
1962	1040.98	751.57	815.69	702.49	800.70	715.22	289.42
1963	687.66	746.88	806.37	701.85	792.57	713.48	-59.23
1964	766.23	742.20	797.05	701.20	784.44	711.73	24.04
1965	749.94	737.51	787.73	700.55	776.30	709.98	12.43
1966	715.43	732.83	778.41	699.90	768.17	708.24	-17.40
1967	748.03	728.14	769.09	699.26	760.04	706.49	19.89
1968	1058.95	723.46	759.77	698.61	751.91	704.74	335.49
1969	953.62	718.78	750.45	697.96	743.78	703.00	234.84
1970	749.62	714.09	741.13	697.31	735.65	701.25	35.52
1971	621.88	709.41	731.81	696.67	727.52	699.50	-87.53
1972	551.64	704.72	722.49	696.02	719.39	697.76	-153.08
1973	677.35	700.04	713.17	695.37	711.26	696.01	-22.69
1974	934.50	695.35	703.85	694.72	703.13	694.27	239.14
1975	931.61	690.67	694.53	694.07	694.99	692.52	240.94
1976	869.51	685.98	685.21	693.43	686.86	690.77	183.52
1977	965.05	681.30	675.89	692.78	678.73	689.03	283.75
1978	1021.81	676.62	666.57	692.13	670.60	687.28	345.20
1979	990.11	671.93	657.25	691.48	662.47	685.53	318.18
1980	803.68	667.25	647.93	690.84	654.34	683.79	136.43
1981	571.92	662.56	638.61	690.19	646.21	682.04	-90.64
1982	657.88	657.88	629.29	689.54	638.08	680.30	0.00
1983	590.15	653.19	619.97	688.89	629.95	678.55	-63.04
1984	610.65	648.51	610.65	688.25	621.81	676.80	-37.85
1985	609.83	643.82	601.33	687.60	613.68	675.06	-33.99
1986	588.37	639.14	592.01	686.95	605.55	673.31	-50.77
1987	687.94	634.45	582.69	686.30	597.42	671.56	53.49
1988	617.66	629.77	573.38	685.65	589.29	669.82	-12.11
1989	534.93	625.09	564.06	685.01	581.16	668.07	-90.16
1990	666.32	620.40	554.74	684.36	573.03	666.32	45.92
1991	596.85	615.72	545.42	683.71	564.90	664.58	-18.86
1992	635.07	611.03	536.10	683.06	556.77	662.83	24.04
1993	549.41	606.35	526.78	682.42	548.63	661.09	-56.94
1994	438.06	601.66	517.46	681.77	540.50	659.34	-163.61
1995	384.25	596.98	508.14	681.12	532.37	657.59	-212.73
1996	526.75	592.29	498.82	680.47	524.24	655.85	-65.54
1997	909.70	587.61	489.50	679.83	516.11	654.10	322.09
1998	211.10	582.93	480.18	679.18	507.98	652.35	-371.83
1999		578.24	470.86	678.53	499.85	650.61	
2000	1059.26	573.56	461.54	677.88	491.72	648.86	485.70
2001	939.05	568.87	452.22	677.23	483.59	647.11	370.18
2002	676.59	564.19	442.90	676.59	475.45	645.37	112.40
2003	240.76	559.50	433.58	675.94	467.32	643.62	-318.74

Appendix 6 continued.

Point values for the chart Observed discharge at Lukulu station 1952 - 1980

Year	Data	Sen's estimate	99 % conf. min	99 % conf. max	95 % conf. min	95 % conf. max	Residual
1952	733.43	691.28	809.39	606.87	774.79	641.69	42.15
1953	667.57	697.52	806.07	621.20	774.08	654.29	-29.95
1954	667.57	703.77	802.75	635.53	773.36	666.90	-36.19
1955	879.51	710.02	799.43	649.86	772.65	679.50	169.49
1956	687.87	716.26	796.11	664.18	771.94	692.11	-28.39
1957	841.35	722.51	792.79	678.51	771.23	704.71	118.84
1958	649.25	728.76	789.47	692.84	770.51	717.32	-79.51
1959	709.10	735.00	786.15	707.16	769.80	729.92	-25.90
1960	816.46	741.25	782.83	721.49	769.09	742.53	75.21
1961	1012.38	747.49	779.50	735.82	768.37	755.14	264.89
1962	1040.98	753.74	776.18	750.14	767.66	767.74	287.24
1963	687.66	759.99	772.86	764.47	766.95	780.35	-72.33
1964	766.23	766.23	769.54	778.80	766.23	792.95	0.00
1965	749.94	772.48	766.22	793.13	765.52	805.56	-22.54
1966	715.43	778.73	762.90	807.45	764.81	818.16	-63.30
1967	748.03	784.97	759.58	821.78	764.10	830.77	-36.94
1968	1058.95	791.22	756.26	836.11	763.38	843.37	267.73
1969	953.62	797.47	752.94	850.43	762.67	855.98	156.15
1970	749.62	803.71	749.62	864.76	761.96	868.59	-54.10
1971	621.88	809.96	746.29	879.09	761.24	881.19	-188.08
1972	551.64	816.21	742.97	893.42	760.53	893.80	-264.56
1973	677.35	822.45	739.65	907.74	759.82	906.40	-145.11
1974	934.50	828.70	736.33	922.07	759.10	919.01	105.80
1975	931.61	834.95	733.01	936.40	758.39	931.61	96.67
1976	869.51	841.19	729.69	950.72	757.68	944.22	28.31
1977	965.05	847.44	726.37	965.05	756.97	956.82	117.61
1978	1021.81	853.69	723.05	979.38	756.25	969.43	168.13
1979	990.11	859.93	719.73	993.71	755.54	982.04	130.18
1980	803.68	866.18	716.41	1008.03	754.83	994.64	-62.50

Appendix 6 continued.

Point values for the chart Observed – Precipitation- Mansa station 1974 - 2012

Year	Data	Sen's estimate	99 % conf. min	99 % conf. max	95 % conf. min	95 % conf. max	Residual
1974	1287.80	1162.91	1278.97	970.47	1255.88	1041.89	124.89
1975	1145.10	1162.58	1271.90	978.25	1250.37	1047.38	-17.48
1976	1218.70	1162.25	1264.83	986.03	1244.85	1052.86	56.45
1977	1065.40	1161.93	1257.76	993.81	1239.34	1058.35	-96.52
1978	1259.00	1161.60	1250.69	1001.59	1233.83	1063.84	97.40
1979	1657.00	1161.27	1243.62	1009.37	1228.32	1069.32	495.73
1980	1227.30	1160.94	1236.55	1017.15	1222.80	1074.81	66.36
1981	956.30	1160.62	1229.48	1024.93	1217.29	1080.30	-204.32
1982	1307.70	1160.29	1222.41	1032.71	1211.78	1085.78	147.41
1983	963.00	1159.96	1215.34	1040.49	1206.27	1091.27	-196.96
1984	1316.40	1159.64	1208.27	1048.27	1200.76	1096.76	156.76
1985	1223.80	1159.31	1201.20	1056.05	1195.24	1102.24	64.49
1986	1358.50	1158.98	1194.14	1063.83	1189.73	1107.73	199.52
1987	841.40	1158.66	1187.07	1071.61	1184.22	1113.22	-317.26
1988	965.40	1158.33	1180.00	1079.39	1178.71	1118.70	-192.93
1989	1164.70	1158.00	1172.93	1087.17	1173.19	1124.19	6.70
1990	1139.80	1157.68	1165.86	1094.95	1167.68	1129.68	-17.88
1991	1057.70	1157.35	1158.79	1102.73	1162.17	1135.16	-99.65
1992	971.50	1157.02	1151.72	1110.51	1156.66	1140.65	-185.52
1993	950.50	1156.69	1144.65	1118.29	1151.14	1146.13	-206.19
1994	833.90	1156.37	1137.58	1126.07	1145.63	1151.62	-322.47
1995	1073.60	1156.04	1130.51	1133.84	1140.12	1157.11	-82.44
1996	1102.50	1155.71	1123.44	1141.62	1134.61	1162.59	-53.21
1997	1124.60	1155.39	1116.37	1149.40	1129.10	1168.08	-30.79
1998	1096.10	1155.06	1109.30	1157.18	1123.58	1173.57	-58.96
1999	1190.90	1154.73	1102.23	1164.96	1118.07	1179.05	36.17
2000	1183.20	1154.41	1095.16	1172.74	1112.56	1184.54	28.79
2001	1180.50	1154.08	1088.10	1180.52	1107.05	1190.03	26.42
2002	1499.60	1153.75	1081.03	1188.30	1101.53	1195.51	345.85
2003	1058.30	1153.43	1073.96	1196.08	1096.02	1201.00	-95.13
2004	1146.40	1153.10	1066.89	1203.86	1090.51	1206.49	-6.70
2005		1152.77	1059.82	1211.64	1085.00	1211.97	
2006	1218.80	1152.44	1052.75	1219.42	1079.49	1217.46	66.36
2007	1090.70	1152.12	1045.68	1227.20	1073.97	1222.95	-61.42
2008	1235.00	1151.79	1038.61	1234.98	1068.46	1228.43	83.21
2009	1293.20	1151.46	1031.54	1242.76	1062.95	1233.92	141.74
2010	850.30	1151.14	1024.47	1250.54	1057.44	1239.41	-300.84
2011	1272.20	1150.81	1017.40	1258.32	1051.92	1244.89	121.39
2012	1191.50	1150.48	1010.33	1266.10	1046.41	1250.38	41.02

Appendix 6 continued.

Point values for the chart Observed –Max-temperature – Mongu station 1975 - 2002

Year	Data	Sen's estimate	99 % conf. min	99 % conf. max	95 % conf. min	95 % conf. max	Residual
1975	30.28	31.47	33.25	29.97	32.60	30.43	-1.19
1976	32.00	31.40	33.03	30.03	32.43	30.45	0.60
1977	30.61	31.32	32.82	30.09	32.26	30.46	-0.71
1978	32.00	31.25	32.60	30.14	32.10	30.48	0.75
1979	31.22	31.18	32.39	30.20	31.93	30.50	0.04
1980	27.78	31.11	32.17	30.26	31.76	30.51	-3.33
1981	33.78	31.04	31.96	30.31	31.59	30.53	2.74
1982	32.33	30.97	31.75	30.37	31.42	30.55	1.36
1983	32.72	30.90	31.53	30.43	31.25	30.57	1.82
1984	29.56	30.82	31.32	30.48	31.08	30.58	-1.26
1985	29.83	30.75	31.10	30.54	30.91	30.60	-0.92
1986	30.17	30.68	30.89	30.60	30.74	30.62	-0.51
1987	32.67	30.61	30.68	30.65	30.57	30.64	2.06
1988	30.50	30.54	30.46	30.71	30.40	30.65	-0.04
1989	32.06	30.47	30.25	30.77	30.24	30.67	1.59
1990	32.67	30.40	30.03	30.82	30.07	30.69	2.27
1991	29.78	30.32	29.82	30.88	29.90	30.71	-0.54
1992	25.22	30.25	29.60	30.94	29.73	30.72	-5.03
1993	29.17	30.18	29.39	30.99	29.56	30.74	-1.01
1994	31.67	30.11	29.18	31.05	29.39	30.76	1.56
1995	30.94	30.04	28.96	31.11	29.22	30.78	0.90
1996	29.28	29.97	28.75	31.16	29.05	30.79	-0.69
1997	30.50	29.90	28.53	31.22	28.88	30.81	0.60
1998	29.11	29.82	28.32	31.28	28.71	30.83	-0.71
1999	26.94	29.75	28.11	31.33	28.54	30.84	-2.81
2000	32.28	29.68	27.89	31.39	28.38	30.86	2.60
2001	31.61	29.61	27.68	31.44	28.21	30.88	2.00
2002	26.56	29.54	27.46	31.50	28.04	30.90	-2.98

Appendix 6 continued.

Point values for the chart Observed discharge for Kalabo station 1959 - 1998

Year	Data	Sen's estimate	99 % conf. min	99 % conf. max	95 % conf. min	95 % conf. max	Residual
1959	26587.82	29532.46	36582.19	22320.43	34271.53	23228.15	-2944.64
1960	20544.56	29124.11	35858.01	22199.70	33634.08	23044.82	-8579.55
1961	22132.67	28715.76	35133.83	22078.97	32996.64	22861.49	-6583.09
1962	28683.98	28307.41	34409.65	21958.25	32359.19	22678.16	376.57
1963	39587.01	27899.07	33685.46	21837.52	31721.75	22494.83	11687.94
1964	19648.73	27490.72	32961.28	21716.79	31084.30	22311.50	-7841.99
1965	18341.92	27082.37	32237.10	21596.06	30446.86	22128.17	-8740.46
1966	26941.69	26674.02	31512.92	21475.33	29809.42	21944.84	267.66
1967	22544.76	26265.68	30788.74	21354.60	29171.97	21761.51	-3720.92
1968	34447.54	25857.33	30064.56	21233.87	28534.53	21578.18	8590.21
1969	35637.96	25448.98	29340.38	21113.14	27897.08	21394.85	10188.98
1970	28253.07	25040.63	28616.20	20992.42	27259.64	21211.52	3212.44
1971	16304.15	24632.29	27892.01	20871.69	26622.20	21028.19	-8328.14
1972	18017.07	24223.94	27167.83	20750.96	25984.75	20844.86	-6206.87
1973	5544.22	23815.59	26443.65	20630.23	25347.31	20661.53	-18271.37
1974	25852.22	23407.24	25719.47	20509.50	24709.86	20478.20	2444.98
1975	30074.96	22998.90	24995.29	20388.77	24072.42	20294.87	7076.07
1976	30854.64	22590.55	24271.11	20268.04	23434.97	20111.54	8264.10
1977	19186.80	22182.20	23546.93	20147.32	22797.53	19928.21	-2995.40
1978	34057.90	21773.85	22822.75	20026.59	22160.09	19744.88	12284.04
1979	26243.35	21365.51	22098.56	19905.86	21522.64	19561.55	4877.85
1980	25358.09	20957.16	21374.38	19785.13	20885.20	19378.22	4400.93
1981	25158.61	20548.81	20650.20	19664.40	20247.75	19194.89	4609.79
1982	8855.51	20140.46	19926.02	19543.67	19610.31	19011.56	-11284.95
1983	15731.62	19732.12	19201.84	19422.94	18972.87	18828.23	-4000.49
1984	16449.63	19323.77	18477.66	19302.21	18335.42	18644.90	-2874.14
1985	21536.25	18915.42	17753.48	19181.49	17697.98	18461.57	2620.83
1986	19007.06	18507.07	17029.30	19060.76	17060.53	18278.24	499.99
1987	16172.36	18098.73	16305.11	18940.03	16423.09	18094.91	-1926.37
1988	21862.61	17690.38	15580.93	18819.30	15785.64	17911.58	4172.23
1989	38588.84	17282.03	14856.75	18698.57	15148.20	17728.25	21306.81
1990	14743.05	16873.68	14132.57	18577.84	14510.76	17544.92	-2130.63
1991	16630.08	16465.34	13408.39	18457.11	13873.31	17361.59	164.75
1992	7616.36	16056.99	12684.21	18336.39	13235.87	17178.27	-8440.63
1993	20765.36	15648.64	11960.03	18215.66	12598.42	16994.94	5116.72
1994	11728.68	15240.29	11235.85	18094.93	11960.98	16811.61	-3511.61
1995	3981.66	14831.95	10511.66	17974.20	11323.53	16628.28	-10850.29
1996	5298.41	14423.60	9787.48	17853.47	10686.09	16444.95	-9125.18
1997	15321.81	14015.25	9063.30	17732.74	10048.65	16261.62	1306.55
1998	13442.16	13606.90	8339.12	17612.01	9411.20	16078.29	-164.75

Appendix 6 continued.

Point values for the chart Observed Precipitation – Mongu station 1974 - 2013

Year	Data	Sen's estimate	99 % conf. min	99 % conf. max	95 % conf. min	95 % conf. max	Residual
1974	1140.70	840.01	972.18	636.35	929.51	681.57	300.69
1975	1037.40	844.23	968.03	650.34	927.38	693.22	193.17
1976	1085.10	848.46	963.88	664.34	925.26	704.87	236.64
1977	846.20	852.69	959.73	678.33	923.13	716.52	-6.49
1978	1310.90	856.92	955.58	692.33	921.01	728.18	453.98
1979	880.20	861.15	951.43	706.33	918.88	739.83	19.05
1980	883.70	865.38	947.28	720.32	916.76	751.48	18.32
1981	925.70	869.61	943.13	734.32	914.63	763.14	56.09
1982	724.30	873.84	938.98	748.31	912.51	774.79	-149.54
1983	761.00	878.06	934.83	762.31	910.38	786.44	-117.06
1984	554.50	882.29	930.68	776.31	908.25	798.10	-327.79
1985	763.30	886.52	926.53	790.30	906.13	809.75	-123.22
1986	937.80	890.75	922.38	804.30	904.00	821.40	47.05
1987	649.80	894.98	918.23	818.29	901.88	833.06	-245.18
1988	833.60	899.21	914.08	832.29	899.75	844.71	-65.61
1989	1074.60	903.44	909.93	846.29	897.63	856.36	171.16
1990	876.20	907.67	905.78	860.28	895.50	868.01	-31.47
1991	867.10	911.90	901.63	874.28	893.37	879.67	-44.80
1992	623.50	916.12	897.48	888.27	891.25	891.32	-292.62
1993	1256.70	920.35	893.33	902.27	889.12	902.97	336.35
1994	620.20	924.58	889.18	916.27	887.00	914.63	-304.38
1995	707.70	928.81	885.03	930.26	884.87	926.28	-221.11
1996	726.50	933.04	880.88	944.26	882.75	937.93	-206.54
1997	941.40	937.27	876.73	958.25	880.62	949.59	4.13
1998	1120.70	941.50	872.58	972.25	878.49	961.24	179.20
1999	865.30	945.73	868.43	986.24	876.37	972.89	-80.43
2000	1228.50	949.96	864.28	1000.24	874.24	984.54	278.54
2001	816.50	954.18	860.13	1014.24	872.12	996.20	-137.68
2002	1060.20	958.41	855.98	1028.23	869.99	1007.85	101.79
2003	813.80	962.64	851.82	1042.23	867.87	1019.50	-148.84
2004	984.40	966.87	847.67	1056.22	865.74	1031.16	17.53
2005	682.20	971.10	843.52	1070.22	863.62	1042.81	-288.90
2006	842.50	975.33	839.37	1084.22	861.49	1054.46	-132.83
2007	1096.40	979.56	835.22	1098.21	859.36	1066.12	116.84
2008	1579.50	983.79	831.07	1112.21	857.24	1077.77	595.71
2009	1158.20	988.02	826.92	1126.20	855.11	1089.42	170.18
2010	1203.30	992.24	822.77	1140.20	852.99	1101.08	211.06
2011	968.40	996.47	818.62	1154.20	850.86	1112.73	-28.07
2012	1244.10	1000.70	814.47	1168.19	848.74	1124.38	243.40
2013	1000.80	1004.93	810.32	1182.19	846.61	1136.03	-4.13

Appendix 6 continued.

Point values for the chart Observed precipitation at Kabompo station 1974 - 2004

Year	Data	Sen's estimate	99 % conf. min	99 % conf. max	95 % conf. min	95 % conf. max	Residual
1974	1131.10	1037.55	1233.57	872.48	1155.65	919.96	93.55
1975	850.80	1032.90	1218.55	879.65	1144.17	924.45	-182.10
1976	1244.00	1028.25	1203.53	886.82	1132.70	928.94	215.75
1977	786.60	1023.60	1188.50	893.99	1121.22	933.43	-237.00
1978	1340.20	1018.95	1173.48	901.16	1109.75	937.91	321.25
1979	1045.80	1014.30	1158.46	908.32	1098.27	942.40	31.50
1980	696.70	1009.65	1143.43	915.49	1086.80	946.89	-312.95
1981	1005.00	1005.00	1128.41	922.66	1075.33	951.38	0.00
1982	995.80	1000.35	1113.39	929.83	1063.85	955.87	-4.55
1983	848.90	995.70	1098.37	937.00	1052.38	960.35	-146.80
1984	965.10	991.05	1083.34	944.16	1040.90	964.84	-25.95
1985	1037.90	986.40	1068.32	951.33	1029.43	969.33	51.50
1986	1277.90	981.75	1053.30	958.50	1017.96	973.82	296.15
1987	964.00	977.10	1038.27	965.67	1006.48	978.31	-13.10
1988	1214.10	972.45	1023.25	972.84	995.01	982.79	241.65
1989	1211.50	967.80	1008.23	980.01	983.53	987.28	243.70
1990	1121.30	963.15	993.21	987.17	972.06	991.77	158.15
1991	996.00	958.50	978.18	994.34	960.59	996.26	37.50
1992	642.00	953.85	963.16	1001.51	949.11	1000.75	-311.85
1993	1142.80	949.20	948.14	1008.68	937.64	1005.23	193.60
1994	818.70	944.55	933.11	1015.85	926.16	1009.72	-125.85
1995	761.60	939.90	918.09	1023.01	914.69	1014.21	-178.30
1996	890.10	935.25	903.07	1030.18	903.21	1018.70	-45.15
1997	918.50	930.60	888.05	1037.35	891.74	1023.19	-12.10
1998	1165.10	925.95	873.02	1044.52	880.27	1027.67	239.15
1999	921.30	921.30	858.00	1051.69	868.79	1032.16	0.00
2000		916.65	842.98	1058.85	857.32	1036.65	
2001	961.40	912.00	827.95	1066.02	845.84	1041.14	49.40
2002	825.90	907.35	812.93	1073.19	834.37	1045.62	-81.45
2003	1078.70	902.70	797.91	1080.36	822.90	1050.11	176.00
2004	884.70	898.05	782.89	1087.53	811.42	1054.60	-13.35